EPIGENETICS OF HUMAN FETAL AND PLACENTAL DEVELOPMENT

by

Ka Chun Yuen

M.Phil., The Chinese University of Hong Kong, 2007

A THESIS SUBMITTED IN PARTIAL FULFILLMENT OF

THE REQUIREMENTS FOR THE DEGREE OF

DOCTOR OF PHILOSOPHY

in

The Faculty of Graduate Studies

(Medical Genetics)

The University of British Columbia

(Vancouver)

June 2011

Abstract

Dysregulation of placental and fetal epigenetics can affect gene expression patterns, including the parent-of-origin dependent expression in imprinted genes. While defects of imprinted genes have been implicated in some adverse pregnancy outcomes, little is currently known about the role of epigenetics in regulating normal or pathological human pregnancy and development. The objective of this thesis is to provide fundamental DNA methylation profiles of human fetal and placental development so as to offer insights into the etiology of human disease and adverse pregnancy outcomes.

Taking advantage of the unbalanced parental genomic constitutions in triploidies, 45 novel imprinted genes were identified by comparing the genome-wide DNA methylation profiles between 10 diandries and 10 digynies. A comparison of DNA methylation profiles between placentas of different gestations and other somatic tissues showed tissue-specific and gestational age-specific DNA methylation changes in many imprinted genes. To gain insight into the genomic pattern of tissue-specific methylation, DNA methylation profile was evaluated in 5 somatic tissues (brain, kidney, lung, muscle and skin) from eight normal second-trimester fetuses. Tissue-specific differentially methylated regions (tDMRs) were identified in 195 loci, suggesting that tissue-specific methylation is established early in the second trimester. Importantly, only 17% of the identified fetal tDMRs were found to maintain this same tissue-specific methylation in adult tissues, implicating an extensive epigenetic reprogramming between fetus and adult. Besides intra-individual differences, there is also substantial DNA methylation variation between individuals. While many sites show a continuous pattern of DNA methylation variation between different placentas, *WNT2*, *TUSC3* and *EPHB4* were identified to have epipolymorphisms at their promoter region. The methylation status at the *TUSC3* promoter showed an association with

preeclampsia, suggesting a role of DNA methylation change in adverse pregnancy outcomes. A further investigation of DNA methylation profiles in 26 placentas from preeclampsia, IUGR and control subjects showed 34 loci were hypomethylated in the early-onset preeclamptic placentas, with *TIMP3* having a potential of being a biomarker for the disorder. These results provided comprehensive DNA methylation profiles for both normal and abnormal fetal and placental tissues, which contribute to the biological and clinical aspects of the pathogenesis of fetal and placental disorders.

Preface

I wrote Chapter 1 in its entirety. Part of the chapter has been published by Yuen RKC and Robinson WP (2011).

A version of Chapter 2 has been submitted for publication by Yuen RKC, Jiang R, Peñaherrera MS, McFadden DE and Robinson WP (2011). This project was conceived by WPR and me. I designed and performed the experiments. RJ prepared and karyotyped the samples. MSP performed the microarray experiment. DEM contributed the tissue samples. I analyzed the data and wrote the manuscript. WPR edited the manuscript.

A version of Chapter 3 has been published by Yuen RKC, Neumann SMA, Fok AK, Peñaherrera MS, McFadden DE, Robinson WP, Kobor MS (2011). WPR, MSK and I conceived and designed the study. SMAN, AKF and MSP performed the microarray experiment. I performed the pyrosequencing experiments. DEM contributed the fetal tissue samples. MSK, WPR and I analyzed the data. I wrote the manuscript with the input and edits from WPR and MSK.

Chapter 4 has been published by Yuen RKC, Avila L, Peñaherrera MS, von Dadelszen P, Lefebvre L, Kobor MS, Robinson WP (2009). The experiments in this study were conceived, designed and performed by myself. LA sampled the placentas and extracted DNA and RNA. I performed the microarray experiment with the help from MSP. PvD and LL provided samples and MSK provided analysis tools. I analyzed the data and wrote the manuscript. WPR edited the manuscript.

Chapter 5 has been published by Yuen RKC, Peñaherrera MS, von Dadelszen P, McFadden DE, Robinson WP (2010). WPR and I conceived the study. I designed and performed

the experiments, and analyzed the data. MSP and I performed the microarray experiment. PvD and DEM provided samples. I wrote the manuscript and WPR edited it.

I wrote Chapter 6 in its entirety.

Ethical approval for the experiments presented was obtained from ethics committees of the University of British Columbia and the Children's & Women's Health Centre of British Columbia (UBC and C&W Research Ethics Board; certificate number H04-70488).

Table of contents

List of tables

List of figures

List of abbreviations

aDMG	age-dependent differentially methylated gene
aDMR	age-dependent differentially methylated region
ANOVA	analysis of variance
BWS	Beckwith-Wiedemann Syndrome
CGIs	CpG islands
CHARM	comprehensive high throughput arrays for relative methylation
CHM	complete hydatidiform mole
CNV	copy number variation
CVS	chorionic villous sampling
DAVID	Database for Annotation, Visualization and Integrated Discovery
DML	differentially methylated loci
DMR	differentially methylated region
DNMT	DNA methyltransferase
EOPET	early-onset preeclampsia
EVT	extravillous cytotrophoblast
FDR	false discovery rate
GO	Gene Ontology
HDAC	histone deacetylase
HIF	hypoxia-inducible factor
ICM	inner cell mass
ICR	imprinting control region
IUGR	intrauterine growth restriction

LOPET	late-onset preeclampsia
MAP	Methylation Allelic Polymorphism
MBD	methyl-CpG-binding domain
MeDIP	methylated DNA immunoprecipitation array
MEG	maternally expressed gene
MMP	matrix metalloproteinase
PcG	Polycomb Group
PCR	polymerase chain reaction
PEG	paternally expressed gene
PET	Preeclampsia (preeclamptic toxemia)
PGC	primordial germ cell
RT-PCR	reverse transcription-polymerase chain reaction
SAM	significance analysis of microarrays
SNP	single-nucleotide polymorphism
SRS	Silver-Russell Syndrome
tDMR	Tissue-specific differentially methylated region
VEGF	vascular endothelial growth factor

Acknowledgements

I would like to thank my supervisor, Dr. Wendy Robinson, for giving me patient guidance and allowing me the freedom to develop my own ideas. Thank you for your support, encouragement and trust on me. To the members of my thesis committee, Dr. Michael Kobor, Dr. Louis Lefebvre and Dr. Peter von Dadelszen, thanks for providing me invaluable advice and inspiration by being knowledgeable and supportive. I would also like to thank Dr. Matthew Lorincz and Dr. Carolyn Brown for stimulating discussions and additional insight. I want to express my gratitude to all the past and present members of the Robinson lab for their help and supports. To Ruby, David, Maria, Dan, Courtney, Danielle, Jennifer, Alicia, Irina, Magda, John, Kristal, to name but a few, thanks for hanging around with me and keeping me entertained. It is my privilege to work with you all.

I would like to thank my family for their support and for always believing in me. I am deeply indebted to my girlfriend Grace. Without her love and support, it would not be possible for me to overcome all the challenges and difficulties.

Chapter 1: Introduction[1]

1.1. Overview

Many thousands of pregnancies with obstetrical complications are encountered each year in Canada. These complications are potentially due to underlying utero-placental defects. Approximately 5% of the pregnancies are complicated by preeclampsia, a condition that leads among the causes of maternal and infant morbidity and mortality world-wide (Roberts and Cooper 2001), and 5% of live births have low birth weight (less than 2,500 grams), which is associated with long-term implication to postnatal health (Pallotto and Kilbride 2006). These conditions are thought to be related to a deficiency in migration and differentiation of trophoblasts at the maternal-fetal interface (Redman and Sargent 2005). However, the specific causes of this deficiency are still unknown. The variety of distinct cell types that compose the placenta, each with very different gene expression patterns and changing distribution throughout pregnancy (Rossant and Cross 2001), makes it difficult to diagnose specific causes of placental failure. The difficulty in distinguishing cause from consequence perhaps explains the lack of progress in our understanding of these conditions.

Epigenetics is the study of processes that produce a heritable phenotype without changing the underlying DNA sequence. While our knowledge of epigenetic changes in fetal and placental development is still limited, they certainly play important roles. Genes exhibiting parent-of-origin effects (imprinting) are prominently expressed in the placenta and regulated by epigenetic mechanisms (Coan *et al*. 2005). Disruption of these genes in mouse often results in abnormal

[1] Part of Chapter 1 has been published. Yuen RKC and Robinson WP. (2011) Review: A high capacity of the human placenta for genetic and epigenetic variation: implications for assessing pregnancy outcome. Placenta. 32 Suppl2: S136-41.

placental development and fetal growth (Coan *et al*. 2005). It has been suggested from studies in mouse that epigenetic regulation of gene expression is less stringent in placental tissue than the fetus proper (Morgan *et al*. 2005). It is possible that defects in epigenetic regulation of these imprinted genes may contribute to human placental disorders. However, there is a remarkable variability in placental structure among different mammals (Carter and Enders 2004; Murphy *et al*. 2001). Thus animal models, while very useful, are limited in their direct application to the study of the human placenta.

The objective of this thesis is to provide fundamental epigenetic profiles of human fetal and placental differentiation that can be used as a basis to understand the etiology of human diseases and adverse pregnancy outcomes. The introduction of this thesis will provide the current knowledge and understanding of the role of epigenetic regulation in fetal and placental development. I will: 1) introduce the importance of early prenatal and placental development in relation to the human disorders; 2) review epigenetic regulations and the role of epigenetic reprogramming during early fetal development; 3) describe the intra-individual DNA methylation variation, including tissue-specific and age-dependent DNA methylation; 4) present the recent findings on the inter-individual DNA methylation, with a focus on the variation in the human placenta; 5) discuss the relationship between epigenetic abnormality and the development of adverse pregnancy outcomes, such as preeclampsia and intrauterine growth restriction (IUGR), and lastly, 6) present the research objectives of this thesis.

1.2. Fetal programming

Traditionally, the intrauterine environment has been regarded as critical only for prenatal development of the fetus. However, there is accumulating evidence showing that adverse influences during early development can increase the risk of developing disease in adult life. It was first observed by Barker and co-workers that the weights at birth were correlated with the risk of developing coronary artery diseases in adults (Barker and Osmond 1986; Barker *et al*. 1989). Subsequently, it has also been found that birth weights were associated with chronic diseases, such as hypertension (Curhan *et al*. 1996a; Curhan *et al*. 1996b) and Type 2 diabetes (Hales *et al*. 1991; Ravelli *et al*. 1998). Based largely on the epidemiological data, Barker suggested an hypothesis that the alterations of fetal nutrition and endocrine status may result in developmental adaptations that permanently change the structure, physiology, and metabolism which then predispose individuals to cardiovascular, metabolic and endocrine disease in adult life (Barker 1992; Barker 2004). This paradigm is referred to as "fetal programming". The term "programming" refers to the permanent or long term effects of a stimulus or insult at a critical or sensitive period (Lucas 1991).

Further studies in experimental animals have provided proof of principle for fetal programming, suggesting that intrauterine environment is important for long term postnatal development (Armitage *et al*. 2004; Gluckman and Hanson 2004b; Hoet and Hanson 1999). The most commonly used approach to study the effect of intrauterine environment has been to alter maternal nutrition during pregnancy, for example, by subjecting the pregnant animals to protein malnutrition. It has been shown that the mice with maternal protein malnutrition result in various degrees of disturbed glucose metabolism (Dahri *et al.* 1991) and cardiovascular function (Langley and Jackson 1994) in the offspring. It has also been shown that other perturbations of

maternal physiology, such as administration of corticosteroids (Dahlgren *et al.* 2001), cytokines (Nyirenda *et al.* 1998) or experimental reduction of uterine blood flow (Jansson and Lambert 1999; Simmons *et al*. 2001) can lead to fetal programming of obesity (Dahlgren *et al.* 2001) or diabetes (Nyirenda *et al*. 1998; Simmons *et al*. 2001). These phenomena were referred to as developmental plasticity of the fetus during pregnancy, which conveys the ability to change the structure and function of the fetus in an irreversible fashion during a critical time window in response to the environmental cue (Gluckman and Hanson 2004a; Gluckman and Hanson 2004b).

The concept of fetal programming has more broadly been defined as developmental and evolutionary strategies, termed "predictive adaptive response" (Gluckman and Hanson 2004a; Gluckman and Hanson 2004b).This theory proposed 'the developmental plasticity as adaptive responses to environmental cues acting early in the life cycle, but where the advantage of the induced phenotype is primarily manifest in a later phase of the life cycle' (Gluckman and Hanson 2004a; Gluckman and Hanson 2004b). Therefore, instead of causing developmental disruption immediately, the plasticity allows the fetus to respond to the environmental influences by following a developmental trajectory that may be associated with an adaptive advantage *in utero* (Gluckman and Hanson 2004a; Gluckman and Hanson 2004b). The resulting phenotype is likely to be advantageous in an anticipated future environment. The cue thus acts as a predictor of the nature of this environment. For instance, if the fetal metabolism and growth are adapted to the predicated postnatal environment by the nutrient supply during fetal life as the primary cue, intrauterine nutrient restriction will cause inappropriate fetal predictive response for subsequent abundance supply of nutrients in postnatal stage. Such mismatch of anticipation will then result in susceptibility for chronic diseases in adulthood (Gluckman and Hanson 2004b). These

observations highlight the importance of investigating the relationship between maternal-fetal interface and the fetal development.

1.3. Placental development

The placenta is a unique organ that constitutes the active interface between the maternal and fetal blood circulations. It serves as a source of hormonal and nutrient supply and immunologic barrier for the fetus, protects the fetus from harmful waste products by acting as an excretory route, allows exchange of respiratory gases between maternal and fetal compartments, and possesses many other functions. The wide ranges of physiological functions are carried out by the lung, kidney, gastrointestinal tract, liver, bone marrow, immune and the endocrine systems of the neonate after birth. The placental function is believed to have both short and long term consequences for the developing fetus and play a key role in fetal programming (Godfrey 2002; Myatt 2006).

Successful placental development is crucial for optimal growth, maturation, and survival of the fetus. Many animal embryonic null mutants die subsequent to placental failure (Rossant and Cross 2001). The human placenta is derived largely from the differentiation of its epithelial stem cells, termed trophoblasts. Although there are several types of trophoblast, they are all believed to be derived from the cytotrophoblast. These specialized placental cells proliferate early in pregnancy and then differentiate into tumor-like cells that establish blood flow to the placenta (Figure 1.1A). The human placenta is hemochorial, which means that the trophoblast comes into direct contact with the maternal blood (Pijnenborg *et al.* 1981). This results in extensive interdigitation of fetal and maternal tissues.

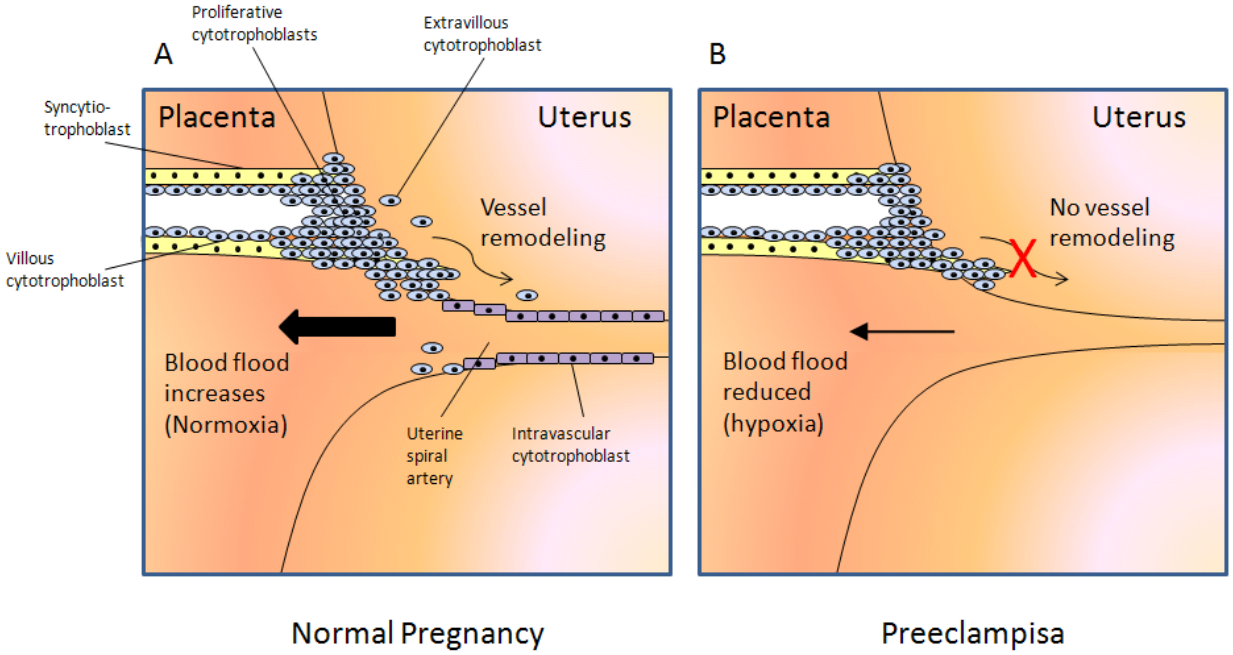

Figure 1.1. Placental development in (A) normal and (B) preeclamptic pregnancy.

A) In a normal development of placenta, extravillous cytotrophoblasts (EVTs) invade into the maternal uterus for vessel remodeling. EVTs will form intravascular cytotrophoblast in order to modulate the uterine spiral artery for normal supply of oxygen. B) In the case of pregnancy with preeclampsia, EVTs are less invasive and results in no vessel remodeling and reduced supply of oxygen.

After fertilization, the morula becomes a blastocyst that forms the central cavity (blastocyst cavity). The outer cell layer will develop into trophoblast while the inner cell mass will form the embryo and will also contribute to the extraembryonic tissues. At days 6 to 12 during implantation, the blastocyst invades the decidua of the uterine wall and the trophoblast cells become invasive as they differentiate (Staun-Ram and Shalev 2005). The trophoblasts closer to the embryo then proliferate and differentiate into mononuclear cytotrophoblast stem

cells (Figure 1.1A). They attach to the trophoblast basement membrane and actively proliferate. The cytotrophoblasts then fuse to form multinucleate syncytiotrophoblasts, which form the outer layer of the chorionic villi responsible for directly contacting the maternal blood for nutrient and gas exchange of the fetus (Kliman 2000). On the other hand, a subset of proliferative cytotrophoblast cells differentiate into proliferative extravillous cytotrophoblasts (EVTs) which are responsible for the penetration of the uterine wall, as well as remodeling of maternal spiral arteries (Staun-Ram and Shalev 2005) (Figure 1.1A). The behaviour of these EVTs closely resembles that of transformed cells that display a tumorigenic phenotype after neoplastic transformation (Gupta *et al.* 2005). The high cell proliferation, migratory and invasive properties of trophoblast cells have led to the statement that the placenta acts as a "pseudo-malignant" type of tissue (Soundararajan and Rao 2004; Strickland and Richards 1992).

The differentiation of cytotrophoblast into syncytiotrophoblast or EVT is highly regulated by the dramatic changes in expression of numerous genes (Aronow *et al.* 2001; Cross *et al.* 1994; Rossant and Cross 2001). Oxygen tension is a crucial determinant of the cytotrophoblast cell differentiation process (Genbacev *et al.* 1997; James *et al.* 2006). The hypoxic condition of early embryogenesis stimulates cytotrophoblast cells specifically to undergo cell division, causing the placenta to grow more rapidly than the embryo. From week 8 to 10 weeks of gestation, the cytotrophoblast tends to proliferate under low oxygen tension (hypoxia) (Rodesch *et al.* 1992). The hypoxic environment during early placental development is essential for normal placental angiogenesis, which is promoted by hypoxia-induced transcriptional and post-transcriptional regulation of angiogenic factors (Charnock-Jones and Burton 2000). The oxygen tension increases steadily after 12 to 13 weeks This leads to the differentiation of cytotrophoblast into invasive EVTs (Rodesch *et al.* 1992) and this allows the maternal blood to perfuse the

intervillous space. Once the intervillous blood flow is established, maternal blood can deliver nutrients to the fetus and allow for gaseous exchange between the maternal and fetal circulations (Figure 1.1A). Through this special regulation, adequate supply of nutrients to the embryo for growth and development can be achieved. The cause of this specific response of trophoblast cells to hypoxia is unknown, but could be mediated through epigenetic factors since the expression of genes involved in the epigenetic mark establishment is significantly altered in the mouse placenta upon hypoxic treatment (Gheorghe *et al.* 2007).

1.4. Epigenetics

There is a growing interest in studying the epigenetics of the placenta as it provides a mechanism by which development can be altered in response to maternal-fetal signals and environmental effects, such as maternal nutrition. Epigenetic processes can alter gene expression independent of DNA sequence and are inherited through mitotic cell division to constitute a form of cellular memory. This property is particularly important for cellular lineage development since the human body contains more than 200 different cell types and each having developed a different function and phenotype despite containing an identical genome. Through the establishment and maintenance of cell-type specific gene expression profiles, epigenetic mechanisms contribute to cellular identity (Illingworth *et al.* 2008). Epigenetic changes are critical for cellular differentiation and provide a means to alter gene expression in response to external cues. In mammals, DNA methylation and histone modifications constitute the most common epigenetic regulations.

1.4.1. DNA methylation

DNA methylation at CpG dinucleotides is one of the best-studied epigenetic modifications. It involves the addition of a methyl group to the 5 position of a cytosine (5-methylcytosine) adjacent to a guanine. DNA methyltransferases (DNMTs) are the enzymes responsible for catalyzing the transfer of the methyl group from a methyl donor, S-adensoyl-methionine, to the cytosine (Herman and Baylin 2003). *DNMT3A* and *DNMT3B* are involved in *de novo* methylation and the establishment of a new DNA methylation pattern, while *DNMT1* is responsible for the maintenance of DNA methylation by restoring hemi-methylated CpG sites to full symmetrical methylation after DNA replication (Laird 2003). Other DNMTs such as *DNMT2* (Yoder and Bestor 1998) and *DNMT3L* (Okano *et al.* 1998) have also been discovered, but they are either a RNA cytosine methyltransferase (Goll *et al*. 2006), or a cofactor for DNA methylation (Bourc'his *et al*. 2001).

The overall frequency of CpG dinucleotides in the human genome is low, but there are small stretches of DNA that are of high CpG density. These are termed CpG islands, and they are often associated with gene promoter regions (Bird 1986) (Defined as GC content >50% and observed/expected CpG >0.6 in a length >200 bp). Most CpG islands are unmethylated, but DNA methylation of CpG islands in the promoter regions are generally linked to gene silencing. Most CpG sites outside of CpG islands are methylated while most CpG sites in the CpG islands of the gene promoters are unmethylated in order to allow active gene transcription (Herman and Baylin 2003). The precise mechanism by which DNA methylation mediates the transcriptional repression is still unresolved, but the process is known to be in part associated with the recognition of methylated DNA by a family of methyl-CpG-binding domain (MBD) proteins (Bird and Wolffe 1999). These MBD proteins can mediate the regulation of gene expression by

interacting with histone protein modifications that regulate DNA accessibility (Cedar and Bergman 2009; Jaenisch and Bird 2003).

1.4.2. Histone modifications

The nucleosome is a protein complex that forms an important constituent of chromatin together with genomic DNA. It consists of two copies of each of the four core histones (H2A, H2B, H3 and H4), and is wrapped by the DNA. Modifications of histones refer to the covalent modifications of the amino-terminal tails and the core of nucleosomal histones. There are several types of histone modifications, including acetylation, methylation, phosphorylation, ADP ribosylation and ubiquitylation. They can extend the information content of the underlying DNA sequence and confer unique transcriptional potential (Turner 2002). Histone modifications can have both repressive and activating functions. The most well-characterized modifications are the trimethylation of Lys9 and Lys27 residues of histone H3 (H3K9me3 and H3K27me3), which have repressive functions, and H3K4me3 and H3K9 acetylation (H3K9ac), which are associated with active genes.

The repressive and activating modifications can also coexist together, which is termed bivalent modification, particularly in the embryonic stem cell (Bernstein *et al.* 2006). The bivalent domains are often the targets of Polycomb Group (PcG) proteins, which are important regulators of cellular development and differentiation (Lee *et al.* 2006). They are predicted to confer the potential for a gene to be driven either to its active or inactive state. Therefore, the genes that are silenced by this mechanism can maintain the possibility of being readily activated during differentiation, whereas genes in their active conformation may also easily revert to the repressed state (Pan *et al.* 2007; Zhao *et al*. 2007). In general, repressive histone modifications

are believed to confer short-term and flexible silencing whereas DNA methylation is believed to be a more stable, long-term silencing mechanism (Boyer *et al*. 2006; Lee *et al*. 2006; Reik 2007).

1.4.3. Epigenetic reprogramming and cell lineage commitment

The development of an organism from a zygote to an adult involves series of reprogramming and differentiation. Given the high plasticity of epigenetic marks, the gene expression changes required in these processes are mainly driven by the coordination of multiple transcriptional factors and epigenetic modifications (Reik 2007). Epigenetic modifications can be inherited through multiple cell divisions and therefore constitute a form of cellular memory (Reik 2007). For most cell types in the body, these epigenetic marks are believed to be fixed once the cells differentiate or exit the cell cycle. However, at certain stages of normal development, cells such as germ cells and embryonic cells need to undergo epigenetic reprogramming in order to acquire the essential characteristics of immorality and totipotency (Sasaki and Matsui 2008; Surani *et al*. 2007). This epigenetic reprogramming involves the removal of epigenetic marks in the nucleus, followed by establishment of a different set of epigenetic marks (Reik 2007).

The first wave of epigenetic reprogramming begins right after fertilization. It is characterized by a rapid active DNA demethylation before the onset of DNA replication (Mayer *et al*. 2000b; Oswald *et al*. 2000; Santos *et al*. 2002) and is followed by passive DNA demethylation up to the morula stage (Howlett and Reik 1991; Monk *et al*. 1987; Rougier *et al*. 1998) (Figure 1.2). This involves the whole genome except for some specific regions that are spared from the reprogramming at this stage such as imprinted regions, heterochromatin around centromeres and some repetitive elements (Reik *et al.* 2001).

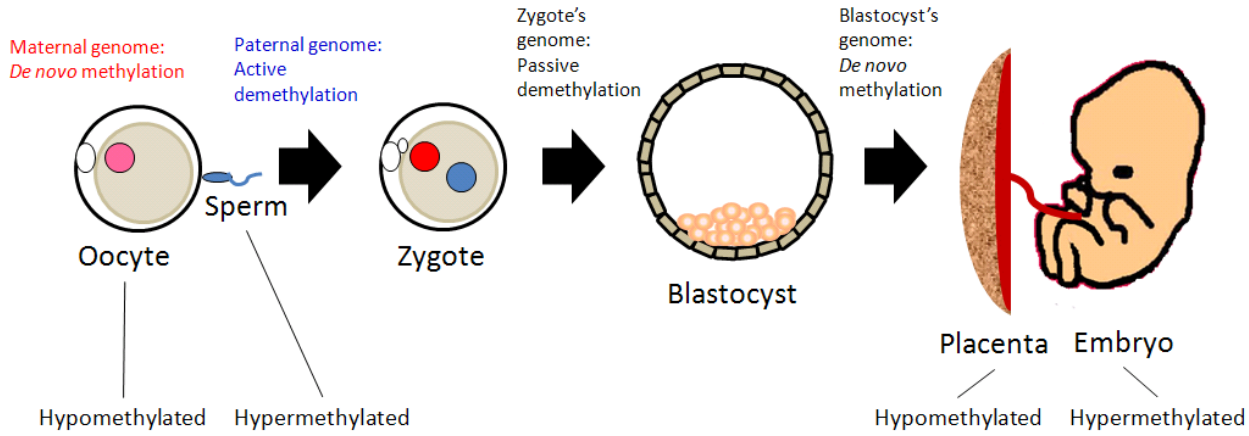

Figure 1.2. Epigenetic reprogramming of fetus and placenta.

Right before fertilization, the maternal genome will undergo *de novo* methylation. The paternal genome will then be actively demethylated after fertilization. With further cell divisions, the coneptuses' genome becomes passively demethylated during the first rounds of cell division. Up to the blastocyst stage, *de novo* methylation occurs for further tissue differentiation. The process results in global DNA hypomethylation in the placenta relative to the embryo.

After erasure of most of the epigenetic marks in the genome, *de novo* DNA methylation is initiated at the earliest differentiation event that separates the embryonic and trophoblast lineages (Santos *et al.* 2002). This developmental progression is a linear process that involves a series of differentiation steps, proceeding from totipotency to pluripotency and multipotency in committed cell lineages towards terminal differentiation. The progressive development is associated with a restriction of cellular plasticity at each stage of progress. This is accompanied by epigenetic modifications that impose a cellular memory and thereby ensure fixation of cell fate (Figure 1.2).

The second wave of epigenetic reprogramming occurs in the primordial germ cells (PGCs), which arise from the inner cell mass and migrate into in the extra-embryonic mesoderm

of the developing embryo. During the early stage of post-fertilization differentiation, the genome-wide methylation level in PGCs decline rapidly as a result of active targeted process of DNA demethylation (Hajkova *et al.* 2002). This profound period of DNA methylation erasure is associated with the essential resetting of parent-of-origin-specific methylation marks that are established during later stages of gametogenesis (paternal imprints in spermatozoa and maternal imprints in oocytes) based on the sex of the developing embryo and maintained during post-zygotic development (Lucifero *et al*. 2004; Swales and Spears 2005). Through this process, a limited number of genes establish gametic memory, which results in transcriptional silencing of one allelic copy of a homologous gene pair in a parent-of-origin-dependent manner. This process is called genomic imprinting.

1.4.4. Genomic imprinting

Imprinted genes are essential to early embryo and placental development of mammals. They are defined by their parent-of-origin dependent monoallelic expression that is caused by a functional non-equivalence of the maternal and paternal copy. The importance of imprinted genes for placental and fetal development was first revealed in mouse by the observations that parthenogenetic embryos (maternal origin in digynic diploid) could show embryonic differentiation but failed to form extraembryonic components (Surani *et al*. 1984). In contrast, androgenetic embryos (paternal origin in diandric diploid) had poorly developed embryos but the trophoblasts showed extensive proliferation (McGrath and Solter 1984). The parallel observations in human are ovarian teratomas (parthenogenetic) which is a rare form of tumor that consists of a variety of embryonic tissues or organs with absence of placental tissues; and complete hydatidiform moles (CHMs) (androgenetic), which exhibit trophoblast hyperplasia but no, or rarely any, embryonic structures.

These findings led to the discovery of several imprinted genes in mice such as *Igf2*, which is a paternally expressed gene (PEG) (DeChiara *et al.* 1991), and *H19* and *Igf2r* which are maternally expressed genes (MEGs) (Barlow *et al*. 1991; Bartolomei *et al*. 1991). Since then, more than 80 imprinted genes have been identified (Morison *et al.* 2005). The majority of imprinted genes since identified in mouse and human, play a role in placental and/or fetal growth. All of these imprinted genes are expressed in the placenta when tested and their imprinted expression is often limited to the placenta (Reik *et al.* 2003).

Imprinted genes are not randomly distributed in the genome, but rather tend to be located in clusters. In each cluster, the parent-of-origin-dependent monoallelic expression of the imprinted genes is regulated by epigenetic modifications at regions called imprinting control regions (ICRs) (Delaval and Feil 2004). DNA methylation is one of the epigenetic modifications for repressing allelic expression. Many imprinted genes possess differentially methylated regions (DMRs) where allelic methylation depends on the parent-of-origin (Reik and Walter 2001). DMRs established through the germline are called gametic DMRs or primary DMRs, which often coincide with ICRs (Henckel and Arnaud 2010; Mann 2001). Their methylation status is thought to be maintained in all somatic lineages once acquired. Other DMRs called somatic or secondary DMRs, are established after fertilization and may be tissue-specific (Henckel and Arnaud 2010; Mann 2001).

The importance of imprinted genes for balancing fetal and placental growth can be demonstrated by many knockout (loss of expression) and transgenic (over-expression) experiments of imprinted genes in mice. For example, *Igf2* is a PEG that has growth enhancing function and its abnormal expression can disturb the normal growth in mice (Ferguson-Smith *et al.* 1991). This is supported by the observation that a knockout of *Igf2* can lead to growth

restriction while over-expressing the *Igf2* transcripts can result in overgrowth of the fetus (DeChiara *et al*. 1990; Leighton *et al*. 1995). In particular, mice with knockout of a placenta-specific promoter of *Igf2* show similar growth retardation to mice with a knockout of the *Igf2* coding sequence, but the former display catch-up growth to become normal-sized adults (Constancia *et al*. 2002). This suggests that *Igf2* expression in the mouse placenta is principally responsible for prenatal growth.

The paternal allelic expression of murine *Igf2* is also present in human and the subsequent phenotypic effects of the imprinting dysregulation are similar. In both species, the allele-specific expression is regulated in *cis* by the paternal DMR at the *H19* ICR, or ICR1 (Cui *et al*. 2001; Frevel *et al*. 1999; Takai *et al*. 2001; Thorvaldsen *et al*. 1998). A loss of methylation at ICR1 in human can be found in a subset of Silver-Russell Syndrome (SRS) cases (Gicquel *et al*. 2005), which is characterized by intrauterine and postnatal growth restriction. It is found to be caused in some cases by the reduction of *IGF2* transcripts as a result of a loss of methylation at ICR1 (Gicquel *et al*. 2005). On the other hand, hypermethylation of ICR1 can be found in 30% cases of Beckwith-Wiedemann Syndrome (BWS) (Cooper *et al*. 2005), which is a overgrowth syndrome that may be caused by the over-expression of *IGF2* transcripts.

While many of the genes imprinted in mice are also imprinted in human, there are some notable exceptions (Morison *et al*. 2005). For example, *Igf2r, Ascl2, Xist* and *Esx1* are imprinted in mouse, but the orthologs in human are either not imprinted or have a less clear imprinting status (Grati *et al*. 2004; Ogawa *et al*. 1993; Westerman *et al*. 2001; Zeng and Yankowitz 2003). This discrepancy is particularly significant at the DNA methylation level in the placenta. For instance, many DMRs of the imprinted genes in the *KCNQ1* domain were found to be unmethylated in human (Monk *et al*. 2006). The lack of conservation of imprinting between

human and mouse has been suggested to be due to the evolutionary differences of placentation and pregnancy between two species (Monk *et al.* 2006).

The parental conflict theory has been developed to explain the evolution of imprinted genes (Moore and Haig 1991). It proposes that PEGs tend to promote growth of the offspring at the expense of the mother, while MEGs act as growth limiting factors in order to conserve maternal resources (Moore and Haig 1991). Mice may have acquired an expansion of imprinting to enable the placenta to become more efficient for supporting multiple offspring over a short gestational period, which may have led to an accelerated requirement for resource provisioning genes and their regulators (Monk *et al.* 2006). On the other hand, human pregnancy is mostly singleton and thus no competition is present, which may relieve the pressure for maintaining placental specific imprinting (Monk *et al.* 2006). Nevertheless, complete maps of DMRs in human and mouse placenta have not been established. It is possible that there are unidentified DMRs in the orthologous imprinted genes. It is also possible that some imprinted genes show tissue-specific imprinting and therefore have not yet been identified in either species.

1.5. Tissue-specific DNA methylation

Given that the human body contains more than 200 different cell types despite sharing an identical genome, it is commonly believed that there is an epigenetic mechanism that regulates the cell lineage differentiation. However, it is not until recently that DNA methylation has widely been proven to play an important role in this process, because it was believed that promoter DNA methylation, particularly in CpG islands, was a hallmark of cancer development (Esteller and Herman 2002); the primary exceptions are those promoters located in X chromosome and

imprinted genes. The advent of molecular technologies has demonstrated tissue-specific DNA methylation patterns both in locus-specific and genome-wide levels.

Evidence for a role of DNA methylation for tissue-specific gene expression was first reported for the human *SERPINB5* gene, which encodes Maspin (Futscher *et al*. 2002). *SERPINB5* was identified by subtractive hybridization analysis of normal mammary tissues and breast cancer cell lines (Zou *et al*. 1994). It is known to be a potential tumor suppressor gene that is unmethylated in normal breast cells and frequently hypermethylated in breast cancers (Domann *et al*. 2000). Further studies in multiple types of normal cells found that although it was unmethylated and expressed in cells of epithelial origin, it was methylated in mesenchymal and haematopoietic cells where expression was repressed (Futscher *et al*. 2002). The promoter of the *SERPINB5* contains differentially methylated transcription factor binding sites. It was found that the inverse correlation between tissue-specific DNA methylation and gene expression leads to changes in chromatin accessibility (Futscher *et al*. 2002). Importantly, demethylation of the *SERPINB5* promoter in fibroblasts, a tissue in which is normally methylated with no gene expression, leads to re-expression of the gene (Futscher *et al*. 2002). This indicates that DNA methylation is the primary regulator of tissue-specific gene expression in *SERPINB5*. Subsequently, other tissue- or cell-type-specific genes, such as *DNAJC15* (Strathdee *et al*. 2004) and *SFN* (Oshiro *et al*. 2005), have been found to also exhibit tissue-specific DNA methylation.

With the advance of high-throughput technologies, measurement of genome-wide DNA methylation patterns has recently made it possible to elucidate how DNA methylation controls gene expression and how those patterns differ in each tissue. The extent by which DNA methylation contributes to the normal somatic tissue has been demonstrated in a study showing that 4% of CpG island promoters are nearly completely methylated in peripheral blood but

unmethylated in the germ line (Shen *et al*. 2007), providing evidence that CpG island methylation is not limited to imprinted genes and the X chromosome in normal tissues. In a comparison of human blood, brain, muscle and spleen, it was found that 6-8% of CpG islands were methylated and that inter- and intra-genic sequences are preferred sites of DNA methylation (Illingworth *et al.* 2008). This study also found that developmental genes show preferential DNA methylation (Illingworth *et al.* 2008). A comparison of DNA methylation levels in embryonic tissues derived from different germ layers (such as brain, spleen and liver) revealed DMRs located about 2kb apart from CpG islands, also known as CpG shores, that may be involved in tissue-specific gene expression (Irizarry *et al*. 2009). Collectively, these studies support the idea that different tissue types have unique DNA methylation patterns that contribute to their lineage specificity.

1.5.1. Placenta-specific DNA methylation

Intriguingly, global DNA methylation levels are markedly different between the embryonic and extraembryonic lineages. In mouse studies, the trophectoderm, which gives rise to the trophoblast lineage of the placenta, is hypomethylated compared with the inner cell mass (ICM), as revealed by 5-methylcytosine staining (Santos *et al.* 2002). These global differences are also maintained throughout development in the embryo and placenta (Chapman *et al*. 1984; Rossant *et al*. 1986). However, genome-wide DNA methylation shows no significant difference in methylation levels at the gene promoters (Borgel *et al*. 2010; Farthing *et al*. 2008). This is consistent with the similarity in overall transcriptional activity between the lineages (Tanaka *et al.* 2002). Therefore, global methylation differences must relate to differences in intergenic regions and non-promoter genic regions.

The importance of DNA methylation for normal development of extra-embryonic tissues has been illustrated in several animal studies. For example, administration of a single dose of demethylating agent, 5-aza-2'-deoxycytidine, to pregnant rats at different stages of development can cause disruption of trophoblast proliferation (Serman *et al*. 2007; Vlahovic *et al*. 1999). Also, homozygous knockout of *Dnmt1* and *Dnmt3L* in mice has shown multiple morphological defects in the placentas which may largely be due to the loss of imprinting (Arima *et al*. 2006; Bourc'his *et al*. 2001; Li *et al*. 1992).

In fact, many placenta-specific genes are regulated by promoter DNA methylation. For example, *Syncytin-1* (*ERVWE1*) is an endogenous retrovirus-derived gene that is specifically unmethylated in placenta (Matouskova *et al.* 2006), and plays a crucial role in placenta development (Mi *et al.* 2000). Since many retrovirus-derived genes are expressed specifically in the human placenta, it is expected that more placental-specific unmethylated endogenous retrovirus-derived genes can be found (Reiss *et al.* 2007). Other than endogenous retrovirus-derived genes, there are also cancer-related genes and tumor-suppressor genes, such as *APC* and *RASSF1A*, that are specifically methylated in the placenta and the silencing of these genes is believed to be involved in cytotrophoblast invasion (Chiu *et al*. 2007; Novakovic *et al*. 2008; Wong *et al*. 2008). The similarity of DNA methylation profiles and many other similarities of physiological properties between trophoblasts and cancer cells has further supported trophoblast as a "pseudo-malignant" type of tissue (Chiu *et al*. 2007; Strickland and Richards 1992).

1.6. Age-dependent DNA methylation

There is a significant correlation between advanced aging and the increased incidence of cancer. Although it was generally believed that epigenetic marks are maintained with high fidelity throughout life once established, accumulating evidence shows that epigenetic signatures can change with age. One of the earliest epigenetic epidemiology studies observed that the CpG island DNA methylation of the *ER* gene in colon increased linearly with age of the colon (Issa *et al*. 1994). Since *ER* hypermethylation is found in almost all colorectal tumors, it was suggested that *ER* hypermethylation could contribute to the increased risk of colorectal cancer with age (Issa *et al*. 1994). Since then, the methylation of many more cancer-related genes have been found to show methylation changes that are correlated with age, and this kind of epigenetic modulation upon aging is collectively referred to as "age-related methylation" (Toyota *et al*. 1999), or "age-dependent DNA methylation" (Teschendorff *et al*. 2010).

Many high-throughput studies have been carried out recently to investigate the pattern of epigenetic changes in human somatic tissues due to aging and environmental exposures. Using microarray to profile the DNA methylation patterns in different somatic tissues from individuals with different ages, it was found that age-dependent DNA methylation is tissue-specific (Christensen *et al*. 2009; Gronniger *et al*. 2010). A similar observation was reported in mice (Maegawa *et al*. 2010). In addition, environmental effects may be tissue-specific and locus-specific (Bork *et al*. 2010; Christensen *et al*. 2009; Gronniger *et al*. 2010), which highlights the importance of tissue-specific consideration to the disease susceptibility. Several studies of human and mouse show that age-dependent DNA hypermethylation preferentially occurs at pre-existing bivalent chromatin domains or PcG proteins targeted domains in embryonic stem cells

(Maegawa *et al*. 2010; Rakyan *et al*. 2010; Teschendorff *et al*. 2010), suggesting the role of stem cell transformation in aging and cancer development.

The accumulation of epigenetic variation over time can depend on genetic, environmental, and stochastic factors (Bjornsson *et al*. 2004). In human, twins are valuable models to distinguish the effect of genetic from non-genetic factors. The rationale lies on the fact that monozygotic twins are genetically identical, while dizygotic twins are genetically similar as ordinary siblings (Poulsen *et al*. 2007). Despite sharing identical genetic sequence, monozygotic twins often show phenotypic discordance, which could be due to the influence of epigenetic changes over time. Although controversial, increased global and locus-specific epigenetic differences have been found in a subset of monozygotic twins, suggesting a role of epigenetic changes in the establishment of phenotype during the lifetime (Fraga *et al*. 2005). This finding was supported by another similar, but more systematic study with a larger cohort of monozygotic and dizygotic twins (Kaminsky *et al*. 2009). Thus epigenetic modifications may contribute a substantial component of phenotypic dissimilarity between twin pairs. Therefore, it is clear that environmental and/or stochastic factors can contribute to the change of epigenetic marks during the lifetime in humans.

A genetic component has also been implicated in the change of DNA methylation over time. It is shown that there is a lower intra- than inter-individual epigenetic difference observed in twin studies (Fraga *et al*. 2005), and that dizygotic twins feature more genome-wide and locus-specific DNA methylation differences than do monozygotic twins (Heijmans *et al*. 2007; Kaminsky *et al*. 2009). Similarly, a familial clustering of methylation changes is observed in longitudinal studies (Bjornsson *et al*. 2008). Therefore, it is important to take both the epigenetic

and genetic factors into consideration when studying phenotypic variation and disease susceptibility.

1.7. Inter-individual DNA methylation variation

Since DNA methylation plays an important role in tissue development, and individual variation in methylation may contribute to disease susceptibility, it has been increasingly popular to characterize the inter-individual epigenetic variation among human population. Population studies of inter-individual epigenetic variation are thus an important part of epigenetic epidemiology. A pilot study of human epigenome that profiled DNA methylation of the 3.8 Mb major histocompatibility locus in several human tissues showed that almost half of the amplicons analyzed showed substantial inter-individual variation in methylation in at least one tissue (Rakyan *et al*. 2004). Since then, many studies have been carried out in a large-scale and genome-wide fashion which confirmed that inter-individual DNA methylation variation can commonly be found between individuals (Bock *et al*. 2008; Byun *et al*. 2009; Flanagan *et al*. 2006; Schneider *et al*. 2010; Siegmund *et al*. 2007).

1.7.1. DNA methylation variation in the placenta

The placenta is one of the organs that show the most highly variable DNA methylation pattern (Reiss *et al*. 2007). Inter-individual variation of DNA methylation was initially observed in studies of imprinted genes in the placenta (Jinno *et al*. 1994; Xu *et al*. 1993). Unlike most other imprinted genes for which parental allele-specific expression is generally maintained across population, the imprinting of *IGF2R* and *WT1* is only found in a subset of individuals (Jinno *et al*. 1994; Xu *et al*. 1993) (Figure 1.3A). Methylation level correlates with biallelic versus monoallelic expression in these cases. Further studies of these polymorphic imprinted

genes revealed that such inter-individual variation can be attributed to both genetic and environmental factors (Sandovici *et al*. 2003).

In addition to inter-placental variation, there can be considerable epigenetic variation within a placenta, suggesting that stochastic and localized effects in the uterine environment may play a role. The imprinting control region of *IGF2* is an example of a site that shows considerable site-to-site variability within a placenta (Bourque *et al*. 2010; Katari *et al*. 2009) (Figure 1.3B). It was hypothesized that this variability might be a function of the number of trophoblast stem cells from which the placental trophoblast derived, with placentas derived from fewer precursors having a greater variance (Katari *et al*. 2009). A correlation between the within-placenta methylation variance at the *PTPN6* and *KISS1* promoters was argued to be due to sample-to-sample fluctuations in cell composition in conjunction with cell-specific methylation (Avila *et al*. 2010) (Figure 1.3C). Correcting for such confounding effects may be difficult as there are many different types of cells, each with potentially distinct methylation profiles, within both the trophoblast and mesenchymal portions of the placenta.

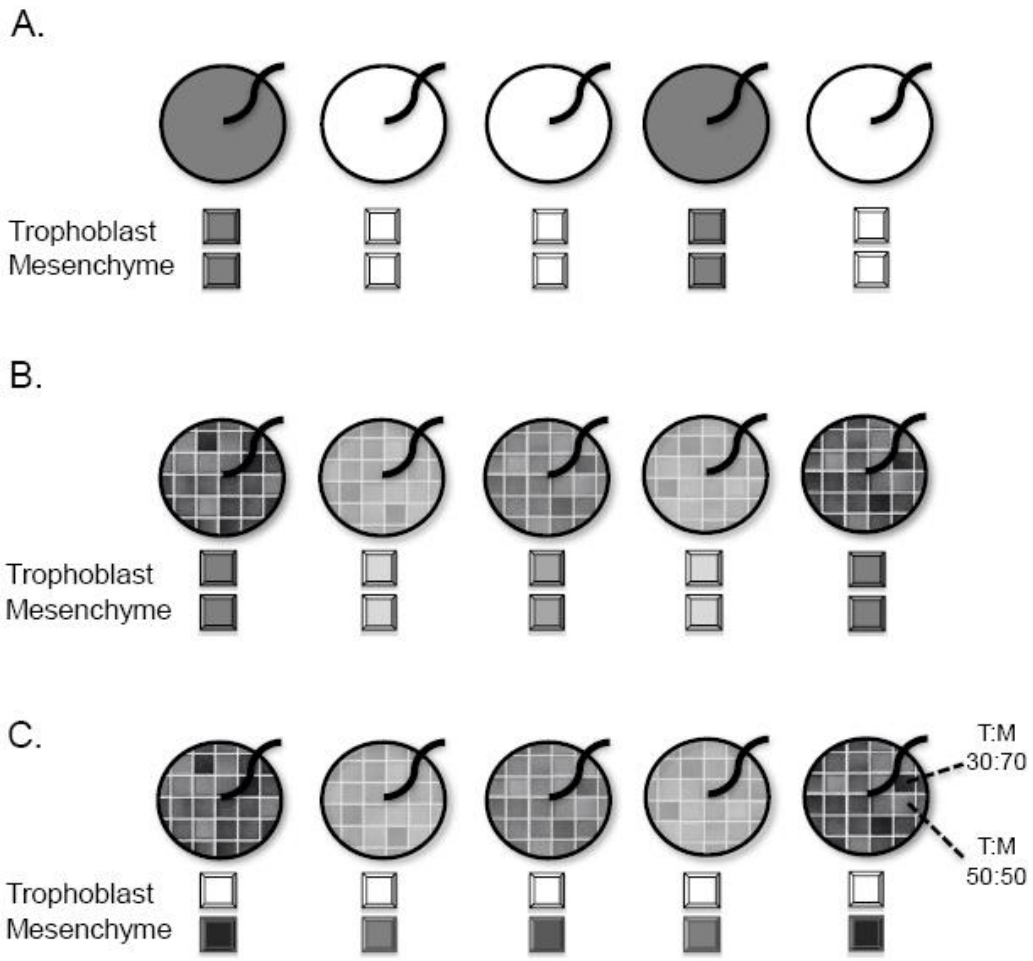

Figure 1.3. Illustration of various types of epigenetic variation.

A) Inter-individual DNA methylation variation. For example, the promoter of *WT1* can be methylated in some placentas (grey) but unmethylated in others (white) with similar level of DNA methylation in trophoblast and mesenchyme. B) Continuous DNA methylation variation. DNA methylation at the *IGF2*/*H19* locus varies continuously and may be mosaic (patchy pattern) among placentas. While there may be some differences in DNA methylation between trophoblast and mesenchyme, these are expected to trend on average in the same direction within a placenta if both are similarly influenced by environmental factors acting on that placenta. C) Inter- and intra-placental DNA methylation variation depends on cell composition. *KISS1* promoter is methylated in mesenchyme but unmethylated in the trophoblast. The observed methylation in placentas is contributed by both variation of methylation level in the mesenchyme and the ratio of cells between trophoblast (T) and mesenchyme (M).

1.7.2. Causes of inter-placental DNA methylation variation

A significant proportion of allele-specific DNA methylation detected in genome-wide studies is associated with the DNA sequence of adjacent SNPs, highlighting that genetic factors may contribute a substantial component of DNA methylation variability (Kerkel *et al*. 2008; Shoemaker *et al*. 2010). Thus some genetic polymorphisms may contribute to disease by affecting epigenetic marks.

A recent study of inter-individual DNA methylation variation in human epigenomes across different tissues, including placenta, found that variation of DNA methylation was significantly related to various environmental exposures, such as tobacco smoking (Christensen *et al*. 2009). More specifically, the intrauterine environmental attribution to the epigenetic state in the placenta is illustrated in two recent studies. The first one demonstrates DNA methylation differences in multiple gene promoters of children conceived *in vitro* or *in vivo* (Katari *et al*. 2009). The other one shows variable DNA methylation at the *IGF2*/*H19* locus in multiple tissues of twin pairs (Ollikainen *et al*. 2010). These two studies implicate that maternal environment may affect the development of the epigenome of the newborn, suggesting that alteration of epigenetic regulation may be a mechanism for "fetal programming" of disease risk (Gluckman *et al*. 2008).

1.8. Clinical aspects of epigenetic abnormalities

Epigenetic alteration has been well studied in association with cancer, but it is now being appreciated to be relevant to other health outcomes as well (Gibbons *et al*. 2000; Grayson *et al*. 2005; Oberle *et al*. 1991; Tufarelli *et al*. 2003). In relation to embryonic and placental development, it was reported that fetuses conceived via assisted reproduction may have

increased imprinting abnormalities which could result in birth defects (Schieve *et al*. 2004a; Schieve *et al*. 2004b). This suggests that preimplantation development is particularly sensitive to epigenetic errors (i.e. the stage at which methylation is more easily be altered). Many other epigenetic errors may occur in a variety of pregnancy disorders but remain undiagnosed. Two potential developmental consequences of epigenetic abnormalities are preeclampsia and IUGR. These two adverse pregnancy outcomes have been suggested to originate from the placenta (Figure 1.4).

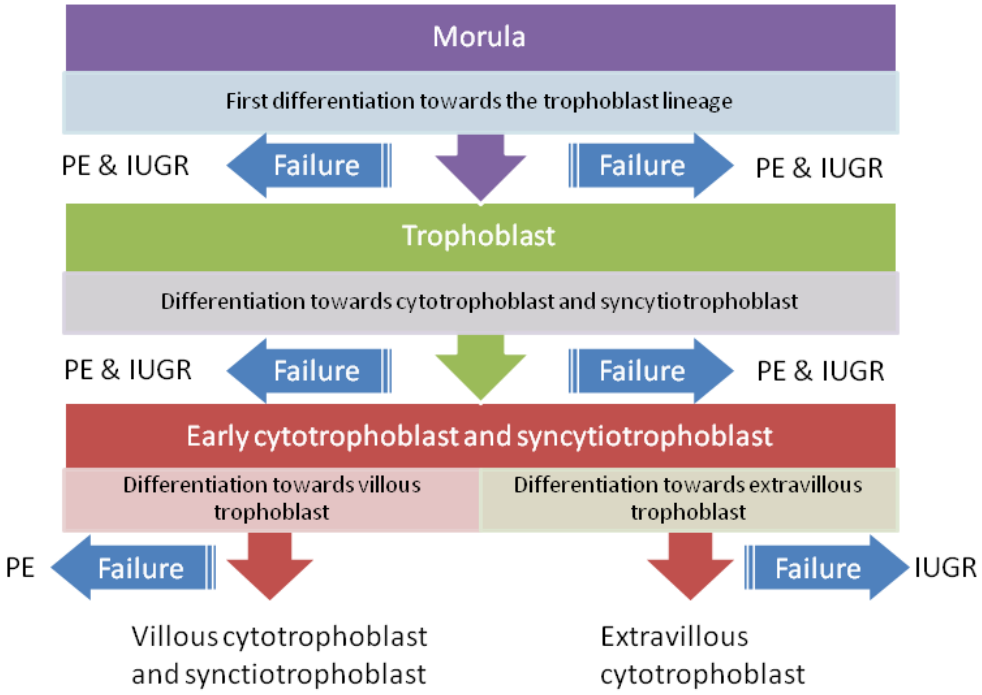

Figure 1.4. Placental origins of preeclampsia and IUGR.

From the placental origin hypothesis, any failure at the early stage of placental development will cause both preeclampsia and IUGR in the pregnancy (severe preeclampsia). While the occurrence of failure at the later stage of development (after villous and extravillous cytotrophoblast differentiation) will cause preeclampsia or IUGR independently, depending on the site of failure occurs.

1.8.1. Preeclampsia

Preeclampsia is one of the leading causes of maternal and fetal morbidity and mortality affecting 2 to 5% of all pregnancies (Redman and Sargent 2005; Roberts and Cooper 2001). It is characterized by high blood pressure in the mother and frequently growth deficiency in the fetus. Diagnosis is defined by hypertension as 140/90mm Hg or higher and proteinuria as 0.3 g or more protein in a 24 h urine sample after 20 weeks gestation and regress after delivery (von Dadelszen *et al.* 2003). Preeclampsia is heterogeneous in etiology and can be further subclassified into early-onset (<34 weeks) and late onset (≥34 weeks) (von Dadelszen *et al.* 2003). The cause of preeclampsia remains unknown and the only known cure is delivery of the fetus and placenta. Over decades, little progress has been made on the disease treatment and management because the disease can only be diagnosed after full-blown manifestation of the condition is developed, by which time treatment options are limited. Therefore, the identification of biomarkers that could be used to accurately identify those women at increase risk for the later development of preeclampsia and to distinguish among clinical subsets of preeclampsia would be a major step forward in antenatal care.

The importance of the placenta in the development of preeclampsia is demonstrated by hydatidiform moles, in which a fetus is absent. Women with hydatidiform moles can develop preeclampsia and the condition remits after removal of the mole, suggesting that the placenta is the primary cause of the symptom (Koga *et al*. 2010). Severe preeclampsia is also often associated with pathologic evidence of placental hypoperfusion and ischemia (Kadyrov *et al*. 2003), which are suggested to be caused by the incomplete transformation of the maternal spiral arteries by the invasive EVTs (Meekins *et al*. 1994). This incomplete remodeling of the uterine spiral arteries from partial cytotrophoblast invasion is known to be a precursor to preeclampsia

development (Figure 1.1B). Whether preeclampsia is caused by or results from the placental hypoxia and ischemia is still unknown, however, constriction of uterine blood flow has been shown to induce hypertension and proteinuria in animal studies (Granger *et al*. 2006; Makris *et al*. 2007) (Figure 1.1B). Also, *in vivo* experiments in mice suggest that placental hypoxia contributes to preeclampsia (Karumanchi and Bdolah 2004).

While the exact cause is still unknown, epigenetic features have been implicated in the pathogenesis of preeclampsia. Mutations in *STOX1*, which is located in an imprinted locus on 10q21.1, were identified in some unique familial cases of preeclampsia identified through apparent maternal transmission of susceptibility (van Dijk *et al.* 2005). Also, deficiency of the imprinted *Cdkn1c* gene in a mouse model leads to hypertension and proteinuria during pregnancy (Kanayama *et al.* 2002), implicating the role of an imprinted gene in the disease susceptibility.

Epigenetic alteration of non-imprinted genes has also been suggested. DNA methylation alteration of *SERPINA3* (Chelbi *et al.* 2007) promoter has been demonstrated. The DNA methylation level at the promoter of the gene was found to be hypomethylated in preeclamptic placentas. It was suggested that the epigenetic alteration of certain genes may be associated with reduced trophoblastic invasion (Dokras *et al.* 2006), *SERPINA3* methylation was also proposed to be useful as a biomarker for preeclampsia (Chelbi *et al*. 2007; Chim *et al*. 2005).

Many investigators have profiled gene expression in human preeclamptic placentas using genomic array technology (Centlow *et al*. 2008; Enquobahrie *et al*. 2008; Farina *et al*. 2009; Founds *et al*. 2009; Gack *et al*. 2005; Hansson *et al*. 2006; Heikkila *et al*. 2005; Hoegh *et al.* 2010; Jarvenpaa *et al*. 2007; Mayor-Lynn *et al*. 2010; Nishizawa *et al*. 2007; Reimer *et al*. 2002;

Sitras *et al*. 2009; Tsai *et al*. 2010; Vaiman *et al*. 2005) (Table 1.1). Up-regulated genes that were consistently identified included obesity-related genes (e.g. *LEP*) (Enquobahrie *et al*. 2008; Hoegh *et al*. 2010; Nishizawa *et al*. 2007; Reimer *et al*. 2002; Sitras *et al*. 2009; Tsai *et al*. 2010), embryonic development genes (e.g. *FLT1*) (Enquobahrie *et al*. 2008; Jarvenpaa *et al*. 2007; Nishizawa *et al*. 2007; Sitras *et al*. 2009; Tsai *et al*. 2010) and many genes involved in cell-cycle regulation or apoptosis (e.g. *INHBA*) (Hoegh *et al*. 2010; Nishizawa *et al*. 2007; Reimer *et al*. 2002; Sitras *et al*. 2009).

Table 1.1. Summary of microarray study of gene expression changes in preeclampsia and/or IUGR

Type	Scale	Sample size	Selected upregulated genes	Selected downregulated genes	Reference
Preeclampsia	~5,600 genes	6 controls; 6 PETs	Integrin α1, ***LEP***, ***INHBA***	N/A	Reimer *et al*, 2002
Preeclampsia	~8,400 genes	2 controls; 2 PETs	Nuclear body protein sp140, Glycoprotein hormones a polypeptide	DHEA sulfotransferase, KIAA0414 protein	Heikkilä *et al*, 2005
Preeclampsia and IUGR	2,304 clones	7 controls; 6 PETs; 3 PE+IUGRs; 3 IUGRs	Preeclampsia: *H19*, *IL8*; IUGR: *IGF2*, *IMP3*	N/A	Vaiman *et al*, 2005
Preeclampsia	~1,600 clones	10 controls; 5 PET+IUGRs; 4 PETs	*ADAM12*, *TIMP1*, *TIMP2*	N/A	Gack *et al*, 2005
Preeclampsia	5,952 genes	7 controls; 9 PETs; 5 Notchs	*ACP5*	Calmodulin 2, *RELA*	Hansson *et al*, 2006
Preeclampsia	~47,000 transcripts	24 controls; 21 PETs	***LEP***, ***FLT1***, ***INHBA***	N/A	Nishizawa *et al*, 2006
Preeclampsia and IUGR	~14,500 genes	3 controls; 2 PET+IUGRs	***FLT1***	*JAG1*, *COL18A1*	Jarvenpaa *et al*, 2007
Preeclampsia	~800 clones	15 controls; 5 PET+Ns; 5 Notchs; 10 PETs	Hemoglobin alpha2 and gamma	N/A	Centlow *et al*, 2008
Preeclampsia	~22,000 genes	18 controls; 18 PETs	***LEP***, ***FLT1***, *CDKN1C*	N/A	Enquobahrie *et al*, 2008
Preeclampsia	~14,500 genes	8 controls; 4 PETs	*CCK*	*IGFBP1*, *MMP12*, *KRT14*	Founds *et al*, 2009
Preeclampsia	18,811 genes	21 controls; 16 PETs	***FLT1***, ***INHBA***, ***PAPPA2***, *CGB5*, ***LEP***	*BHLHB3*, *PDGFD*, *BMP5*	Sitras *et al*, 2009
Preeclampsia	~14,500 genes	23 controls; 23 PETs	*HLA-DRB4*, *CLDN6*, *LTF*	*F8*	Farina *et al*, 2009
Preeclampsia	~15,000 genes	9 controls; 9 PETs	***LEP***, ***INHBA***	*TR1*, *FBLN1*	Hoegh *et al*, 2010
Preeclampsia	18,630 transcripts	7 controls; 7 PETs; 7 Preterms	*MMP1*	*TIMP3*	Mayor-Lynn *et al*, 2010
Preeclampsia	~48,000 transcripts	37 controls; 23 PETs	***LEP***, ***FLT1***, ***PAPPA2***, *ENG*, *INHA*	*CD4*	Tsai *et al*, 2010

It is suggested that many of the gene expression changes are the result of hypoxic conditions in preeclamptic placenta. In particular, hypoxia-inducible factor (HIF) is a heterodimeric transcription factor that initiates many cellular changes in the placenta in response to oxygen tension (Adelman *et al.* 2000). Interestingly, it appears that cross-talk between HIF and histone deacetylase is required for normal trophoblast differentiation (Maltepe *et al.* 2005). This implicates that a hypoxic condition, mediated by HIF, can affect the epigenetic modification of multiple genes. Recently, it was found that low oxygen tension can induce alteration of global DNA methylation in human cells (Shahrzad *et al*. 2007; Watson *et al*. 2009). Also, some genes that are involved in the mechanism of DNA methylation, such as *Dnmt3b*, are differentially expressed in mouse placenta upon hypoxia exposure (Gheorghe *et al*. 2007). It is possible that the low oxygen tension environment may cause DNA methylation changes in the preeclamptic placenta as well.

1.8.2. Intrauterine growth restriction (IUGR)

IUGR is often defined as a birth weight less than the 10^{th} percentile for gestational age, but in obstetric practice is more specifically defined as a baby who does not achieve intrauterine growth potential (representing a more clinically relevant subset of those $<10^{th}$ percentile for gestational age). This later diagnosis requires the presence of one or more ultrasound markers that are suggestive of placental dysfunction. IUGR is associated with significantly increased perinatal morbidity and mortality, as well as with cardiovascular disease, glucose intolerance and psychiatric disorders in later life (Barker 1997; Wiles *et al*. 2005). There are multiple causes for IUGR, but the spectrum and diagnosis are poorly defined. Defective trophoblast invasion and inadequate maternal spiral artery remodeling are common to both preeclampsia and IUGR. Shallow trophoblast invasion clearly contributes to many cases and 25% of the IUGR newborns

are associated with preeclampsia. Changes in placental transport properties can affect nutrient supply to the fetus (Cetin *et al.* 2004).

Confined placenta trisomy has also been reported as increased in placentas associated with IUGR newborns (Amiel *et al*. 2002; Grati *et al*. 2005; Krishnamoorthy *et al*. 1995). An association between loss of normal imprinted gene expression and IUGR is supported by the observation that mosaicism for androgenetic cells in the placenta can also lead to IUGR (Robinson et al. 2007), as can uniparental disomy involving chromosomes 6, 7, 14, 16 and 20 (Kotzot 1999; Robinson 2000). While uniparental disomy may be a rare explanation for IUGR, clearly over- or under-expression of the involved imprinted genes on these same chromosomes would be expected to lead to growth effects as well. This is demonstrated by many mouse knockouts of imprinted genes that show growth restriction as a result of placental defects (Shi *et al*. 2004; Tycko and Morison 2002). This idea is also supported by a recent finding that the gene expression and DNA methylation were altered in the human chromosome 11 imprinted region of the small for gestation age placentas (Guo *et al.* 2008). Since the alteration in that particular region can only be found in isolated cases, it is likely that alteration of DNA methylation can be found in other chromosomal regions of IUGR placenta as well.

1.9. Research objectives

The objective of this thesis is to provide fundamental DNA methylation profiles of human fetal and placental development so as to offer insights into the etiology of human disease and adverse pregnancy outcomes. I hypothesize that epigenetic variation in the fetus and placenta may contribute to human disease and placental insufficiency leading to preeclampsia and IUGR.

To study the role of epigenetic programming and errors in fetal and placental development, I apply the knowledge of epigenetics in human development to the clinical population using the latest genomic and molecular biology tools. Specific aims are to

1) Map the imprinted DMRs in the human placenta.

   It is well known that imprinted genes are important for human fetal and placental development, but a complete map of imprinted genes in the human genome is still lacking. By applying a novel approach, the genomic locations of known and many novel imprinted DMRs are determined in Chapter 2.

2) Characterize intra-individual DNA methylation differences in human fetal tissues.

   Tissue-specific and age-dependent DNA methylation represent the major DNA methylation differences within an individual. Chapter 3 is a study to characterize the poorly defined DNA methylation profiles of human fetal somatic tissues.

3) Assess the inter-individual DNA methylation variation in the human placenta.

   Inter-individual DNA methylation variation may contribute to the development of human disorders. Using the human placenta as a model, the extent of inter-individual DNA methylation variation is evaluated in Chapter 4.

4) Identify genes responsible for the development of preeclampsia and/or IUGR in the human placenta.

In Chapter 5, DNA methylation profiles of normal placentas and placentas with preeclampsia and/or IUGR are compared in order to examine the role of epigenetic dysregulation in placental insufficiency.

In Chapter 6, I will summarize the findings and make a conclusion of this thesis. The goal is to use this data to develop methods to improve diagnosis, counseling and treatment for affected pregnancies, thus leading to improved health of both pregnant mothers and their babies.

Chapter 2: Genome-wide mapping of imprinted genes by DNA methylation profiling of human placentas from triploidies[2]

2.1. Introduction

Genomic imprinting is a phenomenon in which one of the two alleles of a gene is expressed in a parent-of-origin manner (Reik and Walter 2001). The allele-specific expression of imprinted genes is regulated by epigenetic modifications at regions called imprinting control regions (ICRs) (Delaval and Feil 2004). DNA methylation is one of the epigenetic modifications for repressing allelic expression and involves the addition of a methyl group on the cytosine residues of CpG dinucleotides typically within CpG islands of the promoter regions of the gene. To date, around 60 imprinted genes have been identified in human beings (http://www.geneimprint.com). Although the imprints are not necessarily inherited directly from the germline, many imprinted genes possess differentially methylated regions (DMRs) where allelic methylation depends on the parent-of-origin (Reik and Walter 2001). DMRs established through the germline are called gametic DMRs or primary DMRs, which often coincide with ICRs (Henckel and Arnaud 2010; Mann 2001). Their methylation status is thought to be maintained in all somatic lineages once acquired. Other DMRs called somatic or secondary DMRs, are established after fertilization and may be tissue-specific (Henckel and Arnaud 2010; Mann 2001).

The importance of imprinted genes for placental and fetal development was initially demonstrated in mouse by observations that parthenogenetic embryos (maternal origin; digynic

[2] A version of Chapter 2 has been submitted for publication. Yuen RKC, Jiang R, Peñaherrera MS, McFadden DE, Robinson WP. (2011) Genome-wide mapping of imprinted genes by DNA methylation profiling of human placentas from triploidies.

diploid) could show embryonic differentiation but failed to form extraembryonic components (Surani *et al*. 1984). In contrast, androgenetic embryos (paternal origin; diandric diploid) had poorly developed embryos but the trophoblasts showed extensive proliferation (McGrath and Solter 1984). The parallel observations in human are ovarian teratomas (parthenogenetic) which is a rare form of tumor that consists of a variety of embryonic tissues or organs with absence of placental tissues; and complete hydatidiform moles (CHMs) (androgenetic), which exhibit trophoblast hyperplasia but no, or rarely any, embryonic structures. The majority of imprinted genes since identified in mouse and human, play a role in placental and/or fetal growth. The parental conflict theory developed to explain the evolution of imprinted genes (Moore and Haig 1991), suggests that paternally expressed genes (PEGs) tend to promote growth of the offspring at the expense of the mother, while maternally expressed genes (MEGs) act as growth limiting factors in order to conserve maternal resources (Moore and Haig 1991).

Since most imprinted genes contain DMRs, comparing DNA methylation profiles between tissues with unbalanced parental constitutions provides an approach to identify novel imprinted genes in the genome. The most intuitive approach is to compare paternally derived CHMs to maternally derived ovarian teratomas (Cooper and Constancia 2010). Indeed, several novel imprinted genes have been identified previously using this strategy (Strichman-Almashanu *et al*. 2002). Such comparisons are limited by the fact that the tissues present in ovarian teratomas and CHMs are highly abnormal and are not necessarily comparable. CHMs present with highly proliferative trophoblasts that can lead to increased risk of choriocarcinoma, and hypermethylation of non-imprinted genes has been reported in CHMs (Xue *et al*. 2004). Ovarian teratoma is a rare form of tumor that consists of a variety of embryonic tissues or organs with the

absence of placental tissues; thus, comparing it with CHM may result in identification of many DNA methylation differences reflecting tissue-specific methylated genes.

We propose that a comparison between diandric and digynic triploidies, for which development is less severely altered, provides an alternative approach for the identification of novel imprinted genes in the human genome. Triploidy occurs in 2-3% of pregnancies and, while frequently ending in miscarriage, can survive into the fetal period and, very rarely, to term. Consistent with the parental conflict hypothesis, the diandric (extra paternal haploid genome) triploid phenotype is characterized by normal size or only moderately growth restricted fetus with a large and cystic placenta with trophoblast hyperplasia, while the digynic (extra maternal haploid genome) triploid phenotype is characterized by intrauterine growth restricted fetus and a very small placenta with no trophoblast hyperplasia (McFadden and Kalousek 1991).

We recently demonstrated that the DNA methylation status of many known imprinted DMRs is maintained in the triploid placentas (Bourque *et al*. 2011), justifying the further application of triploidy to identify imprinted DMRs. Therefore, in the present study, we compared the DNA methylation profiles of placentas from diandric and digynic triploidies using a well validated methylation microarray, Illumina Infinium HumanMethylation27 panel, which targets over 27,000 CpG loci within the proximal promoter regions of approximately 14,000 genes (Bock *et al*. 2010). Methylation levels in chromosomally normal placentas, CHMs and maternal blood samples were used as a reference for comparison. Using this strategy, we identified the majority of known imprinted ICRs and many novel imprinted DMRs in the genome. We validated these results for a subset of genes by demonstrating parent-of-origin biases in allelic expression in the term placenta by genotyping maternal-fetal pairs. We also demonstrated that complex DNA methylation domains that regulate imprinted genes can be

mapped by comparing the methylation patterns in different tissues and different gestational ages of placentas.

2.2. Methods

2.2.1. Sample collection

This study was approved by the ethics committees of the University of British Columbia and the Children's & Women's Health Centre of British Columbia. Early gestation placental samples (10 diandric triploids, 10 digynic triploids, 6 CHMs and 10 normal controls) were obtained from spontaneous abortions examined in the Children's & Women's Hospital Pathology laboratory. Mid-gestation placental samples (n=10) and fetal tissues (11 muscle samples, 12 kidney samples and 8 brain samples) were obtained from anonymous, chromosomally normal 2^{nd} trimester elective terminations for medical reasons. Term placental samples and the corresponding maternal blood samples were collected from BC Children's & Women's Hospital with informed consent from individuals. For all the placental samples, fragments of ~$1cm^3$ were dissected from the fetal side of each placenta and whole villi were used for investigation. All tissues were karyotyped for chromosomal abnormalities and genomic DNA was extracted from each tissue sample using standard techniques. Total RNA was extracted from term placentas using RNeasy kit (Qiagen) according to manufacturer's instructions.

2.2.2. Illumina DNA methylation array

Genomic DNA was bisulfite converted using the EZ DNA Methylation Kit (Zymo Research) according to the manufacturer's instructions. Bisulfite treatment converted unmethylated cytosines to uracils, while leaving methylated cytosines unchanged. After DNA purification, bisulfite converted DNA samples were randomly arrayed and subjected to the

Illumina Infinium HumanMethylation27 panel array-based assay (Illumina). The array assays methylation levels at 27,578 CpG sites in the genome. The methylation level for each CpG site was measured by the intensity of fluorescent signals corresponding to the methylated allele (Cy5) and the unmethylated allele (Cy3). Cy5 and Cy3 fluorescent intensities were corrected independently for background signal and normalized using GenomeStudio software (Illumina). Continuous beta values that range from 0 (unmethylated) to 1 (methylated) were used to signify the percentage of methylation, from 0% to 100%, for each CpG site. The beta value was calculated based on the ratio of methylated/(methylated + unmethylated) signal outputs. Detection p value of each probe was generated by comparison with a series of negative controls embedded in the assay. Probes with detection p values >0.05 in any of the sample were eliminated from the study. The correlation coefficient for technical replicates was over 0.98.

2.2.3. DNA methylation analyses for targeted loci

Methylation-unbiased PCR and sequencing primers were designed based on the probe sequences provided by Illumina (Supplementary Table 2.1). All primers were designed in regions free of known SNPs. Pyrosequencing was performed on a PyroMark MD System (Biotage). The quantitative levels of methylation for each CpG dinucleotide were evaluated using the Pyro Q-CpG software (Biotage). For bisulfite cloning and sequencing, PCR product from individual samples was generated by non-biotinated primers (Supplementary Table 2.1) and subsequently TA-cloned into pGEM-Teasy vector (Promega). Individual clones were picked and PCR amplified with SP6 and T7 promoter primers. PCR products were sequenced by Sanger sequencing. The sequencing data were analyzed using BiQ Analyser software (Rohde *et al*. 2010) and sequences with less than 80% bisulfite conversion rate were eliminated from analysis.

2.2.4. SNP genotyping

Multiplex genotyping of genomic DNA and cDNA was performed by the iPLEX Gold assay on the MassARRAY Platform (Sequenom) at the Genome Quebec Centre, Montreal Canada. Primers for Sequenom SNP genotyping were designed by primer design software from Sequenom (Supplementary Table 2.2). The primer extended products were analyzed and the genotypes were determined by mass spectrometric detection using the MassARRAY Compact system (Sequenom). Technical replicates showed r=0.92 correlation. Samples or SNPs with less than 70% conversion rates (calls) were eliminated. Genotyping by pyrosequencing was performed on a PyroMark MD System and the relative levels of alleles for the SNP were evaluated with PSQ96MA SNP analysis software (Biotage). Genotyping of exonic SNPs were carried out either with cDNA prepared using Omniscript Reverse Transcriptase Kit (Qiagen) followed by iPLEXing or pyrosequencing, or one-step RT-PCR (Qiagen) followed by pyrosequencing. Primers for pyrosequencing genotyping were designed by primer design software from Biotage (Supplementary Table 2.2). PCR without reverse transcriptase was performed on each sample to confirm no genomic DNA contamination.

2.2.5. Statistical analysis

Unsupervised hierarchical clustering of samples was done using the Illumina GenomeStudio software. Differentially methylated probes in the Illumina array from each comparison were identified using Siggenes package from R with a cut-off of false discovery rate (FDR)<0.1%. FDRs were generated after comparison of 1000 random permutations between samples. Pearson linear correlation was used to determine the similarity of DNA methylation profiles between samples. The Database for Annotation, Visualization and Integrated Discovery

(DAVID) program was used for gene ontology analysis using total number of genes presented in the array as a background for comparison (Dennis *et al*. 2003; Huang da *et al*. 2009).

2.3. Results

2.3.1. DNA methylation profile analysis in placenta and blood samples

To generate DNA methylation profiles from triploidies, we assayed placental DNA from 10 diandric and 10 digynic triploidies on the Illumina Infinium HumanMethylation27 panel. In addition, 10 chromosomally normal placentas, 6 CHMs and 10 maternal whole blood samples were included for comparison. After background adjustment and normalization, we performed unsupervised hierarchical clustering with all the samples based on a distance measure of 1-r, where r is the Pearson correlation coefficient between different samples. This revealed three distinct groups of clusters: (1) CHM, (2) triploid and normal placentas and (3) blood (Figure 2.1). The blood cluster is more distant from the two other clusters of placentas, confirming that there are many DNA methylation differences between blood and placenta (Cotton *et al.* 2009; Papageorgiou *et al.* 2009). Although CHMs are trophoblast derived, they show a distinct methylation profile from the triploid and normal placentas. Within triploid and normal placentas, digynic and diandric triploid placentas are clearly separated by their methylation profiles, but interestingly, they are not separated from the chromosomally normal placentas (Figure 2.1). This suggests that methylation profiles of triploid placentas closely resemble those of chromosomally normal placentas, but digynic and diandric triploid placentas have distinguishing DNA methylation differences.

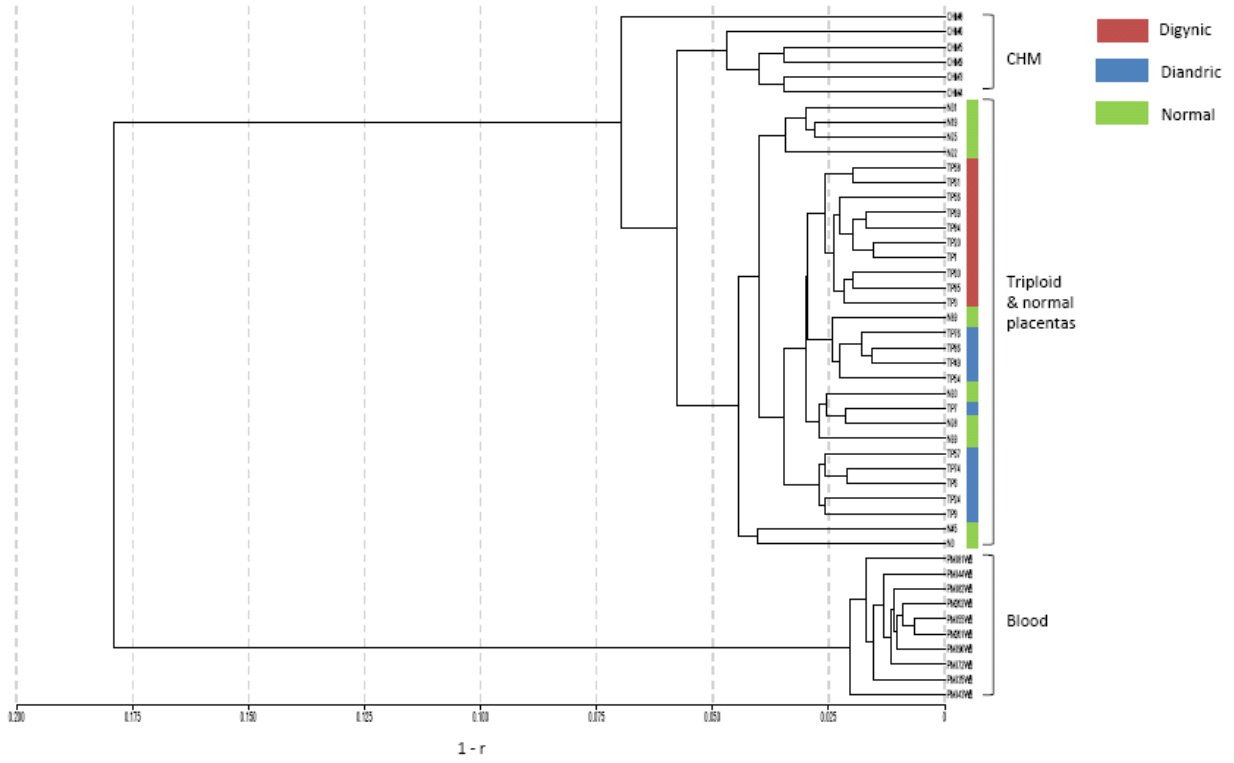

Figure 2.1. Unsupervised clustering of triploid and normal placentas with CHMs and blood samples demonstrates that each tissue type has a distinct methylation profile.

Sample names are shown with labeling of corresponding tissue types. Samples were clustered by hierarchical clustering of beta values based on 1-r (Illumina GenomeStudio software), where r represents the correlation coefficient between samples. Digynic triploids are indicated with red boxes, diandric triploids with blue boxes and normal placentas with green boxes.

Although clustering can be biased by gender differences resulting from inactivation of an X chromosome in females (i.e. higher methylation of the X chromosome CpG islands in female than in male samples) (Cotton *et al.* 2009; Yuen *et al.* 2010), there is no preferential clustering of samples by gender within the triploid and normal placenta cluster (Figure 2.2A). There is a small difference in gestational age (~3 weeks apart on average) between diandric and digynic placentas

($p<0.01$) (Supplementary Table 2.3), but this also does not explain the distinct clustering patterns since their gestational ages overlap with each others for many cases (Supplementary Table 2.3).

We further compared the average DNA methylation of probes between the 5 sample groups (digynic triploid placentas, diandric triploid placentas, normal placentas, CHMs, and blood) (Figure 2.1B). As expected, the correlation of average probe methylation values between different sample groups is consistent with that observed in the cluster analysis. In general, blood has the most distinct DNA methylation profile from all types of placenta with a greater number of highly methylated probes (Figure 2.2B). Triploid and normal placentas are highly correlated for their methylation profiles ($r=0.99$), while CHMs are more similar to diandric and normal placentas ($r=0.98$) than digynic placentas ($r=0.96$).

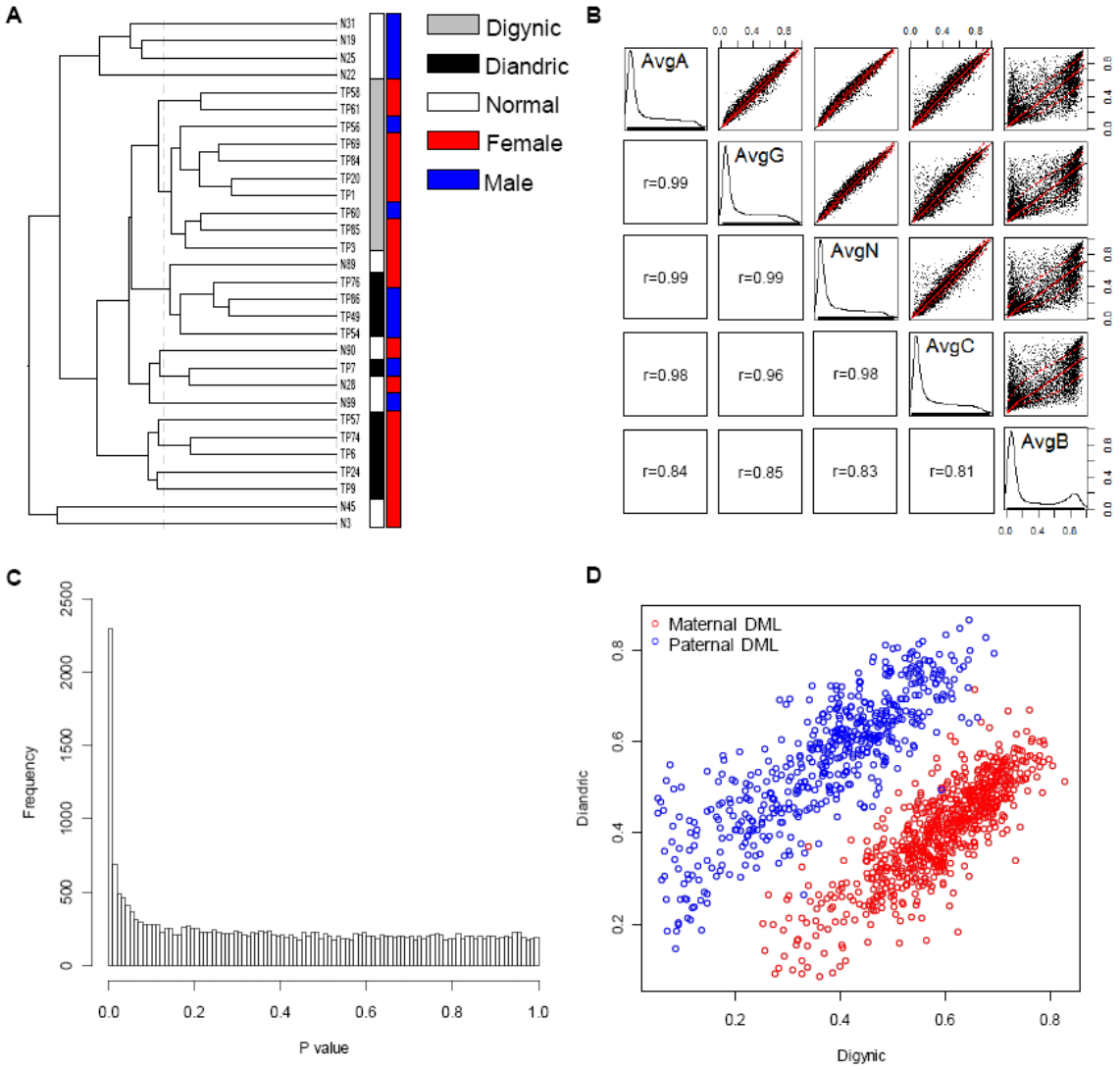
A
Digynic
Diandric
Normal
Female
Male
B
AvgA
AvgG
AvgN
AvgC
AvgB
r=0.99
r=0.99
r=0.98
r=0.96
r=0.98
r=0.84
r=0.85
r=0.83
r=0.81
C
Frequency
P value
D
Maternal DML
Paternal DML
Diandric
Digynic
E
P: r=0.90, p<0.0001 M: r=0.4, p=0.0006
P: r=0.85, p<0.0001 M: r=0.35, p=0.003
P: r=0.81, p<0.0001 M: r=0.23, p=0.03
CHM
P: r=0.94, p<0.0001 M: r=0.94, p<0.0001
P: r=0.94, p<0.0001 M: r=0.96, p<0.0001
Normal
P: r=0.96, p<0.0001 M: r=0.97, p<0.0001
Digynic
Diandric
Avg. Maternal DML
Avg. Paternal DML

Figure 2.2. Analyses of DNA methylation data from the Illumina microarray assay.

(A) Unsupervised hierarchical clustering of placental samples. No preferential clustering by gender is observed. Sample names are shown with labeling of corresponding tissue types. Samples were clustered by hierarchical clustering of beta values based on 1-r (Illumina GenomeStudio software), where r is referring to the correlation coefficient between samples. Digynic triploids are indicated with grey boxes, diandric triploids are indicated with black boxes and normal placentas are indicated with white boxes. Female placentas are labelled in red while male placentas are labelled in blue. (B) Pair-wise comparisons of average methylation of probes between different placental groups. Scatterplots of average methylation of probes between placental pairs are shown on the upper right panel while their correlation coefficients are shown on the lower left panel. Density plots of the methylation distribution of probes in each placental group are shown between two panels. AvgA: average methylation in diandric triploids, AvgG: average methylation in digynic triploids, AvgN: average methylation in chromosomally normal placentas, AvgC: average methylation in CHMs and AvgB: average methylation in blood samples. (C) Distribution of p values calculated by the Student's t test. More than 2000 probes have p values lower than 0.01. (D) Scatterplot of methylation values for identified DML in all digynic vs. diandric triploid samples. The DNA methylation level for comparisons of all samples is given with the maternal DML represented by red circles and paternal DML represented by blue circles. Maternal DML and paternal DML form two independent clusters without much overlap. DML: differentially methylated loci. (E) Scatterplot of average methylation for each maternal DML and paternal DML for each pairwise comparison of placental groups. Scatterplots for each comparison is shown on the lower right panel while the corresponding correlation coefficients are shown on the upper left panel. Average methylation of maternal DML is highlighted in pink while average methylation of paternal DML is highlighted in light blue.

2.3.2. Comparison of DNA methylation profiles between placentas from diandric and digynic triploidies

After comparing methylation at all probes between diandric and digynic placentas by the Student's t-test, nearly 2500 probes were identified with a p value less than 0.01, which is nearly 10 times higher than expected by chance (Figure 2.2C). To adjust for multiple testing, we used a stringent cut-off of <0.1% false discovery rate (FDR) generated by Significant Analysis of Microarray (SAM) with 1000 permutation comparisons for each sample (Tusher *et al*. 2001). To further focus on meaningful differences we also only considered probes with more than 15% absolute magnitude difference between the mean methylation of diandric and digynic triploidies.

While we expect a theoretical difference of 33.3% for imprinted sites, we used a lower cut-off because we have observed that the actual methylation difference may vary for some known imprinted genes (Bourque *et al*. 2011). In total, 122 probes were identified with FDR<0.1% and average absolute methylation difference>15% (average absolute delta beta>0.15 from the Illumina array). Probes with higher average methylation in diandric than digynic triploidies were assigned as putative paternal differentially methylated loci (DML) and probes with higher average methylation in digynic than diandric triploidies were assigned as putative maternal DML. Plotting DNA methylation of putative DML in all samples from diandric against digynic triploidies shows a clear separation of methylation values of paternal and maternal DML (Figure 2.2D), suggesting that most of the identified differentially methylated probes are consistently methylated within each sample group without much overlap, as expected from our application of stringent statistical criteria.

As some methylation differences between diandric and digynic triploids could theoretically arise due to secondary effects, such as altered cell composition, the validity of the identified putative imprinted DML was further evaluated by comparing the methylation levels of diandric and digynic triploid placentas with CHMs and chromosomally normal placentas (Figure 2.3). The average methylation in CHMs was closer in value to diandric triploidies (Figure 2.3A and C), while that for normal placentas fell between that for diandric and digynic triploidies for the majority of putative DML (Figure 2.3B and D). In particular, putative maternal DML had higher correlation with normal placentas than paternal DML (Figure 2.3A and C), while putative paternal DML tended to have higher correlation with CHMs than maternal DML (Figure 2.3B and D). This observation is confirmed by pair-wise comparisons of average methylation of paternal and maternal DML in different placental groups (diandric, digynic, normal and CHM)

(Figure 2.2E). CHMs show particularly low correlation for maternal DML when compared with other placental groups, largely due to the low average methylation of putative maternal DML in CHMs, as well as more variability in values for CHMs (Figure 2.3D).

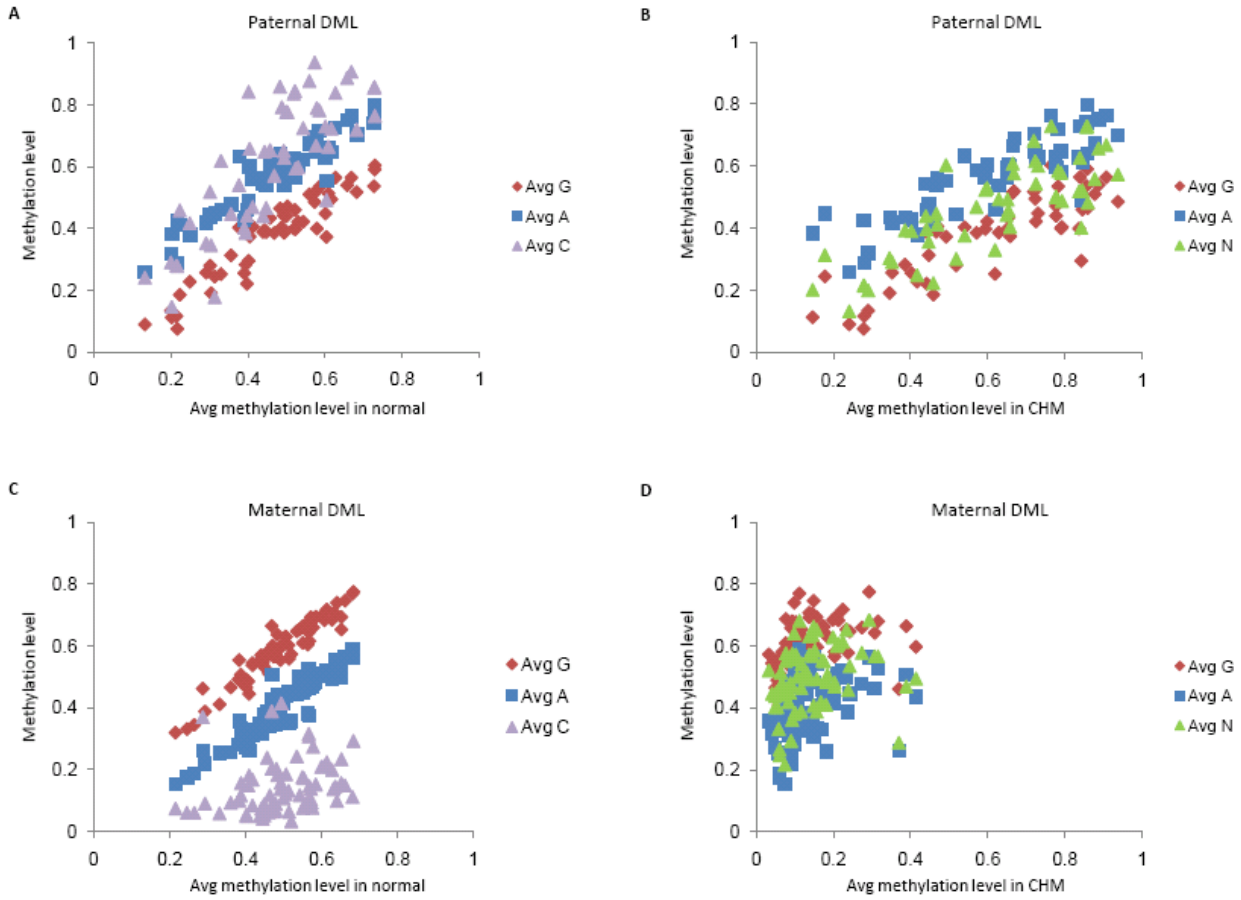

Figure 2.3. Scatterplots of average methylation of paternal (A and B) and maternal (C and D) differentially methylated loci (DML).

(A and C) average methylation values in normal placentas (X-axis) plotted against digynic triploids (Avg G), diandric triploids (Avg A) and CHMs (Avg C) show high correlation. (B and D) Average methylation values in CHMs (X-axis) plotted against digynic triploids (Avg G), diandric triploids (Avg A) and normal placentas (Avg N).

Fourteen probes failed to follow the expected pattern in the comparisons between different placental groups (average methylation in normal placentas with a level in between that in diandric and digynic placentas and average methylation in CMHs with a level closer to that in diandric placenta) and were eliminated as candidates for further analysis. This yielded a final list of 108 identified putative DML that are associated with 63 different DMRs from 62 genes (one gene has both paternal and maternal DML) (Supplementary Table 2.4). Of the 63 DMRs, 37 are maternally and 26 are paternally methylated (Figure 2.4). These imprinted DMRs are distributed across the whole genome with chromosome 7 containing the highest number (9 DMRs), while chromosome 13, 21 and Y are the only chromosomes for which no DMRs were identified (Figure 2.4).

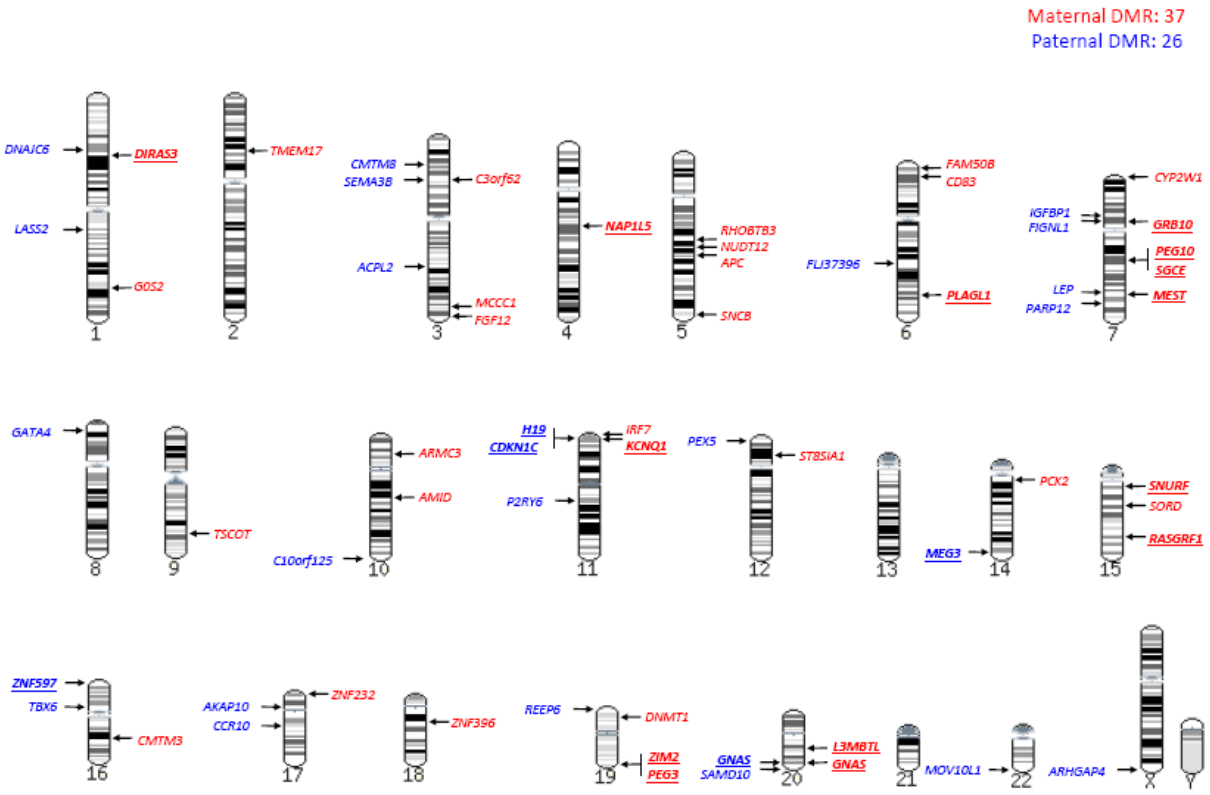

Figure 2.4. Location of the 63 identified differentially methylated regions (DMRs) in the genome.

Relative location of the identified 37 maternal DMRs and 26 paternal DMRs are shown in the human genome according to the genomic sequence released on 2006 in UCSC Genome Browser (hg18). Paternal DMRs are highlighted in blue while maternal DMRs are highlighted in red. Known imprinted genes are bolded and underlined. Chromosome 7 contains the highest number of DMRs (9 DMRs), while there are no DMRs identified on chromosome 13, 21 and Y.

As copy number variation (CNV) can be a potential bias for methylation (Robinson *et al*. 2010), we referred to UCSC Genome Brower (hg18) (http://www.genome.ucsc.edu) and found that the locations of 37 of the 108 probes overlap with known CNVs (Supplementary Table 2.4). However, any effect of the CNVs on methylation of the candidate sites identified by our criteria was minimal since the methylation of maternal and paternal DML were clearly separated from

each other without much overlap (Figure 2.2D). Similarly, differences between the two groups are unlikely to be caused by differences in genetic sequence polymorphisms that influence methylation, as this would require all 10 diandric placentas to by chance be of a differing genotype than all 10 dygynic placentas.

2.3.3. Validation of DNA methylation patterns of identified putative imprinted DMRs

Among the 62 genes identified with parent-of-origin dependent DMRs, 18 are known imprinted genes associated with 15 distinct DMRs based on the literature (Cooper and Constancia 2010) and public databases (http://igc.otago.ac.nz and http://www.geneimprint.com) (Table 1). However, two of these DMRs, associated with the imprinted genes *CDKN1C* and *RASGRF1*, have only been reported in mouse but not human (Cooper and Constancia 2010; Morison *et al*. 2005). Eleven out of the known 15 imprinted DMRs are known to be ICRs, with parental origin of methylation concordant with what we observed based on the comparison of triploidies (Table 2.1).

Table 2.1. Eighteen identified DMRs with known imprinted DMRs

			Methylated allele		
Location	**Gene**	**Expressed allele**	**ICR**	**Known DMR**	**Identified DMR**
1p31	*DIRAS3*	P	-	M	M
4q22.1	*NAP1L5*	P	M	M	M
6q24	*PLAGL1*	P	M	M	M
7p12	*GRB10*	M/P[b]	M	M	M
7q21.3	*PEG10*/*SGCE*	P	M	M	M
7q32.2	*MEST*	P	M	M	M
11p15	*CDKN1C*	M	-	P[c]	P
11p15	*H19*	M	P	P	P
11p15	*KCNQ1*[a]	M	M	M	M
14q32	*MEG3*	M	P	P	P
15q11-q12	*SNURF*	P	M	M	M
15q24	*RASGRF1*	P	-	P[c]	M
16p13	*ZNF597*	M	-	-	P
19q13.43	*PEG3*/*ZIM2*	P	M	M	M
20q13	*GNAS*	M/P[b]	M	M/P	M/P
20q13	*L3MBTL*	P	-	M	M

[a]Region known as KvDMR1

[b]Tissue-specific parental origins of allelic expression

[c]Parental origins based on mouse studies

We performed bisulfite pyrosequencing for a subset of the novel imprinted DMRs to confirm their DNA methylation patterns in the different placental groups. For this purpose, 10 DMRs were selected based on their low FDR (*FAM50B*, *MCCC1*, *DNAJC6*, *SORD* and *RHOBTB3*) or biological significance to the placenta (*APC*, *DNMT1*, *IGFBP1*, *LEP* and *RASGRF1*). A high correlation between the values obtained from microarray and pyrosequencing was observed ($r=0.85$ to 0.98, $p<0.0001$) (Supplementary Figure 2.1A-J). Specifically, the DNA methylation patterns observed by pyrosequencing were concordant with those found by microarray for both (1) CpGs analyzed by the microarray and their the proximal CpGs within the

pyrosequencing assays (Supplementary Figure 2.2A-J) and (2) the average methylation levels of all CpG sites covered by pyrosequencing (Supplementary Figure 2.3A-J). DNA methylation levels of the selected loci were also assessed in sperm DNA and all were unmethylated (data not shown), suggesting they may be either secondary DMRs or maternal imprinted DMRs.

We chose to further evaluate DNA methylation for two genes *FAM50B* and *MCCC1* which contain SNPs with high average heterozygosity (~0.4) in the proximal promoter regions that can be used to distinguish alleles (Figure 2.5A and F). Bisulfite cloning and sequencing confirmed monoallelic methylation patterns for both DMRs (Figure 2.5C and H) and maternal origin of allelic methylation that was concordant with that predicted by the triploidy comparison (Figure 2.5B and G). Furthermore, allelic expression analysis showed preferential expression of the unmethylated paternal allele at the proximal promoter regions (Figure 2.5E and I), consistent with an inverse correlation relationship between methylation and expression. As allelic methylation can occur in a SNP-dependent manner (Kerkel *et al*. 2008), we developed a methylation-specific pyrosequencing assay for *FAM50B* to evaluate allelic methylation in additional samples. The results of this assay were concordant with cloning and sequencing results for the same placental sample (Figure 2.5C and D). As methylation was found in association with either allele (A or G at rs2239713) among 12 heterozygous normal term placental samples and 10 heterozygous maternal blood samples, (Supplementary Table 2.5), the allelic methylation is not linked with the SNP genotypes.

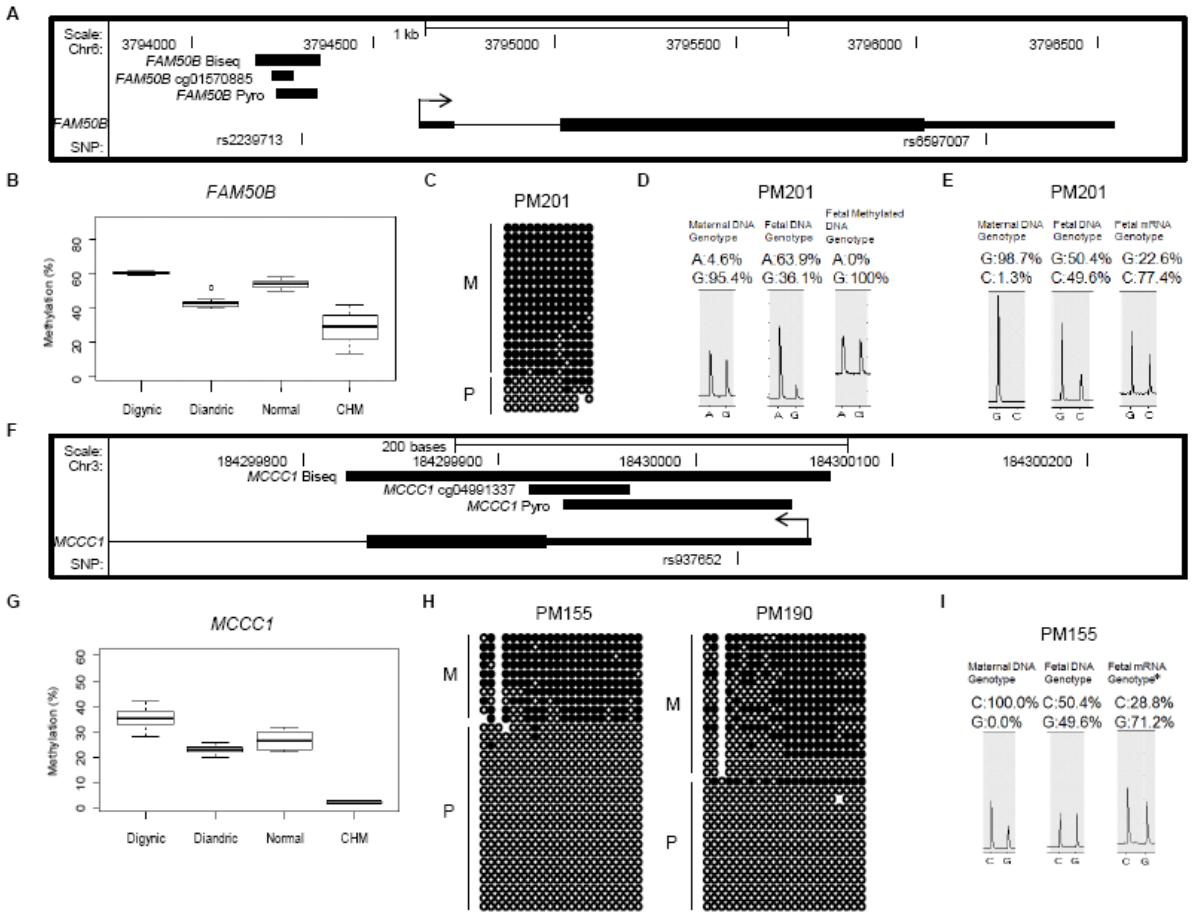

Figure 2.5. Identification of imprinted differentially methylated regions (DMRs) at the proximal promoter regions of FAM50B and MCCC1.

(A and F) Schematic diagrams show the positions of methylation assays (Biseq: bisulfite cloning and sequencing assay, cg code: probe number of Illumina assay, Pyro: bisulfite pyrosequencing assay) and SNPs locations relative to the genes. Directions of arrows represent the transcriptional directions for the genes. Genomic coordinates are retrieved from UCSC Genome Brower (hg18). (B and G) Box plots show the methylation level of samples in each placental group for the DMRs analyzed by bisulfite pyrosequencing. Both DMRs in *FAM50B* and *MCCC1* have higher methylation in digynic than diandric triploid placentas, while they have intermediate methylation in normal placentas and particularly low methylation in CHMs. (C and H) Bisulfite cloning and sequencing shows parental origins of methylated and unmethylated alleles (M: maternal alleles, P: paternal alleles). Parental origin was determined by genotyping heterozygous informative SNPs for each sample. The DMRs in both *FAM50B* and *MCCC1* are maternally methylated. Each black circle represents a methylated CpG dinucleotide and each white circle represents an unmethylated CpG dinucleotide. (D) Quantitative genotyping of methylated alleles by pyrosequencing. SNP rs2239713 is homozygous (GG) in maternal DNA and heterozygous (AG) in fetal (placental) DNA (dispensation order: AAG). Genotyping the placental sample using a methylation-specific pyrosequencing primer shows a homozygous (GG) pattern indicating that the DMR associated with the maternally inherited 'G' allele is methylated while the one

associated with the paternal 'A' allele is not. (E and I) Quantitative genotyping of expressed alleles by pyrosequencing. Both SNPs (E) rs6597007 (dispensation order: GGC) and (I) rs937652 (dispensation order for DNA genotyping: CG, dispensation order for RNA genotyping: CCG) are homozygous in maternal DNA and heterozygous in fetal DNA. Genotyping of cDNA shows a bias towards preferential expression of the paternal alleles. *The pyrosequencing primers used for cDNA genotyping (intron-spanning) in *MCCC1* were different from those used for DNA genotyping (Supplementary Table 2.1), so the peak ratio shown in genotyping the pyrogram of cDNA does not correspond to that for DNA.

Since diandric triploid placentas tend to be associated with trophoblast hyperplasia (McFadden and Kalousek 1991), it is possible that the identified imprinted DMRs were merely a consequence of a different extent of differential methylation between trophoblast and mesenchyme (Avila *et al*. 2010). To address this, we used a non-imprinted trophoblast-specific unmethylated region, *EDNRB* (Supplementary Figure 2.4A), to compare the methylation level between diandric and digynic triploid placentas. We did not find a difference in methylation level between them (Supplementary Figure 2.4B). Likewise, we did not find any difference in allelic methylation between trophoblast and mesenchyme for the novel identified imprinted gene *MCCC1* (Supplementary Figure 2.4C and D).

2.3.4. Confirmation of parent-of-origin allelic expression for the identified putative imprinted genes

Next, we performed a high-throughput genotyping assay to investigate the parental origin of allelic expression for the novel putative imprinted genes using iPLEX Gold assay on the MassARRAY Platform. We selected 38 out of 45 putative novel imprinted genes (the 45 putative imprinted genes including *RASGRF1* for which imprinting expression has not been reported in human) based on the availability of an exonic SNP with high average heterozygosity (>0.1) and the presence of expression in the placenta according to the GNF atlas database

(http://biogps.gnf.org). In addition, two exonic SNPs from *IGF2* were included as positive controls. Thus, a total of 40 SNPs were genotyped in 27 maternal-fetal pairs, including DNA from maternal blood and the corresponding fetal normal term placenta, as well as cDNA from the same placenta.

Of these 40 SNPs, seven did not pass the quality control (less than 70% calls or presence of severe allelic bias) and three had no informative (heterozygous) genotypes in fetal DNA, leaving 30 SNPs for analysis (Supplementary Table 2.6). The two SNPs from *IGF2* showed the expected paternal allelic expression in all informative cases (Supplementary Table 2.6). Of the 28 novel putative imprinted genes, 11 showed monoallelic expression in at least a portion of informative samples (Table 2.2). Among these 11 genes, 8 had cases informative in maternal blood for parental origin assessment. Since most CpGs in the microarray are located at the proximal promoter regions of the genes, we assume that the DNA methylation correlates with silencing for all these genes. Six genes (*FAM50B*, *DNMT1*, *RHOBTB3*, *ARMC3*, *AIFM2* and *LEP*) showed parent-of-origin dependent expression that matched that predicted by the parental origin of the DMRs, while two others (*MOV10L1* and *ST8SIA1*) showed parental expression opposite to that predicted in some informative cases (Table 2.2).

Table 2.2. Eleven genes associated with candidate imprinted genes with confirmed monoallelic expression

Gene	DMR	SNP	Monoallelic cases Obs./Total (%)	Monoallelic expression observed for reciprocal SNP[1]	Matched expected parental origin Obs./Total (%)[2]
FAM50B	M	rs6597007	9/9 (100)	Y	5/5 (100)
DNMT1	M	rs16999593	1/1 (100)	-	1/1 (100)
MOV10L1	P	rs9617066	8/9 (89)	N	1/3 (33)
RHOBTB3	M	rs34896	3/4 (75)	Y	2/2 (100)
SNCB	M	rs2075667	3/4 (75)	N	NI
ARMC3	M	rs12259839	2/3 (67)	N	2/2 (100)
ST8SIA1	M	rs4762737	2/3 (67)	Y	0/1 (0)
ARHGAP4	P	rs2070097	1/2 (50)	-	NI
AIFM2	M	rs7908957	2/8 (25)	N	1/1 (100)
MCCC1	M	rs937652	2/8 (25)	Y	NI
LEP	P	rs2167270	1/15 (7)	-	1/1 (100)

NI: Not informative

[1]Were both alleles of the SNP observed to be expressed among those cases with monoallelic expression. This is impossible if only one case showed monoallelic expression.

[2]Number of cases matching the expected parental origin of those cases informative to determine parent of origin

A number of genes did not show monoallelic expression using the Sequenom approach. For example, for *LEP* only 1 of 15 samples was scored as monoallelic by this approach. To evaluate the sensitivity of the Sequenom genotyping assay we developed a RNA-specific genotyping pyrosequencing assay for *LEP*. Although the two methods were correlated ($r=0.64$, $p<0.02$), we found that pyrosequencing was more sensitive in picking up preferential allelic expression, with 5 of 12 informative cases exhibiting a <0.3 allelic ratio by pyrosequencing (Supplementary Table 2.7). Furthermore, in case PM155 for *MCCC1* we found preferential paternal allelic expression by pyrosequencing (Figure 2.5I), but not by Sequenom (Table 2.2). Thus, the Sequenom assay may not be sufficiently sensitive to detect more subtle allelic expression bias, i.e. when there is a mix of cells with biallelic and monoallelic expression.

2.3.5. Tissue-specific and gestational age-specific methylation of imprinted DMRs

Some genes with imprinted DMRs may not show allele-specific expression biases due to the presence of tissue-specific or gestational age-specific imprinting that is further regulated by DNA methylation at other nearby sites. To study tissue-specific effects and the effect of gestational age on methylation of the putative imprinted DMRs, we further compared methylation at these sites among 3 types of fetal somatic tissues (8 brain samples, 12 kidney samples and 11 muscle samples) and 2 sets of placentas with different gestational ages (10 mid-gestation and 10 term placentas) that had been run in the same Infinium methylation array.

For tissue-specific methylation analysis, we compared the DNA methylation level of the 108 DML (probes) associated with 63 imprinted DMRs in 5 tissues (brain, kidney, muscle, mid-gestation placenta and blood). Multiclass comparison from SAM was performed with 1000 permutations. Using a cut-off of FDR<0.1%, 53 probes of 46 imprinted DMRs show differential DNA methylation between tissues (Table 2.3 and Supplementary Table 2.8). Placenta-specific methylation was observed for 31 of these probes (26 imprinted DMRs), with the average methylation more than 15% higher in placenta than any other tissues (Table 2.3 and Supplementary Table 2.8). A change in methylation of placenta by gestational age was found for 12 probes from 10 DMRs using the same statistical criterion (FDR<0.1%) (Table 2.3 and Supplementary Table 2.9). Thus, imprinted DMRs can show both tissue-specific and gestational age-specific DNA methylation. Nonetheless, 14 of the imprinted DMRs have constant methylation between different tissues and gestational ages (Table 2.3), 11 of which are in ICRs from known imprinted genes. Three novel imprinted DMRs also remained constant across samples, associated with *FAM50B*, *FGF12* and *IRF7*, and are thus potential new ICRs.

Table 2.3. DNA methylation of identified DMRs in different tissues and gestational ages

Index	Gene	Chromosome	Tissue-specific[a]	Change in gestation[b]	Stable non tissue-specific[c]	Known imprinted genes[d]
1	*DNAJC6*	1	Y^P	Y	N	N
2	*LASS2*	1	Y^P	Y	N	N
3	*PEX5*	12	Y^P	Y	N	N
4	*RASGRF1*	15	Y^P	N	N	N
5	*AKAP10*	17	Y^P	N	N	N
6	*AIFM2*	10	Y^P	N	N	N
7	*APC*	5	Y^P	N	N	N
8	*ARHGAP4*	X	Y^P	N	N	N
9	*ARMC3*	10	Y^P	N	N	N
10	*C3orf62*	3	Y^P	N	N	N
11	*CD83*	6	Y^P	N	N	N
12	*CMTM3*	16	Y^P	N	N	N
13	*DNMT1*	19	Y^P	N	N	N
14	*G0S2*	1	Y^P	N	N	N
15	*GATA4*	8	Y^P	N	N	N
16	*LEP*	7	Y^P	N	N	N
17	*MCCC1*	3	Y^P	N	N	N
18	*NUDT12*	5	Y^P	N	N	N
19	*PCK2*	14	Y^P	N	N	N
20	*RHOBTB3*	5	Y^P	N	N	N
21	*SLC46A2*	9	Y^P	N	N	N
22	*SNCB*	5	Y^P	N	N	N
23	*SORD*	15	Y^P	N	N	N
24	*ST8SIA1*	12	Y^P	N	N	N
25	*TBX6*	16	Y^P	N	N	N
26	*TMEM17*	2	Y^P	N	N	N
27	*ZNF232*	17	Y^P	N	N	N
28	*ZNF396*	18	Y^P	N	N	N
29	*AK094715*	6	Y	Y	N	N
30	*DIRAS3*	1	Y	Y	N	Y
31	*CMTM8*	3	Y	Y	N	N
32	*SEMA3B*	3	Y	Y	N	N
33	*CDKN1C*	11	Y	N	N	Y
34	*H19*	11	Y	N	N	Y
35	*KCNQ1*	11	Y	N	N	Y

Table 2.3. DNA methylation of identified DMRs in different tissues and gestational ages

Index	Gene	Chromosome	Tissue-specific[a]	Change in gestation[b]	Stable non tissue-specific[c]	Known imprinted genes[d]
36	*MEG3*	14	Y	N	N	Y
37	*PEG10*	7	Y	N	N	Y
38	*C10orf125*	10	Y	N	N	N
39	*CCR10*	17	Y	N	N	N
40	*CYP2W1*	7	Y	N	N	N
41	*FIGNL1*	7	Y	N	N	N
42	*IGFBP1*	7	Y	N	N	N
43	*MOV10L1*	22	Y	N	N	N
44	*P2RY6*	11	Y	N	N	N
45	*PARP12*	7	Y	N	N	N
46	*SAMD10*	20	Y	N	N	N
47	*L3MBTL*	20	N	Y	N	Y
48	*ACPL2*	3	N	Y	N	N
49	*REEP6*	19	N	Y	N	N
50	*GNAS*(M)	20	N	N	Y	Y
51	*GNAS*(P)	20	N	N	Y	Y
52	*GRB10*	7	N	N	Y	Y
53	*MEST*	7	N	N	Y	Y
54	*NAP1L5*	4	N	N	Y	Y
55	*PEG3*	19	N	N	Y	Y
56	*PLAGL1*	6	N	N	Y	Y
57	*SGCE*	7	N	N	Y	Y
58	*SNURF*	15	N	N	Y	Y
59	*ZIM2*	19	N	N	Y	Y
60	*ZNF597*	16	N	N	Y	Y
61	*FAM50B*	6	N	N	Y	N
62	*FGF12*	3	N	N	Y	N
63	*IRF7*	11	N	N	Y	N

[a]Multiclass comparison of methylation level in brain, kidney, muscle, mid-gestation placenta, and blood with FDR<0.1%

[b]Multiclass comparison of methylation level in early-gestation, mid-gestation and term placenta, FDR<0.1%

[c]DMRs with no statistically significant changes in methylation level in different tissues and gestational ages

[d]Based on the public databases (http://igc.otago.ac.nz and http://www.geneimprint.com)

[p]Placenta-specific methylation

The complexity of DNA methylation associated with imprinted genes can be illustrated by the data for 3 genes, *GNAS, CDKN1C* and *MEST,* for which multiple probes were present on the Infinium array. For *GNAS*, the array contains 30 probes across 3 promoter regions of 3 alternative transcripts (*NESP55, GNASXL* and exon 1A of *GNAS*) (Figure 2.6A). As has been previously reported, the paternal DMR is located at the promoter of *NESP55* transcript (Figure 2.6B), while the maternal DMR is located at the promoter of *GNASXL* (Kelsey 2010). While most of the probes have more or less equal average methylation across the locus, probes cg15160445 to cg1683351 and cg01565918 show clear tissue-specific methylation across different tissues (Figure 2.6B to D). For *CDKN1C,* there are 8 probes present in the array (Figure 2.6E). A previously unidentified paternal DMR was identified by our method at the promoter region of this gene (Figure 2.6F). Interestingly, not only is the imprinted DMR itself tissue-specific (Table 2.3), but there is a probe (cg20919799) that shows differential methylation across different gestational ages (Figure 2.6G) and tissues (Figure 2.6H). Likewise, for *MEST* for which 10 probes span 2 regions of the gene (Figure 2.7A), an imprinted DMR can be found in one region (Figure 2.7B and C), while tissue-specific and gestational age-specific methylation is observed in another region of the *MEST* promoter (Figure 2.7C to G).

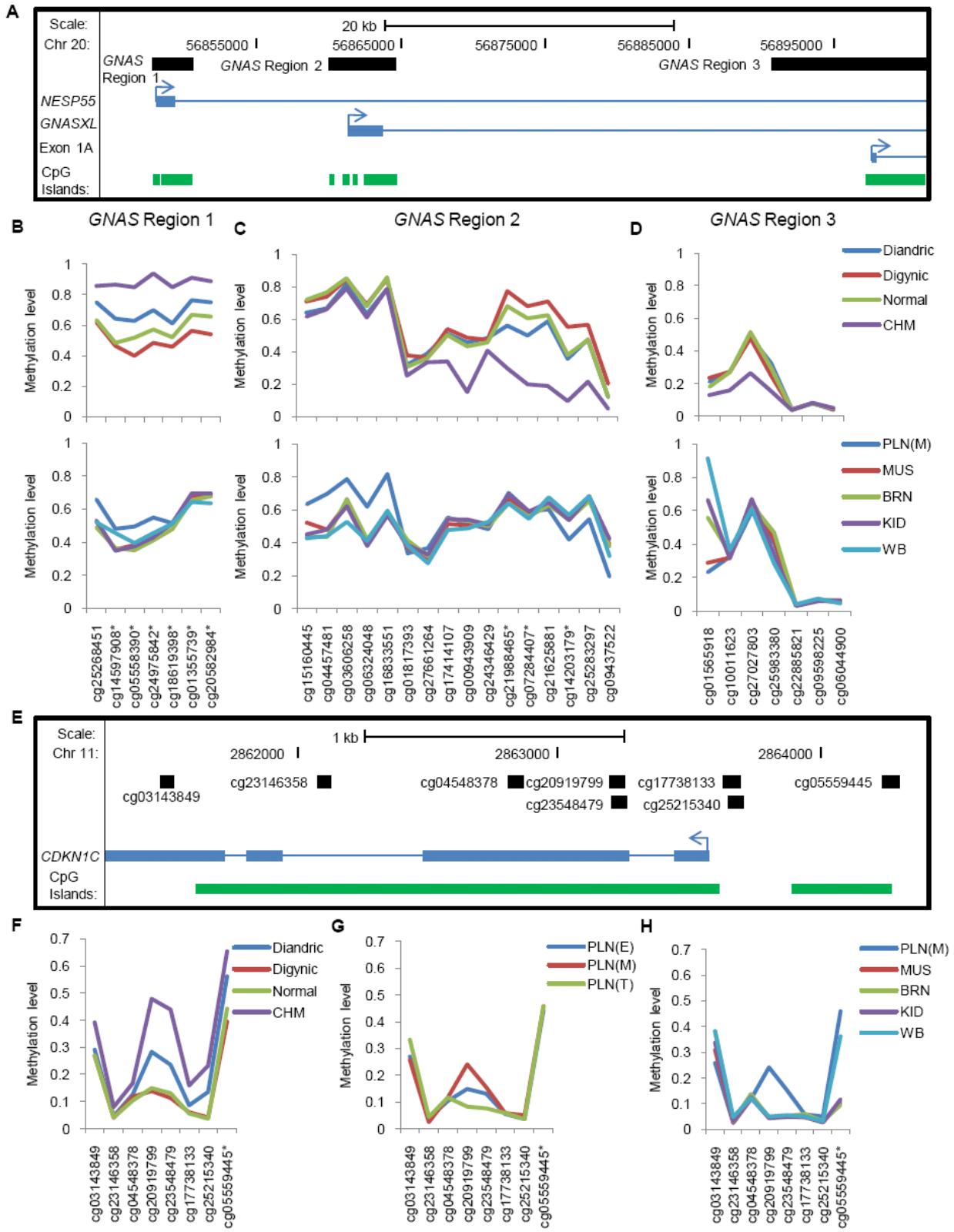
A
Scale:
Chr 20:
20 kb
56855000
56865000
56875000
56885000
56895000
GNAS Region 1
GNAS Region 2
GNAS Region 3
NESP55
GNASXL
Exon 1A
CpG Islands:
B
GNAS Region 1
C
GNAS Region 2
D
GNAS Region 3
Methylation level
Diandric
Digynic
Normal
CHM
PLN(M)
MUS
BRN
KID
WB
cg25268451
cg14597908*
cg05558390*
cg24975842*
cg18619398*
cg01355739*
cg20582984*
cg15160445
cg04457481
cg03606258
cg06324048
cg16833551
cg01817393
cg27661264
cg17414107
cg00943909
cg24346429
cg21988465*
cg07284407*
cg21625881
cg14203179*
cg25283297
cg09437522
cg01565918
cg10011623
cg27027803
cg25983380
cg22885821
cg09598225
cg06044900
E
Scale:
Chr 11:
1 kb
2862000
2863000
2864000
cg03143849
cg23146358
cg04548378
cg20919799
cg17738133
cg05559445
cg23548479
cg25215340
CDKN1C
CpG Islands:
F
G
H
PLN(E)
PLN(M)
PLN(T)
cg03143849
cg23146358
cg04548378
cg20919799
cg23548479
cg17738133
cg25215340
cg05559445*

Figure 2.6. Illustration of tissue-specific and gestational age-specific methylation at the proximal promoter regions of *GNAS* and *CDKN1C*.

(A and E) Schematic diagrams show the positions of the Illumina Infinium probes relative to the genes and transcripts. The directions of the arrows represent the transcriptional directions for the genes or transcripts. Genomic coordinates are retrieved from UCSC Genome Brower (hg18). (B-D) Average methylation level of the Illumina Infinium probes in different placental groups (upper panel) and in different tissues (lower panel). Probe numbers are shown on the x-axis of the figures in the lower panel divided into (B) *GNAS* Region 1, (C) *GNAS* Region 2 and (D) *GNAS* Region 3 according to their proximity to the known transcripts. Tissue-specific methylation can be found from cg15160445 to cg16833551 in *GNAS* Region 2 and at cg01565918 in *GNAS* Region 3. (F-H) Average methylation level of the Illumina Infinium probes of *CDKN1C* in (F) different placental groups, (G) different gestational ages of placenta and (H) different tissues. Probe numbers are shown on the x-axis of the figures. Both tissue-specific and gestational age-specific methylation can be found at cg20919799. PLN(E): early gestation placenta, PLN(M): mid gestation placenta, PLN(T): term placenta, MUS: muscle, BRN: brain, KID: kidney and WB: whole blood.

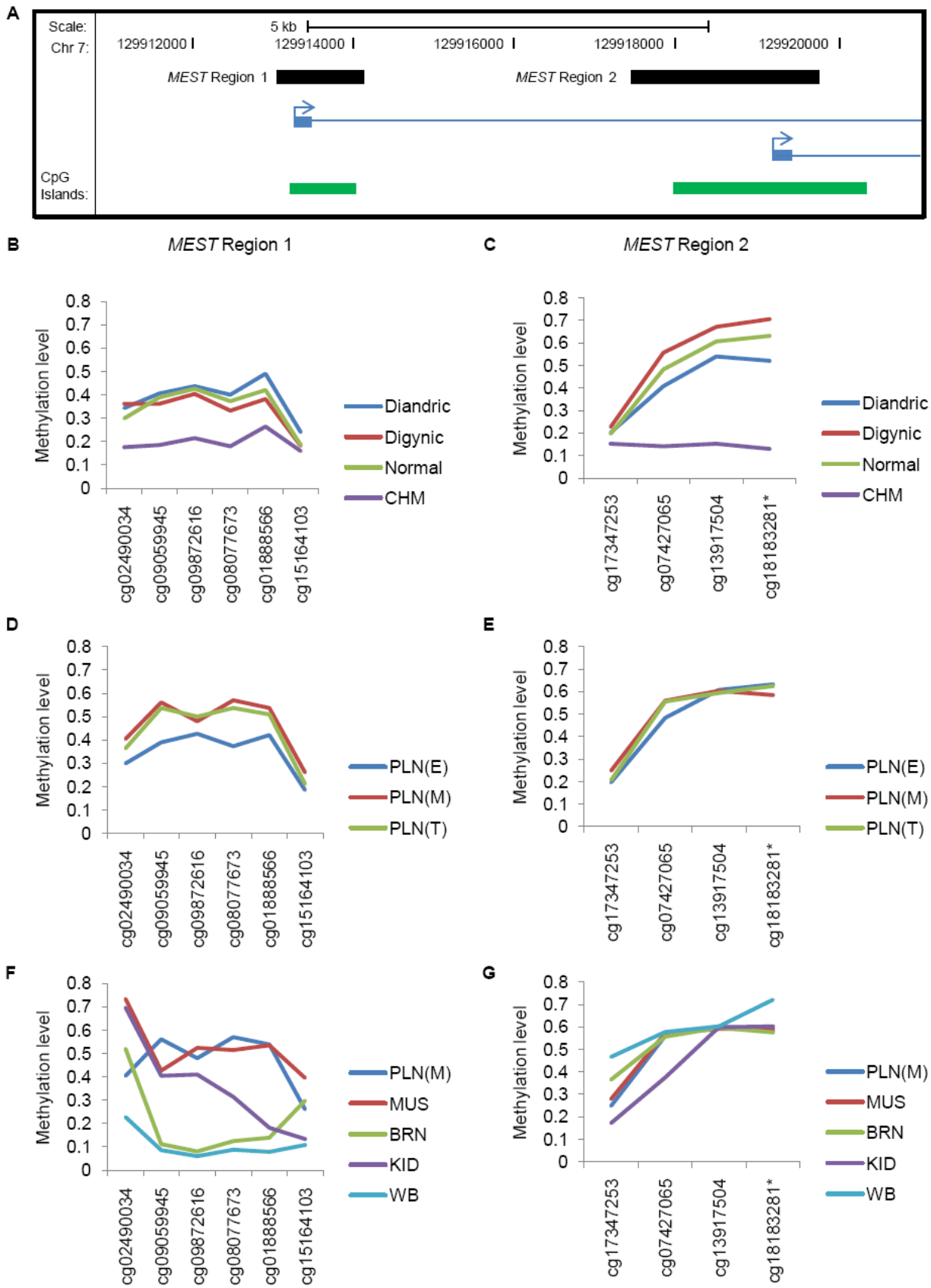
A
Scale:
Chr 7:
5 kb
129912000
129914000
129916000
129918000
129920000
MEST Region 1
MEST Region 2
CpG Islands:
B
MEST Region 1
C
MEST Region 2
Methylation level
0.8
0.7
0.6
0.5
0.4
0.3
0.2
0.1
0
cg02490034
cg09059945
cg09872616
cg08077673
cg01888566
cg15164103
cg17347253
cg07427065
cg13917504
cg18183281*
Diandric
Digynic
Normal
CHM
D
E
PLN(E)
PLN(M)
PLN(T)
F
G
MUS
BRN
KID
WB

Figure 2.7. Illustration of tissue-specific and gestational age-specific methylation at the proximal promoter regions of *MEST*.

(A) Schematic diagram shows the positions of probes contained on the Illumina Infinium methylation array relative to the transcripts. The directions of arrows represent the transcriptional directions. Genomic coordinates are retrieved from the UCSC Genome Browser (hg18). (B-G) Comparison of average methylation level of the Illumina Infinium probes between: (B and C) different placental groups; (D and E) placentas with different gestational ages; (F and G) different tissues. Probe numbers are shown on the x-axis of the figures in the lower panel divided into (B, D, F) *MEST* Region 1 and (C, E, G) *MEST* Region 2 according to their proximity to the known transcripts. PLN(E): early gestation placenta, PLN(M): mid gestation placenta, PLN(T): term placenta, MUS: muscle, BRN: brain, KID: kidney and WB: whole blood.

2.3.6. Functions of identified imprinted genes

To classify the function of the imprinted DMRs, we carried out a gene ontology analysis for all the identified known and novel imprinted DMRs (Table 2.4). Although the functions that were enriched from gene ontology may not be significant after multiple comparison adjustment (FDR ranging from 3.8 to 18%) (Table 2.4), the general functions of maternal DMRs were distinct from the paternal DMRs. The former were enriched for DNA binding and the later for regulation of growth (Table 2.4). A functional difference between PEGs and MEGs was previously suggested by the parental conflict theory (Moore and Haig 1991).

Table 2.4. Gene ontology of identified imprinted genes

DMR	Term	%	P Value	FDR(%)
All	Regulation of myeloid cell differentiation	6.7	0.003	4.9
	DNA-binding	21.7	0.011	12.0
	Domain:SCAN box	5	0.013	16.0
	SCAN	5	0.015	12.0
	Transcriptional regulator SCAN	5	0.015	17.0
	Beckwith-Wiedemann syndrome	3.3	0.019	17.0
Maternal	Domain:SCAN box	8.3	0.005	5.9
	SCAN	8.3	0.005	3.8
	Transcriptional regulator SCAN	8.3	0.006	6.6
	Regulation of myeloid cell differentiation	8.3	0.010	14.0
	Regulation of gene expression, epigenetic	8.3	0.013	17.0
	DNA-binding	25	0.017	18.0
Paternal	Beckwith-Wiedemann syndrome	7.7	0.008	5.9
	Regulation of growth	15.4	0.010	13.0

2.4. Discussion

Many efforts have been made to identify imprinted genes in the human genome due to their importance in fetal growth and development, and their potential for dysregulation (Cooper and Constancia 2010; Henckel and Arnaud 2010). Most imprinted genes known to date were first identified in mouse, but many imprinted genes are not conserved across species (Monk *et al*. 2006). In the present study, we utilized diandric and digynic triploid placentas to map imprinted DMRs in the human genome. We identified 11 of the 18 reported human ICRs covered by the Illumina Infinium HumanMethylation27 panel despite application of stringent statistical criteria, and validated the parent-of-origin dependence of methylation and expression in a subset of our candidate novel imprinted genes by independent experiments.

This approach improves upon previous strategies for mapping imprinted genes, such as comparing parthenogenotes and androgenotes (Strichman-Almashanu *et al*. 2002), which are

grossly abnormal, or comparing maternal and paternal uniparental disomies (UPDs) (Schulz *et al*. 2006; Sharp *et al*. 2010), which is limited by the rarity of UPDs for many chromosomes and the limited tissues available for analysis. Although triploid placentas do exhibit some abnormal pathology, the methylation profiles of both types of triploidy were closely correlated with chromosomally normal placentas and distinct from the androgenote CHMs. Genome-wide transcriptome analysis has also been used to identify imprinted genes (Daelemans *et al*. 2010; Henckel and Arnaud 2010), but it is gene expression and SNP dependent; thus, imprinted genes with tissue-specific expression or lacking a heterozygous exonic SNP would be missed.

As demonstrated, tissue-specific methylation of imprinted DMRs or their flanking regions can readily be assessed by comparing methylation profiles of a variety of tissues, allowing a comprehensive analysis of tissue-specific methylation regulation even at complex loci, such as *GNAS* (Kelsey 2010). While in the present study we identified only loci that were imprinted in placenta, most known imprinted genes show parent-of-origin specific expression in this organ (Frost and Moore 2010). Furthermore, as diandric and digynic triploids can both exist as fetuses, additional comparisons can be made to identify any potential genes that exhibit imprinting specifically in other tissues. A further extension of this analysis could also be made by using microarray or whole-genome sequencing with higher coverage of the genome, since the microarray used in the present study only included CpGs within the proximal promoter regions of genes.

Overall, the number of novel imprinted DMRs identified in the present study was less than that predicted by bioinformatic approaches (Luedi *et al*. 2007). However, the stringent selection criteria (FDR<0.1% and absolute average methylation difference>15%) we used will cause an underestimation of the number of imprinted loci. For instance, a recently confirmed

imprinted gene, *RB1* (Kanber *et al*. 2009), was significantly differentially methylated between diandric and digynic triploidies (FDR<0.1%) with a methylation pattern consistent with being a maternal DMR (data not shown). However, it was excluded because its absolute average methylation difference between diandries and digynies was only 14%. Interestingly, *FAM50B* was predicted to be a potential imprinted gene by bioinformatics (Luedi *et al*. 2007), though our data show that it is a PEG instead of a MEG as originally predicted (Luedi *et al*. 2007).

Only some of the novel putative imprinted DMRs could be confirmed to show monoallelic expression and others did not show strict parent-of-origin expression for all cases (Supplementary Table 2.6). In addition to tissue-specific or gestational age-specific imprinting, there are several other potential explanations. First, as we have shown, the Sequenom assay may not be sensitive enough to pick up subtle allelic expression biases (Supplementary Table 2.5). Second, as previously reported for *STOX1*, some imprinted DMRs may be cell-type-specific (Dijk *et al*. 2010). Given the highly heterogeneous cell types present in the placenta (Avila *et al*. 2010), non-imprinted expression in some cells may mask allele-specific expression in others. The possibility that cell heterogeneity exists is supported by the observation that average methylation of some imprinted DMRs was not strictly 50% in normal placentas (Supplementary Figure 2.3). Third, there may be alternative transcripts regulated by alternative promoters that are not imprinted, so the observed expressed allelic ratio at particular SNP may be complicated by the synergic effect of multiple transcripts. Such complex regulation is observed for known imprinted genes such as *GNAS*, *CDKN1C* and *MEST* (Figure 2.6 and 2.7).

The validation of all the putative imprinted DMRs we identified is limited by the number of samples and common SNPs within the regions, and the availability of intact mRNA from the pathological specimens. A proper validation to demonstrate that the DMRs we have identified

are associated with imprinted methylation and gene expression requires being able trace the parental origin of the methylated and the expressed alleles in multiple members of the same family, which can be done in mouse but is impractical and ethically impossible do across multiple tissues in humans (Moore and Oakey 2011). The best alternative is to trace the origin of the methylated allele and expressed allele in multiple individuals. This requires a SNP adjacent to the methylation site that is heterozygous in the test sample but homozygous in one parent. Using this strategy, we demonstrated for *FAM50B* 1) a maternal origin of the methylated allele in placenta and blood from multiple individuals and on reciprocal genetic backgrounds, 2) the paternal allele is expressed with either SNP allele in the placenta, thus ruling out the possibility of a genetic effect. Confirming that an imprint represents a primary imprinted DMR requires detailed investigations of post-fertilization imprinting dynamics which is difficult to perform in human. Nonetheless, we showed that the methylation level of *FAM50B* is similar in multiple tissues and is unmethylated in sperm, suggesting that it is likely to be a primary maternal DMR. During the preparation of this manuscript, the maternal imprint of *FAM50B* has also been confirmed by other groups using similar validation methods (Nakabayashi et al. 2011; Zhang et al. 2011). The goal of this study was to demonstrate the ability of our approach to identify imprinted DMRs, and not to map and confirm every imprinted DMR on the array. Thus, the putative imprinted DMRs listed in the present study should be taken with caution and further validation is required.

Two genes identified as imprinted in the present study, *APC* and *DNMT1*, were excluded as imprinted in previous studies (Novakovic *et al*. 2010; Wong *et al*. 2008), while *APC* was reported as imprinted in another study (Guilleret *et al*. 2009). We confirmed the methylation at these genes and found parent-of-origin allelic expression at least in *DNMT1*. Of interest, *DNMT1*

is a DNA methyltransferase that is important for maintenance and establishment of DMRs in imprinted genes (Weaver *et al*. 2010), while *APC* is a negative regulator of Wnt signaling pathway which has been implicated in the survival, differentiation and invasion of human trophoblasts (Wong *et al*. 2008). Although *Dnmt1* was found to be dispensable for growth of the extraembryonic lineages in mouse (Sakaue *et al*. 2010), it is not methylated at the orthologous region in mouse (Novakovic *et al*. 2010). Both the *APC* and *DNMT1* DMRs were reported to be specifically methylated in primate placentas (Ng *et al*. 2010), suggesting that the imprinting marks of these genes emerged fairly recently in evolution. This is also consistent with the hypothesis that maternal imprints are under selective pressure over early development for methylation-dependent control since there are disproportionately more maternal DMRs than paternal DMRs (Schulz *et al*. 2010). This could occur by selecting genes with developmental advantage by gain-of-imprinting from epipolymorphisms (Yuen *et al*. 2009).

In conclusion, we have demonstrated that comparison of diandric and digynic triploids is an effective method for mapping imprinted DMRs in the human genome. This approach can be extended to different tissues, gestational ages or species, thereby generating a comprehensive view of imprinting regulation and evolution. The ability to map novel imprinted genes in the human genome should improve our understanding of the causes of placental dysfunction and birth defects. With the rapid advancement of molecular genetics technologies, a complete map of imprinted DMRs may ultimately be generated by the use of whole-genome sequencing. However, the present approach is a convenient and cost-effective way of imprinted gene mapping currently available.

Chapter 3: Extensive epigenetic reprogramming in human somatic tissues between fetus and adult[3]

3.1. Introduction

The human body contains more than 200 different cell types, each having developed a different function and phenotype despite containing an identical genome. Through the establishment and maintenance of cell-type specific gene expression profiles, epigenetic mechanisms contribute to cellular identity (Illingworth *et al*. 2008). Perhaps the best understood component of the epigenetic machinery is DNA methylation, which most often occurs on cytosine residues in the context of CpG dinucleotides.

In addition to tissue-specific gene expression, a number of intriguing biological phenomena are closely linked to DNA methylation, including the inactivation of the extra X-chromosome in females (Cotton *et al.* 2009), the allele-specific expression of imprinted genes (Strichman-Almashanu *et al*. 2002), and biological aging (Baccarelli *et al*. 2009; Boks *et al*. 2009). All of these processes are examples for developmental programming of DNA methylation, which generally are considered to be relatively stable. However, recent studies have revealed that DNA methylation can be dynamic and capable of temporally changing (Kangaspeska *et al*. 2008; Metivier *et al*. 2008). This plasticity may be modulated in part by a diverse set of environmental influences, all of which have been correlated with changes in DNA methylation. These include nutritional factors such as folate intake (Fryer *et al.* 2009), social factors such as maternal care (McGowan *et al*. 2009), as well as exposure to pollutants (Baccarelli *et al*. 2009; Bollati *et al*.

[3] A version of Chapter 3 has been published. Yuen RKC, Neumann SMA, Fok AK, Peñaherrera MS, McFadden DE, Robinson WP, Kobor MS. (2011) Extensive epigenetic reprogramming in human somatic tissues between fetus and adult. Epigenetics Chromatin. In press.

2007). Therefore, it is likely that DNA methylation serves as an important mediator between the environment and genome function. The malleable features of DNA methylation are important for its role in health and disease, as improper regulation of this epigenetic mark during development has been associated with a number of pathological conditions including birth defects and various kinds of cancer (Robertson 2005).

One particularly well-understood specialized aspect of epigenetics during development is genomic imprinting. It refers to the parent-of-origin specific allelic expression of a small number of genes. While this epigenetic program is established early in development and thought to be maintained throughout life (Reik 2007; Reik and Walter 2001), relatively little is known about its tissue-specific manifestation and temporal dynamics across different developmental stages in humans. In addition to imprinting, a number of findings connecting DNA methylation changes to biological development have emerged over the last few years, largely fuelled by the advent of genome-wide technologies. For example, substantial alterations in DNA methylation occur during stem cell differentiation, supporting a general role for DNA methylation in early development (Brunner *et al*. 2009; Cohen *et al*. 2009; Straussman *et al*. 2009). Similarly, profiling of adult human tissues revealed striking differences in DNA methylation, manifested most pronouncedly in tissue-specific differentially methylated regions (tDMRs) (Eckhardt *et al*. 2006; Rakyan *et al*. 2010; Shen *et al*. 2007; Weber *et al*. 2007). DNA methylation in adult somatic tissues can undergo striking changes during the adult lifespan, with a tendency for gain of DNA methylation with age for loci (CpG sites) residing in CpG islands (CGIs) and loss of DNA methylation with age for CpG loci residing outside of CGIs (Christensen *et al*. 2009). It has not yet been determined whether such changes reflect an instability in the maintenance of DNA methylation over time leading to more variable methylation in the older samples or,

alternatively, is indicative of intrinsic programmed changes over time due to changing biological requirements at different developmental and life-stages.

It is also not clear to what extent epigenetic programming may be altered by the abnormal development of cells and tissues. Dramatic changes in DNA methylation occur in connection with altered cellular changes in cancer (Esteller 2008; Herman and Baylin 2003). Reminiscent of cancer, chromosomal trisomy is also associated with altered cell growth parameters (generally slower growth and increased apoptosis) and a global disruption of the transcriptome (Dauphinot *et al*. 2005; FitzPatrick *et al*. 2002; Saran *et al*. 2003), which could similarly be associated with altered DNA methylation at a subset of genes. However, comprehensive mapping of DNA methylation has not been performed in trisomic subjects, especially as it relates to tissue-specific manifestations.

Mechanistically, DNA methylation exerts its effects on gene expression in close partnership with histone proteins (Cedar and Bergman 2009). DNA methylation is sensed by proteins that turn gene expression on or off, often through altering posttranslational modifications of histones. Numerous histone modifications are associated with different levels of gene expression, most prominently H3K4 trimethylation as an indicator of active transcription and H3K27 trimethylation as an indicator of inactive genes. Curiously, in stem cells these marks are sometimes found together in "bivalent domains", which might poise genes for rapid expression changes necessary during development (Bernstein *et al*. 2006).

Here, we investigate the characteristics and functional significance of the differentially methylated CpG loci in normal and abnormal fetal development. Using a well-validated array platform, DNA methylation status of around 1000 CpG dinucleotides located in the regulatory

regions of nearly 800 genes was measured semi-quantitatively in 5 somatic tissues (brain, kidney, lung, muscle and skin) from second-trimester elective terminations of eight normal, five trisomy 21 and four trisomy 18 fetuses. We found tissue-specific clustering of DNA methylation at this early stage of development, while relatively few sites with altered DNA methylation were observed for trisomies. Through a detailed comparison of fetal DNA methylation data with published data on normal somatic tissues from adult autopsies obtained on an identical platform (Byun *et al*. 2009), we identified substantial age-related DNA methylation changes. Lastly, the plasticity of DNA methylation was also evident when we compared fetal DNA methylation profiles to embryonic stem cells (Calvanese *et al*. 2008), with the most variable marks being linked to domains with bivalent histone modifications. Collectively these data fill an important gap between DNA methylation patterns in stem cells and in adult tissues and illustrate the complexity that may arise in trying to identify more subtle effects of environment or disease.

3.2. Methods

3.2.1. Sample collection

This study was approved by the ethics committees of the University of British Columbia and the Children's & Women's Health Centre of British Columbia. Fetal tissues (muscle, skin, kidney, lung, and brain) were obtained from anonymous chromosomally normal 2nd trimester (15-24 weeks in gestational age, mostly 19-20 weeks) elective terminations for medical reasons (i.e. termination for premature rupture of membranes or diaphragmatic hernia). Only information on gestational age and reason for pregnancy termination was recorded. All were either dilation or evacuation, with the extractions being of intact fetuses or inductions of labour, which results in delivery of an intact fetus. Samples were collected by the Children's & Women's Pathology lab

on autopsy as follows: Skin (normally abdominal area), kidney (1/4 of a kidney including cortex and medulla), brain (cerebrum), lung (small sample from edges) and muscle (psoas muscle). Genomic DNA was extracted from each tissue sample using standard techniques. In addition, samples from pregnancy terminations for trisomy 18 and 21 were obtained in a similar manner for comparison. No discernible growth delay was observed in the trisomic fetuses and the age distribution was similar for trisomies and controls.

3.2.2. Illumina DNA methylation array

Bisulfite conversion of 750ng of genomic DNA was performed using the EZ DNA Methylation Kit (Zymo Research, Orange, CA, USA) according to the manufacturer instructions. After bisulfite treatment, unmethylated cytosines were converted to uracils, while methylated cytosines were not changed. Bisulfite converted DNA samples were subjected to the Illumina GoldenGate methylation Cancer Panel I array-based assay (Illumina, San Diego, CA, USA) as described in our previous studies (Yuen *et al*. 2009; Yuen *et al*. 2010). All samples were run on the same Illumina GoldenGate chip to avoid and chip/batch effects. This platform is well-validated and its use allows us to compare our data to that in the literature. The Illumina array targets specifically promoter regions of the genes (1.5 kb upstream and 500 bp downstream from the transcription start site) and the location of specific sites is well annotated in the Illumina probe database. Briefly, two allele-specific probes are designed for each CpG site on the array: one for the methylated sequence and one for the unmethylated sequence. After annealing to the target sequence, the probes were extended and ligated to locus-specific oligos. The ligated products were then amplified by PCR using fluorescently labelled primers and hybridized to the bead array. The methylation levels for each CpG sites were measured by the intensity of fluorescent signals corresponding to the methylated allele (Cy5) and the unmethylated allele

(Cy3). Cy5 and Cy3 fluorescent intensities were corrected independently for background signal and normalized using BeadStudio software (Illumina, San Diego, CA, USA). Continuous β values that range from 0 (unmethylated) to 1 (methylated) were used to signify the percentage of DNA methylation, from 0% to 100%, for each CpG site. Detection *p*-value of each probe was generated by comparison with a series of negative controls embedded in the assay. Probes with detection *p*-value >0.05 in any of the sample was eliminated from the study. Furthermore, to concentrate on substantially altered sites and to reduce the statistical complexities associated with large numbers of tests being done in a small sample set, CpG loci considered to be non-variant (β values <0.1 or >0.9 in all samples) were eliminated from the analyses. This is being done throughout the study, but it yields different numbers depending on individual comparison due to different number of probes being invariant.

3.2.3. Statistical analysis

Tissue-specific differentially methylated regions in fetus and adult tissues were identified by ANOVA for statistically significant CpG loci after Bonferroni correction using SPSS. Differentially methylated loci between tissues from normal and trisomy fetuses as well as from normal fetal and adult tissues were identified using significance analysis of microarrays (SAM) with a cut-off of false discovery rate (FDR) <5%. Characteristics of DNA methylation in tDMRs and aDMRs were analyzed by Pearson Chi-Square test. Pearson linear correlation was used to analyze the similarities of average DNA methylation at each autosomal locus between tissue samples. The Database for Annotation, Visualization and Integrated Discovery (DAVID) program was used for gene ontology (GO) analysis (Dennis *et al*. 2003; Huang da *et al*. 2009). Using total number of genes presented in the array as a background for comparison, enriched GO terms were identified using a cut-off of FDR <5%.

3.2.4. Bisulfite pyrosequencing

Loci identified with tissue-specific DNA methylation in fetal tissues were confirmed using bisulfite pyrosequencing. Pyrosequencing was performed on a Biotage Pyromark Q96 MD Pyrosequencer and the quantitative levels of methylation for each CpG dinucleotide were evaluated with the Pyro Q-CpG software (Biotage, Uppsala, Sweden). DNA Methylation-unbiased pyrosequencing primers that cover the same CpG sites interrogated by the Illumina probes and their assay conditions are listed in Supplementary Table 3.1.

3.3. Results

3.3.1. Tissue-specific DNA methylation in fetal tissues

To determine the extent of tissue-specific DNA methylation during fetal development we used the Illumina GoldenGate DNA Methylation Cancer Panel to measure the DNA methylation status in 5 somatic tissues (brain, kidney, lung, muscle and skin) from second-trimester elective terminations of eight normal, five trisomy 21 and four trisomy 18 fetuses. For each sample, relative DNA methylation was measured at 1315 CpG loci located in the promoter regions of 752 genes after eliminating probes with detection *p*-value >0.05 and those located on the X-chromosome. Only CpG loci located on autosomes were included in the analysis to eliminate gender-specific effects caused by differential methylation of the X-chromosome, which tends to be hypermethylated at gene regulatory regions in females (Yuen *et al*. 2009; Yuen *et al*. 2010).

Unsupervised hierarchical clustering of the remaining 877 CpG loci was performed based on 1-r (Illumina Beadstudio software), where r refers to the correlation coefficient between sample methylation values at the included loci. Methylation profile for samples of the same tissue type were highly correlated (r>0.925) and therefore clustered together (Figure 3.1 and

Supplementary Figure 3.1). Brain showed the most distinct clustering, from the other groups, while only one muscle sample from T21 (FT1_t21_muscle) clustered with the skin sample from the same fetus.

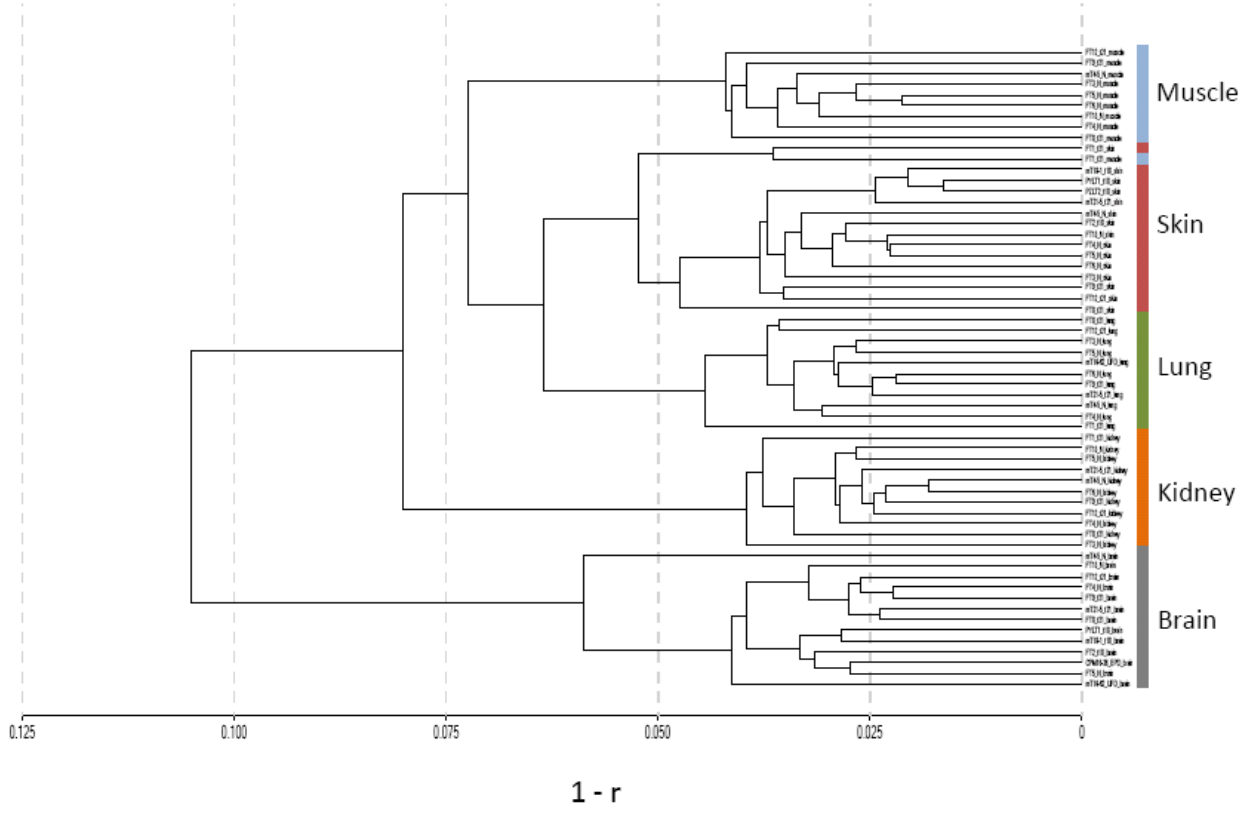

Figure 3.1. Unsupervised clustering of fetal tissues demonstrates that each tissue has a distinct DNA methylation profile.

Sample names are shown with labeling of the corresponding tissue types. Tissue samples were clustered by hierarchical clustering of β values based on 1-r (Illumina Beadstudio software), where r is referring to the correlation coefficient between samples. Specific tissue types clustered together with a high correlation between samples derived from the same tissue. All tissues have distinct clustering from the other groups except one muscle sample from T21 (FT1_t21_muscle) clustered with the skin sample from the same fetus.

The tight clustering of tissues enabled the identification of CpG loci with tissue-specific DNA methylation profiles. To eliminate potential confounding factors resulting from chromosomal trisomy, this analysis was confined to 5 somatic tissues (brain, kidney, lung, muscle and skin) from the 8 normal fetuses. Of the 834 sites being studied, 195 (23%) showed statistically significant differences between tissues as determined by ANOVA using a Bonferroni corrected *p*-value of 5.99×10^{-5} (Supplementary Table 3.2).

Among the 195 tissue-specific differentially methylated regions (tDMRs), only 63 (32%) were located within a CpG island (CGI; Defined as GC content >50% and observed/expected CpG >0.6 in a length >200 bp). By comparison, 586 (70%) of the original 834 sites tested were CGI associated, suggesting that low density CpG regions are more likely to dictate tissue-specific DNA methylation patterns ($p<0.0001$; Chi-Square test).

To identify changes that are most likely to be biological meaningful, we selected 98 tDMRs which showed an absolute difference in average DNA methylation level for a given CpG site of at least 20% in a particular tissue for subsequent analysis. Hypermethylated and hypomethylated loci are thus defined as those having an average β value in that tissue of >0.2 above or below the overall mean for all tissues (A β value of zero represents an unmethylated locus and a value of one represents a completely methylated locus). Using this cut-off, fetal brain had the highest number of tDMRs (Figure 3.2) with 30 hyper- and 23 hypo-methylated loci. This is consistent with its more distinct clustering as a separate group (Figure 3.1). Muscle was the next most distinct tissue with 24 hyper- and 16 hypo-methylated tDMRs (Supplementary Table 3.2).

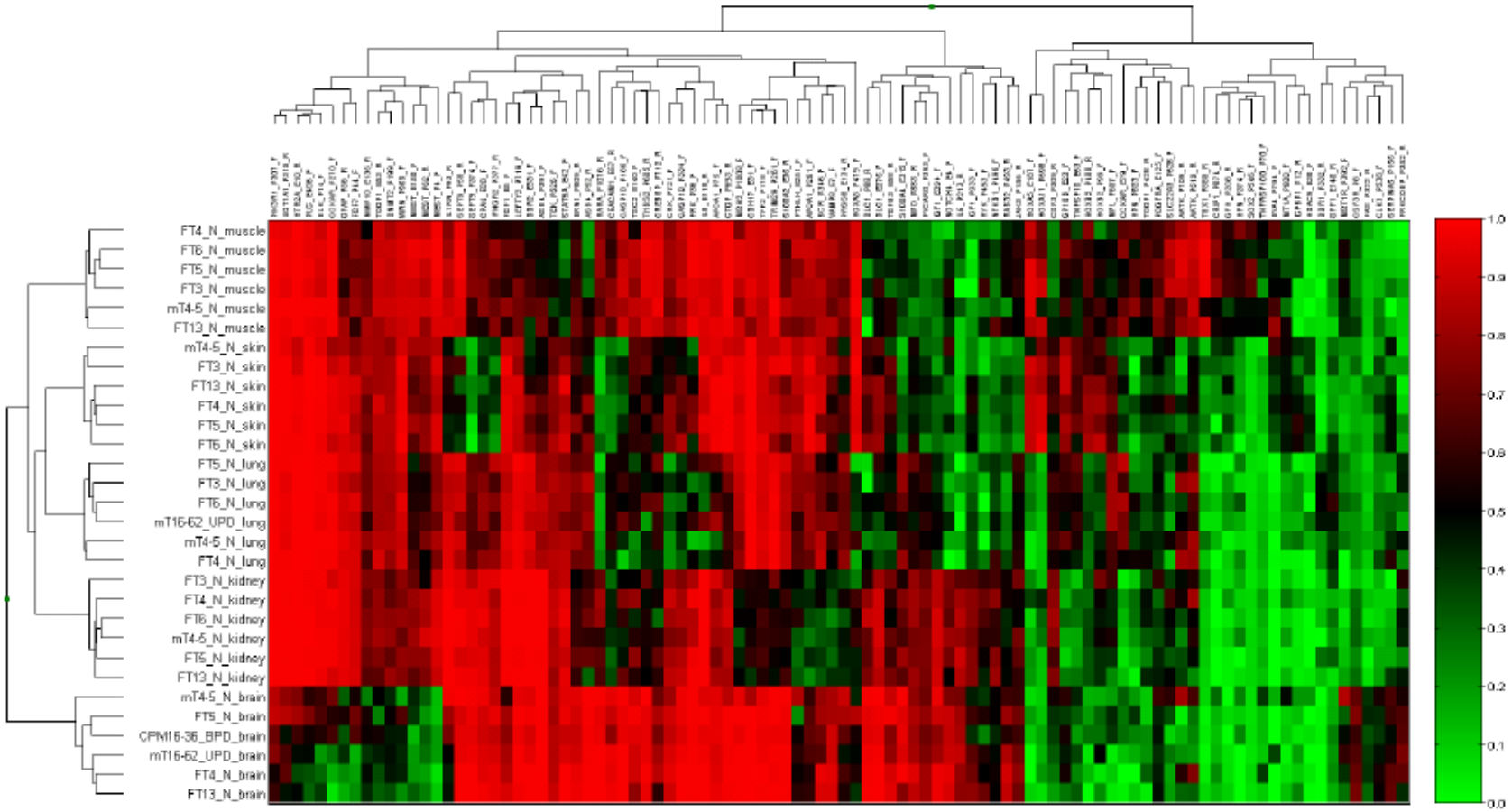

Figure 3.2. Heat-map of 98 loci showing hyper- or hypo- methylated tDMRs in particular tissues.

Probes and sample names are shown and with hierarchical clustering of β values based on 1-r (Illumina Beadarray software). A β value of zero (indicated in bright green) represents an unmethylated locus and one (indicated in bright red) represents a methylated locus. Hypermethylated and hypomethylated loci are defined as those having an average β value in that tissue of >0.2 above or below the overall mean for all tissues. Fetal brain had the highest number of tDMRs with 30 hyper- and 23 hypo-methylated loci.

The ability to identify the tissue source of DNA samples could be useful in determining the developmental origin of pathologically abnormal tissue or other samples of unclear origin. In order to identify sites that could be used as key indicator markers to identify tissue source, we searched for sites within the fetal tissue data for which the mean of one tissue was maximally different from the mean for other tissues and, in addition, did not show any overlap in the range of DNA methylation values. Using these more stringent criteria, one locus with tissue-specific DNA methylation for each tissue type (5 in total: CDH17_E31 for kidney, CRK_P721 for lung, HOXA5_P479 for skin, MUSK_P308 for muscle and MEST_P4 for brain) was identified (Supplementary Table 3.2) and their tissue-specificity was confirmed with bisulfite pyrosequencing, with the correlation between values from the Illumina array and pyrosequencing ranging from r=0.77 to 0.97 (Supplementary Figure 3.2). These loci are associated with genes (within the promoter region as defined by the Illumina annotation) that are important for the development of their respective tissues (DeChiara *et al*. 1996; Horsfield *et al*. 2002; Stelnicki *et al*. 1998). For example, MUSK_P208 is associated with the *MUSK* (muscle skeletal receptor tyrosine kinase) gene that is responsible for synapse formation in mammalian muscle during development (DeChiara *et al*. 1996).

3.3.2. DNA methylation in somatic tissues from trisomy 21 and trisomy 18 showed relatively few differences compared to normal fetuses

To identify potential epigenetic differences associated with chromosomal trisomies, the DNA methylation profile in 5 somatic tissues (brain, kidney, lung, muscle and skin) from the 8 normal fetuses (3 males and 5 females) was compared with the identical tissue from the fetuses with either T18 (N=4; 3 males and 1 female) or T21 (N=5; 2 males and 3 females). Using a cut-off of <5% false discovery rate (FDR) from significance analysis of microarrays (SAM) (Tusher

et al. 2001) and a previously suggested Δβ value of >0.17 (Bibikova *et al*. 2006), we identified 17 hypermethylated loci in the skin of T18, 7 hypermethylated loci in the skin and 1 hypermethylated locus in the muscle of T21 (Table 3.1). None of these were located on chromosome 18 or 21. One CpG (DDB2_P407) was hypermethylated in both skin and muscle of T21 and one CpG (ZNF264_P397) was hypermethylated in the skin of T18 and T21 (Table 3.1). However, no differentially methylated loci were identified in brain, kidney or lung. Furthermore, the tDMRs identified as key indicators of normal fetal tissue types maintained their tissue-specific DNA methylation patterns in the trisomy samples (data not shown). Thus the significant differences between chromosomally normal and abnormal fetuses in DNA methylation were largely tissue-specific and limited compared to the number of tissue specific differences observed.

Table 3.1. Loci demonstrating differential methylation between trisomic and control subjects

					Controls		Trisomies			
Type	**Tissue**	**Feature ID**	**Chromosome**	**False-Discovery Rate (%)**	**Mean**	**SD**	**Mean**	**SD**	**Difference**	**GO term**
T18	Skin	HOXA9_E252_R	7	0	0.04	0.09	0.58	0.21	0.54	Developmental process
		ZNF264_P397_F	19	0	0.52	0.17	0.92	0.01	0.40	Biological regulation
		RYK_P493_F	3	0	0.17	0.08	0.56	0.12	0.39	Developmental process
		CASP10_P186_F	2	0	0.37	0.12	0.72	0.11	0.35	Developmental process
		IL1RN_P93_R	2	0	0.51	0.07	0.78	0.04	0.27	Immune response
		RBL2_P250_R	16	0	0.04	0.05	0.26	0.11	0.22	Biological regulation
		MAP2K6_P297_R	17	0	0.30	0.05	0.49	0.03	0.19	Metabolic process
		JAK3_P156_R	19	0	0.25	0.05	0.44	0.07	0.19	Developmental process
		MST1R_P392_F	3	0	0.15	0.05	0.32	0.05	0.17	Metabolic process
		RARA_P1076_R	17	2.08	0.19	0.08	0.52	0.19	0.33	Metabolic process
		CPA4_E20_F	7	2.08	0.37	0.07	0.61	0.13	0.24	Metabolic process
		CEACAM1_E57_R	19	2.08	0.27	0.05	0.46	0.09	0.19	Developmental process
		ARHGDIB_P148_R	12	3.38	0.74	0.10	0.92	0.02	0.19	Immune response
		SEPT9_P374_F	17	4.24	0.14	0.08	0.37	0.15	0.24	Immune response
		S100A4_E315_F	1	4.24	0.25	0.09	0.43	0.10	0.19	Developmental process
		RAD54B_P227_F	8	4.24	0.16	0.05	0.33	0.12	0.17	DNA repair
		CASP10_E139_F	2	4.24	0.74	0.10	0.92	0.01	0.17	Developmental process
T21	Skin	ZNF264_P397_F	19	0	0.52	0.17	0.85	0.06	0.33	Biological regulation
		WNT10B_P993_F	12	0	0.16	0.04	0.38	0.08	0.22	Developmental process
		DIO3_E230_R	14	0	0.45	0.11	0.65	0.05	0.19	Biological regulation
		TSC2_E140_F	16	0	0.61	0.06	0.79	0.08	0.18	Biological regulation
		IPF1_P750_F	13	3.89	0.33	0.12	0.56	0.12	0.23	Biological regulation
		DDB2_P407_F	11	3.89	0.12	0.09	0.35	0.16	0.23	DNA repair
		HLA-DRA_P77_R	6	3.89	0.70	0.10	0.87	0.05	0.17	Immune response
T21	Muscle	DDB2_P407_F	11	0	0.11	0.05	0.30	0.08	0.19	DNA repair

3.3.3. DNA methylation of a significant portion of CpG loci was age-dependent

The establishment of semi-quantitative DNA methylation maps from fetuses reported here allowed us to determine the extent of age-dependent DNA methylation changes. To this end, we compared our data to published DNA methylation measurements obtained from adult human autopsy specimens using the same Illumina methylation array (Byun *et al*. 2009). This analysis was limited to the three tissues (brain, kidney and lung) that overlapped between the two studies. After eliminating all non-variable CpG loci in the combined fetal + adult tissue group (β value <0.1 or >0.9 in all samples), 756 loci in brain, 1026 loci in kidney and 849 loci in lung were compared. In general, the average DNA methylation at each autosomal locus in normal fetal tissues was more highly correlated with the average DNA methylation for the corresponding locus in the trisomic fetal tissues (r=0.99) than for the comparable adult tissues (Figure 3.3).

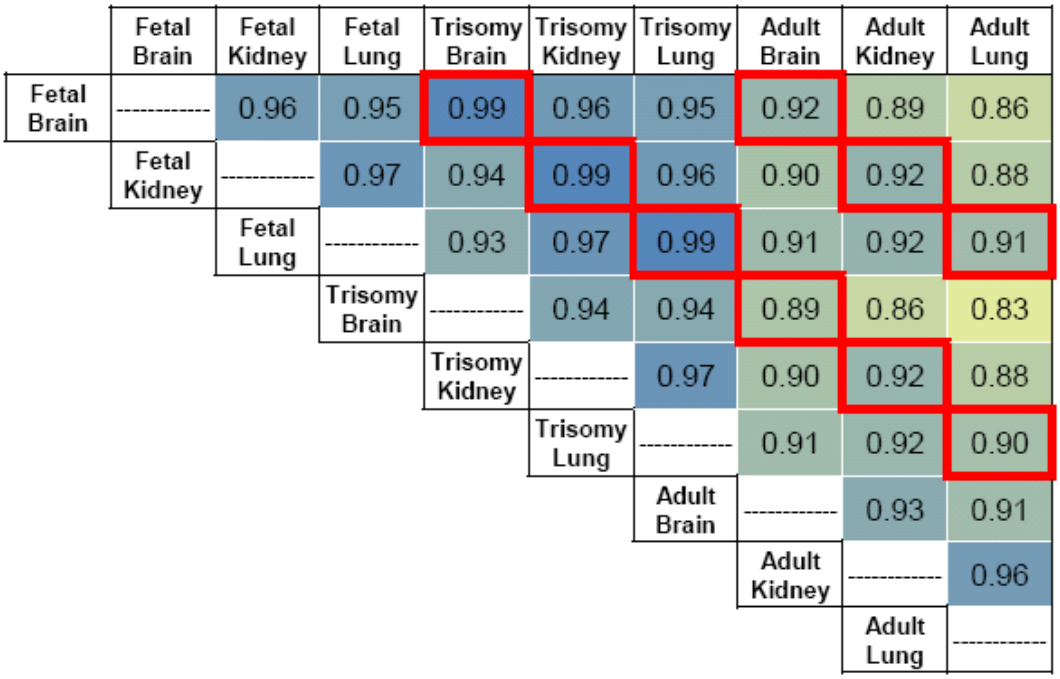

Figure 3.3. Correlations of average methylation β values between different tissues.

The correlation coefficients between paired tissues are indicated and can range from 0 (yellow) to 1 (blue). Boxes highlighted in red indicate the comparisons between the same tissue type by comparing control to trisomic tissues, or fetal to adult tissues. Trisomic and chromosomally normal fetal show high correlation relative to the same tissue at different developmental time points.

To identify significantly altered sites between fetuses and adult, we analyzed raw CpG methylation data using stringent criteria (FDR <5% and $\Delta\beta$ value >0.4). This high cut-off for average DNA methylation difference (more than double the suggested 0.17 β value difference) was applied to avoid any discrepancies arising from signal differences between arrays due to different hybridization efficiencies or different laboratory facilities performing the experiments (Bibikova *et al*. 2006). Using this approach, we identified 89 CpG loci representing 75 distinct genes for which DNA methylation status was different between fetal and adult tissues. We refer

to these as aDMRs for age-dependent differentially methylated regions. This represented 10% of the autosomal genes present in the Illumina GoldenGate DNA methylation arrays employed in the two studies (Figure 3.4A and B and Supplementary Table 3.3). Of these, only 4 loci (ALOX12_P223, APC_E117, GABRB3_P92 and PEG3_E496) showed significant (using our criteria) age related changes in all three tissues. More commonly, the aDMRs were specific for one tissue, with 24 such loci identified in brain, 11 in kidney, and 25 in lung (Figure 3.4A). Interestingly, these differentially methylated loci included some imprinted regions, such as *GABRB3*, *ZNF264* and *PEG3* (Supplementary Figure. 3.3A-C), in which DNA methylation is believed to play a central role in regulating allelic expression in a parent-of-origin manner during normal development (Beatty *et al*. 2006; Hogart *et al*. 2007; Huang and Kim 2009). There were also many immune-related genes (e.g. HLA-class II genes) that were hypermethylated in the fetus as compared to adult, presumably reflecting that the immune system is not yet developed fully in the fetus (Levy 2007).

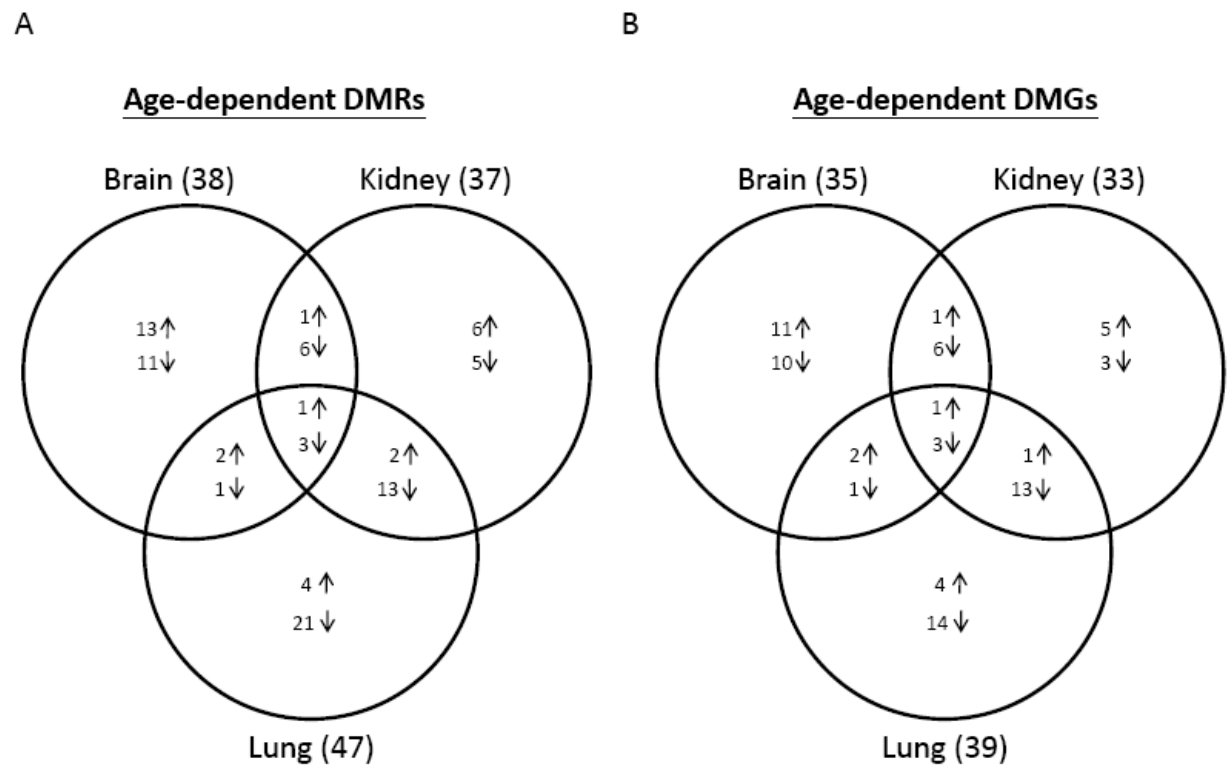

Figure 3.4. Venn diagram having the number of age-dependent methylated loci/genes between brain, kidney and lung.

(A) Among 89 age-dependent methylated loci (CpG sites) in total, only 4 loci were in common between tissues. (B) For the 75 associated genes in the 89 age-dependent methylated loci, only 4 genes were in common between tissues. Most aDMRs were specific for one tissue, with 24 such loci identified in brain, 11 in kidney, and 25 in lung. DMRs: differentially methylated regions, DMGs: differentially methylation genes. ↑ : Hypermethylated; ↓ : Hypomethylated.

Together, these data suggest that fetal-to-adult programmed DNA methylation changes occur in a variety of genes within specific tissues. To examine this tissue-specificity in more detail, we next focused on comparing tDMRs between fetal and adult tissues. While similar number of tDMRs was identified in fetus and adult (93 in fetus and 82 in adult), only 25 of those were in common (Supplementary Table 3.3). Moreover, of the 25 loci identified as tDMRs in both fetus and adult, only 16 of these had the same relative tissue-specific DNA methylation

pattern in both fetus and adult. Thus, only ~17% (16 out of 93) of fetal tDMRs remained as clear tDMRs in adult tissues. Similarly, 57 tDMRs in adult were not identified as differentially methylated in fetus (Figure 3.5). For example, PTPN6_E171 shows kidney-specific hypomethylation in adult, but is hypomethylated in all the tissues examined (brain, kidney, lung, skin and muscle) in the fetus. Furthermore, the fetal tissue-specific indicative loci MEST_P4 (for brain), CDH17_E31 (for kidney) and CRK_P721 (for lung) were not indicative of tissue origin in adult tissues (Figure 3.6). For example, MEST_P4 is specifically hypomethylated in fetal brain, but in the adult all tissues exhibit an intermediate level of DNA methylation consistent with genomic imprinting (Figure 3.6 and Supplementary Figure. 3.3D).

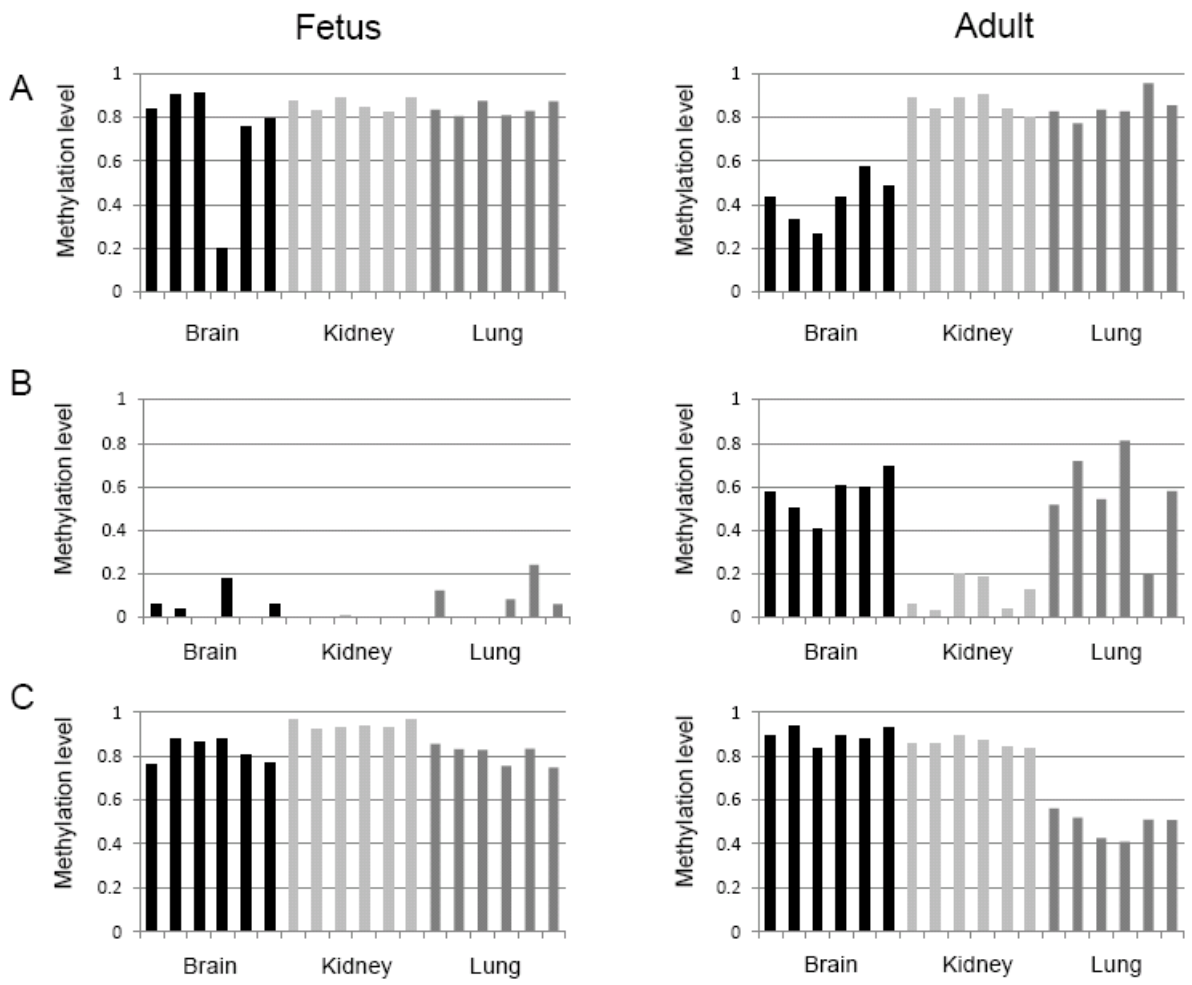

Figure 3.5. Lack of conservation of tissue-specific differentially methylated loci in fetus and adult.

Methylation level (β value) of (A) FGF1_P357 (B) PTPN6_E171 (C) MST1R_E42 in fetal and adult tissues is given. Each bar represents a different sample. Hypomethylation of FGF1_P357 in brain and MST1R_E42 in lung is specific to adult tissue, whereas hypomethylation of PTPN6_E171 observed in adult kidney represents the fetal status.

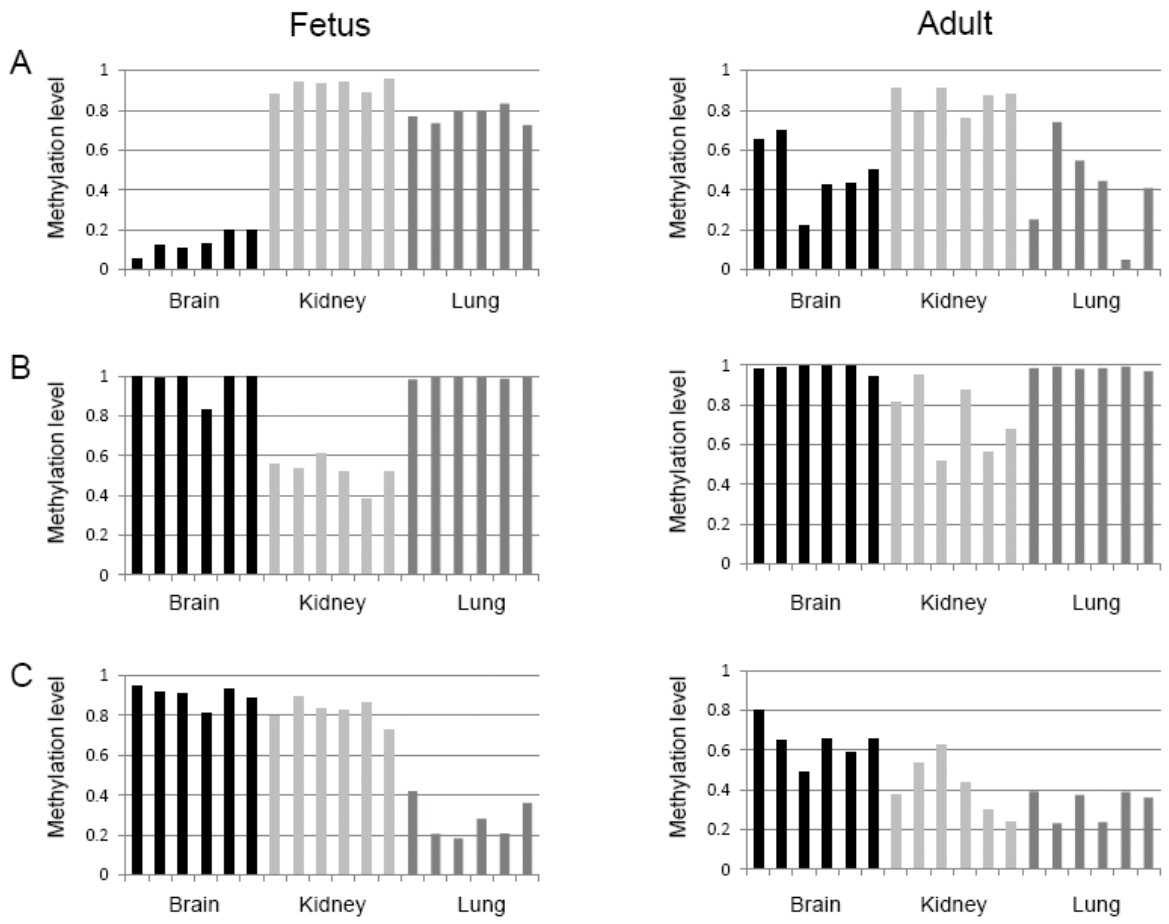

Figure 3.6. Lack of conservation in tissue-specific differentially methylated loci between fetus and adult.

Methylation level (β value) of (A) MEST_P4 of *MEST* gene, (B) CDH17_E31 of *CDH17* gene and (C) CRK_P721 of *CRK* gene in fetus and adult tissues. Each bar represents a different sample. Fetal tissue-specific indicator loci were not indicative of tissue origin in adult tissues.

To understand in a developmental context the general function of genes that are differentially methylated between fetus and adult, we carried out a Gene Ontology (GO) analysis using DAVID (Dennis *et al*. 2003; Huang da *et al*. 2009). Thus, we tested whether specific GO terms of the genes associated with one or more aDMRs were enriched when compared to the GO distribution of all the 752 autosomal genes associated with CpG sites present on the array that we analyzed. Using this approach, specific GO terms could be assigned to aDMR-associated groups of genes in all three tissues. For brain, there was no GO term enriched for the genes showing age-dependent DNA methylation. For kidney, enriched function was "positive regulation of steroid metabolic process" (p=0.00057). Lastly, for lung "atp-binding" (p=0.0013) was enriched for the differentially methylated genes. When we did a similar analysis of all aDMRs irrespective of tissue origin, we found that those genes associated with CpG sites that were hypomethylated in the adult compared to fetus were enriched in "NOD-like receptor signaling pathway" (p=0.000017), while genes associated with hypermethylated sites (increased DNA methylation in the adult) were enriched for "embryonic morphogenesis" (p=0.0019) (Table 3.2).

Table 3.2. Summary of differentially methylated loci between normal fetal and adult tissues

Tissue	No. of hyper loci	No. of hypo loci	Total aDMR	Total associated genes	GO terms	P-Value	FDR(%)
Brain	17	21	38	36	----------	----------	--------
Kidney	10	27	37	33	positive regulation of steroid metabolic process	0.00057	0.87
					transport	0.0042	4.7
					regulation of steroid metabolic process	0.0031	4.7
Lung	9	38	47	39	atp-binding	0.0013	1.6
					positive regulation of steroid metabolic process	0.0013	2
					positive regulation of lipid metabolic process	0.0015	2.3
					ATP binding	0.0022	2.5
					adenyl ribonucleotide binding	0.0023	2.7
					transport	0.0026	3
					adenyl nucleotide binding	0.0028	3.3
					nucleoside binding	0.003	3.5
					purine nucleoside binding	0.003	3.5
					nucleotide-binding	0.0035	4
All hyper*	29	--------	29	25	embryonic morphogenesis	0.0019	2.8
All hypo*	--------	60	60	50	NOD-like receptor signaling pathway	0.000017	0.018

*Redundant loci eliminated

Key:

Hyper: Hypermethylated

Hypo: Hypomethylated

3.3.4. Characteristics of differentially methylated loci

DNA methylation has been associated with variety of histone marks and protein binding targets (Brunner *et al*. 2009; Cohen *et al*. 2009; Straussman *et al*. 2009). Understanding how such features are associated with the temporal changes in DNA methylation may add insight into the regulatory process involved. To test if any chromatin features set up during embryonic stem (ES) cell stage might affect the fate of tDMRs and aDMRs, we also compared our DNA methylation data with previously published studies of H3K4me3 and H3K27me3 status and Polycomb group (PcG) protein binding targets in ES cells (Lee *et al*. 2006; Pan *et al*. 2007; Zhao *et al*. 2007).

Epigenetic marks associated with adult tDMRs showed both similarities and differences when compared with those associated with fetal tDMRs. The adult tDMRs were deficient in H3K4me3 regions (p=0.004) and CGI (p<0.0001), but were strikingly enriched amongst the loci that contained neither H3K4me3 nor H3K27me3 when compared with all genes studied (p<0.0001) (Figure 3.7A), which is consistent with a recent report by Byun *et al*. (Byun *et al*. 2009). While fetal tDMRs displayed similar characteristics (less prevalent in H3K4me3 regions, p=0.006 and in CGI, p<0.0001; more prevalent in regions with neither H3K4me3 nor H3K27me3, p<0.0001), they were less likely to involve loci containing PcG binding targets (p=0.006) and regions that were occupied by both H3K4me3 and H3K27me3 ('bivalent' regions) in ES cells (p<0.0001) (Figure 3.7A).

For the aDMRs, hypermethylated loci were only enriched in bivalent regions (p=0.03) (Figure 3.7B), while hypomethylated loci were enriched in regions lacking H3K4me3 or H3K27me3 (p<0.0002), but reduced in PcG binding regions (p<0.03), CGI (p<0.0001) and

bivalent regions (p<0.0002) (Figure 3.7B). The reduced number of hypomethylated loci in CGI was also revealed by plotting the DNA methylation distribution of all loci in CGI or non-CGI in fetus and adult independently (Supplementary Figure 3.4).

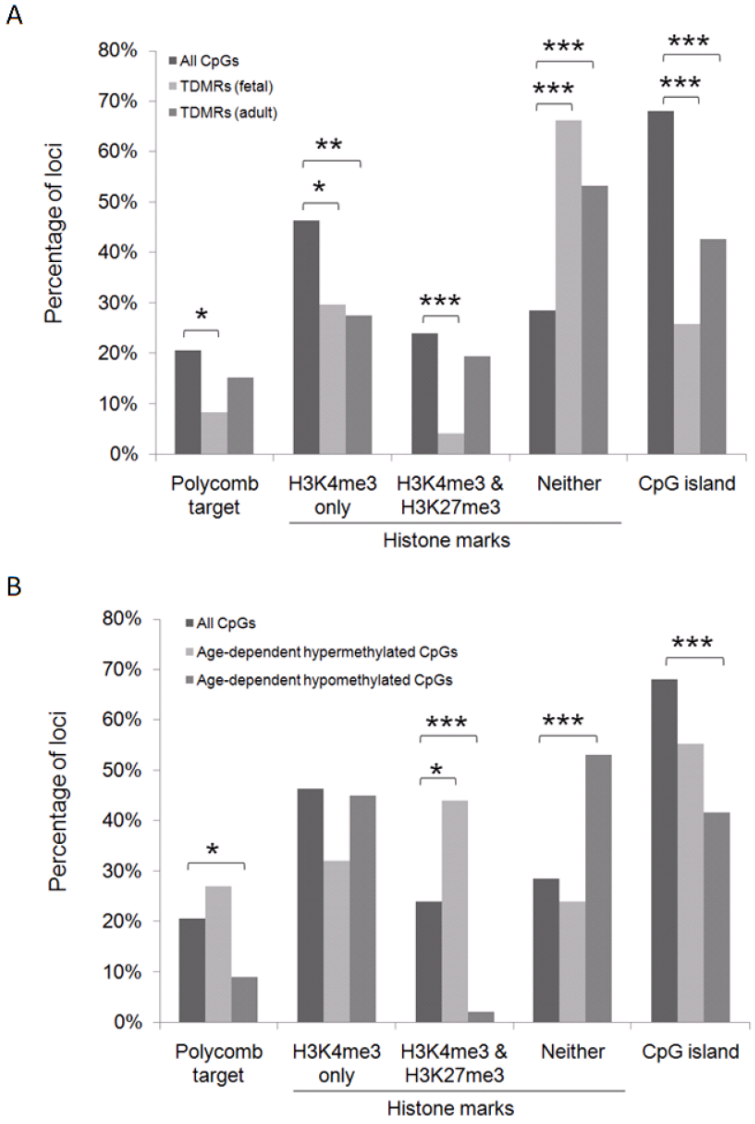

Figure 3.7. Characteristics of (A) tissue-specific differentially methylated regions (tDMRs) and (B) age-dependent differentially methylated regions (aDMRs).

The characteristics of Polycomb complex binding targets and histone marks were based on the previous report on ES cells while the CGI location information was available from Illumina. "*" represents p-value <0.05, "**" represents p-value <0.005 and "***" represents p-value <0.0005. Percentage of loci refers to the percentage loci in the microarray that contains the specified features.

3.3.5. Comparison to embryonic stem cells identified dynamic DNA methylation changes

The observed age-dependent DNA methylation changes may represent a distinct temporal program or instead simply reflect a continuum of change from ES cell-to-fetus-to-adult. To determine if the fetal DNA methylation profile was largely intermediate between stem cell and adult, the identified aDMRs were compared with the DNA methylation pattern of embryonic stem cells, obtained from another study using the same Illumina GoldenGate Methylation array (Calvanese *et al*. 2008). Methylation statuses of 571 CpG sites in the ES cells were reported from that study. Multiple patterns were observed with DNA methylation levels at some loci changing dynamically throughout development (Figure 3.8 and 3.9). For example, *RAB32* was *de novo* methylated in the fetus from ES cell but showed loss of DNA methylation in adult tissue (Figure 3.8A). In contrast, *HPN* showed loss of DNA methylation from ES cell to fetus but was hypermethylated in adult tissue (Figure 3.8B). This shows that DNA methylation changes dynamically during tissue development.

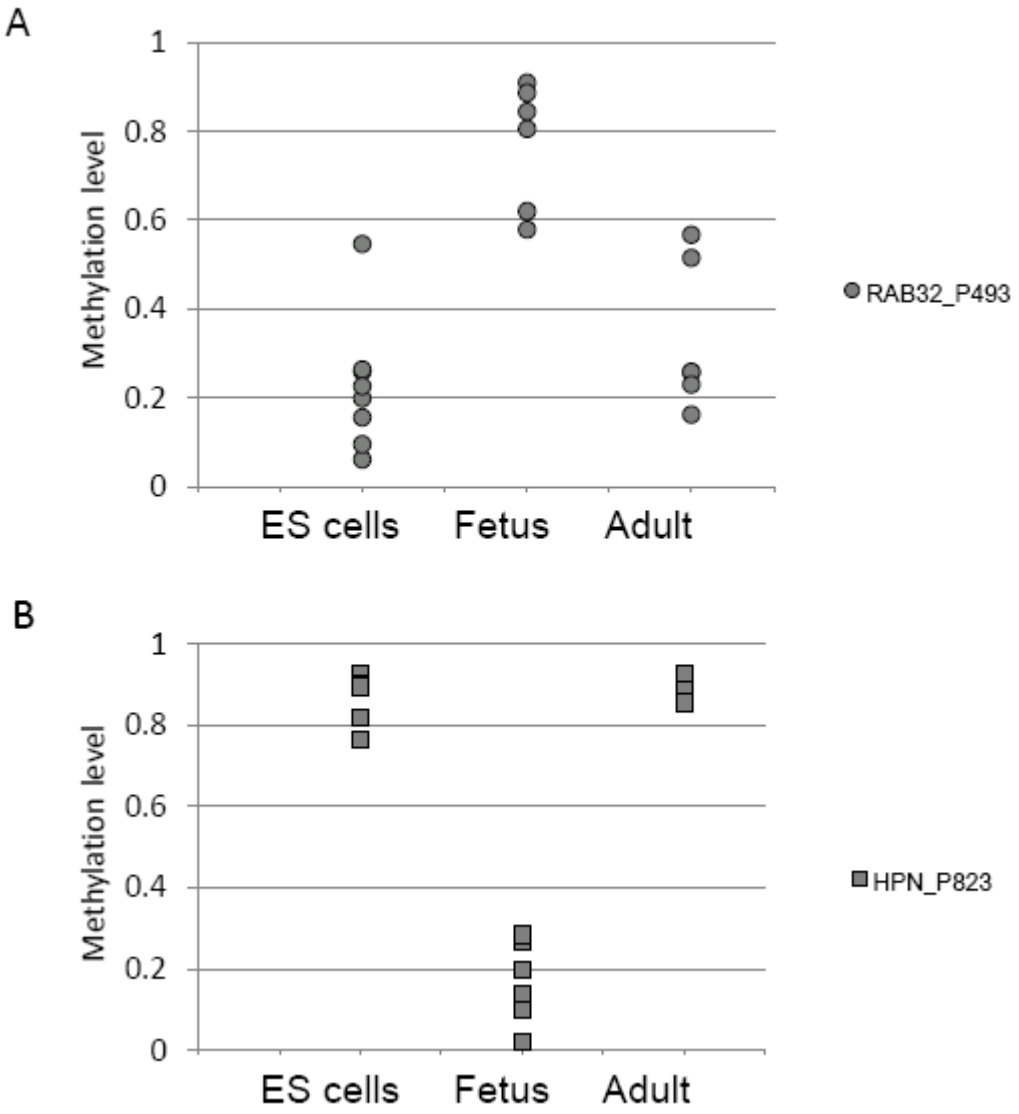

Figure 3.8. Dynamic changes of DNA methylation.

(A) RAB32_P493 shows hypermethylation in fetal brain, but hypomethylation in ES cells and adult brain. (B) HPN_P823 shows hypermethylation in ES cells and adult kidney, but hypomethylation in fetal kidney.

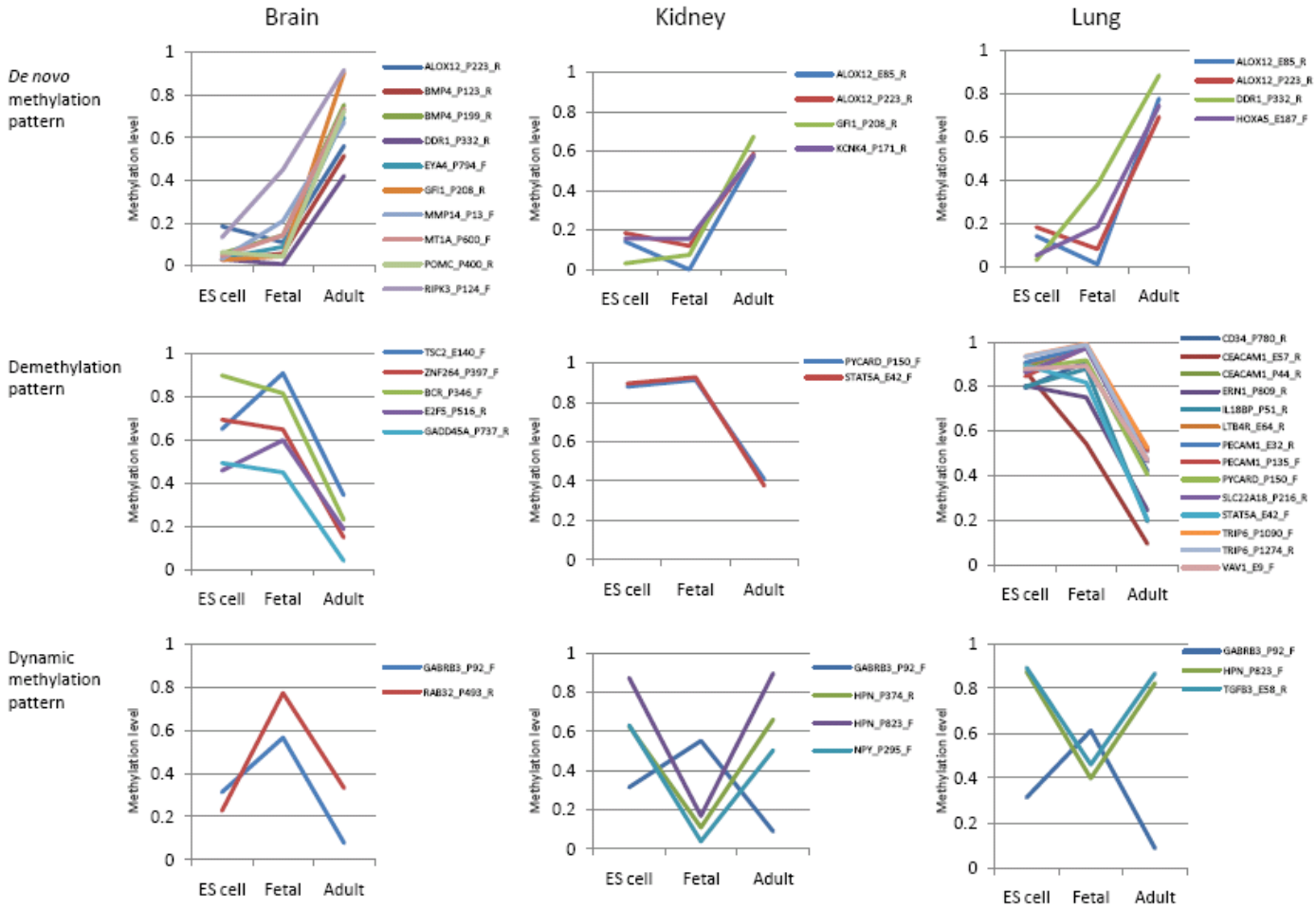

Figure 3.9. Patterns of DNA methylation changes from ES cell to adult tissues.

Examples are given of loci in different tissues that show either *de novo* methylation in adult tissue as compared to fetus and ES cell, demethylation in adult tissue as compared to fetus and ES cell or dynamic (changing) methylation pattern from ES cell to adult tissues. Each data point is an average of the methylation values observed for that site in either ES cell, fetal, or adult samples.

3.4. Discussion

The establishment and maintenance of tissue-specific gene expression profiles during development of multicellular organisms is tightly linked to a network of transcription factors and epigenetic modifications. Among the latter, DNA methylation is currently best understood, with a great number of tissue-specific differentially methylated regions (tDMRs) having been identified (Byun *et al*. 2009; Christensen *et al*. 2009; Eckhardt *et al*. 2006; Illingworth *et al*. 2008; Rakyan *et al*. 2008; Straussman *et al*. 2009), primarily in adult tissues. In particular, a recent high-throughput DNA methylation study of 11 somatic tissue from six individuals (age 35 to 60) provided valuable data for adult tissue- and individual-specific DNA methylation patterns (Byun *et al*. 2009). Here, we present several findings relevant to assessing the contribution of DNA methylation to tissue-specificity during the course of normal and abnormal development. First, we found clustering of fetal tissues according to their DNA methylation patterns, and identified DNA methylation marks that are indicative of tissue origin. Second, while distinct significantly altered DNA methylation marks were present in skin of fetuses with trisomy 18 and trisomy 21, overall these differences were much less dramatic than tissue and age related effects. Third, DNA methylation in adult tissues was remarkably different from that in fetal tissues, with these age-dependent changes being most often tissue-specific. This was also true for imprinted loci, suggesting an unexpected plasticity of these classical epigenetic marks. Lastly, the dynamic nature of DNA methylation marks became even more evident through comparisons to stem cells, with the most plastic regions being linked to bivalent histone modification domains. Collectively, this work not only complements recent studies identifying DNA methylation changes during aging in blood, but also expands the age-range of epigenetic interrogations in somatic tissues, as these have been previously primarily been done in adults.

Using an array-based approach, we were able to establish tissue-specific patterns of DNA methylation in fetuses from second trimester terminations. Unsupervised clustering clearly separated the five tissues interrogated here, confirming that distinct patterns of DNA methylation occur during early embryo or fetal development. Consistent with this, 23% of all sites included in the analysis were statistically significantly different between tissues and thus classified as tDMRs. Interestingly, tDMRs were more likely to reside in regions of low CpG density as opposed to CGIs, indicating that these regions are particularly receptive for the establishment of tissue-specific DNA methylation marks.

While fetal tissue-specific DNA methylation was generally maintained in pathological conditions caused by trisomy 18 and 21, these chromosomal abnormalities were associated with epigenetic differences. Specifically, we identified 17 hypermethylated loci in the skin of T18, 7 hypermethylated loci in the skin and 1 hypermethylated locus in the muscle of T21. Interestingly, none of the loci with an altered DNA methylation pattern was located on the affected chromosome (chromosome 18 or 21). This suggests that the extra chromosome may exert a trans-acting effect to change the overall epigenetic patterning of the genome and is consistent with the global disruption in gene expression reported in association with trisomy and a recent study of genome-wide DNA methylation of leukocytes with trisomy 21 (Dauphinot *et al*. 2005; FitzPatrick *et al*. 2002; Kerkel *et al*. 2010; Saran *et al*. 2003). Many of the differentially methylated genes were related to developmental processes and immune response, perhaps reflecting an important functional difference between normal and trisomic tissues. The lack of obvious DNA methylation differences in brain, kidney and lung between normal and trisomic fetuses may be in part due to our somewhat low sample size (4 cases of T18 and 5 cases of T21) or the relatively small number of CpG loci interrogated here.

In contrast to the relatively subtle changes in DNA methylation associated with the two trisomies, DNA methylation changes occurring over time in normal development were much more pronounced. In total, 10% of the investigated genes had striking changes in DNA methylation between somatic tissues (brain, lung and kidney) of second-trimester fetus compared to adult. As a high statistical stringency was used to avoid technical artefacts, even more differences would be expected when applying less strict criteria. While cellular composition of each tissue may also change with time, the dramatic differences in DNA methylation between fetus and adult would require major changes in cell composition to explain. However, it may be worth noticing that the study is based on the comparison between fetal samples originating from a small time window with adult samples of wide range of ages (age 35 to 60), so there is naturally greater variation in the age of adults than in 2nd trimester fetuses. This may explain the wider variation of DNA methylation observed in adult tissues (Figure 3.5 and 3.6). Furthermore, while SNPs and sequence repeats overlapping with some probes present on the array may potentially interfere with DNA methylation analysis (Byun *et al*. 2009), DNA sequence polymorphisms would be unlikely to cause the consistent large DNA methylation differences observed between groups. In accordance with this, we did not find an enrichment of known SNPs and repeats located in the differentially methylated loci we identified (p=0.92).

Focusing more specifically on tDMRs that differ between fetal and adult tissues supports of the existence of extensive reprogramming of the epigenome occurring during development. Many tDMRs (~80%) identified in the fetus were no longer distinctly methylated in the same tissue-specific pattern in adult. This suggests that the tissue-specific DNA methylation, and likely expression of these genes, is required only at an early stage of development and thus, not maintained in the adult. It is possible that the loss of fetal tDMRs was due either to the reduced

function of DNA methyltransferases (Richardson 2003), or responses to the changing environmental influences, and/or stochastic changes which occur over time (Christensen *et al*. 2009). However, the emergence of some tDMRs in adult that were not present in the fetus suggests that tDMRs also result from major programmed developmental changes occurring postnatally.

One clue as to the significance of re-programming of tDMRs might emerge from the differences in associated biological functions, depending on whether these tDMRs were hypo- or hypermethylated in adult relative to fetus. The age-dependent hypermethylated loci (i.e. those that are most likely associated with a decreased gene expression in the adult) were enriched for genes involved in embryonic morphogenesis, perhaps reflecting a decreased need for such genes to be expressed in fully differentiated adult tissue. Age-dependent hypomethylated loci were enriched for immune response which may reflect the general activation of the immune system after birth.

Mechanistically, chromatin features set in embryonic stem cells might be linked to developmental plasticity of tDMRs. Both fetal and adult tDMRs were deficient in H3K4me3 regions and CGI while were more prevalent for regions lacking H3K4me3 or H3K27me3, suggesting that tDMRs are identified by other epigenetic marks. Specifically, tDMRs from fetal tissues were less enriched for bivalent chromatin domains, which are characterized by the coexistence of an activating H3K4me3 mark and repressive H3K27me3 mark. These domains likely function to silence genes encoding developmental regulators while simultaneously keeping them 'poised' for activation in ES cells (Bernstein *et al*. 2006). Fetal tDMRs also less often contained PcG protein binding regions, another hallmark of bivalent domains. PcG proteins are important regulators of cellular development and differentiation (Lee *et al*. 2006). In contrast,

there is no significant enrichment of either bivalent chromatin domains or PcG protein binding regions in adult tDMRs. Together, these findings suggest two conclusions. First, tDMRs present at the fetal stage might regulate processes other than differentiation. Second, the mechanism for tissue-specific regulation of gene expression might differ between developmental stages. However, these conclusions should be taken with caution given that the actual DNA methylation status of the ES cells being investigated has not been taken into account. Further investigation is needed to confirm our conclusions.

These principles are further supported by the observation that CpG loci undergoing DNA methylation changes between fetal and adult tissues often have a distinct DNA methylation pattern in embryonic stem cells. For example, while it might be expected that *de novo* DNA methylation of genes bound by PcG proteins in ES cells would be irreversible to permanently silence their expression, we found dramatic plasticity at these loci during development. This is well illustrated by *RAB32*, which showed considerable increase in DNA methylation during the transition from ES cells to fetal brain but then lost DNA methylation in the adult tissues. Thus, DNA methylation is not only reversible during development but can be changed in a non-linear, dynamic fashion throughout life. These changes may occur through passive or active processes. These data have important practical implications for DNA methylation studies. Specifically, the developmental plasticity of DNA methylation emphasizes the necessity of using age-matched case-control subjects for epigenetic studies and considering in what age group the hypothesized differences may be most apparent.

In addition to bivalent chromatin domains being associated with differences between fetal and adult tDMRs, we identified several imprinted loci associated with differential DNA methylation during development. In general, imprinted genes are associated with DMRs that

exhibit ~50% DNA methylation, corresponding to their parent-of-origin allelic gene expression pattern. These DMRs are generally classified as either primary (gametic) imprints, inherited from the gametes and maintained throughout tissue differentiation, or secondary DMRs, which are generally assumed to be acquired prior to or during tissue differentiation (Reik and Walter 2001). Although it has been reported that DNA methylation of imprinted genes can moderately change during aging (Bjornsson *et al*. 2008; Christensen *et al*. 2009) and tissue- and developmental-specific imprinting of *Igf2* has been reported in mouse (Feil *et al*. 1994), this may be more common than previously appreciated.

Here we found strong evidence for an erosion of methylation over time for CpGs associated with the promoter regions of several imprinted genes such as *GABRB3* and *ZNF264*, having an average of ~50% methylation in the fetus but only ~5% in different adult tissues (for some sites this occurred in all tissues while for others this was only in one specific tissue). Interestingly, *GABRB3* is biallelically expressed in normal brain, including newborns, but is imprinted in some cases of autistic-spectrum disorders (Hogart *et al*. 2007). Although we did not measure allelic expression of *GABRB3* in our fetal samples, the approximately 50% DNA methylation at the *GABRB3* locus is indicative of it being imprinted early in fetal development. This then postulates that the early imprinting would have to be erased in brain perinatally to establish biallelic gene expression reported in newborns and adults. Although speculative, it is interesting to consider that autistic disorders might be linked to the maintenance of parent-of-origin allelic expression of *GABRB3* due to a failure to erase the fetal imprint.

In addition to loss of imprinting, we also identified gain of DNA methylation at imprinted loci, suggesting that imprinting can be established later in development long after tissue-differentiation. For example, *MEST* (Region 1 in Chapter 2) was unmethylated in fetal brain and

highly methylated in fetal lung, but had the expected 50% DNA methylation in both adult brain and lung. Thus, DMRs associated with imprinted genes can not only be tissue-specific but also modulated during the transition from second-trimester to postnatal development. This unexpected plasticity raises the possibility that the number of imprinted genes in our genome may greatly exceed those yet identified, as the correct tissue and time point in development may be needed to assessed to detect their presence.

While the full biological significance of dynamic changes in tissue-specific DNA methylation over time has yet to be elucidated, the patterns and magnitude of differences indicate that many of the changes observed here are programmed rather than stochastic changes (Figure 3.9). Obtaining well matched normal human samples over different developmental stages is difficult, thus, more detailed investigations in model organisms such as mouse are needed. Nonetheless, the investigation of fetal pathologies such as trisomy 18 and 21 cannot be fully replicated in other organisms and these results suggest that epigenetic changes between disease groups can be identified, as long as there is careful control for all confounding factors such as gestational age and consideration of the effects of tissue composition. These data also suggest that caution should be used in applying DNA methylation analysis to prenatal diagnosis (e.g. to diagnose disorders of genomic imprinting) without prior confirmatory studies demonstrating the predictive value of such prenatally determined DNA methylation.

Chapter 4: Human placental-specific epipolymorphism and its association with adverse pregnancy outcomes[4]

4.1. Introduction

Gene expression within various human tissues displays inter-individual variability that can contribute to phenotypic variation (Morley *et al*. 2004; Sood *et al*. 2006; Whitney *et al*. 2003). Some of this variability is due to DNA sequence differences, such as single nucleotide polymorphism (SNP) and copy number variation (CNV) (Pastinen and Hudson 2004), while environmentally mediated or stochastic effects on epigenetic programming may also affect gene expression (Pastinen and Hudson 2004). Investigation of monozygotic twins suggests a genetic contribution to gene expression variation (Cheung *et al*. 2008; Cheung *et al*. 2003); however, non-Mendelian inheritance of allelic variation is also observed (Pastinen *et al*. 2004; Serre *et al*. 2008). A large-scale analysis of allele-specific gene expression showed that allelic differences in expression level may affect up to 50% of human genes (Lo *et al*. 2003). As only a small fraction of genetic polymorphisms are located in gene regulatory regions, epigenetic variation, that is independent of local sequence changes, may also contribute to a significant portion of variation in gene expression.

DNA methylation is a well-characterized form of epigenetic modification in mammals, and methylation of CpG sites in the promoter regions of genes can critically affect transcriptional regulation (Bird 2002). However, evidence for a gene silencing effect of promoter DNA methylation mainly comes from cancer studies, while this relationship in normal tissues has been

[4] A version of Chapter 4 has been published. Yuen RKC, Avila L, Peñaherrera MS, von Dadelszen P, Lefebvre L, Kobor MS, Robinson WP. (2009) Human placental-specific epipolymorphism and its association with adverse pregnancy outcomes. PLoS One. 4(10):e7389.

less clear (Illingworth *et al.* 2008; Walsh and Bestor 1999). Identifying a correlation between gene expression and promoter methylation compared across normal tissues may be confounded by the presence of multiple tissue-specific differentially methylated regions (tDMRs), as well as presence of other tissue-specific regulatory factors that affect the level of expression (Pastinen and Hudson 2004). Also, some tDMRs exhibit a composite methylation pattern, i.e. a mix of methylated and unmethylated alleles, possibly due to cellular heterogeneity. Even if DNA methylation silences the promoter completely, large changes in gene expression level may not be observed (Illingworth *et al.* 2008). Thus, identifying distinct DNA methylation differences among individuals within a particular tissue would be useful for demonstrating the regulatory role of DNA methylation on gene expression.

While DNA methylation variation at specific loci, such as imprinted genes, genes on the X-chromosome and transposable elements has been reported (Busque *et al*. 1996; Carrel and Willard 2005; McMinn *et al*. 2006; Sandovici *et al*. 2005; Sandovici *et al*. 2003), inter-individual differences in DNA methylation for other genes in human tissues is less well-studied. A genome-wide study of inter-individual DNA methylation variation in the human germline revealed that DNA methylation differences can be established during development (Flanagan *et al*. 2006). Skewed allelic expression associated with sequence-dependent DNA methylation has also been reported (Kerkel *et al*. 2008). Further understanding of the extent of tissue-specific methylation variability, its etiology, and its role in affecting gene expression variation is needed.

We hypothesize that sequence-independent effects on DNA methylation set in early development may contribute an additional layer to human phenotypic variation. In order to identify distinct DNA methylation differences between individuals and assess the regulatory role

of DNA methylation on gene expression and phenotypic variation, we surveyed the human genome using the Illumina GoldenGate Methylation Cancer Panel I. We chose to study placenta as it plays a vital role in human health due to its essential role in regulating fetal growth and development and the long term consequences of *in utero* development on disease in adulthood (Godfrey 2002). In addition, placenta has been reported to have high variability in overall DNA methylation compared to other tissues as investigated by the same Illumina methylation array (Houseman *et al*. 2008), and increased epigenetic variability in the placenta may have evolved in response to its role in mediating the conflicting demands of mother and fetus (Constancia *et al*. 2004). Although the Illumina GoldenGate Methylation Cancer panel I targets mainly cancer-related genes, the pseudomalignant nature of the placenta makes it suitable for this study (Chiu *et al*. 2007; Novakovic *et al*. 2008).

4.2. Methods

4.2.1. Sample collection

This study was approved by the ethics committees of the University of British Columbia and the Children's & Women's Health Centre of British Columbia. Samples from 128 placenta were collected from Vancouver BC Children's & Women's Hospital with informed consent from individuals. Clinical information was collected on prenatal findings, pregnancy complications and birth parameters (gestational age, sex, birth weight etc). Preeclampsia was defined as at least two of the following: (1) hypertension (systolic blood pressure ≥140mmHg and/or diastolic blood pressure ≥90mmHg, twice, >4h apart) after 20 weeks, and proteinuria defined as ≥0.3g/d or ≥2+ dipstick proteinuria after 20 weeks, (2) non-hypertensive and non-proteinuric HELLP syndrome or (3) an isolated eclamptic seizure without preceding hypertension or proteinuria.

Intrauterine growth retardation (IUGR) was defined as either (1) birth weight <3rd percentile for gender and gestational age using Canadian charts, or (2) birth weight <10th percentile with either: (a) persistent uterine artery notching at 22+0 to 24+6 weeks gestation, (b) absent or reversed end diastolic velocity on umbilical artery Doppler, and/or (c) oligohydramnios (amniotic fluid index <50mm). At least two sites were sampled from each placenta. DNA was extracted and RNAlater (Qiagen) was added for follow up RNA extraction. First-trimester normal placental tissues, peripheral blood samples from normal individuals and fetal tissue biopsies from abortuses were obtained with review board approval and were anonymous to individual identifiers. Outbred mouse placental tissues were obtained from pregnant mice with institutional animal ethics approval.

4.2.2. DNA methylation analysis

Bisulfite modification of 500ng of genomic DNA was performed using the EZ DNA Methylation Kit (Zymo Research) according to the manufacturer instructions. After bisulfite treatment, DNA samples were subjected to the Illumina GoldenGate methylation Cancer Panel I array-based assay, using Illumina-supplied reagents and conditions. A β-value of 0 to 1 was reported for each CpG site, signifying the percentage of methylation, from 0% to 100%. β-values were calculated by subtracting background with use of negative controls on the array and taking the ratio of the methylated signal intensity to the sum of both methylated and unmethylated signals.

To identify genes with the most highly variable distribution of methylation values, the variance of β-values among placentas was calculated for each CpG site, as well as the standard deviation of this value relative to the mean variance observed for all CpGs. Those sites with

variance values >1.5 standard deviation from the mean were considered to be "highly variable". To then select for findings not likely to be due to artefact (such as variable hybridization or local sequence variants), only genes with at least two associated highly variable CpGs were considered. The identified pairs of highly variable CpGs associated with the same gene tended to show a good degree of correlation of methylation values and several appeared to have a bimodal distribution in methylation values suggestive of on/off methylation. Four autosomal genes which had the highest correlation in methylation values between the two associated CpGs were selected for follow-up confirmation. Methylation-unbiased PCR and sequencing primers were designed based on the sequences from Illumina probes on the CpG site (Supplementary Table 4.1). Pyrosequencing was performed on a Biotage PSQ HS96 Pyrosequencer and the quantitative levels of methylation for each CpG dinucleotide were evaluated with Pyro Q-CpG software (Biotage). A test run for each assay was performed in triplicate to confirm reproducibility. For clonal bisulfite pyrosequencing, PCR product from individual samples was generated by non-biotinated primers (Supplementary Table 4.1) and subsequently TA-cloned into pGEM-Teasy vector (Promega). Individual clones were picked and analyzed by pyrosequencing as described.

4.2.3. SNP genotyping

Multiplex genotyping on genomic DNA was performed by iPlex (Sequenom) in Quebec Genome Centre. Primer sequences for individual SNP genotyping are available upon request. The primer extended products were analyzed and the genotypes determined by mass spectrometric detection using the MassARRAY Compact system (Sequenom). For *Bst*UI predigestion assay followed by pyrosequencing on *TUSC3*, 200ng of genomic DNA was digested with 100 units of *Bst*UI (New England Biolabs) for 18 hours. 20 ng was used for PCR

and *ID2* was used as internal control for validation of complete enzyme digestion in each sample. Pyrosequencing was performed on a Biotage PSQ HS96 Pyrosequencer and the relative levels of allele for the SNP were evaluated with PSQ96MA SNP analysis software (Biotage). Genotyping on mRNA was carried out either with cDNA prepared using Omniscript Reverse Transcriptase Kit (Qiagen) followed by iPlex (Sequenom) or one step RT-PCR (Qiagen) followed by sequencing or pyrosequencing. Primers for the one step RT-PCR assays were designed to span at least one intron (Supplementary Table 4.1). PCR without reverse transcriptase was performed on each sample to confirm no genomic DNA contamination.

4.2.4. Statistical analysis

All the statistical analysis in this study was performed using VassarStats (http://faculty.vassar.edu/lowry/VassarStats.html).

4.3. Results

4.3.1. Identifying genes with "on-or-off" polymorphic DNA methylation

Using the Illumina GoldenGate methylation Beadarray, we initially investigated DNA samples from whole villi (fetus side) of 13 normal placentas (5 female and 8 male) without pregnancy complication. To identify probes (CpG sites) that have distinct classes of DNA methylation levels among placentas, we first calculated the variance of the β-value (proportional to level of DNA methylation) for each probe. The majority of sites (1210 of 1505) showed very little variability (variance <0.01) (Figure 4.1) and these were generally either always methylated or always unmethylated. However, the distribution of variances has a broad tail and many sites showed extremely variable methylation patterns. While not all CpG sites associated with a single

gene necessarily are expected to be methylated similarly, to reduce the probability of variability due to technical artefact or to SNPs in the associated primer sequences, we identified genes for which at least 2 associated CpG sites demonstrated a β-value variance greater than 1.5 SD from the mean variance for all samples. Using this criterion, 19 out of 576 genes that had probes targeting two or more CpG sites were identified as having highly variable DNA methylation among individual placentas (Figure 4.2A). Among these 19 genes, 14 genes are located on the autosome while 5 are on the X chromosome. As expected, methylation at these X-linked sites (all in gene promoter regions) correlates with sex of the placental sample (i.e. higher methylation in female than in male) given that promoter DNA methylation is enriched on the inactive X chromosome of females (Weber *et al*. 2007). Detection of additional X-linked genes was limited by our strict criteria for this screen (i.e. two sites, both >1.5 SD above the mean). *WT1*, an imprinted gene with polymorphic imprinting in placenta (Jinno *et al*. 1994), was detected, which further validates this approach. Variable DNA methylation identified at another imprinted gene, *MKRN3* (Supplementary Figure 4.1A), suggests it may also be polymorphically imprinted in placenta.

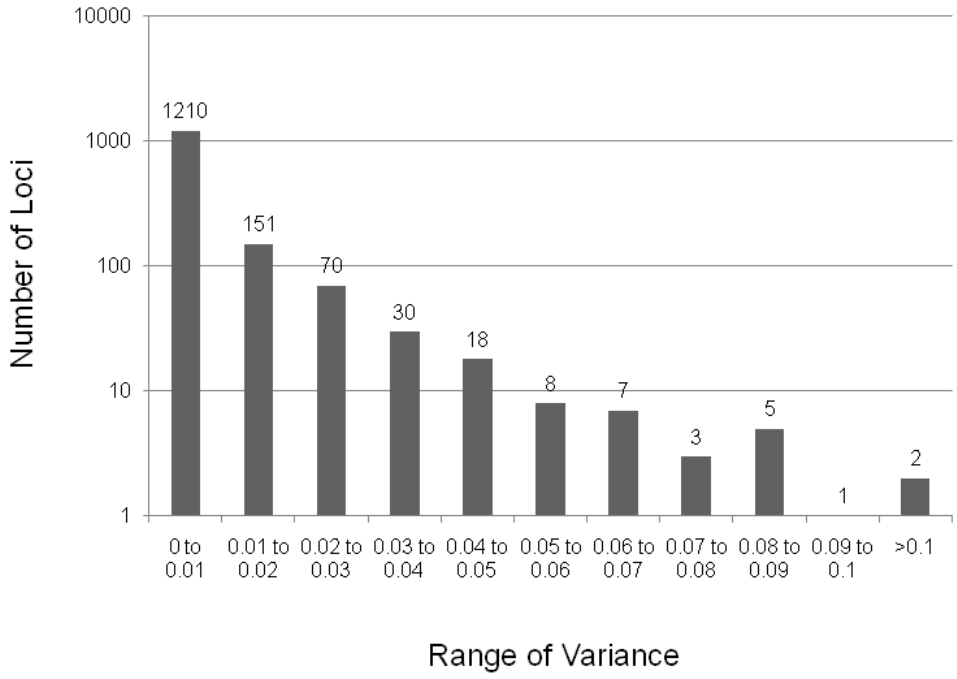

Figure 4.1. Frequency distribution of DNA methylation variances for 1505 CpG sites in 13 normal placental samples.

The average variance is 0.007. The value for 1.5 SD above the mean variance is 0.025. There are 106 CpG sites with variance greater than 1.5 SD.

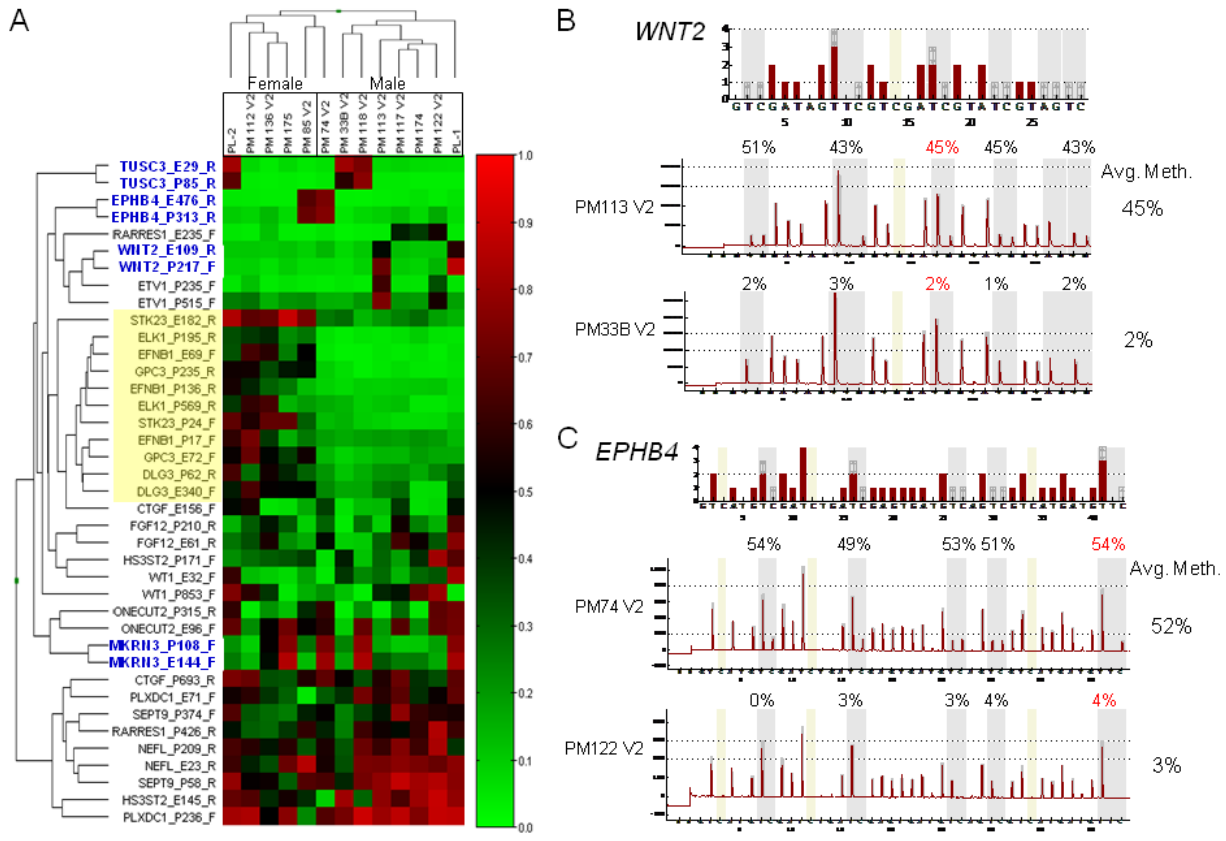

Figure 4.2. Genes exhibiting high inter-individual variance in methylation values in the human placentas.

(A) Heat-map of 19 genes with at least 2 probes having methylation variance greater than 1.5 SD from the mean. Probes and sample names are shown and with hierarchical clustering of beta values based on 1-r (Illumina Beadarray software). A beta value of zero (indicated in bright green) represents an unmethylated locus and one (indicated in bright red) represents a methylated locus. Probes for genes on the X chromosome are highlighted by a yellow box and the probes being further investigated here are bolded in blue. (B and C) Validation of variable methylation by bisulfite pyrosequencing for (B) *WNT2* and (C) *EPHB4*. CpG sites that are targeted by the Illumina probes are highlighted in red. One methylated sample and one unmethylated sample are shown for each gene. Reference pyrograms are shown on top.

We chose three autosomal genes which had the most concordant methylation patterns between the two associated CpG sites assayed for further follow-up: *WNT2*, *EPHB4*, and *TUSC3* (Figure 4.2A). These genes also appeared to have a bimodal distribution of methylation suggestive of an on/off switch. The methylation pattern for these genes was confirmed and quantified more accurately by gene-specific bisulfite pyrosequencing using primers without any known SNP or CpG site bias (Figure 4.2B, Supplementary Figure 4.1B). A similar methylation level was found for every CpG investigated within the sample group with around 50% methylation in "methylated" cases and almost no methylation in "unmethylated" cases (Figure 4.2B, Supplementary Figure 4.1B). No within-placenta variability was observed as different sites sampled from the same placenta always displayed concordant methylation levels (Supplementary Figure 4.2). We further investigated samples from more than 100 placentas by the Illumina array (49 placentas run on separate Beadarrays than the original set) and bisulfite pyrosequencing (all placentas). Using the same threshold to search for distinct methylation polymorphism, 12 genes met the criteria in the Illumina methylation analysis of the additional 49 placental samples (Supplementary Figure 4.3A). Nine out of the 12 genes, including *TUCS3* and *WNT2*, were in common with those found in the initial analysis of 13 placental samples. Although *EPHB4* did not meet the variance cut-off observed in the initial set, distinct polymorphic methylation was observed with 3 of the 49 samples exhibiting a "methylated" state (Supplementary Figure 4.3B). The lower variance was thus a consequence of the lower frequency of "methylated" alleles in the larger sample set. All samples for the initially identified three CpGs could be classified as "methylated" or "unmethylated" (i.e. the distribution of values was again distinctly bimodal) and the methylation frequency (ratio of number methylated cases to total number cases) for these genes ranged from 0.07 to 0.25 (Table 4.1).

Table 4.1. Correlation between MAP and clinical status

Gene Name	M/U	Total	MF	MA (year)	GA (week)	BW (g)	Gender (M:F)	IUGR	No IUGR	*p*-value	EOPET	LOPET	No PET	*p*-value
EPHB4	M	9	0.07	33.0	36.9	2878.3	4:5	2	7	1.00	1	1	7	1.00
	U	115		34.6	36.9	2802.0	56:59	30	85		15	17	83	
TUSC3	M	31	0.25	34.5	36.2	2776.7	15:16	10	21	0.48	3	9	19	<0.05
	U	91		34.3	37.1	2836.3	48:43	22	69		13	9	69	
WNT2	M	25	0.20	33.6	37.7	3100.7	12:13	3	22	0.08	1	4	20	0.37
	U	97		34.7	36.6	2715.5	46:51	29	68		15	14	68	

M = Methylated;
U = Unmethylated;
MF = Methylation frequency (Number of methylated cases / Total number of cases);
MA = Maternal age;
GA = gestational age;
BW = birth weight;
EOPET = early onset preeclampsia (<34 weeks' gestation);
LOPET = late onset preeclampsia (≥34 weeks' gestation)

4.3.2. Correlation of DNA methylation and gene expression

Since the average methylation level of the CpGs in those cases classified as "methylated" was close to 50% based on bisulfite pyrosequencing, we speculated that the DNA methylation may cause allele-specific variation in gene expression. Therefore, heterozygous SNPs in the coding regions of these genes were identified and the genotype of DNA and cDNA extracted from the same placenta were compared by primer extension assay (Figure 4.3 and 4.4). Clonal bisulfite pyrosequencing of the *WNT2* promoter demonstrated monoallelic DNA methylation in the methylated cases (Figure 4.3B). Furthermore, biallelic gene expression was observed in the unmethylated cases, while monoallelic expression was found in the methylated cases (Figure 4.3C, Supplementary Figure 4.4). A similar observation was found for *EPHB4* (Figure 4.4). To determine the relationship between promoter DNA methylation and gene expression, we identified four cases heterozygous for SNP rs12550009 located within the 5' UTR of *TUSC3* (Figure 4.5A). Methylation-sensitive enzyme digestion followed by pyrosequencing genotyping revealed allele-specific methylation of the "T" alleles in the two of these cases which were methylated at this gene (Figure 4.5D). Genotyping cDNA with pyrosequencing using RNA-specific RT-PCR primers demonstrated biallelic expression in the unmethylated cases while the "C" alleles were predominantly expressed in the methylated cases. Thus, lack of DNA methylation of the gene promoter is correlated with gene expression. Unlike the sequence-dependent allele-specific DNA methylation described in another study (Kerkel *et al*. 2008), the present polymorphic DNA methylation had no correlation with the genotypes of the SNPs (Supplementary Table 4.2). To distinguish this on-off type of epigenetic polymorphism, we suggest a term called Methylation Allelic Polymorphism (MAP). This term can generally be used

to apply to any polymorphic methylation, including that attributable to imprinting or local sequence effects, as well as that due to other causes (stochastic, environment etc).

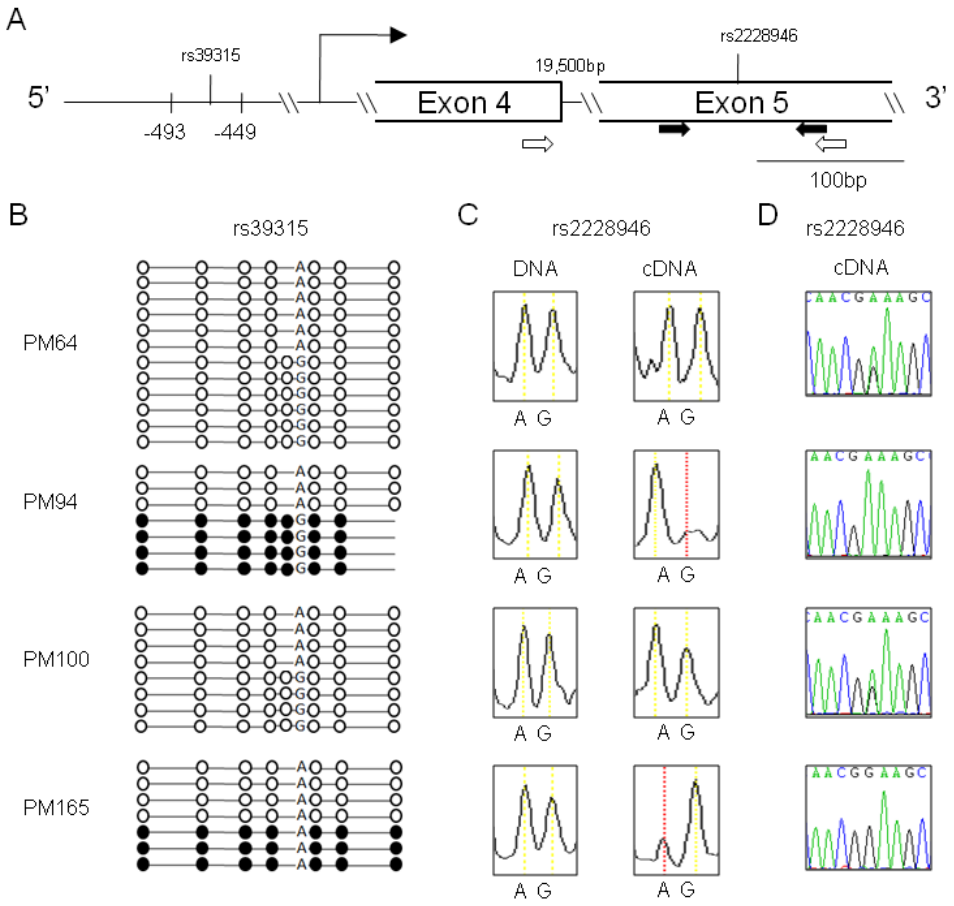

Figure 4.3. Allele-specific DNA methylation and mRNA expression of *WNT2*.

(A) Schematic of the *WNT2* locus showing the regions investigated by clonal bisulfite pyrosequencing of the promoter (-493 to -449 relative to the transcriptional start site according to NM_003391) and genotyping assays within exon 5. PCR primers for DNA and cDNA genotyping by iPlex are indicated by black arrows while RT-PCR primers for mRNA genotyping are indicated by arrows highlighted in white. (B) Bisulfite pyrosequencing of single clones from four placental samples. The A/G polymorphism of SNP rs39315 is indicated. Each row represents one clone and each circle represents one CpG. Methylated CpGs are shown in black while unmethylated CpGs are shown in white. The presence of a cytosine proximal to this A/G SNP site creates a polymorphic CpG site. (C) Allele-specific expression of *WNT2* based on the analysis of the A/G allele of rs2228946 in DNA and cDNA by iPlex. Peak height of the alleles corresponds to the relative amount of alleles present in the sample. (D) Validation of allele-specific expression of *WNT2* by cDNA-specific primers. Double peaks are observed in unmethylated samples while single peaks are found in methylated samples.

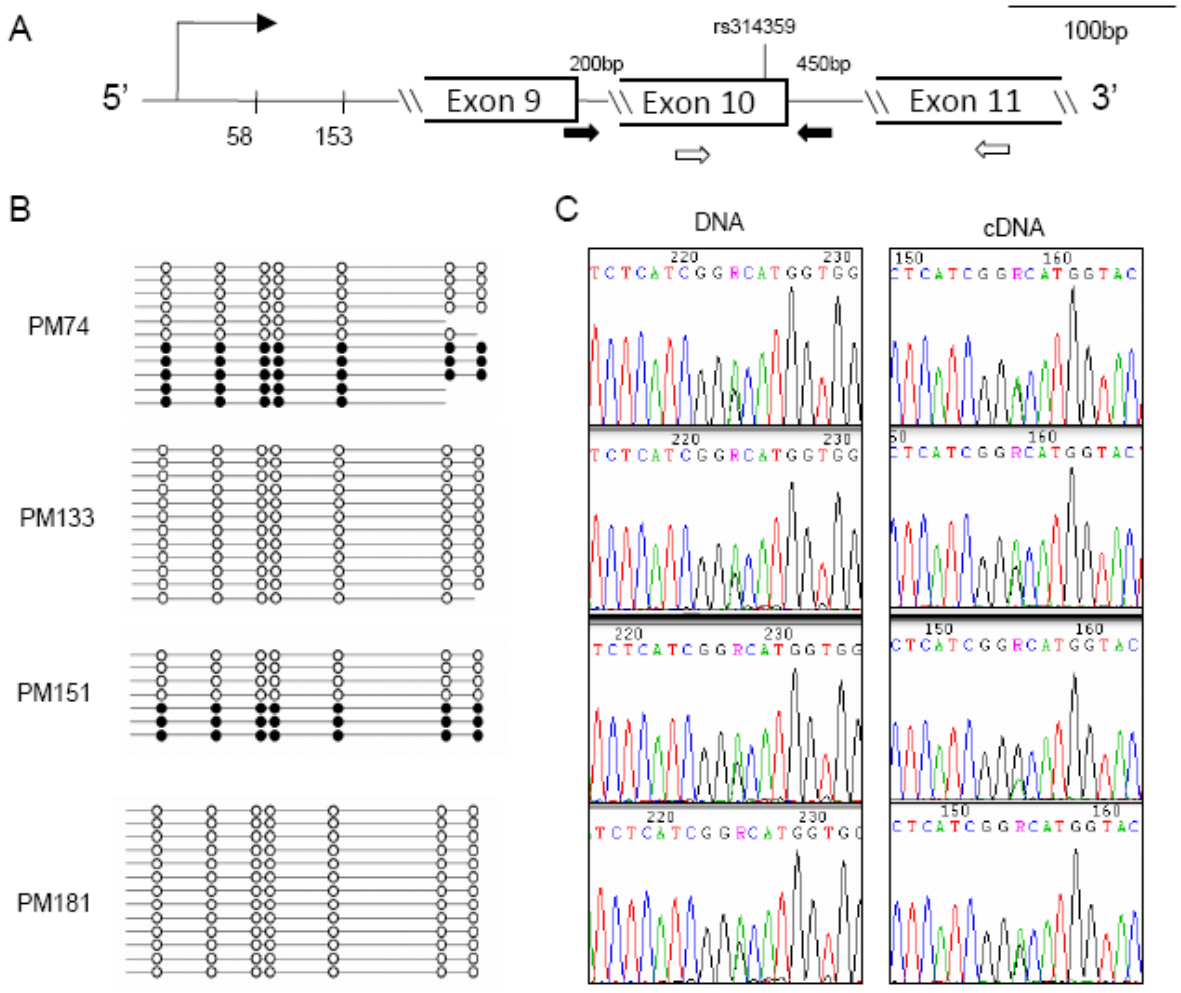

Figure 4.4. Allele-specific DNA methylation and mRNA expression in *EPHB4*.

(A) Schematic of the *EPHB4* locus showing the regions investigated by clonal bisulfite pyrosequencing on the exon 1 (58 to 153 relative to the transcriptional start site according to NM_004444) and genotyping assays for exon 10. PCR primers for DNA by sequencing are indicated by black arrows while RT-PCR primers for mRNA genotyping are indicated by arrows highlighted in white. (B) Bisulfite pyrosequencing of single clones from four placenta samples. Each row represents one clone and each circle represents one CpG. Methylated CpGs are shown in black while unmethylated CpGs are shown in white. (C) Allele-specific expression of *EPHB4* at A/G allele of rs314359 in DNA and cDNA by sequencing. Double peaks are shown in unmethylated samples. However, peaks on the SNP were skewed only in cDNA from methylated samples.

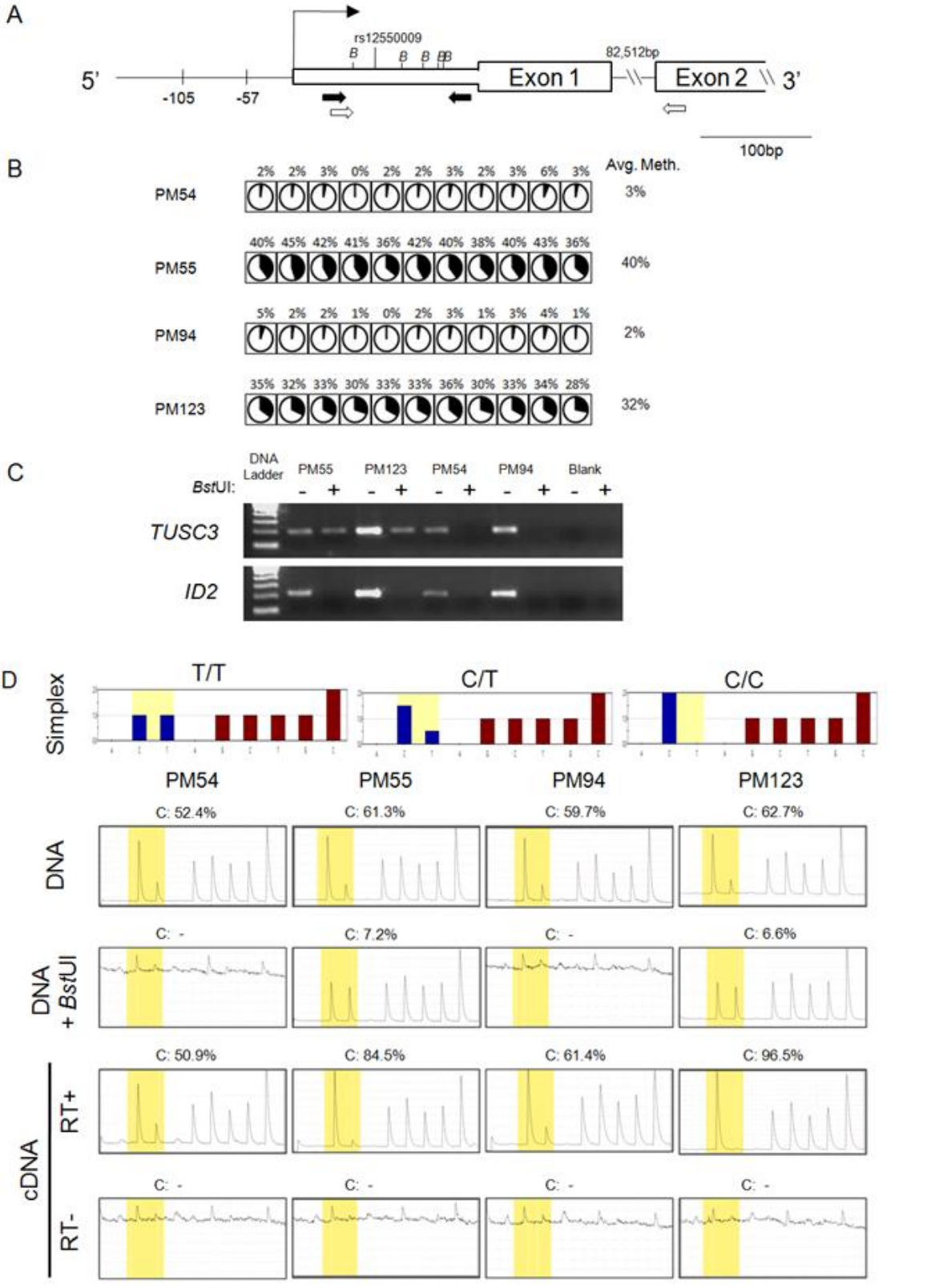
A
rs12550009
82,512bp
5'
-105
-57
Exon 1
Exon 2
3'
100bp
B
Avg. Meth.
PM54
2% 2% 3% 0% 2% 2% 3% 2% 3% 6% 3%
3%
PM55
40% 45% 42% 41% 36% 42% 40% 38% 40% 43% 36%
40%
PM94
5% 2% 2% 1% 0% 2% 3% 1% 3% 4% 1%
2%
PM123
35% 32% 33% 30% 33% 33% 36% 30% 33% 34% 28%
32%
C
DNA Ladder
PM55
PM123
PM54
PM94
Blank
BstUI:
- + - + - + - + - +
TUSC3
ID2
D
Simplex
T/T
C/T
C/C
PM54
PM55
PM94
PM123
DNA
C: 52.4%
C: 61.3%
C: 59.7%
C: 62.7%
DNA + BstUI
C: -
C: 7.2%
C: -
C: 6.6%
cDNA
RT+
C: 50.9%
C: 84.5%
C: 61.4%
C: 96.5%
RT-
C: -
C: -
C: -
C: -

Figure 4.5. Promoter CpG methylation correlates with lack of *TUSC3* gene expression.

(A) Schematic of *TUSC3* locus showing the regions investigated by bisulfite pyrosequencing on the promoter (-105 to -57 relative to the transcriptional start site according to NM_006765) and genotyping assays of the 5' untranslated region. PCR primers for DNA genotyping are indicated by black arrows while RT-PCR primers for mRNA genotyping are indicated by arrows highlighted in white. Enzyme recognition sites for *Bst*UI are indicated by "*B*". (B) Methylation status of *TUSC3* promoter region studied by bisulfite pyrosequencing. A similar methylation level of every CpG within each sample is observed and the gene follows "on-or-off" methylation pattern. Each circle represents a CpG site in a sample. Area shaded in black is proportional to the methylation level of the CpG site indicated by pyrosequencing. (C) Validation of complete methylation-sensitive restriction enzyme digestion on unmethylated molecules. Genomic DNA was predigested with *Bst*UI followed by PCR amplification with *TUSC3* and *ID2* specific primers (Supplementary Table 4.1). *Bst*UI digestion sites within the *ID2* region were unmethylated (Supplementary Figure 4.5) and, therefore, no PCR product was generated after enzyme digestion. (D) Allele-specific methylation of *TUSC3* on the fragment containing SNP rs12550009 demonstrated by enzyme digestion pyrosequencing. The "Simplex" diagrams (top) show the reference pyrograms by genotype. A heterozygous CT in the methylated samples (PM55 and PM123) displays a homozygous T pattern after *Bst*UI digestion indicating predominant methylation of the T allele. Allele-specific mRNA expression is concordant with allele-specific methylation on the same SNP rs1250009. Predominant expression of C alleles was observed in the cDNAs generated by RNA specific primers (bottom). RT+ and RT- represent assays with Reverse Transcriptase and without Reverse Transcriptase, respectively.

4.3.3. Correlation between MAP and pregnancy complication

Intriguingly, the genes exhibiting MAP identified here are highly expressed in the placenta (Su *et al*. 2002). Furthermore, *WNT2* and *EPHB4*, are crucial for placenta development (Gerety *et al*. 1999; Monkley *et al*. 1996; Red-Horse *et al*. 2005). The variable allelic gene expression caused by MAP may have functional consequences to placental physiology. In particular, the expression of *TUSC3* was downregulated in trophoblast upon hypoxic (a characteristic feature in preeclampsia) *in vitro* culturing (Pak *et al*. 1998). To determine whether there is a correlation between MAP and pregnancy disorders, the studied samples were categorized according to the presence or absence of intrauterine growth restriction and/or preeclampsia (Table 4.1). We found a significant difference in DNA methylation frequency of

TUSC3 between normal and preeclamptic pregnancies (Table 4.1). Specifically, *TUSC3* promoter methylation was found more frequently in the late-onset preeclampsia than normal placentas (P=0.02; Fisher's test). There was no significant correlation of MAP with maternal age, gestational age, and fetus gender or birth weight (Table 4.1).

4.3.4. No conservation of MAP in *Ephb4*, *Tusc3* and *Wnt2* of mice

As we observed no cases exhibiting 100% methylation for any of these analyzed sites, the MAP is likely regulated in a specific manner. In order to better understand the regulatory mechanism as well as the functional effect of MAP, we investigated the methylation status of these genes in mice, for which embryonic lethality has been reported in *Wnt2* and *Ephb4* knock-outs (Gerety *et al*. 1999; Monkley *et al*. 1996). However, the conserved regions of the three genes were unmethylated in the placentas of 21 outbred mice (Figure 4.6), suggesting MAP in these genes may not be conserved in rodent placenta and implicating a discrepancy of inter-individual variation of these genes between human and mouse placentas. Further analysis of MAP in other placental mammals would be interesting to find out if MAP is unique to human placentas.

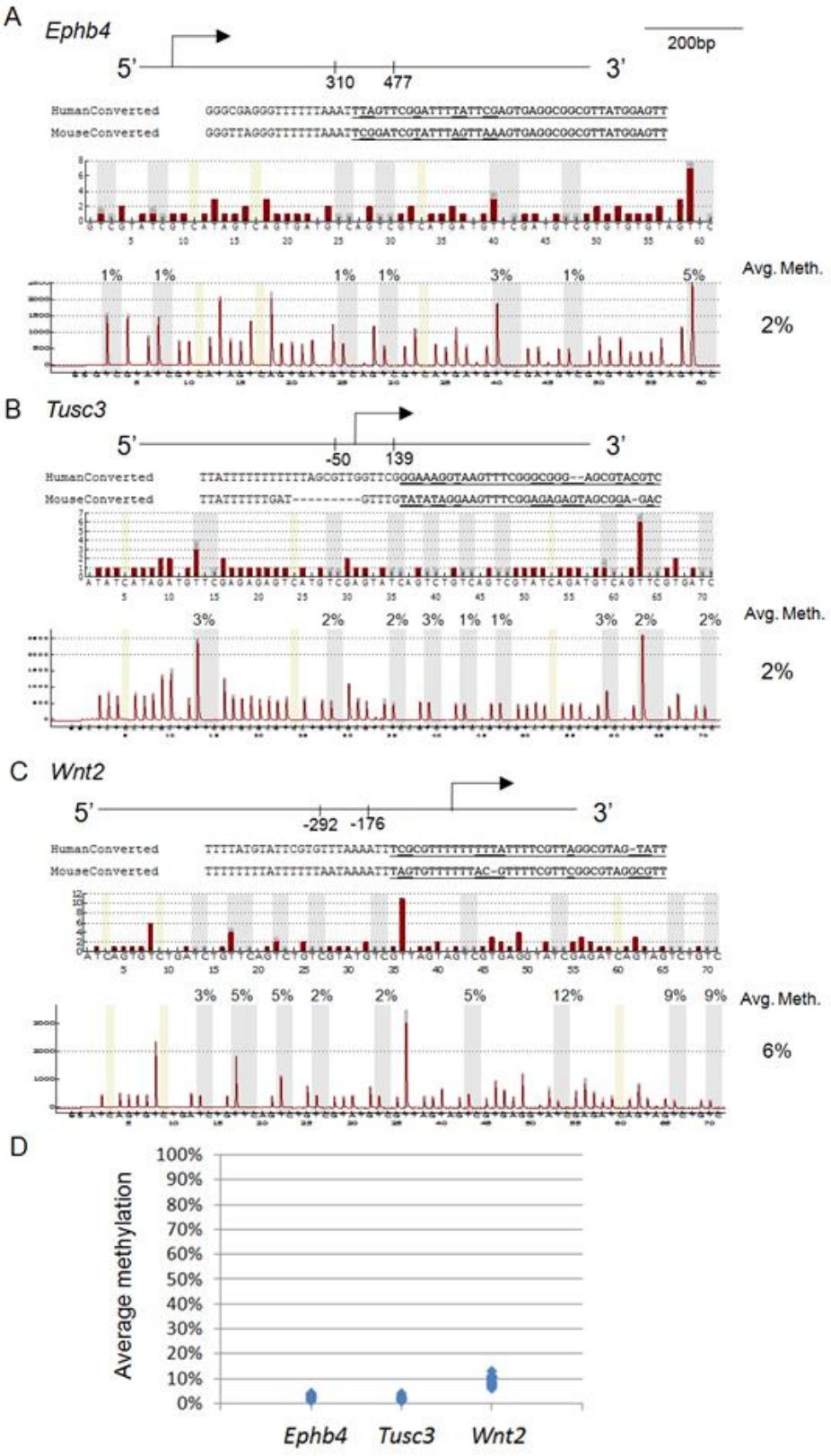
A
Ephb4
200bp
5'
3'
310
477
HumanConverted
MouseConverted
1% 1% 1% 1% 3% 1% 5%
Avg. Meth.
2%
B
Tusc3
5'
3'
-50
139
HumanConverted
MouseConverted
3% 2% 2% 3% 1% 1% 3% 2% 2%
Avg. Meth.
2%
C
Wnt2
5'
3'
-292
-176
HumanConverted
MouseConverted
3% 5% 5% 2% 2% 5% 12% 9% 9%
Avg. Meth.
6%
D
Average methylation
100%
90%
80%
70%
60%
50%
40%
30%
20%
10%
0%
Ephb4
Tusc3
Wnt2

Figure 4.6. DNA methylation status of MAP conserved regions in mouse.

Schematic of (A) *Ephb4* locus (310 to 477 relative to the transcriptional start site according to NM_010144), (B) *Tusc3* locus (-50 to 139 relative to the transcriptional start site according to NM_030254) and (C) *Wnt2* locus (-292 to -176 relative to the transcriptional start site according to NM_003391), showing the regions investigated by bisulfite pyrosequencing. Sequence alignments on bisulfite converted DNA between human and mouse at the first 60 nucleotides including the sequencing primers are shown. Sequences highlighted in red are the nucleotides being investigated while the nucleotides highlighted in blue are the differences between them. Reference pyrograms are provided and one representative sample for each locus is shown. (D) Summary of methylation level at *Ephb4*, *Tusc3* and *Wnt2* in 21 outbred mice. No "on-or-off" methylation variation is found in the mouse conserved regions.

4.3.5. Tissue-specificity of MAP

To determine the tissue specificity of MAP in human, the fetal tissues of abortuses with DNA methylation of *TUSC3* and *WNT2* in the associated placentas were studied. DNA methylation in the promoter of *TUSC3* and *WNT2* was not observed in any of 10 fetal tissues other than placenta (Figure 4.7). Also, there was no methylation in the maternal blood cells from women carrying placentas with DNA methylation of the *TUSC3* gene (Supplementary Figure 4.6A). Even within the methylated placenta, trophoblastic chorionic villi was the only tissue methylated (Supplementary Figure 4.6B).

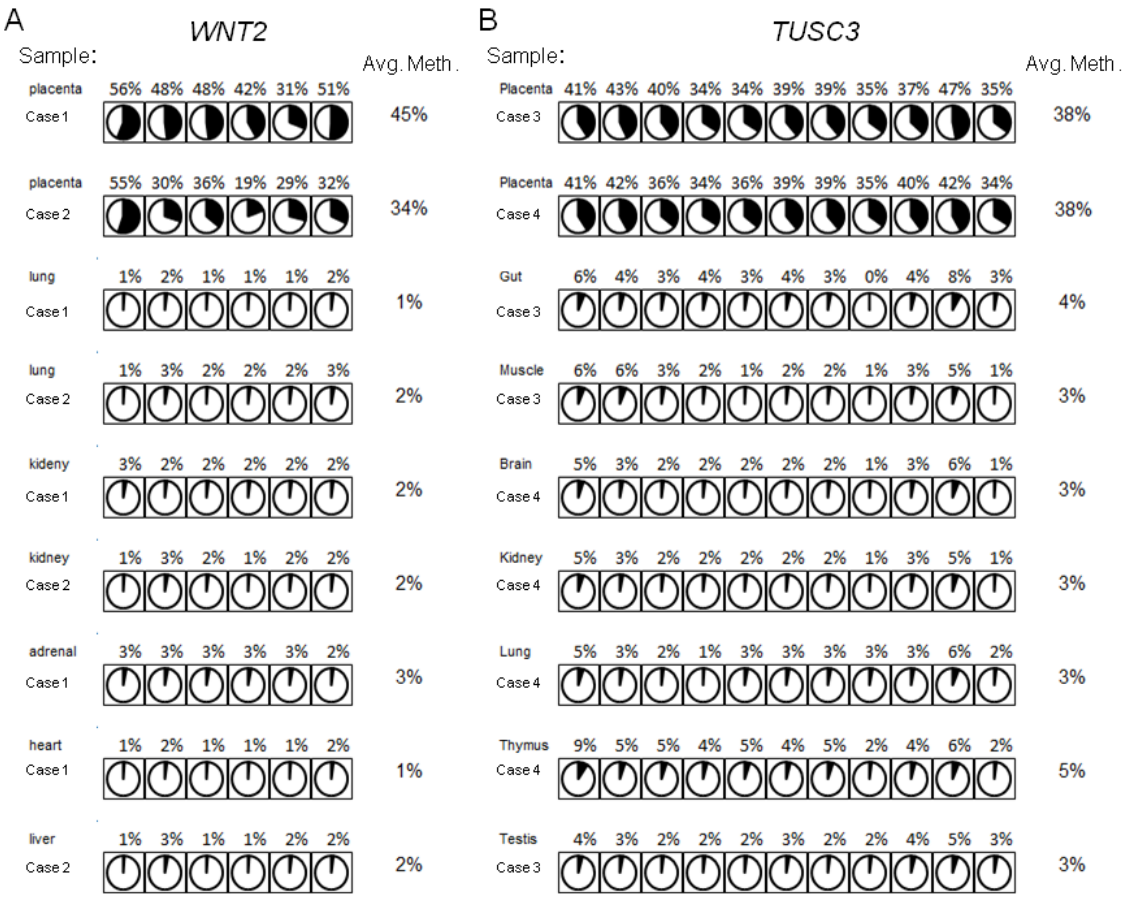

Figure 4.7. Tissue-specific DNA methylation of *WNT2* and *TUSC3*.

(A) DNA samples from two independent fetuses associated with placental methylation at the *WNT2* promoter were investigated by bisulfite pyrosequencing. None of the tissues (lung, kidney, adrenal, heart and liver) other than placenta was methylated. (B) DNA samples from two independent fetuses with placental methylation at the *TUSC3* promoter were investigated by bisulfite pyrosequencing. None of the tissues (lung, kidney, gut, muscle, brain, thymus and testis) other than placenta was methylated. Each circle represents a CpG site in a sample. Area shaded in black is proportional to the methylation level of the CpG site indicated by pyrosequencing.

We further tested the genome-wide DNA methylation patterns in blood cells of 18 normal individuals by the Illumina methylation array. Using the same criteria as we analyzed in placentas, 15 genes have highly variable methylation in two associated CpGs (defined as >1.5 SD above the mean) (Supplementary Figure 4.7A). 14 of the identified genes were located on the X chromosome, indicating that blood cells are less variably methylated than placenta, which is consistent with a previous study (Houseman *et al*. 2008). As expected, we found no MAP in *EPHB4*, *TUSC3* and *WNT2* (Supplementary Figure 4.7B). Two distinct CpGs associated with *TRIP6* genes were identified with highly variable methylation, while CpGs associated with two other genes, *NOD2* and *ALOX12*, nearly met these criteria. While the variation was not distributed in a clearly bimodal fashion, the levels of methylation for each pair of CpGs showed a very high degree of correlation, suggesting this is not methodological (measurement error or sequence variants directly affecting probe binding). The variable methylation at *NOD2* was further confirmed by pyrosequencing (Supplementary Figure 4.7C). A high degree of allelic variation of *NOD2* expression has been reported elsewhere (Yan *et al*. 2002), suggesting this variable methylation reflects this variable expression. As whole blood consists of a mixture of various types of cells, distinct on/off methylation patterns confined to a specific cell type may appear to be continuously distributed due to confounding by the varying proportions of cells among individuals. Analysis of individual blood cell populations would be necessary to determine if this is the case for these genes.

4.4. Discussion

Understanding the source of phenotypic variation among individuals is a fundamental aspect of human biology. Current studies mainly focus on searching for genetic sequence

variation which might miss the important phenotypic effects exerted by epigenetic polymorphisms. A study of the *MHC* locus on chromosome 6 in 7 human tissues across 32 individuals showed that around half of the studied loci had some inter-individual variability for DNA methylation in at least one tissue (Rakyan *et al*. 2004). However, this was not extensively quantified and its effect on gene expression was not investigated. Other loci with variable DNA methylation have also been found recently (Flanagan *et al*. 2006; Kerkel *et al*. 2008), but most, if not all, are dependent on DNA sequence variation within the differentially methylated region. In this report, we identify tissue-specific DNA methylation polymorphisms that can be found in as many as 25% of individuals and cannot simply be explained by the DNA sequence differences generated by common flanking SNPs. They are sequence-independent epigenetic polymorphisms that can act as a *cis*-acting regulator of gene expression.

The silencing effect of DNA methylation on single allele in *EPHB4*, *TUSC3* and *WNT2* resembles the characteristic of imprinted genes. With limited parental DNA and RNA samples from the "methylated" cases, we were unable to rule out the possibility that the genes with MAP are novel polymorphic imprinted genes. Polymorphic imprinting has been reported in humans for *IGF2R* (paternal or biallelic expression) (Xu *et al*. 1993) and *WT1* (maternal or biallelic expression) (Jinno *et al*. 1994). By screening 70 maternal-fetal pairs for rs1250009 in *TUSC3*, we identified three cases informative for parental origin of the methylation and all three were methylated on the maternal allele (Supplementary Figure 4.8). Similarly we identified one "methylated" case of *EPHB4* with paternal expression suggesting the maternal allele was methylated in this case. While the MAPs were maternally methylated in all informative cases we identified, we cannot rule out the possibility that this happened only by chance due to the small sample size. Of the roughly 80 imprinted loci identified to date, few are imprinted in human but

not in mouse (Morison *et al*. 2005). Thus these results could be consistent with an abnormal or stochastic failure of erasure of this "imprint" in the trophoblastic villi or specifically to a failure to erase a maternal methylation mark.

Alternatively, there may be a lineage-specific acquisition of DNA methylation by a *de novo* mechanism early in development. In this case, either allele could be methylated, or there may be a preference for acquiring methylation on one parental allele due to other epigenetic marks differentiating the two parental chromosomes. It is possible that a random acquisition of DNA methylation on single allele of these genes reflects a selection for reduced expression of these genes which may be relevant to the generation of imprinted genes during evolution (Spencer 2000). Further investigation of parental origins of the allelic methylation is needed to test this hypothesis.

The fact that none of the cases in this study has complete methylation on both alleles suggested that the regulation of developmental important genes by MAP in placenta is functionally significant. The correlation of *TUSC3* promoter methylation with preeclampsia, a pregnancy disorder that is complicated by placental hypoxia implies a biological relevance to MAP. *TUSC3* is an ortholog of the yeast *Ost3* protein which catalyzes the transfer of an oligosaccharide chain on nascent proteins in the process of N-glycosylation (Kelleher and Gilmore 2006). While the function of *TUSC3* in placenta is unknown, its paralog, *MAGT1*, is believed to be associated with embryonic implantation and hypertension (Sontia and Touyz 2007). In addition, *TUSC3* is highly expressed in the human placenta, but expression was reduced after *in vitro* hypoxic culturing of trophoblast (Pak *et al*. 1998). These observations suggest that *TUSC3* may be important in the development of preeclampsia. Further studies are

necessary to confirm this association and to identify the intrinsic function of *TUSC3* in the human placenta and its relation to preeclampsia development. Although the clinical status of the placentas did not appear to be related to the methylation pattern of *EPHB4* and *WNT2* in human, a phenotypic effect of these MAP genes on the human placenta cannot be excluded as only two clinical features, IUGR and preeclampsia were evaluated.

The discrepancy of DNA methylation profile between human and mouse might also suggest an evolutionary role. Several DNA methylation studies of placenta revealed a number of tumor-related genes specifically methylated in the human placenta (Chiu *et al*. 2007; Novakovic *et al*. 2008). It is believed that the difference in DNA methylation profile between rodents and primates may account for the disparity of placentation, such as different degree of trophoblast invasiveness, between species. Intriguingly, *EPHB4* and *WNT2* were found to be responsible for vascularisation of placenta which associated with the invasion of spiral arteries (Monkley *et al*. 1996; Red-Horse *et al*. 2005). It is possible that the DNA methylation polymorphism in these genes causes a subtle difference in the degree of trophoblast invasiveness among individual human placentas. Many of the other genes detected in our initial screen likewise may play an important role in placentation (Figure 4.2). For example *CTGF* is an important regulator of VEGF, a factor critical in vascularisation of the placenta and decidua (Inoki *et al*. 2002). However, biological effects may be difficult to discern when considering only the methylation status of individual genes as it may be the combined effects of multiple genes that is critical in development of traits, which may explain the marginal significance of disease association for *TUSC3*. The identification of MAP in other genes could be tested for association with complex traits by whole-epigenome association studies (Bjornsson *et al*. 2004; Hatchwell and Greally 2007).

Recently, "epimutation" has been found for *MLH1* and *MSH2* in cancer patients (Chan *et al*. 2006; Suter *et al.* 2004). Similar to the MAP identified here, epimutation can silence the genes in an allelic-specific manner. The distinction is that MAP is more frequent and appears to be set early in development, as we observed no within-placenta heterogeneity and found MAP even in first-trimester placentas (Data not shown). Although additional biological effects of such "epipolymorphism" in human remains to be determined, the functional consequence of imbalanced allelic gene expression is substantial (Cui *et al*. 2003; Yan and Zhou 2004). A genome-wide study of gene expression found that the variation of gene expression between alleles is common in human and it is believed to be the basis for variation in the transmission of some diseases (Lo *et al*. 2003; Yan *et al*. 2002). Thus the study of MAP as a method of identifying allelic expression differences, through measures at the DNA level, should open up a new dimension for future disease association studies. The Illumina methylation array used in this study only targets 807 genes, of which we only considered the limited set of those with multiple CpGs exhibiting correlated methylation patterns. Looking at these same genes more exhaustively, and considering the more than 20,000 genes in the human genome, there should be many more genes identified with MAP which might contribute to the disease susceptibility in a multifactorial and tissue-specific way. The future study of MAP is important for our understanding of inter-individual phenotypic variability, as well as complex disease susceptibility.

Chapter 5: DNA methylation profiling of human placentas reveals promoter hypomethylation of multiple genes in early-onset preeclampsia[5]

5.1. Introduction

Preeclampsia is one of the leading causes of maternal and fetal morbidity and mortality, and affects 5% of all pregnancies (Redman and Sargent 2005; Roberts and Cooper 2001). It is characterized by high blood pressure in the mother and, frequently, growth deficiency in the fetus. Preeclampsia is heterogeneous in etiology and can be further subclassified into early-onset (<34 weeks) and late onset (≥34 weeks) (von Dadelszen *et al*. 2003). Intrauterine growth restriction (IUGR), even in the absence of preeclampsia shows similar placental pathology, and is also associated with significantly increased perinatal morbidity and mortality, as well as with cardiovascular disease, glucose intolerance and psychiatric disorders later in life (Barker 1997; Wiles *et al*. 2005). Over decades, little progress has been made in the treatment and management of these disorders because they can only be diagnosed after full-blown manifestation of the condition is developed, by which time, treatment options are limited. Therefore, the identification of biomarkers that could be used to diagnose abnormal outcomes during early pregnancy would be a major step forward in antenatal care.

While the exact cause is still unknown, epigenetic features are implicated in the pathogenesis of preeclampsia. Mutations in *STOX1* were identified in some unique familial cases of preeclampsia with apparent maternal transmission of susceptibility (van Dijk *et al*. 2005). Also, deficiency of the imprinted *Cdkn1c* gene in mice can lead to hypertension and proteinuria

[5] A version of Chapter 5 has been published. Yuen RKC, Peñaherrera MS, von Dadelszen P, McFadden DE, Robinson WP. (2010) DNA methylation profiling of human placentas reveals promoter hypomethylation of multiple genes in early-onset preeclampsia. Eur J Hum Genet. 18(9):1006-12.

during pregnancy (Kanayama *et al*. 2002), further implicating the role of imprinted genes in the development of preeclampsia. Epigenetic alterations of non-imprinted genes have also been suggested to be involved. For example, the *SERPINA3* promoter was found to be hypomethylated in preeclampsia-associated placenta (Chelbi *et al*. 2007), suggesting that the epigenetic alteration of this gene may be associated with reduced trophoblastic invasion and implicating this change as a potential biomarker for preeclampsia.

Many studies have investigated the gene expression profile in human placentas with preeclampsia and IUGR using genomic array technology (Enquobahrie *et al*. 2008; Founds *et al*. 2009; Nishizawa *et al*. 2007). However, many factors may cause short-lived temporal changes in gene expression and (Torricelli *et al*. 2008; Torricelli *et al*. 2007a; Torricelli *et al*. 2007b), furthermore, placental RNA can degrade during parturition and rapidly after delivery of the placenta (Fajardy *et al*. 2009), making it difficult to obtain useful samples. DNA methylation is generally more stable and provides an alternative marker for underlying processes in the cell. In our previous study, we focused on the identification of highly variable 'epipolymorphisms' in the placenta. We then showed an association of one such epipolymorphism with *TUSC3* with late-onset preeclampsia, suggesting a role of DNA methylation change in adverse pregnancy outcomes (Yuen *et al*. 2009). In the present study we use a statistical analysis of the microarray data to compare the patterns of DNA methylation in placental samples from pregnant women with and without preeclampsia and IUGR in order to search for potential biomarkers for these disorders.

5.2. Methods

5.2.1. Sample collection

Fifty-seven placentas with or without associated preeclampsia and/or IUGR were collected from Vancouver BC Children's & Women's Hospital with informed consent from individuals, and was approved by the ethics committees of the University of British Columbia and the Children's & Women's Health Centre of British Columbia. Some data on these placentas have been previously published including analysis of trisomy in the placenta (Robinson *et al*. 2009), analysis of altered imprinting for 11p15.5 imprinting control regions (Bourque *et al*. 2010), and an investigation of methylation variability in the placenta (Yuen *et al*. 2009). Clinical information was collected on prenatal findings, pregnancy complications and birth parameters. Preeclampsia was defined as at least two of the following: (1) hypertension (systolic blood pressure ≥140mmHg and/or diastolic blood pressure ≥90mmHg, twice, >4h apart) after 20 weeks, and proteinuria defined as ≥0.3g/d or ≥2+ dipstick proteinuria after 20 weeks, (2) non-hypertensive and non-proteinuric HELLP syndrome, using Sibai's criteria (Audibert *et al*. 1996) or (3) an isolated eclamptic seizure without preceding hypertension or proteinuria, using the British Eclampsia Survey Team (BEST) criteria to define eclampsia (Douglas and Redman 1994). The preeclamptic placentas were subclassified into EOPET (onset before 34 weeks) and LOPET (onset after 34 weeks) (von Dadelszen *et al*. 2003). Intrauterine growth retardation (IUGR) was defined as either (1) birth weight <3rd percentile for gender and gestational age using Canadian charts,(Kramer *et al*. 2001) or (2) birth weight <10th percentile with either: (a) persistent uterine artery notching at 22+0 to 24+6 weeks gestation, (b) absent or reversed end diastolic velocity on umbilical artery Doppler, and/or (c) oligohydramnios (amniotic fluid index <50mm). All the

LOPET and IUGR cases and 16 of the 17 EOPET cases have been used in our previous study of placental methylation variability (Yuen *et al*. 2009). Detailed clinical information is provided in Supplementary Table 5.1. Although clinical details such as blood pressure and urine protein level were not always available in our controls, we excluded any cases with hypertension or low birth weight. Fragments of ~1cm^3 were dissected from the fetal side of each placenta and DNA was extracted immediately after collection. Total RNA was extracted from 5 control placentas with 2 sites sampled from each placenta using RNeasy kit (Qiagen) according to manufacturer's instructions. Peripheral blood samples from normal individuals and fetal tissue biopsies (brain, kidney and lung) from abortuses were obtained with review board approval and were anonymous to individual identifiers.

5.2.2. Illumina microarray

DNA samples from 26 placentas were used for the DNA methylation array analysis. Samples were classified into 3 groups (EOPET, LOPET and IUGR) with their gestation-matched controls. The groups did not differ by maternal or gestational age (Table 5.1). In addition, DNA samples from 5 additional control placentas with two sites dissected from each placenta were used to test for intra-individual DNA methylation variation. DNA samples extracted from blood of 5 normal female individuals and fetal tissues (brain, kidney and lung) from 3 abortuses were used to assess the tissue-specificity of methylation in the candidate loci. 500ng of genomic DNA was bisulfite modified using the EZ DNA Methylation Kit (Zymo Research) according to the manufacturer instructions. After bisulfite treatment, DNA samples were subjected to the Illumina GoldenGate Methylation Cancer Panel I array-based assay, which contains 1505 probes targeting 807 genes, using Illumina-supplied reagents and conditions.

Table 5.1. Clinical characteristics of the study groups

	Early controls (N=4)	EOPET (N=4)	*p* value	Late controls (N=5)	LOPET (N=4)	*p* value	Controls (N=5)	IUGR (N=4)	*p* value
Gestational age (weeks)	29.64	30.86	0.60	38.00	37.96	0.95	37.80	32.79	0.15
Maternal age (years)	36.03	33.30	0.53	37.16	36.45	0.61	35.94	37.28	0.62
Birth weight (g)	1381.00	1172.50	0.63	3184.00	3348.75	0.72	3313.00	1466.25	0.008

Bisulfite converted DNA was mixed with allele-specific oligonucleotides in the assay which target either the unmethylated cytosine (U) or methylated cytosine (C). A beta-value of 0 to 1 was reported for each CpG site, which is related to the percentage of methylation, from 0% to 100%. Beta-values were calculated by subtracting background with the use of negative controls on the array and taking the ratio of the methylated signal intensity to the sum of both methylated and unmethylated signals. As a quality control step for Illumina array data analysis, we eliminated the probes with detection *p* value >0.05 in any sample. To control for the possibility of methylation differences arising due to gender bias, we excluded all the probes on the X chromosome from our analysis. Differentially methylated loci between groups were identified based on the average DNA methylation level difference (delta beta) comparison and significance analysis of microarrays (SAM) (Tusher *et al.* 2001).

DNA methylation and RNA expression of 10 placental sites from 5 normal term placentas were further assayed using the Illumina GoldenGate Methylation array and the Illumina Human Gene Expression array, respectively. Total RNA quality was verified and processed samples were hybridized to an 8-well microarray chip (HumanRef-8 v2). The BeadChip array was processed in the Centre for Molecular Medicine and Therapeutics (CMMT) BioAnalyzer Core Facility (Vancouver, BC, Canada). Output was analyzed using Illumina's BeadStudio software (v3.2.7, 2007).

5.2.3. Bisulfite pyrosequencing

Loci with absolute delta beta >10% and false discovery rate (FDR) <10% in SAM were considered candidates of interest. To validate the differentially methylated loci identified from the Illumina array, bisulfite pyrosequencing was carried out for a subset of the candidate loci. In

addition to the 26 samples run on the Illumina array, an independent set of 26 DNA samples from 13 EOPET and 13 control placentas were studied to validate the array findings. Pyrosequencing was performed on a Biotage PSQ HS96 Pyrosequencer and the quantitative levels of methylation for each CpG dinucleotide were evaluated using Pyro Q-CpG software (Biotage). All methylation-unbiased PCR and sequencing primers were designed to cover the same CpG sites interrogated by the Illumina probes (Supplementary Table 5.2). Methylation analysis of LINE1 elements was performed according to manufacturer's instructions (Biotage), as this measurement is commonly used as an indirect measure of global methylation.

5.2.4. Statistical analysis

Data from bisulfite pyrosequencing were analyzed with two-tailed Student's T-test. Linear correlation was used to analyse the intra-individual methylation variation in different sites of placentas, the correlation between DNA methylation and gene expression, as well as the correlation between data obtained from Illumina array and bisulfite pyrosequencing assays.

5.3. Results

Unsupervised hierarchical clustering was performed on the Illumina GoldenGate methylation bead-array result from the 26 placental samples using the Illumina software and based on a distance measure of 1 - r, where r is the Pearson correlation coefficient (Supplementary Figure 5.1). There was no obvious clustering of EOPET, LOPET, IUGR and control placentas. However, there was a preferential clustering of placentas according to gender (Figure 5.1A), which is caused by the inactivation of X chromosome in females (i.e. higher methylation of X chromosome CpG islands in female than in male samples). After eliminating loci on the X chromosome from our analysis, the samples preferentially clustered according to

their gestational age (i.e. 83% samples with gestational week <34 clustered together and 76% samples with gestational week >34 clustered together) (Figure 5.1B). In particular, only 2 out of 14 control placentas did not cluster using this classification. These results suggested that gender and gestational age of samples were potential biases for DNA methylation analysis.

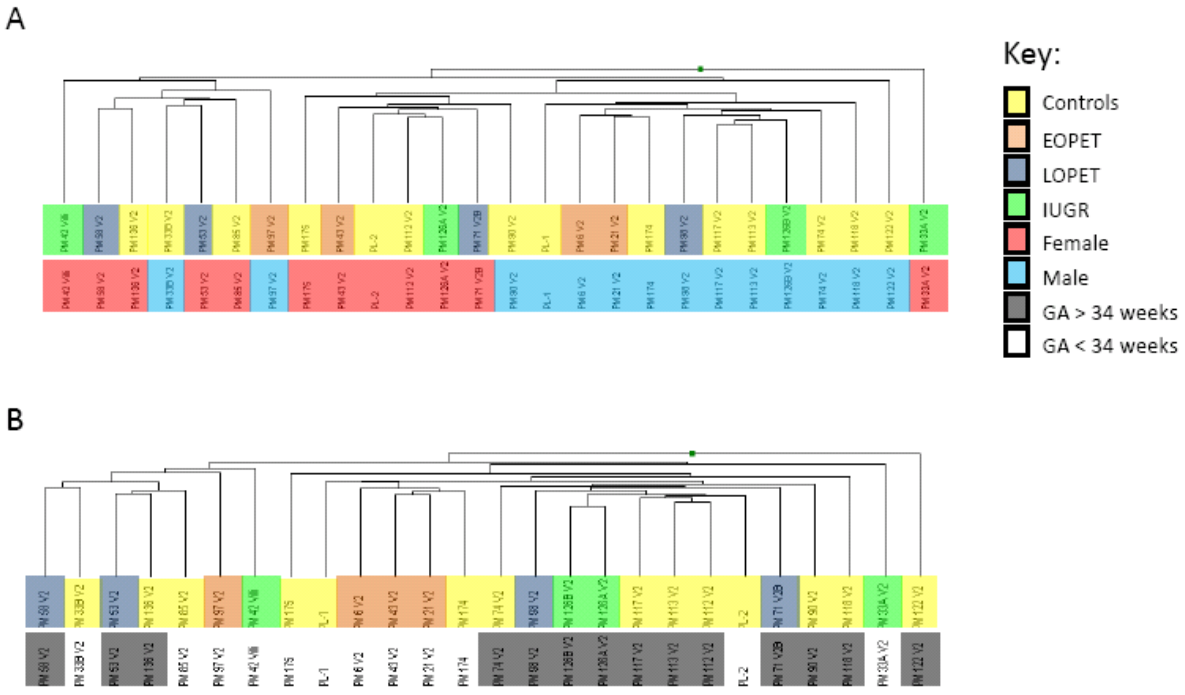

Figure 5.1. Cluster analysis of placental samples.

(A) Samples preferentially clustered by gender and (B) samples preferentially clustered by gestational age.

To eliminate these potential biases in the search of differentially methylated loci between placentas with and without adverse pregnancy outcomes, all Illumina probes on the X chromosome were excluded from our study. Furthermore, cases and controls were compared separately for each gestational age-matched group (i.e. 3 comparison groups: EOPET, LOPET

and IUGR, with their corresponding gestational age-matched controls). Within these matched groups, there was no significant difference of gestational age or maternal age (Table 5.1). Using a cut-off of <10% FDR from SAM, 192 loci were identified as being differentially methylated in EOPET as compared to controls, 16 loci in IUGR, but none in LOPET (Figure 5.2). Because differences of small magnitude are less likely to be meaningful, we only considered differences between the mean methylation of patient and control groups of at least 10% absolute magnitude difference. Of the 192 loci with <10% FDR for EOPET, 34 had methylation difference >10% (delta beta >0.1 from Illumina array) and all of them were hypomethylated in EOPET compared to the controls (Table 5.2). Of the 16 loci identified by SAM for IUGR, 5 had more than 10% methylation difference between controls and IUGR, all of them were highly variable in methylation value consistent with being a methylation allelic polymorphism (MAP) – epipolymorphism as is commonly found in normal placentas (Yuen *et al*. 2009).

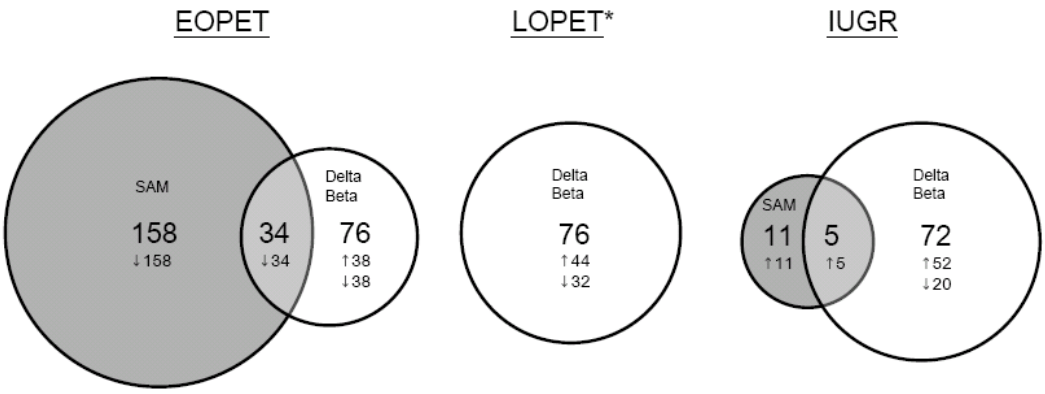

Figure 5.2. Venn diagram summary of differentially methylated loci.

Differentially methylated loci were defined as false discovery rate (FDR) <10% as calculated by significance analysis of microarrays (indicated as "SAM") and average DNA methylation difference >10% as represented by delta beta (indicated as "Delta Beta"). The number of differentially methylated loci is indicated in the overlapping area between circles. 34 hypomethylated loci and 5 hypermethylated loci were identified in EOPET group and IUGR group, respectively. *No differentially methylated loci was identified by SAM with FDR <10%. ↑: Hypermethylated comparing to the controls. ↓: Hypomethylated comparing to the controls.

Table 5.2. Loci demonstrating differential methylation between EOPET and controls

Feature ID	False-Discovery Rate (%)	Controls		EOPET		Difference
		Mean	SD	Mean	SD	
GLI2_E90_F[2]	0	0.66	0.06	0.44	0.08	0.22
CHI3L2_E10_F	0	0.85	0.06	0.64	0.12	0.21
MEST_P62_R	0	0.71	0.05	0.52	0.11	0.19
KRT13_P676_F[2]	0	0.66	0.03	0.48	0.12	0.18
MEST_P4_F	0	0.85	0.04	0.70	0.08	0.16
MEST_E150_F[2]	0	0.55	0.05	0.39	0.06	0.16
MYOD1_E156_F	0	0.20	0.11	0.05	0.01	0.15
PSCA_E359_F[1]	0	0.74	0.04	0.59	0.04	0.15
GABRB3_P92_F	0	0.50	0.08	0.37	0.02	0.14
NES_P239_R	0	0.63	0.02	0.49	0.13	0.14
CYP2E1_E53_R	0	0.42	0.09	0.29	0.07	0.13
CCL3_E53_R	0	0.66	0.06	0.53	0.04	0.13
CDKN1C_P6_R[1]	0	0.22	0.07	0.09	0.02	0.13
LIF_P383_R	0	0.77	0.04	0.64	0.10	0.13
ABCB4_P51_F[1]	0	0.73	0.04	0.60	0.05	0.13
SRC_P164_F	0	0.80	0.05	0.68	0.04	0.11
AATK_P519_R[1]	0	0.80	0.05	0.70	0.03	0.10
FRZB_E186_R[1]	6.69	0.66	0.09	0.45	0.24	0.22
TIMP3_P690_R[2]	6.69	0.66	0.08	0.47	0.10	0.19
SH3BP2_P771_R[1]	6.69	0.56	0.06	0.37	0.15	0.19
PENK_P447_R	6.69	0.41	0.09	0.24	0.14	0.17
ARHGDIB_P148_R	6.69	0.30	0.08	0.16	0.05	0.14
TRIM29_E189_F	6.69	0.65	0.03	0.52	0.13	0.13
EMR3_P39_R[1]	6.69	0.73	0.06	0.59	0.10	0.13
MLF1_E243_F	6.69	0.31	0.10	0.19	0.06	0.13
ZMYND10_P329_F	6.69	0.18	0.19	0.06	0.02	0.13
NOTCH4_P938_F	6.69	0.50	0.08	0.39	0.07	0.12
MPO_P883_R	6.69	0.19	0.10	0.08	0.02	0.11
CXCL9_E268_R	6.69	0.61	0.09	0.50	0.07	0.11
PI3_P274_R	6.69	0.77	0.03	0.66	0.09	0.11
CAPG_E228_F[2]	6.69	0.66	0.07	0.56	0.07	0.11
PTPN6_E171_R	6.69	0.47	0.09	0.37	0.07	0.11
POMC_P400_R	6.69	0.32	0.04	0.22	0.07	0.10
SFN_P248_F	6.69	0.58	0.07	0.48	0.06	0.10

[1]Sites showing a significant effect of gestational age on methylation level.

[2]Sites chosen for follow-up study by pyrosequencing.

In order to identify candidate sites at which methylation quantification could potentially be used for diagnostic purposes, it is important to select sites that are not greatly influenced by gestational age. Seven of the 34 candidate methylation changes associated with EOPET were significantly affected by gestational age as judged by comparing mean methylation in control placentas <34 gestational week as compared to controls ≥34 gestational weeks (AATK_P519_R, ABCB4_P51_F, CDKN1C_P6_R, EMR3_P39_R, FRZB_E186_R, PSCA_E359_F, SH3BP2_P771_R; Student's T-test, $p<0.05$). From the remaining 27 loci, 5 sites (CAPG_E228_F, GLI2_E90_F, KRT13_P676_F, TIMP3_P690_R, and MEST_E150_F) were selected for further validation by bisulfite pyrosequencing based on their magnitude of difference (*GLI2*, *MEST* and *KRT13*) and biological relevance to the preeclampsia development (*CAPG*, *MEST* and *TIMP3*) (Mayer *et al*. 2000a; Qi *et al*. 2003; Zhang *et al*. 2009).

Bisulfite pyrosequencing validation of the five selected hypomethylated loci in EOPET showed that the Illumina array data correlate significantly with the pyrosequencing measurements for the same CpG site, as well as the mean of multiple sites in the pyrosequencing assays (Supplementary Table 5.3). To allow better representation of the methylation patterns in the associated regions, means of multiple CpG sites in pyrosequencing assays were used for all the comparisons. Therefore, an independent set of 26 placental samples, which consisted of 13 EOPET and 13 controls (gestational age was not significantly different between the two groups $p=0.49$; clinical information of the samples can be found in Supplementary Table 5.1), was analysed by bisulfite pyrosequencing to confirm the differential methylation of the selected loci between EOPET and control placentas. All selected loci, except *MEST* ($p=0.60$) showed significant hypomethylation in EOPET ($p=0.01$ for *CAPG*, $p=0.03$ for *GLI2*, $p=0.00003$ for *KRT13* and $p=0.00001$ for *TIMP3*) (Figure 5.3).

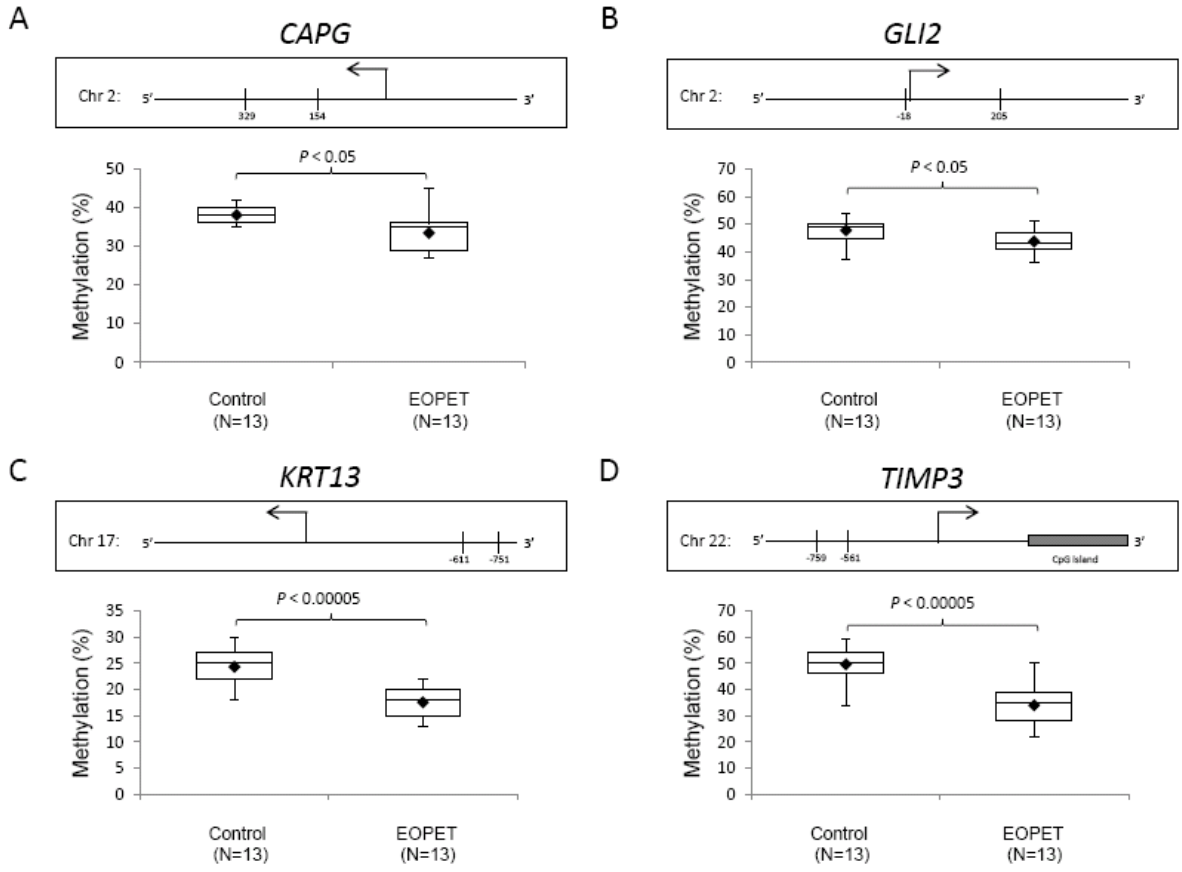

Figure 5.3. Box-plot of differentially methylated loci between EOPET and control subjects and their corresponding locations in the genome.

Percentage of DNA methylation was assessed with bisulfite pyrosequencing for (A) *CAPG*, (B) *GLI2*, (C) *KRT13* and (D) *TIMP3* in 13 placentas with (indicated as "EOPET") and 13 placentas without EOPET (indicated as "Control"). *P*-values (indicated as "*P*") were calculated by Student's t-test. Simplified UCSC genome browser views of the locations for the differentially methylated loci targeted by pyrosequencing assays are shown in the box above the plots.

The most significant and largest absolute methylation difference (over 15%) was observed between EOPET and control at the *TIMP3* locus. We tested the correlation in methylation values at this locus for two separately sampled sites from same placenta of 5 term control samples and these were well correlated with each other (R=0.90; p=0.038)

(Supplementary Figure 5.2A). We further studied the methylation values at more than 10 sampled sites from each of two term placentas. The standard deviations of methylation values in two placentas were only 2.5% and 1.6% (Supplementary Figure 5.2B), suggesting that there is little intra-placental variation of DNA methylation. We also tested the feasibility of developing it as a non-invasive prenatal diagnostic marker. From the Illumina array data, the *TIMP3* locus was completely methylated in adult female blood and fetal tissues (99% methylated on average) with significant (p=0.001) differential methylation compared to the placental samples (73% methylated on average), which is comparable to that of *SERPINB5* (Figure 5.4), a marker that was previously proposed feasible for non-invasive prenatal diagnosis (Chim *et al*. 2005).

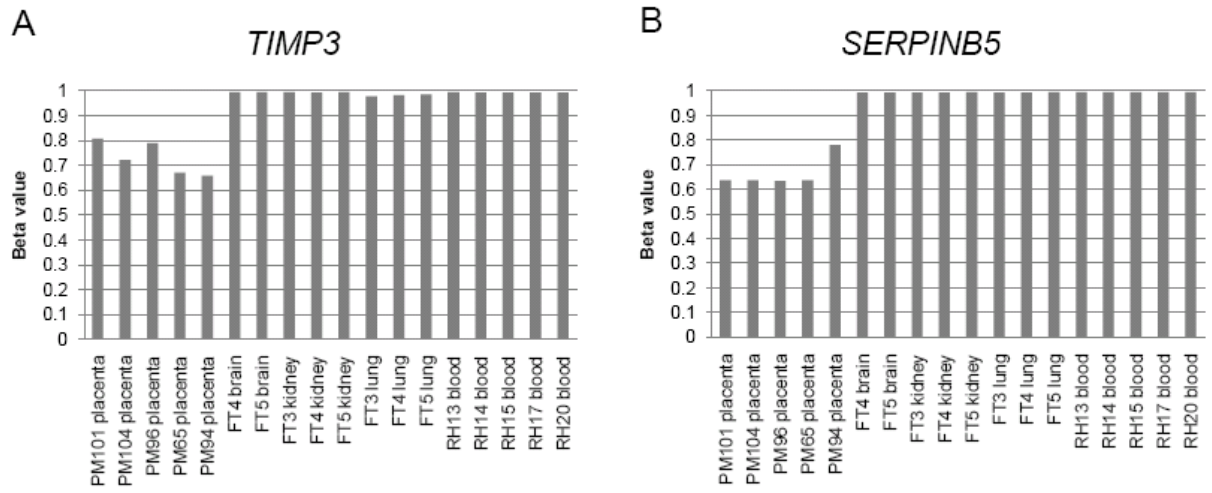

Figure 5.4. Comparison of DNA methylation levels of *TIMP3* and *SERPINB5* between placentas, blood and fetal tissues.

Both *TIMP3* and *SERPINB5* show lower methylation level in control placentas (5 cases) than fetal brain (2 cases), kidney (3 cases), lung (3 cases) and female blood (5 cases). Beta-value of 0 to 1 represents the relative percentage of methylation from 0% to 100%.

Finally, we studied the relationship between the promoter DNA methylation and mRNA expression of the candidate genes in a subset of 5 term control placenta (2 sampled sites each) that had been analysed on the Illumina expression array. From the Illumina array data, we found that the DNA methylation of *TIMP3* locus was inversely correlated with its gene expression (R=-0.72; p=0.019), while none of the other three genes were significantly correlated based on this small sample size (N=10 samples) (Supplementary Figure 5.3).

5.4. Discussion

Despite many suggestions that epigenetic changes might be involved in adverse pregnancy outcomes (Chelbi *et al*. 2007; Chelbi and Vaiman 2008; van Dijk *et al*. 2005), no genome-wide study has searched for epigenetic abnormalities in preeclampsia and IUGR. In the present study, we profiled the DNA methylation of placentas from preeclampsia and IUGR pregnancies and their control counterparts using Illumina GoldenGate Methylation Cancer panel I array. Although the array mainly targets cancer-related genes, the pseudomalignant nature of the placenta makes it suitable for this study (Chiu *et al*. 2007). Among the 1505 CpG loci targeted by the array, 34 loci were identified hypomethylated in EOPET but none was differentially methylated in LOPET. The different epigenetic profiles in EOPET and LOPET placentas support the hypothesis that the two forms are caused by different mechanisms (Huppertz 2008; Oudejans *et al*. 2007). EOPET, which is often associated with IUGR, is a severe form of preeclampsia (76% of our cases associated with IUGR). It is suggested to be initiated by abnormal placentation, caused by reduced perfusion with increased apoptosis of trophoblasts (Goswami *et al*. 2006; Oudejans *et al*. 2007; Redman and Sargent 2005). On the other hand, LOPET, which is considered as being a maternal syndrome, is a mild form of preeclampsia. It is

usually associated with normal placental development and a predisposed maternal constitution, such as hypertension or diabetes (Oudejans *et al*. 2007; Redman and Sargent 2005). Epigenetic change may play a role in EOPET by altering gene expression and, as a consequence, normal placental development. Epigenetic changes may also result from hypoxic conditions associated with preeclampsia or an altered trophoblast composition in these placentas. Hypomethylation was found in many gene promoter regions in EOPET, but there was no difference in the global DNA methylation level as indirectly assessed by methylation at the LINE1 repeat sequence compared to other groups of placentas (data not shown). As LINE1 methylation is a measure of global methylation, these results imply that CpG hypomethylation observed is a gene-specific effect. Interestingly, many of the associated genes, such as the imprinted gene *CDKN1C*, are known to be important for normal placentation (Mayer *et al*. 2000a; Takahashi *et al*. 2000).

In order to control for maternal and gestational age factors, the sample size used for array profiling in the present study is small (8 to 10 samples per group). The small sample size likely explains why we do not find an association between polymorphic DNA methylation of *TUSC3* and LOPET as we did in a previous investigation over 100 placentas (p=0.02) (Yuen *et al*. 2009). This later study was focused on the identification of epipolymorphisms and did not involve the statistical comparison of all methylation sites between groups, as was done for the present study.

Recently, we reported a reduction of methylation at the *H19*/*IGF2* imprinting control region in IUGR-associated placentas, but we did not find altered methylation at *CDKN1C* or other imprinted genes in IUGR and/or preeclampsia (Bourque *et al*. 2010). The discrepancy can be attributed to the different ways of grouping samples, since we divided preeclampsia cases into PET and PET+IUGR previously without considering the effect of gestational changes on DNA

methylation. Global changes of gene expression have been previously reported in association with gestational age (Winn *et al*. 2007). Our current finding suggests this is important also in regard to DNA methylation. Thus, the gestational-age dependent profile is important to evaluate and control for when considering any methylation change identified as a potential biomarker. This is particularly important in the study of preeclampsia as such pregnancies tend to be delivered early and comparisons to term births may be inappropriate.

The DNA methylation differences of CpGs in *CAPG*, *GLI2*, *KRT13* and *TIMP3* were confirmed in an independent set of 26 placentas with EOPET and gestational age-matched control pregnancies. Among these four genes, *TIMP3* had the largest difference in DNA methylation level with an over 15% reduction in EOPET compared to control placentas. A previous study demonstrated that *TIMP3* gene expression can be regulated by promoter DNA methylation in the placental tissues (Feng *et al*. 2004). While our assays target CpG sites upstream of the CpG island where previous groups investigated (Figure 5.3D), we also found a significant inverse correlation between its DNA methylation and gene expression in placentas. Therefore, hypomethylation of the *TIMP3* promoter may alter its gene expression in EOPET.

TIMP3 is a family member of the matrix metalloproteinase (MMP) inhibitors, which have an important function in regulating a wide range of physiological processes such as cell growth, invasion, migration transformation and apoptosis. This gene is highly expressed in placenta and suggested to be important for implantation and decidualization by regulating trophoblast invasion.(Apte *et al*. 1994; Higuchi *et al*. 1995) Elevated expression of many TIMPs, including *TIMP3*, has been reported in preeclamptic placentas (Montagnana *et al*. 2009; Pang and Xing 2003). The hypomethylation of the *TIMP3* promoter found in this study may increase

TIMP3 expression and, in turn, reduce the invasiveness of trophoblast during placental development, which leads to placental hypoperfusion in EOPET. Intriguingly, hypermethylation of the *TIMP3* promoter has been reported in choriocarcinoma and hydatidiform mole, conditions that have increased trophoblast invasiveness (Feng *et al.* 2004; Xue *et al.* 2004), which further supports the inverse relationship between *TIMP3* promoter methylation and trophoblast invasiveness. It has also been demonstrated that TIMP3 could inhibit angiogenesis by blocking the vascular endothelial growth factor (VEGF) from binding its receptor (Qi *et al*. 2003), a well-known defect that found in the trophoblast of preeclamptic pregnancies (Noris *et al*. 2005). Although the cause of the epigenetic modification is unknown, it may be related to the hypoxic environment of the cells (Gheorghe *et al*. 2007; Shahrzad *et al*. 2007). Intriguingly, *TIMP3* expression was increased in the first-trimester trophoblasts upon hypoxic treatment (Koklanaris *et al*. 2006). This implicates that the increased expression of *TIMP3* under hypoxic condition, a hallmark in preeclamptic trophoblast, may be mediated by the epigenetic alteration on its promoter.

Early detection of preeclampsia is necessary for effective treatment. We identified several genes with hypomethylation in their promoter regions. In particular, the significant reduction of DNA methylation in *TIMP3* promoter of EOPET placentas could be useful as a biomarker for the disorder. Importantly, this site showed no significant change of DNA methylation by gestational age and there was a good intra-placental correlation in DNA methylation values. If further study demonstrates that this methylation change is also conserved earlier in pregnancy, then measuring the DNA methylation level of *TIMP3* in chorionic villous sampling (CVS) from pregnant women could reflect subsequent risk for EOPET.

In addition, recent advances in measuring circulating fetal DNA from maternal plasma opens up an additional approach for non-invasive prenatal diagnosis (Dennis Lo and Chiu 2007). This strategy takes advantage of the fact that during pregnancy, 3 to 6% of cell-free DNA in maternal blood plasma is derived from the placenta (Dennis Lo and Chiu 2007). Therefore, one can detect abnormalities in the fetal DNA directly from the maternal blood without going through conventional invasive methods such as amniocentesis and CVS. It has been demonstrated that there is an over 5 fold increase in circulating fetal DNA in the maternal plasma of preeclamptic pregnancies compared to their control counterparts as estimated by measuring the placental-specific unmethylated *SERPINB5* DNA fragments (Chim *et al*. 2005). However, *SERPINB5* is not differentially methylated between normal and preeclamptic placentas. The same extent of increase in circulating fetal DNA can also be found in preeclamptic maternal plasma by measuring *SRY* (Lo *et al*. 1999), suggesting that *SERPINB5* is not a specific marker for preeclampsia. As *TIMP3* is significantly hypomethylated in EOPET placentas the detection of an increased level of unmethylated *TIMP3* cell-free DNA in the maternal plasma could provide increased sensitivity for the non-invasive diagnosis or screening of the pregnancies for EOPET. Importantly, it possesses the same characteristics as *SERPINB5* for being a potential universal non-invasive prenatal diagnostic marker: its methylation is specifically reduced in placenta but it is completely methylated in other tissues, including blood samples. *SERPINA3*, another gene in the SERPIN family, has been reported to be hypomethylated in severe preeclamptic placentas, but the extent of methylation and its potential for being a clinical marker have not been examined thoroughly (Chelbi *et al*. 2007). We therefore propose that the level of unmethylated *TIMP3* DNA in maternal plasma could be a useful biomarker for early detection of severe preeclampsia.

In summary, we report the application of DNA methylation analysis to the elucidation of abnormal placental development associated with preeclampsia. While DNA methylation at critical sites can reflect the availability of a gene for transcription, which may lead to altered expression depending on other regulatory factors present, it has a number of advantages over expression studies. Firstly, it may be more resistant to the transient changes in gene expression associated with labor and delivery (Torricelli *et al*. 2008; Torricelli *et al*. 2007a; Torricelli *et al*. 2007b), as well as the effects of placental storage prior to sample processing (Fajardy *et al*. 2009). While we did in this case observe an inverse association between *TIMP3* methylation and expression, expression studies at term may not always reflect that which occurred during relevant periods of development. Secondly, the trend to hypomethylation of a variety of genes in EOPET, suggest that loss of methylation may generally be involved in the response to hypoxia. Lastly, DNA methylation differences provide an alternative approach for pre-symptomatic diagnosis of at risk pregnancies.

Chapter 6: Conclusion

My thesis has focused on the DNA methylation profiles of human fetal somatic tissues and placentas. This included mapping of imprinted DMRs in the human placental genome, analyzing the aging effect on the DNA methylation profiles in human somatic tissues, characterizing the inter-individual DNA methylation variation in the human placentas, and identifying the aberrant DNA methylation changes in the human placenta with adverse pregnancy outcomes. I will hereby summarize the findings in this thesis, discuss the strength and limitation of the studies, suggest the future directions of the research in this field, and state the significance and contribution of the findings.

6.1. Summary

In this thesis, I showed that genome-wide methylation arrays can be a powerful technique to pinpoint functionally important changes associated with 1) allele-specific methylation, both that associated with imprinting and with MAP; 2) tissue and age-specific methylation; and 3) pregnancy disorders, such as preeclampsia and IUGR

Genomic imprinting is one of the most important and remarkable epigenetic mechanisms of allele-specific gene regulation. Parent-of-origin dependent monoallelic expression of imprinted genes is often mediated by DNA methylation at imprinted DMRs. Many efforts have been made to identify imprinted genes in the human genome due to their importance in fetal growth and development, and their potential for dysregulation. Taking advantage of the unbalanced parental genomic constitutions in triploidies, 62 genes with apparently imprinted DMRs were identified in Chapter 2 by comparing the genome-wide DNA methylation profiles between diandries (extra paternal haploid set) and digynies (extra maternal haploid set). Of these

62 genes, 45 have been not reported previously as imprinted genes. These putative imprinted DMRs were further validated by bisulfite sequencing and allelic expression analysis. Parent-of-origin-specific expression was confirmed, leading to the identification of novel imprinted genes, including *FAM50B*, *DNMT1*, *RHOBTB3*, *ARMC3*, *AIFM2* and *LEP*. While many imprinted DMRs show stable epigenetic regulation between normal individuals, allele-specific methylation in some loci can be highly polymorphic. To identify loci with a high degree of inter-individual DNA methylation variation, over 60 human placentas were profiled using the Illumina GoldenGate Methylation Cancer panel in Chapter 4 of this thesis. While many sites show a continuous pattern of methylation levels, *WNT2*, *TUSC3* and *EPHB4* were identified to have polymorphic "on-or-off" patterns of DNA methylation variation at their promoter region which was confirmed by pyrosequencing. Methylation of these genes can be found in 7%-25% of over 100 placentas tested. The methylation state at the promoter of these genes is concordant with mRNA allelic expression. Similar to epimutations, such as *MLH1* and *MSH2* identified in cancer patients (Chan *et al*. 2006; Suter *et al*. 2004), methylation can silence the genes in an allele-specific manner for these epipolymorphism phenomena. However, epipolymorphisms appear to be set early in development. Since the placenta plays a critical role in regulating fetal growth and development in ways that have lifelong effects on health, characterizing the nature of allele-specific methylation regulation, including its tissue-specific nature, may help in understand the role it plays in human phenotypic variation and disease.

Comparison of DNA methylation profiles between placentas of different gestations and other somatic tissues allowed detailed analysis of tissue-specific and gestational age-specific methylation changes in the genome. In Chapter 2, I showed that there are different regions within the imprinted gene promoter responsible for the complex epigenetic regulation of tissue-specific

imprinting and gestational age-specific methylation. The gestational age effect on global DNA methylation pattern was shown in Chapter 5, where there was a higher correlation of DNA methylation profiles between placentas with similar gestational ages. To gain insight into the pattern of tissue-specific methylation in early tissue development, DNA methylation status of CpGs located in the regulatory regions of nearly 800 genes was evaluated in 5 somatic tissues (brain, kidney, lung, muscle and skin) from eight normal second-trimester fetuses in Chapter 3. Tissue-specific DMRs were identified in 195 loci, suggesting tissue-specific methylation is established as early as in the second trimester. Importantly, only 17% of the identified fetal tDMRs were found to maintain this same tissue-specific DNA methylation in adult tissues. Furthermore, 10% of the sites analyzed, including sites associated with imprinted genes, demonstrated an extensive DNA methylation difference between fetus and adult. This plasticity of DNA methylation over development was further demonstrated by comparison with similar data from embryonic stem cells, with the most altered marks being linked to domains with bivalent histone modifications. Most fetal tDMRs thus appear to reflect transient DNA methylation changes during development rather than permanent epigenetic signatures. These comparisons characterized the acquisition and loss of epigenetic marks during fetal and postnatal development, which can be influenced by a combination of intrinsic biological signals and extrinsic environmental stimuli mediated through epigenetic regulation.

Preeclampsia and IUGR are two of the most common adverse pregnancy outcomes, but their underlying causes are mostly unknown. While multiple studies have investigated gene expression changes in these disorders, few studies have examined epigenetic changes. Analysis of the DNA methylation pattern associated with such pregnancies provides an alternative approach to identifying cellular changes involved in these disorders. In Chapter 4, the

methylation status at the *TUSC3* promoter showed an association with late-onset preeclampsia, suggesting a role of DNA methylation change in adverse pregnancy outcomes. In Chapter 5, I then systematically investigated 1505 CpG methylation sites associated with 807 genes in 26 placentas from EOPET, LOPET, IUGR and control subjects using an Illumina GoldenGate Methylation panel. Thirty-four loci were hypomethylated in the early-onset preeclamptic placentas while no and only 5 differentially methylated loci were found in late-onset preeclamptic and IUGR placentas, respectively. Hypomethylation of 4 loci in EOPET was further confirmed by bisulfite pyrosequencing of 26 independent placental samples. While the promoter of *TIMP3* was significantly hypomethylated in EOPET placentas, no intra-individual variation in the placenta was detected for the *TIMP3* CpG locus. These results suggest that gene-specific hypomethylation may be a common phenomenon in EOPET placentas. Also, DNA methylation profiles of human placentas may change dramatically throughout gestation. I further proposed *TIMP3* as a potential prenatal diagnostic marker for EOPET.

6.2. Strength and limitations

The use of high throughput genomic and molecular technologies for epigenetic profiling is one of the strengths in this thesis. Traditional approaches for epigenetic studies, such as bisulfite sequencing and methylation-specific PCR only allow assessment of DNA methylation at a limited number of CpG sites which restricts the study to relatively localized regions of the genome (Frommer *et al*. 1992; Herman *et al*. 1996). With the rapid development of genomic technology, such as microarrays, DNA methylation analysis has been scaled to a genome-wide level. This thesis utilizes the array-hybridization techniques developed by Illumina, which targets thousands of CpG sites in the human genome (Bibikova *et al*. 2006). The technology involves

multiplexed probes specific for methylated and unmethylated CpG sites following the bisulfite conversion of DNA (Bibikova *et al*. 2006). There are other genome-wide DNA methylation analysis systems currently available, such as affinity-based methylated DNA immunoprecipitation array (MeDIP) (Weber *et al*. 2005) or enzyme digestion based comprehensive high throughput arrays for relative methylation (CHARM) (Irizarry *et al*. 2008). However, the Illumina methylation array system possesses several advantages over the use of other systems. For example, the Illumina GoldGate methylation Cancer panel can accommodate up to 96 samples per run with one chip. This significantly reduced the batch effect and other technical variability that is commonly encountered by other microarray system. Also, as validated by other locus-specific DNA methylation analyzing methods such as pyrosequencing technology or other microarray platforms, the relative DNA methylation level measured by the Illumina array is highly reliable and reproducible (Bibikova and Fan 2009; Grafodatskaya *et al*. 2010).

In this thesis, I was also able to use both fetal and placental tissue samples available for a comprehensive study of fetal and placental DNA methylation profiling. This was possible due to the establishment and maintenance of clinical samples recruitment and processing in the Robinson lab, large number of available placentas, and various precious early aborted fetal tissues that were available for investigations. The good clinical records of the pregnancies also allowed epigenetic studies to be associated with various pregnancy complications. These data provided useful information for the understanding of DNA methylation through different angles in this thesis. For instance, the placentas were taken from different ages of gestation, processing times and sites within a placenta. Taken together, the information allows the exploration of the intra- and inter-individual epigenetic variability and the correlation of epigenetic changes and the

clinical outcomes, which makes the in-depth investigation and discussion of epigenetic variability possible in this thesis.

However, this thesis is not without limitation. First, the Illumina methylation array applied in this thesis only targets the promoter regions of the genes in the human genome. Although it is generally accepted that gene promoter is the region that has functional consequence with epigenetic changes, epigenetic variation in regions other than promoter, such as intra- or inter-genic regions has also been reported (Illingworth *et al*. 2008; Illingworth *et al*. 2010; Meissner *et al*. 2008). Functional significance of epigenetic changes in those area remains to be investigated, but there is immediate diagnostic value for them. For example, by comparing the DNA methylation profiles between disease and control groups, the identified differentially methylated non-promoter regions can be act as a biomarker for the disease regardless of its biological function. Therefore, it would be important to extend the analysis to the rest of the genome.

The Illumina array technology used is also limited in studying single CpG sites in the genome. The problem is two-fold. First, it assumes that a single CpG site can represent the DNA methylation status of a give region, which is not always true. Though we found high correlation of methylation status between the array target CpG and its surrounding CpG sites in most loci, variation can occur within a CpG island, based on some DNA methylation studies using mass spectrometry-based methods or deep bisulfite sequencing (Hodges *et al*. 2009; Talens *et al*. 2010). Therefore, more CpG sites should be included in the array or validated with additional nearby CpG sites using locus-specific methods such as bisulfite sequencing. The GoldenGate methylation array was only a first generation panel with 1505 CpG sites, whereas current

Illumina arrays are much more comprehensive. The Illumina methylation array continues to evolve and the current one evaluates over 450,000 CpG sites per run, which should improve the resolution. Second, non-CpG DNA methylation exists in which the addition of methyl group on the cytosine residue is not necessarily adjacent to a guanine (Grafstrom *et al*. 1985; Woodcock *et al*. 1987). Although it is currently found to be prevalent in embryonic stem cells (Ramsahoye *et al*. 2000) and germline (Tomizawa *et al*. 2011), its effect on disease or normal cell development remains to be explored. Along the same line, epigenetic variation other than DNA methylation, such as histone modification, has not been investigated thoroughly in this thesis, which poses a limitation on a complete picture of epigenetic profiles in fetus and placenta.

Perhaps the most critical component missing in this thesis is the gene expression profiles in fetus and placenta for functional and regulatory correlation with the epigenetic changes. The dismissal of profiling gene expression stemmed from our observation that mRNA degraded rapidly in different rate for different genes soon after delivery of the placenta (Avila *et al*. 2010). Therefore, comparing gene expression in placentas with different processing time may not truly reflect the genuine biological difference between samples, particularly for methods that require standard gene referencing such as Realtime RT-PCR. Despite this challenge, comparing the ratio of allelic expression has been used as an alternative mean for studying the regulatory consequence of epigenetic modification in this thesis because the relative allelic expression rate is a self-referencing method which eliminates the degradation rate bias.

6.3. Future directions

The findings in this thesis have opened up many new directions that are worth pursuing in the future. For example, as DNA methylation profile may change dramatically throughout

gestations in the human placenta, it would be interesting to compare the DNA methylation profiles of placentas from different gestations. The information obtained would be useful for understanding the role of epigenetic regulation to the placental development. It may also help to differentiate loci that are susceptible to environmental change from those that are required for development. Furthermore, it can provide a resource for the development of epigenetic diagnostic markers which require relatively stable epigenetic signature throughout gestations.

Isolating homogeneous cell populations from human placental tissues (e.g. cytotrophoblast, syncytiotrophoblast, EVT and mesenchyme) is technically challenging and requires specific biomarkers (e.g. antibodies) to confirm the cellular origin and purity (Hannan et al. 2010). Although Cytokeratin 7 antbody staining is commonly used to cofirm a trophoblast origin, differentiating subtypes of trophoblast cells require many additional antibody markers which can be time-consuming and very inefficient (Hannan et al. 2010). Cell-type-specific methylation may act as an alternative marker of cellular origin (Grigoriu et al. 2011). Therefore, a futher comparison of methylation profiles between different subtypes of placental cells would be useful to identify cell-type specific DNA methylation markers useful for checking the origin or purity of the isolated trophoblast cell population.

Although epigenetic variability has been investigated in the placenta, the extent to which placental epigenetic variability compares to somatic tissue has not been evaluated. Placental variation in DNA methylation has been reported to be greater than that in somatic tissues for isolated loci, such as Alu and LINE1 elements, and many regions across X chromosomes in females (Cotton *et al.* 2009; Reiss *et al*. 2007). This phenomenon is unlikely to be solely caused by a failure of DNA methylation maintenance as a functional role for such variation has been

hypothesized in many of the genes that exhibit highly variable DNA methylation and also play an important role in the placental development, for example *TUSC3* in this thesis. By comparing the epigenetic variability in the human placenta to that in the somatic tissues, it may be possible to test the hypothesis that the human placenta has a higher tolerance to the epigenetic variability (Yuen and Robinson 2011). However, it is important to control for variation in cell composition in such studies as tissues deemed as being "highly variable" can also be subject to greater variance in cell composition.

To further delineate the tolerance of epigenetic variability in the human placenta, genome-wide epigenetic changes that occur in the presence of identified causes for IUGR or preeclampsia, such as some confined placental trisomies, may be evaluated. The information may be useful to determine whether the DNA methylation changes reported in association with placental dysfunction represent just one of the multiple changes occurring and to determine if they are a cause of dysfunction or instead compensatory changes in response to other abnormalities. These may also be accompanied by the use of cell culture experiments to identify epigenetic changes that are likely to be the consequence of cell composition and/or environmental factors, such as hypoxia, that can be done by separating the subpopulation of the trophoblast cells and culturing them under different oxygen tension. Animal models with specific mutations or environment exposures affecting placental function would also provide a basis to test for epigenetic adaptation in the placenta.

The discovery of multiple loci with epigenetic abnormalities in placenta from pregnancies affected by maternal preeclampsia provides opportunities for early detection of the disorder. However, a specific diagnostic approach still needs to be further developed and

evaluated. Ideally, more epigenetic markers should be identified for preeclampsia in order to increase the sensitivity and specificity in the clinical aspect. This would require further profiling of genome-wide DNA methylation status in EOPET with the use of a higher resolution microarray or a whole methylome sequencing approach, particularly at the early stage of the preeclampsia development. Together with the rapid advancement of sequencing technology, the identification of practical epigenetic diagnostic markers for preeclampsia should soon be achieved.

The identification of novel imprinted DMRs may improve our knowledge in the biological roles of the imprinted genes. Although GO analysis suggested a functional discrepancy between maternal and paternal imprinted genes from the identified DMRs, caution should be taken since not all the identified DMRs were properly valided. In particular, *LEP* is a well-known growth promoting gene that highly expressed in the placenta (Maymo et al. 2011). Yet, it showed maternal expression in a subset of individuals which seemingly contradicts what the inter-genomic conflict theory would predict. In fact, the basis for the genomic conflict theory was origined from early studies in mouse, but recent studies have shown that many imprinted genes are not conserved between mouse and human, which may stem from the reduced conflict between maternal and paternal genomes at the maternal-fetal interface in human pregnancy (Monk et al. 2006). Intriguingly, some imprinted DMRs identified in this thesis are possibly unique to human, which may suggest that there are other forces driving the evolution of new imprinted genes. Although speculative, the driving force may be originated from other tissue, such as brain, which is rapidly evolved from mouse to human and where sex-specific parent-of-origin allelic expression can readily be found (Gregg et al. 2010a; Gregg et al. 2010b). It would

be interesting to find out whether the function of the identified imprinted genes in human supports such hypothesis.

6.4. Significance and contribution

Preeclampsia accounts for 15-20% of maternal mortality in developed countries, as well as being associated with significant perinatal deaths and IUGR. Both maternal preeclampsia and fetal IUGR are associated with many long-term health risks. Even a small reduction in their incidence can effectively cause a significant reduction in health care costs. While it seems obvious that altered imprinted gene expression or altered epigenetic regulation can lead to defects in placentation, there is no study suggesting how commonly (or rarely) this may occur. To address this issue, a comprehensive study of epigenetic profiles for both normal and abnormal fetal and placental tissues is needed. This thesis has provided the fundamental DNA methylation profiles of human somatic tissue and placenta. These can help in understanding the mechanisms of epigenetic regulation, the developmental epigenetic programming of tissues throughout life in relation to fetal programming, and the extent of inter-individual variation in placenta contributing to the development of adverse pregnancy outcomes. It also provided evidence for the involvement of epigenetic changes in the development of EOPET.

The approach of using triploid tissues for identification of imprinted DMRs yielded many novel imprinted genes in the human placenta. The findings contribute to the ever-growing list of imprinted genes important for the study of human growth and development. This approach improves upon the conventional strategies in the sense that it is entirely gene expression and SNP independent. More importantly, this approach allows the comparison of DNA methylation profiles of multiple tissues, so that regions responsible for tissue-specific regulation or

imprinting expression regulation can be identified at once, which may assist the study of complex epigenetic regulation in imprinted regions. The lack of conservation of imprinting marks between human and other organisms also implicates a gain of imprinting for some genes in human throughout evolution, which may shed light on the relationship between imprinted genes and placental mammal evolution.

Secondly, the comparison of DNA methylation profiles between ES cells, fetal and adult somatic tissues showed that developmental changes in DNA methylation can be very dynamic. Although similar studies have been carried out recently to investigate the effect of aging on DNA methylation, these were focused on correlating the ages of individuals with the DNA methylation patterns, but ignored the potential flexibility of DNA methylation regulation upon development (Boks *et al*. 2009; Christensen *et al*. 2009; Maegawa *et al*. 2010; Rakyan *et al*. 2010; Teschendorff *et al*. 2010). The flexibility of DNA methylation is particularly reflected by the observation that the majority of tDMRs identified are not conserved between fetus and adult. This dynamic methylation pattern raises questions about the current concept that DNA methylation is a stable silencing regulator for tissue development and well-maintained once it has been established after fertilization.

Thirdly, the discovery of novel sequence-independent epipolymorphisms offers a new dimension for future disease association studies. Using the MAPs identified in the human placenta, various adverse pregnancy outcomes were correlated with the on-or-off DNA methylation status of the genes which led to the finding of association between MAP of *TUSC3* and preeclampsia. This approach has been used by another group to correlate a MAP of *CGB5* with pregnancy loss (Uuskula *et al*. 2010) and that of *WNT2* with fetal birthweights (Ferreira *et*

al. 2011). Since MAP is DNA sequence-independent and can potentially regulate gene expression, carrying out MAP association in addition to SNP association studies may add extra power to identifying factors contributing to complex diseases.

Finally, the identification of hypomethylation in multiple loci of EOPET placenta linked preeclampsia with epigenetic dysregulation in the human placenta. This is supported by a current finding of altered global DNA methylation in EOPET placenta versus normal placenta (Gao *et al*. 2011; Kulkarni et al. 2010). These findings can contribute to the understanding of the pathology of preeclampsia and help improve diagnosis of the disorder. In particular, DNA methylation is a chemically stable epigenetic mark that has tremendous potential for disease diagnosis. The finding of hypomethylation of *TIMP3* locus in EOPET placenta may be applicable for the early detection of severe preeclampsia in the pregnant women and thus improve the management and treatment for the disorder before its full-blown manifestation.

In conclusion, I have provided comprehensive DNA methylation profiles for both normal and abnormal fetal and placental tissues. This information contributes to the biological and clinical aspects of the pathogenesis of fetal and placental disorders. The findings in this thesis also illuminate new areas of research in this field, which should ultimately lead to improved health of both mothers and their babies.

References

Adelman, D.M., M. Gertsenstein, A. Nagy, M.C. Simon, and E. Maltepe. 2000. Placental cell fates are regulated in vivo by HIF-mediated hypoxia responses. *Genes Dev* **14:** 3191-3203.

Amiel, A., N. Bouaron, D. Kidron, R. Sharony, E. Gaber, and M.D. Fejgin. 2002. CGH in the detection of confined placental mosaicism (CPM) in placentas of abnormal pregnancies. *Prenat Diagn* **22:** 752-758.

Apte, S.S., M.G. Mattei, and B.R. Olsen. 1994. Cloning of the cDNA encoding human tissue inhibitor of metalloproteinases-3 (TIMP-3) and mapping of the TIMP3 gene to chromosome 22. *Genomics* **19:** 86-90.

Arima, T., K. Hata, S. Tanaka, M. Kusumi, E. Li, K. Kato, K. Shiota, H. Sasaki, and N. Wake. 2006. Loss of the maternal imprint in Dnmt3Lmat-/- mice leads to a differentiation defect in the extraembryonic tissue. *Dev Biol* **297:** 361-373.

Armitage, J.A., I.Y. Khan, P.D. Taylor, P.W. Nathanielsz, and L. Poston. 2004. Developmental programming of the metabolic syndrome by maternal nutritional imbalance: how strong is the evidence from experimental models in mammals? *J Physiol* **561:** 355-377.

Aronow, B.J., B.D. Richardson, and S. Handwerger. 2001. Microarray analysis of trophoblast differentiation: gene expression reprogramming in key gene function categories. *Physiol Genomics* **6:** 105-116.

Audibert, F., S.A. Friedman, A.Y. Frangieh, and B.M. Sibai. 1996. Clinical utility of strict diagnostic criteria for the HELLP (hemolysis, elevated liver enzymes, and low platelets) syndrome. *Am J Obstet Gynecol* **175:** 460-464.

Avila, L., R.K. Yuen, D. Diego-Alvarez, M.S. Penaherrera, R. Jiang, and W.P. Robinson. 2010. Evaluating DNA methylation and gene expression variability in the human term placenta. *Placenta* **31:** 1070-1077.

Baccarelli, A., R.O. Wright, V. Bollati, L. Tarantini, A.A. Litonjua, H.H. Suh, A. Zanobetti, D. Sparrow, P.S. Vokonas, and J. Schwartz. 2009. Rapid DNA methylation changes after exposure to traffic particles. *Am J Respir Crit Care Med* **179:** 572-578.

Barker, D.J. 1992. Fetal growth and adult disease. *Br J Obstet Gynaecol* **99:** 275-276.

Barker, D.J. 1997. The long-term outcome of retarded fetal growth. *Clin Obstet Gynecol* **40:** 853-863.

Barker, D.J. 2004. The developmental origins of adult disease. *J Am Coll Nutr* **23:** 588S-595S.

Barker, D.J. and C. Osmond. 1986. Infant mortality, childhood nutrition, and ischaemic heart disease in England and Wales. *Lancet* **1:** 1077-1081.

Barker, D.J., C. Osmond, J. Golding, D. Kuh, and M.E. Wadsworth. 1989. Growth in utero, blood pressure in childhood and adult life, and mortality from cardiovascular disease. *Bmj* **298:** 564-567.

Barlow, D.P., R. Stoger, B.G. Herrmann, K. Saito, and N. Schweifer. 1991. The mouse insulin-like growth factor type-2 receptor is imprinted and closely linked to the Tme locus. *Nature* **349:** 84-87.

Bartolomei, M.S., S. Zemel, and S.M. Tilghman. 1991. Parental imprinting of the mouse H19 gene. *Nature* **351:** 153-155.

Beatty, L., R. Weksberg, and P.D. Sadowski. 2006. Detailed analysis of the methylation patterns of the KvDMR1 imprinting control region of human chromosome 11. *Genomics* **87:** 46-56.

Bernstein, B.E., T.S. Mikkelsen, X. Xie, M. Kamal, D.J. Huebert, J. Cuff, B. Fry, A. Meissner, M. Wernig, K. Plath, R. Jaenisch, A. Wagschal, R. Feil, S.L. Schreiber, and E.S. Lander. 2006. A bivalent chromatin structure marks key developmental genes in embryonic stem cells. *Cell* **125:** 315-326.

Bibikova, M. and J.B. Fan. 2009. GoldenGate assay for DNA methylation profiling. *Methods Mol Biol* **507:** 149-163.

Bibikova, M., Z. Lin, L. Zhou, E. Chudin, E.W. Garcia, B. Wu, D. Doucet, N.J. Thomas, Y. Wang, E. Vollmer, T. Goldmann, C. Seifart, W. Jiang, D.L. Barker, M.S. Chee, J. Floros, and J.B. Fan. 2006. High-throughput DNA methylation profiling using universal bead arrays. *Genome Res* **16:** 383-393.

Bird, A. 2002. DNA methylation patterns and epigenetic memory. *Genes Dev* **16:** 6-21.

Bird, A.P. 1986. CpG-rich islands and the function of DNA methylation. *Nature* **321:** 209-213.

Bird, A.P. and A.P. Wolffe. 1999. Methylation-induced repression--belts, braces, and chromatin. *Cell* **99:** 451-454.

Bjornsson, H.T., M.D. Fallin, and A.P. Feinberg. 2004. An integrated epigenetic and genetic approach to common human disease. *Trends Genet* **20:** 350-358.

Bjornsson, H.T., M.I. Sigurdsson, M.D. Fallin, R.A. Irizarry, T. Aspelund, H. Cui, W. Yu, M.A. Rongione, T.J. Ekstrom, T.B. Harris, L.J. Launer, G. Eiriksdottir, M.F. Leppert, C. Sapienza, V. Gudnason, and A.P. Feinberg. 2008. Intra-individual change over time in DNA methylation with familial clustering. *Jama* **299:** 2877-2883.

Bock, C., E.M. Tomazou, A.B. Brinkman, F. Muller, F. Simmer, H. Gu, N. Jager, A. Gnirke, H.G. Stunnenberg, and A. Meissner. 2010. Quantitative comparison of genome-wide DNA methylation mapping technologies. *Nat Biotechnol* **28:** 1106-1114.

Bock, C., J. Walter, M. Paulsen, and T. Lengauer. 2008. Inter-individual variation of DNA methylation and its implications for large-scale epigenome mapping. *Nucleic Acids Res* **36:** e55.

Boks, M.P., E.M. Derks, D.J. Weisenberger, E. Strengman, E. Janson, I.E. Sommer, R.S. Kahn, and R.A. Ophoff. 2009. The relationship of DNA methylation with age, gender and genotype in twins and healthy controls. *PLoS One* **4:** e6767.

Bollati, V., A. Baccarelli, L. Hou, M. Bonzini, S. Fustinoni, D. Cavallo, H.M. Byun, J. Jiang, B. Marinelli, A.C. Pesatori, P.A. Bertazzi, and A.S. Yang. 2007. Changes in DNA methylation patterns in subjects exposed to low-dose benzene. *Cancer Res* **67:** 876-880.

Borgel, J., S. Guibert, Y. Li, H. Chiba, D. Schubeler, H. Sasaki, T. Forne, and M. Weber. 2010. Targets and dynamics of promoter DNA methylation during early mouse development. *Nat Genet* **42:** 1093-1100.

Bork, S., S. Pfister, H. Witt, P. Horn, B. Korn, A.D. Ho, and W. Wagner. 2010. DNA methylation pattern changes upon long-term culture and aging of human mesenchymal stromal cells. *Aging Cell* **9:** 54-63.

Bourc'his, D., G.L. Xu, C.S. Lin, B. Bollman, and T.H. Bestor. 2001. Dnmt3L and the establishment of maternal genomic imprints. *Science* **294:** 2536-2539.

Bourque, D., M. Penaherrera, R. Yuen, M. Van Allen, D. McFadden, and W. Robinson. 2011. The utility of quantitative methylation assays at imprinted genes for the diagnosis of fetal and placental disorders. *Clin Genet* **79:** 169-175.

Bourque, D.K., L. Avila, M. Penaherrera, P. von Dadelszen, and W.P. Robinson. 2010. Decreased placental methylation at the H19/IGF2 imprinting control region is associated with normotensive intrauterine growth restriction but not preeclampsia. *Placenta* **31:** 197-202.

Boyer, L.A., K. Plath, J. Zeitlinger, T. Brambrink, L.A. Medeiros, T.I. Lee, S.S. Levine, M. Wernig, A. Tajonar, M.K. Ray, G.W. Bell, A.P. Otte, M. Vidal, D.K. Gifford, R.A.

Young, and R. Jaenisch. 2006. Polycomb complexes repress developmental regulators in murine embryonic stem cells. *Nature* **441:** 349-353.

Brunner, A.L., D.S. Johnson, S.W. Kim, A. Valouev, T.E. Reddy, N.F. Neff, E. Anton, C. Medina, L. Nguyen, E. Chiao, C.B. Oyolu, G.P. Schroth, D.M. Absher, J.C. Baker, and R.M. Myers. 2009. Distinct DNA methylation patterns characterize differentiated human embryonic stem cells and developing human fetal liver. *Genome Res* **19:** 1044-1056.

Busque, L., R. Mio, J. Mattioli, E. Brais, N. Blais, Y. Lalonde, M. Maragh, and D.G. Gilliland. 1996. Nonrandom X-inactivation patterns in normal females: lyonization ratios vary with age. *Blood* **88:** 59-65.

Byun, H.M., K.D. Siegmund, F. Pan, D.J. Weisenberger, G. Kanel, P.W. Laird, and A.S. Yang. 2009. Epigenetic profiling of somatic tissues from human autopsy specimens identifies tissue- and individual-specific DNA methylation patterns. *Hum Mol Genet* **18:** 4808-4817.

Calvanese, V., A. Horrillo, A. Hmadcha, B. Suarez-Alvarez, A.F. Fernandez, E. Lara, S. Casado, P. Menendez, C. Bueno, J. Garcia-Castro, R. Rubio, P. Lapunzina, M. Alaminos, L. Borghese, S. Terstegge, N.J. Harrison, H.D. Moore, O. Brustle, C. Lopez-Larrea, P.W. Andrews, B. Soria, M. Esteller, and M.F. Fraga. 2008. Cancer genes hypermethylated in human embryonic stem cells. *PLoS One* **3:** e3294.

Carrel, L. and H.F. Willard. 2005. X-inactivation profile reveals extensive variability in X-linked gene expression in females. *Nature* **434:** 400-404.

Carter, A.M. and A.C. Enders. 2004. Comparative aspects of trophoblast development and placentation. *Reprod Biol Endocrinol* **2:** 46.

Cedar, H. and Y. Bergman. 2009. Linking DNA methylation and histone modification: patterns and paradigms. *Nat Rev Genet* **10:** 295-304.

Centlow, M., P. Carninci, K. Nemeth, E. Mezey, M. Brownstein, and S.R. Hansson. 2008. Placental expression profiling in preeclampsia: local overproduction of hemoglobin may drive pathological changes. *Fertil Steril* **90:** 1834-1843.

Cetin, I., J.M. Foidart, M. Miozzo, T. Raun, T. Jansson, V. Tsatsaris, W. Reik, J. Cross, S. Hauguel-de-Mouzon, N. Illsley, J. Kingdom, and B. Huppertz. 2004. Fetal growth restriction: a workshop report. *Placenta* **25:** 753-757.

Chan, T.L., S.T. Yuen, C.K. Kong, Y.W. Chan, A.S. Chan, W.F. Ng, W.Y. Tsui, M.W. Lo, W.Y. Tam, V.S. Li, and S.Y. Leung. 2006. Heritable germline epimutation of MSH2 in a family with hereditary nonpolyposis colorectal cancer. *Nat Genet* **38:** 1178-1183.

Chapman, V., L. Forrester, J. Sanford, N. Hastie, and J. Rossant. 1984. Cell lineage-specific undermethylation of mouse repetitive DNA. *Nature* **307:** 284-286.

Charnock-Jones, D.S. and G.J. Burton. 2000. Placental vascular morphogenesis. *Baillieres Best Pract Res Clin Obstet Gynaecol* **14:** 953-968.

Chelbi, S.T., F. Mondon, H. Jammes, C. Buffat, T.M. Mignot, J. Tost, F. Busato, I. Gut, R. Rebourcet, P. Laissue, V. Tsatsaris, F. Goffinet, V. Rigourd, B. Carbonne, F. Ferre, and D. Vaiman. 2007. Expressional and epigenetic alterations of placental serine protease inhibitors: SERPINA3 is a potential marker of preeclampsia. *Hypertension* **49:** 76-83.

Chelbi, S.T. and D. Vaiman. 2008. Genetic and epigenetic factors contribute to the onset of preeclampsia. *Mol Cell Endocrinol* **282:** 120-129.

Cheung, V.G., A. Bruzel, J.T. Burdick, M. Morley, J.L. Devlin, and R.S. Spielman. 2008. Monozygotic twins reveal germline contribution to allelic expression differences. *Am J Hum Genet* **82:** 1357-1360.

Cheung, V.G., L.K. Conlin, T.M. Weber, M. Arcaro, K.Y. Jen, M. Morley, and R.S. Spielman. 2003. Natural variation in human gene expression assessed in lymphoblastoid cells. *Nat Genet* **33:** 422-425.

Chim, S.S., Y.K. Tong, R.W. Chiu, T.K. Lau, T.N. Leung, L.Y. Chan, C.B. Oudejans, C. Ding, and Y.M. Lo. 2005. Detection of the placental epigenetic signature of the maspin gene in maternal plasma. *Proc Natl Acad Sci U S A* **102:** 14753-14758.

Chiu, R.W., S.S. Chim, I.H. Wong, C.S. Wong, W.S. Lee, K.F. To, J.H. Tong, R.K. Yuen, A.S. Shum, J.K. Chan, L.Y. Chan, J.W. Yuen, Y.K. Tong, J.F. Weier, C. Ferlatte, T.N. Leung, T.K. Lau, K.W. Lo, and Y.M. Lo. 2007. Hypermethylation of RASSF1A in human and rhesus placentas. *Am J Pathol* **170:** 941-950.

Christensen, B.C., E.A. Houseman, C.J. Marsit, S. Zheng, M.R. Wrensch, J.L. Wiemels, H.H. Nelson, M.R. Karagas, J.F. Padbury, R. Bueno, D.J. Sugarbaker, R.F. Yeh, J.K. Wiencke, and K.T. Kelsey. 2009. Aging and environmental exposures alter tissue-specific DNA methylation dependent upon CpG island context. *PLoS Genet* **5:** e1000602.

Coan, P.M., G.J. Burton, and A.C. Ferguson-Smith. 2005. Imprinted genes in the placenta--a review. *Placenta* **26 Suppl A:** S10-20.

Cohen, N.M., V. Dighe, G. Landan, S. Reynisdottir, A. Palsson, S. Mitalipov, and A. Tanay. 2009. DNA methylation programming and reprogramming in primate embryonic stem cells. *Genome Res* **19:** 2193-2201.

Constancia, M., M. Hemberger, J. Hughes, W. Dean, A. Ferguson-Smith, R. Fundele, F. Stewart, G. Kelsey, A. Fowden, C. Sibley, and W. Reik. 2002. Placental-specific IGF-II is a major modulator of placental and fetal growth. *Nature* **417:** 945-948.

Constancia, M., G. Kelsey, and W. Reik. 2004. Resourceful imprinting. *Nature* **432:** 53-57.

Cooper, W.N. and M. Constancia. 2010. How genome-wide approaches can be used to unravel the remaining secrets of the imprintome. *Brief Funct Genomics* **9:** 315-328.

Cooper, W.N., A. Luharia, G.A. Evans, H. Raza, A.C. Haire, R. Grundy, S.C. Bowdin, A. Riccio, G. Sebastio, J. Bliek, P.N. Schofield, W. Reik, F. Macdonald, and E.R. Maher. 2005. Molecular subtypes and phenotypic expression of Beckwith-Wiedemann syndrome. *Eur J Hum Genet* **13:** 1025-1032.

Cotton, A.M., L. Avila, M.S. Penaherrera, J.G. Affleck, W.P. Robinson, and C.J. Brown. 2009. Inactive X chromosome-specific reduction in placental DNA methylation. *Hum Mol Genet* **18:** 3544-3552.

Cross, J.C., Z. Werb, and S.J. Fisher. 1994. Implantation and the placenta: key pieces of the development puzzle. *Science* **266:** 1508-1518.

Cui, H., M. Cruz-Correa, F.M. Giardiello, D.F. Hutcheon, D.R. Kafonek, S. Brandenburg, Y. Wu, X. He, N.R. Powe, and A.P. Feinberg. 2003. Loss of IGF2 imprinting: a potential marker of colorectal cancer risk. *Science* **299:** 1753-1755.

Cui, H., E.L. Niemitz, J.D. Ravenel, P. Onyango, S.A. Brandenburg, V.V. Lobanenkov, and A.P. Feinberg. 2001. Loss of imprinting of insulin-like growth factor-II in Wilms' tumor commonly involves altered methylation but not mutations of CTCF or its binding site. *Cancer Res* **61:** 4947-4950.

Curhan, G.C., G.M. Chertow, W.C. Willett, D. Spiegelman, G.A. Colditz, J.E. Manson, F.E. Speizer, and M.J. Stampfer. 1996a. Birth weight and adult hypertension and obesity in women. *Circulation* **94:** 1310-1315.

Curhan, G.C., W.C. Willett, E.B. Rimm, D. Spiegelman, A.L. Ascherio, and M.J. Stampfer. 1996b. Birth weight and adult hypertension, diabetes mellitus, and obesity in US men. *Circulation* **94:** 3246-3250.

Daelemans, C., M.E. Ritchie, G. Smits, S. Abu-Amero, I.M. Sudbery, M.S. Forrest, S. Campino, T.G. Clark, P. Stanier, D. Kwiatkowski, P. Deloukas, E.T. Dermitzakis, S. Tavare, G.E. Moore, and I. Dunham. 2010. High-throughput analysis of candidate imprinted genes and allele-specific gene expression in the human term placenta. *BMC Genet* **11:** 25.

Dahlgren, J., C. Nilsson, E. Jennische, H.P. Ho, E. Eriksson, A. Niklasson, P. Bjorntorp, K. Albertsson Wikland, and A. Holmang. 2001. Prenatal cytokine exposure results in obesity and gender-specific programming. *Am J Physiol Endocrinol Metab* **281:** E326-334.

Dahri, S., A. Snoeck, B. Reusens-Billen, C. Remacle, and J.J. Hoet. 1991. Islet function in offspring of mothers on low-protein diet during gestation. *Diabetes* **40 Suppl 2:** 115-120.

Dauphinot, L., R. Lyle, I. Rivals, M.T. Dang, R.X. Moldrich, G. Golfier, L. Ettwiller, K. Toyama, J. Rossier, L. Personnaz, S.E. Antonarakis, C.J. Epstein, P.M. Sinet, and M.C. Potier. 2005. The cerebellar transcriptome during postnatal development of the Ts1Cje mouse, a segmental trisomy model for Down syndrome. *Hum Mol Genet* **14:** 373-384.

DeChiara, T.M., D.C. Bowen, D.M. Valenzuela, M.V. Simmons, W.T. Poueymirou, S. Thomas, E. Kinetz, D.L. Compton, E. Rojas, J.S. Park, C. Smith, P.S. DiStefano, D.J. Glass, S.J. Burden, and G.D. Yancopoulos. 1996. The receptor tyrosine kinase MuSK is required for neuromuscular junction formation in vivo. *Cell* **85:** 501-512.

DeChiara, T.M., A. Efstratiadis, and E.J. Robertson. 1990. A growth-deficiency phenotype in heterozygous mice carrying an insulin-like growth factor II gene disrupted by targeting. *Nature* **345:** 78-80.

DeChiara, T.M., E.J. Robertson, and A. Efstratiadis. 1991. Parental imprinting of the mouse insulin-like growth factor II gene. *Cell* **64:** 849-859.

Delaval, K. and R. Feil. 2004. Epigenetic regulation of mammalian genomic imprinting. *Curr Opin Genet Dev* **14:** 188-195.

Dennis, G., Jr., B.T. Sherman, D.A. Hosack, J. Yang, W. Gao, H.C. Lane, and R.A. Lempicki. 2003. DAVID: Database for Annotation, Visualization, and Integrated Discovery. *Genome Biol* **4:** P3.

Dennis Lo, Y.M. and R.W. Chiu. 2007. Prenatal diagnosis: progress through plasma nucleic acids. *Nat Rev Genet* **8:** 71-77.

Dijk, M., S. Drewlo, and C.B. Oudejans. 2010. Differential methylation of STOX1 in human placenta. *Epigenetics* **5:** 736-742.

Dokras, A., J. Coffin, L. Field, A. Frakes, H. Lee, A. Madan, T. Nelson, G.Y. Ryu, J.G. Yoon, and A. Madan. 2006. Epigenetic regulation of maspin expression in the human placenta. *Mol Hum Reprod* **12:** 611-617.

Domann, F.E., J.C. Rice, M.J. Hendrix, and B.W. Futscher. 2000. Epigenetic silencing of maspin gene expression in human breast cancers. *Int J Cancer* **85:** 805-810.

Douglas, K.A. and C.W. Redman. 1994. Eclampsia in the United Kingdom. *Bmj* **309:** 1395-1400.

Eckhardt, F., J. Lewin, R. Cortese, V.K. Rakyan, J. Attwood, M. Burger, J. Burton, T.V. Cox, R. Davies, T.A. Down, C. Haefliger, R. Horton, K. Howe, D.K. Jackson, J. Kunde, C. Koenig, J. Liddle, D. Niblett, T. Otto, R. Pettett, S. Seemann, C. Thompson, T. West, J. Rogers, A. Olek, K. Berlin, and S. Beck. 2006. DNA methylation profiling of human chromosomes 6, 20 and 22. *Nat Genet* **38:** 1378-1385.

Enquobahrie, D.A., M. Meller, K. Rice, B.M. Psaty, D.S. Siscovick, and M.A. Williams. 2008. Differential placental gene expression in preeclampsia. *Am J Obstet Gynecol* **199:** 566 e561-511.

Esteller, M. 2008. Epigenetics in cancer. *N Engl J Med* **358:** 1148-1159.

Esteller, M. and J.G. Herman. 2002. Cancer as an epigenetic disease: DNA methylation and chromatin alterations in human tumours. *J Pathol* **196:** 1-7.

Fajardy, I., E. Moitrot, A. Vambergue, M. Vandersippe-Millot, P. Deruelle, and J. Rousseaux. 2009. Time course analysis of RNA stability in human placenta. *BMC Mol Biol* **10:** 21.

Farina, A., D. Morano, D. Arcelli, P. De Sanctis, A. Sekizawa, Y. Purwosunu, C. Zucchini, G. Simonazzi, T. Okai, and N. Rizzo. 2009. Gene expression in chorionic villous samples at 11 weeks of gestation in women who develop preeclampsia later in pregnancy: implications for screening. *Prenat Diagn* **29:** 1038-1044.

Farthing, C.R., G. Ficz, R.K. Ng, C.F. Chan, S. Andrews, W. Dean, M. Hemberger, and W. Reik. 2008. Global mapping of DNA methylation in mouse promoters reveals epigenetic reprogramming of pluripotency genes. *PLoS Genet* **4:** e1000116.

Feil, R., J. Walter, N.D. Allen, and W. Reik. 1994. Developmental control of allelic methylation in the imprinted mouse Igf2 and H19 genes. *Development* **120:** 2933-2943.

Feng, H., A.N. Cheung, W.C. Xue, Y. Wang, X. Wang, S. Fu, Q. Wang, H.Y. Ngan, and S.W. Tsao. 2004. Down-regulation and promoter methylation of tissue inhibitor of metalloproteinase 3 in choriocarcinoma. *Gynecol Oncol* **94:** 375-382.

Ferguson-Smith, A.C., B.M. Cattanach, S.C. Barton, C.V. Beechey, and M.A. Surani. 1991. Embryological and molecular investigations of parental imprinting on mouse chromosome 7. *Nature* **351:** 667-670.

Ferreira, J.C., S. Choufani, D. Grafodatskaya, D.T. Butcher, C. Zhao, D. Chitayat, C. Shuman, J. Kingdom, S. Keating, and R. Weksberg. 2011. WNT2 promoter methylation in human placenta is associated with low birthweight percentile in the neonate. *Epigenetics* **6**.

FitzPatrick, D.R., J. Ramsay, N.I. McGill, M. Shade, A.D. Carothers, and N.D. Hastie. 2002. Transcriptome analysis of human autosomal trisomy. *Hum Mol Genet* **11:** 3249-3256.

Flanagan, J.M., V. Popendikyte, N. Pozdniakovaite, M. Sobolev, A. Assadzadeh, A. Schumacher, M. Zangeneh, L. Lau, C. Virtanen, S.C. Wang, and A. Petronis. 2006. Intra- and interindividual epigenetic variation in human germ cells. *Am J Hum Genet* **79:** 67-84.

Founds, S.A., Y.P. Conley, J.F. Lyons-Weiler, A. Jeyabalan, W.A. Hogge, and K.P. Conrad. 2009. Altered global gene expression in first trimester placentas of women destined to develop preeclampsia. *Placenta* **30:** 15-24.

Fraga, M.F., E. Ballestar, M.F. Paz, S. Ropero, F. Setien, M.L. Ballestar, D. Heine-Suner, J.C. Cigudosa, M. Urioste, J. Benitez, M. Boix-Chornet, A. Sanchez-Aguilera, C. Ling, E. Carlsson, P. Poulsen, A. Vaag, Z. Stephan, T.D. Spector, Y.Z. Wu, C. Plass, and M. Esteller. 2005. Epigenetic differences arise during the lifetime of monozygotic twins. *Proc Natl Acad Sci U S A* **102:** 10604-10609.

Frevel, M.A., S.J. Sowerby, G.B. Petersen, and A.E. Reeve. 1999. Methylation sequencing analysis refines the region of H19 epimutation in Wilms tumor. *J Biol Chem* **274:** 29331-29340.

Frommer, M., L.E. McDonald, D.S. Millar, C.M. Collis, F. Watt, G.W. Grigg, P.L. Molloy, and C.L. Paul. 1992. A genomic sequencing protocol that yields a positive display of 5-methylcytosine residues in individual DNA strands. *Proc Natl Acad Sci U S A* **89:** 1827-1831.

Frost, J.M. and G.E. Moore. 2010. The importance of imprinting in the human placenta. *PLoS Genet* **6:** e1001015.

Fryer, A.A., T.M. Nafee, K.M. Ismail, W.D. Carroll, R.D. Emes, and W.E. Farrell. 2009. LINE-1 DNA methylation is inversely correlated with cord plasma homocysteine in man: a preliminary study. *Epigenetics* **4:** 394-398.

Futscher, B.W., M.M. Oshiro, R.J. Wozniak, N. Holtan, C.L. Hanigan, H. Duan, and F.E. Domann. 2002. Role for DNA methylation in the control of cell type specific maspin expression. *Nat Genet* **31:** 175-179.

Gack, S., A. Marme, F. Marme, G. Wrobel, B. Vonderstrass, G. Bastert, P. Lichter, P. Angel, and M. Schorpp-Kistner. 2005. Preeclampsia: increased expression of soluble ADAM 12. *J Mol Med* **83:** 887-896.

Gao, W.L., D. Li, Z.X. Xiao, Q.P. Liao, H.X. Yang, Y.X. Li, L. Ji, and Y.L. Wang. 2011. Detection of global DNA methylation and paternally imprinted H19 gene methylation in preeclamptic placentas. *Hypertens Res*.

Genbacev, O., Y. Zhou, J.W. Ludlow, and S.J. Fisher. 1997. Regulation of human placental development by oxygen tension. *Science* **277:** 1669-1672.

Gerety, S.S., H.U. Wang, Z.F. Chen, and D.J. Anderson. 1999. Symmetrical mutant phenotypes of the receptor EphB4 and its specific transmembrane ligand ephrin-B2 in cardiovascular development. *Mol Cell* **4:** 403-414.

Gheorghe, C.P., S. Mohan, K.C. Oberg, and L.D. Longo. 2007. Gene expression patterns in the hypoxic murine placenta: a role in epigenesis? *Reprod Sci* **14:** 223-233.

Gibbons, R.J., T.L. McDowell, S. Raman, D.M. O'Rourke, D. Garrick, H. Ayyub, and D.R. Higgs. 2000. Mutations in ATRX, encoding a SWI/SNF-like protein, cause diverse changes in the pattern of DNA methylation. *Nat Genet* **24:** 368-371.

Gicquel, C., S. Rossignol, S. Cabrol, M. Houang, V. Steunou, V. Barbu, F. Danton, N. Thibaud, M. Le Merrer, L. Burglen, A.M. Bertrand, I. Netchine, and Y. Le Bouc. 2005. Epimutation of the telomeric imprinting center region on chromosome 11p15 in Silver-Russell syndrome. *Nat Genet* **37:** 1003-1007.

Gluckman, P.D. and M.A. Hanson. 2004a. The developmental origins of the metabolic syndrome. *Trends Endocrinol Metab* **15:** 183-187.

Gluckman, P.D. and M.A. Hanson. 2004b. Living with the past: evolution, development, and patterns of disease. *Science* **305:** 1733-1736.

Gluckman, P.D., M.A. Hanson, C. Cooper, and K.L. Thornburg. 2008. Effect of in utero and early-life conditions on adult health and disease. *N Engl J Med* **359:** 61-73.

Godfrey, K.M. 2002. The role of the placenta in fetal programming-a review. *Placenta* **23 Suppl A:** S20-27.

Goll, M.G., F. Kirpekar, K.A. Maggert, J.A. Yoder, C.L. Hsieh, X. Zhang, K.G. Golic, S.E. Jacobsen, and T.H. Bestor. 2006. Methylation of tRNAAsp by the DNA methyltransferase homolog Dnmt2. *Science* **311:** 395-398.

Goswami, D., D.S. Tannetta, L.A. Magee, A. Fuchisawa, C.W. Redman, I.L. Sargent, and P. von Dadelszen. 2006. Excess syncytiotrophoblast microparticle shedding is a feature of early-onset pre-eclampsia, but not normotensive intrauterine growth restriction. *Placenta* **27:** 56-61.

Grafodatskaya, D., S. Choufani, J.C. Ferreira, D.T. Butcher, Y. Lou, C. Zhao, S.W. Scherer, and R. Weksberg. 2010. EBV transformation and cell culturing destabilizes DNA methylation in human lymphoblastoid cell lines. *Genomics* **95:** 73-83.

Grafstrom, R.H., R. Yuan, and D.L. Hamilton. 1985. The characteristics of DNA methylation in an in vitro DNA synthesizing system from mouse fibroblasts. *Nucleic Acids Res* **13:** 2827-2842.

Granger, J.P., B.B. LaMarca, K. Cockrell, M. Sedeek, C. Balzi, D. Chandler, and W. Bennett. 2006. Reduced uterine perfusion pressure (RUPP) model for studying cardiovascular-renal dysfunction in response to placental ischemia. *Methods Mol Med* **122:** 383-392.

Grati, F.R., M. Miozzo, B. Cassani, F. Rossella, P. Antonazzo, B. Gentilin, S.M. Sirchia, L. Mori, S. Rigano, G. Bulfamante, I. Cetin, and G. Simoni. 2005. Fetal and placental chromosomal mosaicism revealed by QF-PCR in severe IUGR pregnancies. *Placenta* **26:** 10-18.

Grati, F.R., S.M. Sirchia, B. Gentilin, F. Rossella, L. Ramoscelli, P. Antonazzo, U. Cavallari, G. Bulfamante, I. Cetin, G. Simoni, and M. Miozzo. 2004. Biparental expression of ESX1L gene in placentas from normal and intrauterine growth-restricted pregnancies. *Eur J Hum Genet* **12:** 272-278.

Grayson, D.R., X. Jia, Y. Chen, R.P. Sharma, C.P. Mitchell, A. Guidotti, and E. Costa. 2005. Reelin promoter hypermethylation in schizophrenia. *Proc Natl Acad Sci U S A* **102:** 9341-9346.

Gregg, C., J. Zhang, J.E. Butler, D. Haig, and C. Dulac. 2010a. Sex-specific parent-of-origin allelic expression in the mouse brain. *Science* **329:** 682-685.

Gregg, C., J. Zhang, B. Weissbourd, S. Luo, G.P. Schroth, D. Haig, and C. Dulac. 2010b. High-resolution analysis of parent-of-origin allelic expression in the mouse brain. *Science* **329:** 643-648.

Grigoriu, A., J.C. Ferreira, S. Choufani, D. Baczyk, J. Kingdom, and R. Weksberg. 2011. Cell specific patterns of methylation in the human placenta. *Epigenetics* **6:** 368-379.

Gronniger, E., B. Weber, O. Heil, N. Peters, F. Stab, H. Wenck, B. Korn, M. Winnefeld, and F. Lyko. 2010. Aging and chronic sun exposure cause distinct epigenetic changes in human skin. *PLoS Genet* **6:** e1000971.

Guilleret, I., M.C. Osterheld, R. Braunschweig, V. Gastineau, S. Taillens, and J. Benhattar. 2009. Imprinting of tumor-suppressor genes in human placenta. *Epigenetics* **4:** 62-68.

Guo, L., S. Choufani, J. Ferreira, A. Smith, D. Chitayat, C. Shuman, R. Uxa, S. Keating, J. Kingdom, and R. Weksberg. 2008. Altered gene expression and methylation of the human chromosome 11 imprinted region in small for gestational age (SGA) placentae. *Dev Biol* **320:** 79-91.

Gupta, P.B., C. Kuperwasser, J.P. Brunet, S. Ramaswamy, W.L. Kuo, J.W. Gray, S.P. Naber, and R.A. Weinberg. 2005. The melanocyte differentiation program predisposes to metastasis after neoplastic transformation. *Nat Genet* **37:** 1047-1054.

Hajkova, P., S. Erhardt, N. Lane, T. Haaf, O. El-Maarri, W. Reik, J. Walter, and M.A. Surani. 2002. Epigenetic reprogramming in mouse primordial germ cells. *Mech Dev* **117:** 15-23.

Hales, C.N., D.J. Barker, P.M. Clark, L.J. Cox, C. Fall, C. Osmond, and P.D. Winter. 1991. Fetal and infant growth and impaired glucose tolerance at age 64. *Bmj* **303:** 1019-1022.

Hannan, N.J., P. Paiva, E. Dimitriadis, and L.A. Salamonsen. 2010. Models for study of human embryo implantation: choice of cell lines? *Biol Reprod* **82:** 235-245.

Hansson, S.R., Y. Chen, J. Brodszki, M. Chen, E. Hernandez-Andrade, J.M. Inman, O.A. Kozhich, I. Larsson, K. Marsal, P. Medstrand, C.C. Xiang, and M.J. Brownstein. 2006. Gene expression profiling of human placentas from preeclamptic and normotensive pregnancies. *Mol Hum Reprod* **12:** 169-179.

Hatchwell, E. and J.M. Greally. 2007. The potential role of epigenomic dysregulation in complex human disease. *Trends Genet* **23:** 588-595.

Heijmans, B.T., D. Kremer, E.W. Tobi, D.I. Boomsma, and P.E. Slagboom. 2007. Heritable rather than age-related environmental and stochastic factors dominate variation in DNA methylation of the human IGF2/H19 locus. *Hum Mol Genet* **16:** 547-554.

Heikkila, A., T. Tuomisto, S.K. Hakkinen, L. Keski-Nisula, S. Heinonen, and S. Yla-Herttuala. 2005. Tumor suppressor and growth regulatory genes are overexpressed in severe early-onset preeclampsia--an array study on case-specific human preeclamptic placental tissue. *Acta Obstet Gynecol Scand* **84:** 679-689.

Henckel, A. and P. Arnaud. 2010. Genome-wide identification of new imprinted genes. *Brief Funct Genomics* **9:** 304-314.

Herman, J.G. and S.B. Baylin. 2003. Gene silencing in cancer in association with promoter hypermethylation. *N Engl J Med* **349:** 2042-2054.

Herman, J.G., J.R. Graff, S. Myohanen, B.D. Nelkin, and S.B. Baylin. 1996. Methylation-specific PCR: a novel PCR assay for methylation status of CpG islands. *Proc Natl Acad Sci U S A* **93:** 9821-9826.

Higuchi, T., H. Kanzaki, H. Nakayama, M. Fujimoto, H. Hatayama, K. Kojima, M. Iwai, T. Mori, and J. Fujita. 1995. Induction of tissue inhibitor of metalloproteinase 3 gene expression during in vitro decidualization of human endometrial stromal cells. *Endocrinology* **136:** 4973-4981.

Hodges, E., A.D. Smith, J. Kendall, Z. Xuan, K. Ravi, M. Rooks, M.Q. Zhang, K. Ye, A. Bhattacharjee, L. Brizuela, W.R. McCombie, M. Wigler, G.J. Hannon, and J.B. Hicks. 2009. High definition profiling of mammalian DNA methylation by array capture and single molecule bisulfite sequencing. *Genome Res* **19:** 1593-1605.

Hoegh, A.M., R. Borup, F.C. Nielsen, S. Sorensen, and T.V. Hviid. 2010. Gene expression profiling of placentas affected by pre-eclampsia. *J Biomed Biotechnol* **2010:** 787545.

Hoet, J.J. and M.A. Hanson. 1999. Intrauterine nutrition: its importance during critical periods for cardiovascular and endocrine development. *J Physiol* **514 (Pt 3):** 617-627.

Hogart, A., R.P. Nagarajan, K.A. Patzel, D.H. Yasui, and J.M. Lasalle. 2007. 15q11-13 GABAA receptor genes are normally biallelically expressed in brain yet are subject to epigenetic dysregulation in autism-spectrum disorders. *Hum Mol Genet* **16:** 691-703.

Horsfield, J., A. Ramachandran, K. Reuter, E. LaVallie, L. Collins-Racie, K. Crosier, and P. Crosier. 2002. Cadherin-17 is required to maintain pronephric duct integrity during zebrafish development. *Mech Dev* **115:** 15-26.

Houseman, E.A., B.C. Christensen, R.F. Yeh, C.J. Marsit, M.R. Karagas, M. Wrensch, H.H. Nelson, J. Wiemels, S. Zheng, J.K. Wiencke, and K.T. Kelsey. 2008. Model-based clustering of DNA methylation array data: a recursive-partitioning algorithm for high-dimensional data arising as a mixture of beta distributions. *BMC Bioinformatics* **9:** 365.

Howlett, S.K. and W. Reik. 1991. Methylation levels of maternal and paternal genomes during preimplantation development. *Development* **113:** 119-127.

Huang da, W., B.T. Sherman, and R.A. Lempicki. 2009. Systematic and integrative analysis of large gene lists using DAVID bioinformatics resources. *Nat Protoc* **4:** 44-57.

Huang, J.M. and J. Kim. 2009. DNA methylation analysis of the mammalian PEG3 imprinted domain. *Gene* **442:** 18-25.

Huppertz, B. 2008. Placental origins of preeclampsia: challenging the current hypothesis. *Hypertension* **51:** 970-975.

Illingworth, R., A. Kerr, D. Desousa, H. Jorgensen, P. Ellis, J. Stalker, D. Jackson, C. Clee, R. Plumb, J. Rogers, S. Humphray, T. Cox, C. Langford, and A. Bird. 2008. A novel CpG island set identifies tissue-specific methylation at developmental gene loci. *PLoS Biol* **6:** e22.

Illingworth, R.S., U. Gruenewald-Schneider, S. Webb, A.R. Kerr, K.D. James, D.J. Turner, C. Smith, D.J. Harrison, R. Andrews, and A.P. Bird. 2010. Orphan CpG islands identify numerous conserved promoters in the mammalian genome. *PLoS Genet* **6**.

Inoki, I., T. Shiomi, G. Hashimoto, H. Enomoto, H. Nakamura, K. Makino, E. Ikeda, S. Takata, K. Kobayashi, and Y. Okada. 2002. Connective tissue growth factor binds vascular endothelial growth factor (VEGF) and inhibits VEGF-induced angiogenesis. *Faseb J* **16:** 219-221.

Irizarry, R.A., C. Ladd-Acosta, B. Carvalho, H. Wu, S.A. Brandenburg, J.A. Jeddeloh, B. Wen, and A.P. Feinberg. 2008. Comprehensive high-throughput arrays for relative methylation (CHARM). *Genome Res* **18:** 780-790.

Irizarry, R.A., C. Ladd-Acosta, B. Wen, Z. Wu, C. Montano, P. Onyango, H. Cui, K. Gabo, M. Rongione, M. Webster, H. Ji, J.B. Potash, S. Sabunciyan, and A.P. Feinberg. 2009. The human colon cancer methylome shows similar hypo- and hypermethylation at conserved tissue-specific CpG island shores. *Nat Genet* **41:** 178-186.

Issa, J.P., Y.L. Ottaviano, P. Celano, S.R. Hamilton, N.E. Davidson, and S.B. Baylin. 1994. Methylation of the oestrogen receptor CpG island links ageing and neoplasia in human colon. *Nat Genet* **7:** 536-540.

Jaenisch, R. and A. Bird. 2003. Epigenetic regulation of gene expression: how the genome integrates intrinsic and environmental signals. *Nat Genet* **33 Suppl:** 245-254.

James, J.L., P.R. Stone, and L.W. Chamley. 2006. The regulation of trophoblast differentiation by oxygen in the first trimester of pregnancy. *Hum Reprod Update* **12:** 137-144.

Jansson, T. and G.W. Lambert. 1999. Effect of intrauterine growth restriction on blood pressure, glucose tolerance and sympathetic nervous system activity in the rat at 3-4 months of age. *J Hypertens* **17:** 1239-1248.

Jarvenpaa, J., J.T. Vuoristo, E.R. Savolainen, O. Ukkola, T. Vaskivuo, and M. Ryynanen. 2007. Altered expression of angiogenesis-related placental genes in pre-eclampsia associated with intrauterine growth restriction. *Gynecol Endocrinol* **23:** 351-355.

Jinno, Y., K. Yun, K. Nishiwaki, T. Kubota, O. Ogawa, A.E. Reeve, and N. Niikawa. 1994. Mosaic and polymorphic imprinting of the WT1 gene in humans. *Nat Genet* **6:** 305-309.

Kadyrov, M., C. Schmitz, S. Black, P. Kaufmann, and B. Huppertz. 2003. Pre-eclampsia and maternal anaemia display reduced apoptosis and opposite invasive phenotypes of extravillous trophoblast. *Placenta* **24:** 540-548.

Kaminsky, Z.A., T. Tang, S.C. Wang, C. Ptak, G.H. Oh, A.H. Wong, L.A. Feldcamp, C. Virtanen, J. Halfvarson, C. Tysk, A.F. McRae, P.M. Visscher, G.W. Montgomery, Gottesman, II, N.G. Martin, and A. Petronis. 2009. DNA methylation profiles in monozygotic and dizygotic twins. *Nat Genet* **41:** 240-245.

Kanayama, N., K. Takahashi, T. Matsuura, M. Sugimura, T. Kobayashi, N. Moniwa, M. Tomita, and K. Nakayama. 2002. Deficiency in p57Kip2 expression induces preeclampsia-like symptoms in mice. *Mol Hum Reprod* **8:** 1129-1135.

Kanber, D., T. Berulava, O. Ammerpohl, D. Mitter, J. Richter, R. Siebert, B. Horsthemke, D. Lohmann, and K. Buiting. 2009. The human retinoblastoma gene is imprinted. *PLoS Genet* **5:** e1000790.

Kangaspeska, S., B. Stride, R. Metivier, M. Polycarpou-Schwarz, D. Ibberson, R.P. Carmouche, V. Benes, F. Gannon, and G. Reid. 2008. Transient cyclical methylation of promoter DNA. *Nature* **452:** 112-115.

Karumanchi, S.A. and Y. Bdolah. 2004. Hypoxia and sFlt-1 in preeclampsia: the "chicken-and-egg" question. *Endocrinology* **145:** 4835-4837.

Katari, S., N. Turan, M. Bibikova, O. Erinle, R. Chalian, M. Foster, J.P. Gaughan, C. Coutifaris, and C. Sapienza. 2009. DNA methylation and gene expression differences in children conceived in vitro or in vivo. *Hum Mol Genet* **18:** 3769-3778.

Kelleher, D.J. and R. Gilmore. 2006. An evolving view of the eukaryotic oligosaccharyltransferase. *Glycobiology* **16:** 47R-62R.

Kelsey, G. 2010. Imprinting on chromosome 20: tissue-specific imprinting and imprinting mutations in the GNAS locus. *Am J Med Genet C Semin Med Genet* **154C:** 377-386.

Kerkel, K., N. Schupf, K. Hatta, D. Pang, M. Salas, A. Kratz, M. Minden, V. Murty, W.B. Zigman, R.P. Mayeux, E.C. Jenkins, A. Torkamani, N.J. Schork, W. Silverman, B.A. Croy, and B. Tycko. 2010. Altered DNA methylation in leukocytes with trisomy 21. *PLoS Genet* **6:** e1001212.

Kerkel, K., A. Spadola, E. Yuan, J. Kosek, L. Jiang, E. Hod, K. Li, V.V. Murty, N. Schupf, E. Vilain, M. Morris, F. Haghighi, and B. Tycko. 2008. Genomic surveys by methylation-sensitive SNP analysis identify sequence-dependent allele-specific DNA methylation. *Nat Genet* **40:** 904-908.

Kliman, H.J. 2000. Uteroplacental blood flow. The story of decidualization, menstruation, and trophoblast invasion. *Am J Pathol* **157:** 1759-1768.

Koga, K., Y. Osuga, T. Tajima, Y. Hirota, T. Igarashi, T. Fujii, T. Yano, and Y. Taketani. 2010. Elevated serum soluble fms-like tyrosine kinase 1 (sFlt1) level in women with hydatidiform mole. *Fertil Steril* **94:** 305-308.

Koklanaris, N., J.C. Nwachukwu, S.J. Huang, S. Guller, K. Karpisheva, M. Garabedian, and M.J. Lee. 2006. First-trimester trophoblast cell model gene response to hypoxia. *Am J Obstet Gynecol* **194:** 687-693.

Kotzot, D. 1999. Abnormal phenotypes in uniparental disomy (UPD): fundamental aspects and a critical review with bibliography of UPD other than 15. *Am J Med Genet* **82:** 265-274.

Kramer, M.S., R.W. Platt, S.W. Wen, K.S. Joseph, A. Allen, M. Abrahamowicz, B. Blondel, and G. Breart. 2001. A new and improved population-based Canadian reference for birth weight for gestational age. *Pediatrics* **108:** E35.

Krishnamoorthy, A., L.C. Gowen, K.E. Boll, R.A. Knuppel, and L.J. Sciorra. 1995. Chromosome and interphase analysis of placental mosaicism in intrauterine growth retardation. *J Perinatol* **15:** 47-50.

Kulkarni, A., P. Chavan-Gautam, S. Mehendale, H. Yadav, and S. Joshi. 2010. Global DNA methylation patterns in placenta and its association with maternal hypertension in pre-eclampsia. *DNA Cell Biol* **30:** 79-84.

Laird, P.W. 2003. The power and the promise of DNA methylation markers. *Nat Rev Cancer* **3:** 253-266.

Langley, S.C. and A.A. Jackson. 1994. Increased systolic blood pressure in adult rats induced by fetal exposure to maternal low protein diets. *Clin Sci (Lond)* **86:** 217-222; discussion 121.

Lee, T.I., R.G. Jenner, L.A. Boyer, M.G. Guenther, S.S. Levine, R.M. Kumar, B. Chevalier, S.E. Johnstone, M.F. Cole, K. Isono, H. Koseki, T. Fuchikami, K. Abe, H.L. Murray, J.P. Zucker, B. Yuan, G.W. Bell, E. Herbolsheimer, N.M. Hannett, K. Sun, D.T. Odom, A.P. Otte, T.L. Volkert, D.P. Bartel, D.A. Melton, D.K. Gifford, R. Jaenisch, and R.A. Young. 2006. Control of developmental regulators by Polycomb in human embryonic stem cells. *Cell* **125:** 301-313.

Leighton, P.A., R.S. Ingram, J. Eggenschwiler, A. Efstratiadis, and S.M. Tilghman. 1995. Disruption of imprinting caused by deletion of the H19 gene region in mice. *Nature* **375:** 34-39.

Levy, O. 2007. Innate immunity of the newborn: basic mechanisms and clinical correlates. *Nat Rev Immunol* **7:** 379-390.

Li, E., T.H. Bestor, and R. Jaenisch. 1992. Targeted mutation of the DNA methyltransferase gene results in embryonic lethality. *Cell* **69:** 915-926.

Lo, H.S., Z. Wang, Y. Hu, H.H. Yang, S. Gere, K.H. Buetow, and M.P. Lee. 2003. Allelic variation in gene expression is common in the human genome. *Genome Res* **13:** 1855-1862.

Lo, Y.M., T.N. Leung, M.S. Tein, I.L. Sargent, J. Zhang, T.K. Lau, C.J. Haines, and C.W. Redman. 1999. Quantitative abnormalities of fetal DNA in maternal serum in preeclampsia. *Clin Chem* **45:** 184-188.

Lucas, A. 1991. Programming by early nutrition in man. *Ciba Found Symp* **156:** 38-50; discussion 50-35.

Lucifero, D., J.R. Chaillet, and J.M. Trasler. 2004. Potential significance of genomic imprinting defects for reproduction and assisted reproductive technology. *Hum Reprod Update* **10:** 3-18.

Luedi, P.P., F.S. Dietrich, J.R. Weidman, J.M. Bosko, R.L. Jirtle, and A.J. Hartemink. 2007. Computational and experimental identification of novel human imprinted genes. *Genome Res* **17:** 1723-1730.

Maegawa, S., G. Hinkal, H.S. Kim, L. Shen, L. Zhang, J. Zhang, N. Zhang, S. Liang, L.A. Donehower, and J.P. Issa. 2010. Widespread and tissue specific age-related DNA methylation changes in mice. *Genome Res* **20:** 332-340.

Makris, A., C. Thornton, J. Thompson, S. Thomson, R. Martin, R. Ogle, R. Waugh, P. McKenzie, P. Kirwan, and A. Hennessy. 2007. Uteroplacental ischemia results in proteinuric hypertension and elevated sFLT-1. *Kidney Int* **71:** 977-984.

Maltepe, E., G.W. Krampitz, K.M. Okazaki, K. Red-Horse, W. Mak, M.C. Simon, and S.J. Fisher. 2005. Hypoxia-inducible factor-dependent histone deacetylase activity determines stem cell fate in the placenta. *Development* **132:** 3393-3403.

Mann, J.R. 2001. Imprinting in the germ line. *Stem Cells* **19:** 287-294.

Matouskova, M., J. Blazkova, P. Pajer, A. Pavlicek, and J. Hejnar. 2006. CpG methylation suppresses transcriptional activity of human syncytin-1 in non-placental tissues. *Exp Cell Res* **312:** 1011-1020.

Mayer, W., M. Hemberger, H.G. Frank, R. Grummer, E. Winterhager, P. Kaufmann, and R. Fundele. 2000a. Expression of the imprinted genes MEST/Mest in human and murine placenta suggests a role in angiogenesis. *Dev Dyn* **217:** 1-10.

Mayer, W., A. Niveleau, J. Walter, R. Fundele, and T. Haaf. 2000b. Demethylation of the zygotic paternal genome. *Nature* **403:** 501-502.

Maymo, J.L., A.P. Perez, Y. Gambino, J.C. Calvo, V. Sanchez-Margalet, and C.L. Varone. 2011. Review: Leptin gene expression in the placenta--regulation of a key hormone in trophoblast proliferation and survival. *Placenta* **32 Suppl 2:** S146-153.

Mayor-Lynn, K., T. Toloubeydokhti, A.C. Cruz, and N. Chegini. 2010. Expression profile of microRNAs and mRNAs in human placentas from pregnancies complicated by preeclampsia and preterm labor. *Reprod Sci* **18:** 46-56.

McFadden, D.E. and D.K. Kalousek. 1991. Two different phenotypes of fetuses with chromosomal triploidy: correlation with parental origin of the extra haploid set. *Am J Med Genet* **38:** 535-538.

McGowan, P.O., A. Sasaki, A.C. D'Alessio, S. Dymov, B. Labonte, M. Szyf, G. Turecki, and M.J. Meaney. 2009. Epigenetic regulation of the glucocorticoid receptor in human brain associates with childhood abuse. *Nat Neurosci* **12:** 342-348.

McGrath, J. and D. Solter. 1984. Completion of mouse embryogenesis requires both the maternal and paternal genomes. *Cell* **37:** 179-183.

McMinn, J., M. Wei, Y. Sadovsky, H.M. Thaker, and B. Tycko. 2006. Imprinting of PEG1/MEST isoform 2 in human placenta. *Placenta* **27:** 119-126.

Meekins, J.W., R. Pijnenborg, M. Hanssens, I.R. McFadyen, and A. van Asshe. 1994. A study of placental bed spiral arteries and trophoblast invasion in normal and severe pre-eclamptic pregnancies. *Br J Obstet Gynaecol* **101:** 669-674.

Meissner, A., T.S. Mikkelsen, H. Gu, M. Wernig, J. Hanna, A. Sivachenko, X. Zhang, B.E. Bernstein, C. Nusbaum, D.B. Jaffe, A. Gnirke, R. Jaenisch, and E.S. Lander. 2008. Genome-scale DNA methylation maps of pluripotent and differentiated cells. *Nature* **454:** 766-770.

Metivier, R., R. Gallais, C. Tiffoche, C. Le Peron, R.Z. Jurkowska, R.P. Carmouche, D. Ibberson, P. Barath, F. Demay, G. Reid, V. Benes, A. Jeltsch, F. Gannon, and G. Salbert. 2008. Cyclical DNA methylation of a transcriptionally active promoter. *Nature* **452:** 45-50.

Mi, S., X. Lee, X. Li, G.M. Veldman, H. Finnerty, L. Racie, E. LaVallie, X.Y. Tang, P. Edouard, S. Howes, J.C. Keith, Jr., and J.M. McCoy. 2000. Syncytin is a captive retroviral envelope protein involved in human placental morphogenesis. *Nature* **403:** 785-789.

Monk, D., P. Arnaud, S. Apostolidou, F.A. Hills, G. Kelsey, P. Stanier, R. Feil, and G.E. Moore. 2006. Limited evolutionary conservation of imprinting in the human placenta. *Proc Natl Acad Sci U S A* **103:** 6623-6628.

Monk, M., M. Boubelik, and S. Lehnert. 1987. Temporal and regional changes in DNA methylation in the embryonic, extraembryonic and germ cell lineages during mouse embryo development. *Development* **99:** 371-382.

Monkley, S.J., S.J. Delaney, D.J. Pennisi, J.H. Christiansen, and B.J. Wainwright. 1996. Targeted disruption of the Wnt2 gene results in placentation defects. *Development* **122:** 3343-3353.

Montagnana, M., G. Lippi, A. Albiero, S. Scevarolli, G.L. Salvagno, M. Franchi, and G.C. Guidi. 2009. Evaluation of metalloproteinases 2 and 9 and their inhibitors in physiologic and pre-eclamptic pregnancy. *J Clin Lab Anal* **23:** 88-92.

Moore, G. and R. Oakey. 2011. The role of imprinted genes in humans. *Genome Biol* **12:** 106.

Moore, T. and D. Haig. 1991. Genomic imprinting in mammalian development: a parental tug-of-war. *Trends Genet* **7:** 45-49.

Morgan, H.D., F. Santos, K. Green, W. Dean, and W. Reik. 2005. Epigenetic reprogramming in mammals. *Hum Mol Genet* **14 Spec No 1:** R47-58.

Morison, I.M., J.P. Ramsay, and H.G. Spencer. 2005. A census of mammalian imprinting. *Trends Genet* **21:** 457-465.

Morley, M., C.M. Molony, T.M. Weber, J.L. Devlin, K.G. Ewens, R.S. Spielman, and V.G. Cheung. 2004. Genetic analysis of genome-wide variation in human gene expression. *Nature* **430:** 743-747.

Murphy, W.J., E. Eizirik, W.E. Johnson, Y.P. Zhang, O.A. Ryder, and S.J. O'Brien. 2001. Molecular phylogenetics and the origins of placental mammals. *Nature* **409:** 614-618.

Myatt, L. 2006. Placental adaptive responses and fetal programming. *J Physiol* **572:** 25-30.

Nakabayashi, K., A.M. Trujillo, C. Tayama, C. Camprubi, W. Yoshida, P. Lapunzina, A. Sanchez, H. Soejima, H. Aburatani, G. Nagae, T. Ogata, K. Hata, and D. Monk. 2011. Methylation screening of reciprocal genome-wide UPDs identifies novel human specific imprinted genes. *Hum Mol Genet*.

Ng, H.K., B. Novakovic, S. Hiendleder, J.M. Craig, C.T. Roberts, and R. Saffery. 2010. Distinct patterns of gene-specific methylation in mammalian placentas: implications for placental evolution and function. *Placenta* **31:** 259-268.

Nishizawa, H., K. Pryor-Koishi, T. Kato, H. Kowa, H. Kurahashi, and Y. Udagawa. 2007. Microarray analysis of differentially expressed fetal genes in placental tissue derived from early and late onset severe pre-eclampsia. *Placenta* **28:** 487-497.

Noris, M., N. Perico, and G. Remuzzi. 2005. Mechanisms of disease: Pre-eclampsia. *Nat Clin Pract Nephrol* **1:** 98-114; quiz 120.

Novakovic, B., V. Rakyan, H.K. Ng, U. Manuelpillai, C. Dewi, N.C. Wong, R. Morley, T. Down, S. Beck, J.M. Craig, and R. Saffery. 2008. Specific tumour-associated methylation in normal human term placenta and first-trimester cytotrophoblasts. *Mol Hum Reprod* **14:** 547-554.

Novakovic, B., N.C. Wong, M. Sibson, H.K. Ng, R. Morley, U. Manuelpillai, T. Down, V.K. Rakyan, S. Beck, S. Hiendleder, C.T. Roberts, J.M. Craig, and R. Saffery. 2010. DNA methylation-mediated down-regulation of DNA methyltransferase-1 (DNMT1) is coincident with, but not essential for, global hypomethylation in human placenta. *J Biol Chem* **285:** 9583-9593.

Nyirenda, M.J., R.S. Lindsay, C.J. Kenyon, A. Burchell, and J.R. Seckl. 1998. Glucocorticoid exposure in late gestation permanently programs rat hepatic phosphoenolpyruvate carboxykinase and glucocorticoid receptor expression and causes glucose intolerance in adult offspring. *J Clin Invest* **101:** 2174-2181.

Oberle, I., F. Rousseau, D. Heitz, C. Kretz, D. Devys, A. Hanauer, J. Boue, M.F. Bertheas, and J.L. Mandel. 1991. Instability of a 550-base pair DNA segment and abnormal methylation in fragile X syndrome. *Science* **252:** 1097-1102.

Ogawa, O., L.A. McNoe, M.R. Eccles, I.M. Morison, and A.E. Reeve. 1993. Human insulin-like growth factor type I and type II receptors are not imprinted. *Hum Mol Genet* **2:** 2163-2165.

Okano, M., S. Xie, and E. Li. 1998. Cloning and characterization of a family of novel mammalian DNA (cytosine-5) methyltransferases. *Nat Genet* **19:** 219-220.

Ollikainen, M., K.R. Smith, E.J. Joo, H.K. Ng, R. Andronikos, B. Novakovic, N.K. Abdul Aziz, J.B. Carlin, R. Morley, R. Saffery, and J.M. Craig. 2010. DNA methylation analysis of multiple tissues from newborn twins reveals both genetic and intrauterine components to variation in the human neonatal epigenome. *Hum Mol Genet* **19:** 4176-4188.

Oshiro, M.M., B.W. Futscher, A. Lisberg, R.J. Wozniak, W.T. Klimecki, F.E. Domann, and A.E. Cress. 2005. Epigenetic regulation of the cell type-specific gene 14-3-3sigma. *Neoplasia* **7:** 799-808.

Oswald, J., S. Engemann, N. Lane, W. Mayer, A. Olek, R. Fundele, W. Dean, W. Reik, and J. Walter. 2000. Active demethylation of the paternal genome in the mouse zygote. *Curr Biol* **10:** 475-478.

Oudejans, C.B., M. van Dijk, M. Oosterkamp, A. Lachmeijer, and M.A. Blankenstein. 2007. Genetics of preeclampsia: paradigm shifts. *Hum Genet* **120:** 607-612.

Pak, B.J., H. Park, E.R. Chang, S.C. Pang, and C.H. Graham. 1998. Differential display analysis of oxygen-mediated changes in gene expression in first trimester human trophoblast cells. *Placenta* **19:** 483-488.

Pallotto, E.K. and H.W. Kilbride. 2006. Perinatal outcome and later implications of intrauterine growth restriction. *Clin Obstet Gynecol* **49:** 257-269.

Pan, G., S. Tian, J. Nie, C. Yang, V. Ruotti, H. Wei, G.A. Jonsdottir, R. Stewart, and J.A. Thomson. 2007. Whole-genome analysis of histone H3 lysine 4 and lysine 27 methylation in human embryonic stem cells. *Cell Stem Cell* **1:** 299-312.

Pang, Z.J. and F.Q. Xing. 2003. Expression profile of trophoblast invasion-associated genes in the pre-eclamptic placenta. *Br J Biomed Sci* **60:** 97-101.

Papageorgiou, E.A., H. Fiegler, V. Rakyan, S. Beck, M. Hulten, K. Lamnissou, N.P. Carter, and P.C. Patsalis. 2009. Sites of differential DNA methylation between placenta and peripheral blood: molecular markers for noninvasive prenatal diagnosis of aneuploidies. *Am J Pathol* **174:** 1609-1618.

Pastinen, T. and T.J. Hudson. 2004. Cis-acting regulatory variation in the human genome. *Science* **306:** 647-650.

Pastinen, T., R. Sladek, S. Gurd, A. Sammak, B. Ge, P. Lepage, K. Lavergne, A. Villeneuve, T. Gaudin, H. Brandstrom, A. Beck, A. Verner, J. Kingsley, E. Harmsen, D. Labuda, K. Morgan, M.C. Vohl, A.K. Naumova, D. Sinnett, and T.J. Hudson. 2004. A survey of genetic and epigenetic variation affecting human gene expression. *Physiol Genomics* **16:** 184-193.

Pijnenborg, R., W.B. Robertson, I. Brosens, and G. Dixon. 1981. Review article: trophoblast invasion and the establishment of haemochorial placentation in man and laboratory animals. *Placenta* **2:** 71-91.

Poulsen, P., M. Esteller, A. Vaag, and M.F. Fraga. 2007. The epigenetic basis of twin discordance in age-related diseases. *Pediatr Res* **61:** 38R-42R.

Qi, J.H., Q. Ebrahem, N. Moore, G. Murphy, L. Claesson-Welsh, M. Bond, A. Baker, and B. Anand-Apte. 2003. A novel function for tissue inhibitor of metalloproteinases-3 (TIMP3): inhibition of angiogenesis by blockage of VEGF binding to VEGF receptor-2. *Nat Med* **9:** 407-415.

Rakyan, V.K., T.A. Down, S. Maslau, T. Andrew, T.P. Yang, H. Beyan, P. Whittaker, O.T. McCann, S. Finer, A.M. Valdes, R.D. Leslie, P. Deloukas, and T.D. Spector. 2010. Human aging-associated DNA hypermethylation occurs preferentially at bivalent chromatin domains. *Genome Res* **20:** 434-439.

Rakyan, V.K., T.A. Down, N.P. Thorne, P. Flicek, E. Kulesha, S. Graf, E.M. Tomazou, L. Backdahl, N. Johnson, M. Herberth, K.L. Howe, D.K. Jackson, M.M. Miretti, H. Fiegler, J.C. Marioni, E. Birney, T.J. Hubbard, N.P. Carter, S. Tavare, and S. Beck. 2008. An integrated resource for genome-wide identification and analysis of human tissue-specific differentially methylated regions (tDMRs). *Genome Res* **18:** 1518-1529.

Rakyan, V.K., T. Hildmann, K.L. Novik, J. Lewin, J. Tost, A.V. Cox, T.D. Andrews, K.L. Howe, T. Otto, A. Olek, J. Fischer, I.G. Gut, K. Berlin, and S. Beck. 2004. DNA methylation profiling of the human major histocompatibility complex: a pilot study for the human epigenome project. *PLoS Biol* **2:** e405.

Ramsahoye, B.H., D. Biniszkiewicz, F. Lyko, V. Clark, A.P. Bird, and R. Jaenisch. 2000. Non-CpG methylation is prevalent in embryonic stem cells and may be mediated by DNA methyltransferase 3a. *Proc Natl Acad Sci U S A* **97:** 5237-5242.

Ravelli, A.C., J.H. van der Meulen, R.P. Michels, C. Osmond, D.J. Barker, C.N. Hales, and O.P. Bleker. 1998. Glucose tolerance in adults after prenatal exposure to famine. *Lancet* **351:** 173-177.

Red-Horse, K., M. Kapidzic, Y. Zhou, K.T. Feng, H. Singh, and S.J. Fisher. 2005. EPHB4 regulates chemokine-evoked trophoblast responses: a mechanism for incorporating the human placenta into the maternal circulation. *Development* **132:** 4097-4106.

Redman, C.W. and I.L. Sargent. 2005. Latest advances in understanding preeclampsia. *Science* **308:** 1592-1594.

Reik, W. 2007. Stability and flexibility of epigenetic gene regulation in mammalian development. *Nature* **447:** 425-432.

Reik, W., W. Dean, and J. Walter. 2001. Epigenetic reprogramming in mammalian development. *Science* **293:** 1089-1093.

Reik, W., F. Santos, K. Mitsuya, H. Morgan, and W. Dean. 2003. Epigenetic asymmetry in the mammalian zygote and early embryo: relationship to lineage commitment? *Philos Trans R Soc Lond B Biol Sci* **358:** 1403-1409; discussion 1409.

Reik, W. and J. Walter. 2001. Genomic imprinting: parental influence on the genome. *Nat Rev Genet* **2:** 21-32.

Reimer, T., D. Koczan, B. Gerber, D. Richter, H.J. Thiesen, and K. Friese. 2002. Microarray analysis of differentially expressed genes in placental tissue of pre-eclampsia: up-regulation of obesity-related genes. *Mol Hum Reprod* **8:** 674-680.

Reiss, D., Y. Zhang, and D.L. Mager. 2007. Widely variable endogenous retroviral methylation levels in human placenta. *Nucleic Acids Res* **35:** 4743-4754.

Richardson, B. 2003. Impact of aging on DNA methylation. *Ageing Res Rev* **2:** 245-261.

Roberts, J.M. and D.W. Cooper. 2001. Pathogenesis and genetics of pre-eclampsia. *Lancet* **357:** 53-56.

Robertson, K.D. 2005. DNA methylation and human disease. *Nat Rev Genet* **6:** 597-610.

Robinson, M.D., C. Stirzaker, A.L. Statham, M.W. Coolen, J.Z. Song, S.S. Nair, D. Strbenac, T.P. Speed, and S.J. Clark. 2010. Evaluation of affinity-based genome-wide DNA methylation data: Effects of CpG density, amplification bias, and copy number variation. *Genome Res* **20:** 1719-1729.

Robinson, W.P. 2000. Mechanisms leading to uniparental disomy and their clinical consequences. *Bioessays* **22:** 452-459.

Robinson, W.P., J.L. Lauzon, A.M. Innes, K. Lim, S. Arsovska, and D.E. McFadden. 2007. Origin and outcome of pregnancies affected by androgenetic/biparental chimerism. *Hum Reprod* **22:** 1114-1122.

Robinson, W.P., M.S. Penaherrera, R. Jiang, L. Avila, J. Sloan, D.E. McFadden, S. Langlois, and P. von Dadelszen. 2009. Assessing the role of placental trisomy in preeclampsia and intrauterine growth restriction. *Prenat Diagn*.

Rodesch, F., P. Simon, C. Donner, and E. Jauniaux. 1992. Oxygen measurements in endometrial and trophoblastic tissues during early pregnancy. *Obstet Gynecol* **80:** 283-285.

Rohde, C., Y. Zhang, R. Reinhardt, and A. Jeltsch. 2010. BISMA--fast and accurate bisulfite sequencing data analysis of individual clones from unique and repetitive sequences. *BMC Bioinformatics* **11:** 230.

Rossant, J. and J.C. Cross. 2001. Placental development: lessons from mouse mutants. *Nat Rev Genet* **2:** 538-548.

Rossant, J., J.P. Sanford, V.M. Chapman, and G.K. Andrews. 1986. Undermethylation of structural gene sequences in extraembryonic lineages of the mouse. *Dev Biol* **117:** 567-573.

Rougier, N., D. Bourc'his, D.M. Gomes, A. Niveleau, M. Plachot, A. Paldi, and E. Viegas-Pequignot. 1998. Chromosome methylation patterns during mammalian preimplantation development. *Genes Dev* **12:** 2108-2113.

Sakaue, M., H. Ohta, Y. Kumaki, M. Oda, Y. Sakaide, C. Matsuoka, A. Yamagiwa, H. Niwa, T. Wakayama, and M. Okano. 2010. DNA methylation is dispensable for the growth and survival of the extraembryonic lineages. *Curr Biol* **20:** 1452-1457.

Sandovici, I., S. Kassovska-Bratinova, J.C. Loredo-Osti, M. Leppert, A. Suarez, R. Stewart, F.D. Bautista, M. Schiraldi, and C. Sapienza. 2005. Interindividual variability and parent of origin DNA methylation differences at specific human Alu elements. *Hum Mol Genet* **14:** 2135-2143.

Sandovici, I., M. Leppert, P.R. Hawk, A. Suarez, Y. Linares, and C. Sapienza. 2003. Familial aggregation of abnormal methylation of parental alleles at the IGF2/H19 and IGF2R differentially methylated regions. *Hum Mol Genet* **12:** 1569-1578.

Santos, F., B. Hendrich, W. Reik, and W. Dean. 2002. Dynamic reprogramming of DNA methylation in the early mouse embryo. *Dev Biol* **241:** 172-182.

Saran, N.G., M.T. Pletcher, J.E. Natale, Y. Cheng, and R.H. Reeves. 2003. Global disruption of the cerebellar transcriptome in a Down syndrome mouse model. *Hum Mol Genet* **12:** 2013-2019.

Sasaki, H. and Y. Matsui. 2008. Epigenetic events in mammalian germ-cell development: reprogramming and beyond. *Nat Rev Genet* **9:** 129-140.

Schieve, L.A., C. Ferre, H.B. Peterson, M. Macaluso, M.A. Reynolds, and V.C. Wright. 2004a. Perinatal outcome among singleton infants conceived through assisted reproductive technology in the United States. *Obstet Gynecol* **103:** 1144-1153.

Schieve, L.A., S.A. Rasmussen, G.M. Buck, D.E. Schendel, M.A. Reynolds, and V.C. Wright. 2004b. Are children born after assisted reproductive technology at increased risk for adverse health outcomes? *Obstet Gynecol* **103:** 1154-1163.

Schneider, E., G. Pliushch, N. El Hajj, D. Galetzka, A. Puhl, M. Schorsch, K. Frauenknecht, T. Riepert, A. Tresch, A.M. Muller, W. Coerdt, U. Zechner, and T. Haaf. 2010. Spatial, temporal and interindividual epigenetic variation of functionally important DNA methylation patterns. *Nucleic Acids Res* **38:** 3880-3890.

Schulz, R., T.R. Menheniott, K. Woodfine, A.J. Wood, J.D. Choi, and R.J. Oakey. 2006. Chromosome-wide identification of novel imprinted genes using microarrays and uniparental disomies. *Nucleic Acids Res* **34:** e88.

Schulz, R., C. Proudhon, T.H. Bestor, K. Woodfine, C.S. Lin, S.P. Lin, M. Prissette, R.J. Oakey, and D. Bourc'his. 2010. The Parental Non-Equivalence of Imprinting Control Regions during Mammalian Development and Evolution. *PLoS Genet* **6:** e1001214.

Serman, L., M. Vlahovic, M. Sijan, F. Bulic-Jakus, A. Serman, N. Sincic, R. Matijevic, G. Juric-Lekic, and A. Katusic. 2007. The impact of 5-azacytidine on placental weight, glycoprotein pattern and proliferating cell nuclear antigen expression in rat placenta. *Placenta* **28:** 803-811.

Serre, D., S. Gurd, B. Ge, R. Sladek, D. Sinnett, E. Harmsen, M. Bibikova, E. Chudin, D.L. Barker, T. Dickinson, J.B. Fan, and T.J. Hudson. 2008. Differential allelic expression in

the human genome: a robust approach to identify genetic and epigenetic cis-acting mechanisms regulating gene expression. *PLoS Genet* **4:** e1000006.

Shahrzad, S., K. Bertrand, K. Minhas, and B.L. Coomber. 2007. Induction of DNA hypomethylation by tumor hypoxia. *Epigenetics* **2:** 119-125.

Sharp, A.J., E. Migliavacca, Y. Dupre, E. Stathaki, M.R. Sailani, A. Baumer, A. Schinzel, D.J. Mackay, D.O. Robinson, G. Cobellis, L. Cobellis, H.G. Brunner, B. Steiner, and S.E. Antonarakis. 2010. Methylation profiling in individuals with uniparental disomy identifies novel differentially methylated regions on chromosome 15. *Genome Res* **20:** 1271-1278.

Shen, L., Y. Kondo, Y. Guo, J. Zhang, L. Zhang, S. Ahmed, J. Shu, X. Chen, R.A. Waterland, and J.P. Issa. 2007. Genome-wide profiling of DNA methylation reveals a class of normally methylated CpG island promoters. *PLoS Genet* **3:** 2023-2036.

Shi, W., L. Lefebvre, Y. Yu, S. Otto, A. Krella, A. Orth, and R. Fundele. 2004. Loss-of-imprinting of Peg1 in mouse interspecies hybrids is correlated with altered growth. *Genesis* **39:** 65-72.

Shoemaker, R., J. Deng, W. Wang, and K. Zhang. 2010. Allele-specific methylation is prevalent and is contributed by CpG-SNPs in the human genome. *Genome Res* **20:** 883-889.

Siegmund, K.D., C.M. Connor, M. Campan, T.I. Long, D.J. Weisenberger, D. Biniszkiewicz, R. Jaenisch, P.W. Laird, and S. Akbarian. 2007. DNA methylation in the human cerebral cortex is dynamically regulated throughout the life span and involves differentiated neurons. *PLoS One* **2:** e895.

Simmons, R.A., L.J. Templeton, and S.J. Gertz. 2001. Intrauterine growth retardation leads to the development of type 2 diabetes in the rat. *Diabetes* **50:** 2279-2286.

Sitras, V., R.H. Paulssen, H. Gronaas, J. Leirvik, T.A. Hanssen, A. Vartun, and G. Acharya. 2009. Differential placental gene expression in severe preeclampsia. *Placenta* **30:** 424-433.

Sontia, B. and R.M. Touyz. 2007. Magnesium transport in hypertension. *Pathophysiology* **14:** 205-211.

Sood, R., J.L. Zehnder, M.L. Druzin, and P.O. Brown. 2006. Gene expression patterns in human placenta. *Proc Natl Acad Sci U S A* **103:** 5478-5483.

Soundararajan, R. and A.J. Rao. 2004. Trophoblast 'pseudo-tumorigenesis': significance and contributory factors. *Reprod Biol Endocrinol* **2:** 15.

Spencer, H.G. 2000. Population genetics and evolution of genomic imprinting. *Annu Rev Genet* **34:** 457-477.

Staun-Ram, E. and E. Shalev. 2005. Human trophoblast function during the implantation process. *Reprod Biol Endocrinol* **3:** 56.

Stelnicki, E.J., L.G. Komuves, A.O. Kwong, D. Holmes, P. Klein, S. Rozenfeld, H.J. Lawrence, N.S. Adzick, M. Harrison, and C. Largman. 1998. HOX homeobox genes exhibit spatial and temporal changes in expression during human skin development. *J Invest Dermatol* **110:** 110-115.

Strathdee, G., B.R. Davies, J.K. Vass, N. Siddiqui, and R. Brown. 2004. Cell type-specific methylation of an intronic CpG island controls expression of the MCJ gene. *Carcinogenesis* **25:** 693-701.

Straussman, R., D. Nejman, D. Roberts, I. Steinfeld, B. Blum, N. Benvenisty, I. Simon, Z. Yakhini, and H. Cedar. 2009. Developmental programming of CpG island methylation profiles in the human genome. *Nat Struct Mol Biol* **16:** 564-571.

Strichman-Almashanu, L.Z., R.S. Lee, P.O. Onyango, E. Perlman, F. Flam, M.B. Frieman, and A.P. Feinberg. 2002. A genome-wide screen for normally methylated human CpG islands that can identify novel imprinted genes. *Genome Res* **12:** 543-554.

Strickland, S. and W.G. Richards. 1992. Invasion of the trophoblasts. *Cell* **71:** 355-357.

Su, A.I., M.P. Cooke, K.A. Ching, Y. Hakak, J.R. Walker, T. Wiltshire, A.P. Orth, R.G. Vega, L.M. Sapinoso, A. Moqrich, A. Patapoutian, G.M. Hampton, P.G. Schultz, and J.B. Hogenesch. 2002. Large-scale analysis of the human and mouse transcriptomes. *Proc Natl Acad Sci U S A* **99:** 4465-4470.

Surani, M.A., S.C. Barton, and M.L. Norris. 1984. Development of reconstituted mouse eggs suggests imprinting of the genome during gametogenesis. *Nature* **308:** 548-550.

Surani, M.A., K. Hayashi, and P. Hajkova. 2007. Genetic and epigenetic regulators of pluripotency. *Cell* **128:** 747-762.

Suter, C.M., D.I. Martin, and R.L. Ward. 2004. Germline epimutation of MLH1 in individuals with multiple cancers. *Nat Genet* **36:** 497-501.

Swales, A.K. and N. Spears. 2005. Genomic imprinting and reproduction. *Reproduction* **130:** 389-399.

Takahashi, K., T. Kobayashi, and N. Kanayama. 2000. p57(Kip2) regulates the proper development of labyrinthine and spongiotrophoblasts. *Mol Hum Reprod* **6:** 1019-1025.

Takai, D., F.A. Gonzales, Y.C. Tsai, M.J. Thayer, and P.A. Jones. 2001. Large scale mapping of methylcytosines in CTCF-binding sites in the human H19 promoter and aberrant hypomethylation in human bladder cancer. *Hum Mol Genet* **10:** 2619-2626.

Talens, R.P., D.I. Boomsma, E.W. Tobi, D. Kremer, J.W. Jukema, G. Willemsen, H. Putter, P.E. Slagboom, and B.T. Heijmans. 2010. Variation, patterns, and temporal stability of DNA methylation: considerations for epigenetic epidemiology. *Faseb J* **24:** 3135-3144.

Tanaka, T.S., T. Kunath, W.L. Kimber, S.A. Jaradat, C.A. Stagg, M. Usuda, T. Yokota, H. Niwa, J. Rossant, and M.S. Ko. 2002. Gene expression profiling of embryo-derived stem cells reveals candidate genes associated with pluripotency and lineage specificity. *Genome Res* **12:** 1921-1928.

Teschendorff, A.E., U. Menon, A. Gentry-Maharaj, S.J. Ramus, D.J. Weisenberger, H. Shen, M. Campan, H. Noushmehr, C.G. Bell, A.P. Maxwell, D.A. Savage, E. Mueller-Holzner, C. Marth, G. Kocjan, S.A. Gayther, A. Jones, S. Beck, W. Wagner, P.W. Laird, I.J. Jacobs, and M. Widschwendter. 2010. Age-dependent DNA methylation of genes that are suppressed in stem cells is a hallmark of cancer. *Genome Res* **20:** 440-446.

Thorvaldsen, J.L., K.L. Duran, and M.S. Bartolomei. 1998. Deletion of the H19 differentially methylated domain results in loss of imprinted expression of H19 and Igf2. *Genes Dev* **12:** 3693-3702.

Tomizawa, S., H. Kobayashi, T. Watanabe, S. Andrews, K. Hata, G. Kelsey, and H. Sasaki. 2011. Dynamic stage-specific changes in imprinted differentially methylated regions during early mammalian development and prevalence of non-CpG methylation in oocytes. *Development* **138:** 811-820.

Torricelli, M., L. Galleri, C. Voltolini, G. Biliotti, P. Florio, M. De Bonis, and F. Petraglia. 2008. Changes of placental Kiss-1 mRNA expression and maternal/cord kisspeptin levels at preterm delivery. *Reprod Sci* **15:** 779-784.

Torricelli, M., A. Giovannelli, E. Leucci, G. De Falco, F.M. Reis, A. Imperatore, P. Florio, and F. Petraglia. 2007a. Labor (term and preterm) is associated with changes in the placental mRNA expression of corticotrophin-releasing factor. *Reprod Sci* **14:** 241-245.

Torricelli, M., A. Giovannelli, E. Leucci, P. Florio, G. De Falco, P.B. Torres, F.M. Reis, L. Leoncini, and F. Petraglia. 2007b. Placental neurokinin B mRNA expression increases at preterm labor. *Placenta* **28:** 1020-1023.

Toyota, M., N. Ahuja, M. Ohe-Toyota, J.G. Herman, S.B. Baylin, and J.P. Issa. 1999. CpG island methylator phenotype in colorectal cancer. *Proc Natl Acad Sci U S A* **96:** 8681-8686.

Tsai, S., N.E. Hardison, A.H. James, A.A. Motsinger-Reif, S.R. Bischoff, B.H. Thames, and J.A. Piedrahita. 2010. Transcriptional profiling of human placentas from pregnancies complicated by preeclampsia reveals disregulation of sialic acid acetylesterase and immune signalling pathways. *Placenta*.

Tufarelli, C., J.A. Stanley, D. Garrick, J.A. Sharpe, H. Ayyub, W.G. Wood, and D.R. Higgs. 2003. Transcription of antisense RNA leading to gene silencing and methylation as a novel cause of human genetic disease. *Nat Genet* **34:** 157-165.

Turner, B.M. 2002. Cellular memory and the histone code. *Cell* **111:** 285-291.

Tusher, V.G., R. Tibshirani, and G. Chu. 2001. Significance analysis of microarrays applied to the ionizing radiation response. *Proc Natl Acad Sci U S A* **98:** 5116-5121.

Tycko, B. and I.M. Morison. 2002. Physiological functions of imprinted genes. *J Cell Physiol* **192:** 245-258.

Uuskula, L., K. Rull, L. Nagirnaja, and M. Laan. 2010. Methylation Allelic Polymorphism (MAP) in Chorionic Gonadotropin {beta}5 (CGB5) and Its Association with Pregnancy Success. *J Clin Endocrinol Metab*.

Vaiman, D., F. Mondon, A. Garces-Duran, T.M. Mignot, B. Robert, R. Rebourcet, H. Jammes, S.T. Chelbi, F. Quetin, G. Marceau, V. Sapin, F. Piumi, J.L. Danan, V. Rigourd, B. Carbonne, and F. Ferre. 2005. Hypoxia-activated genes from early placenta are elevated in preeclampsia, but not in Intra-Uterine Growth Retardation. *BMC Genomics* **6:** 111.

van Dijk, M., J. Mulders, A. Poutsma, A.A. Konst, A.M. Lachmeijer, G.A. Dekker, M.A. Blankenstein, and C.B. Oudejans. 2005. Maternal segregation of the Dutch preeclampsia locus at 10q22 with a new member of the winged helix gene family. *Nat Genet* **37:** 514-519.

Vlahovic, M., F. Bulic-Jakus, G. Juric-Lekic, A. Fucic, S. Maric, and D. Serman. 1999. Changes in the placenta and in the rat embryo caused by the demethylating agent 5-azacytidine. *Int J Dev Biol* **43:** 843-846.

von Dadelszen, P., L.A. Magee, and J.M. Roberts. 2003. Subclassification of preeclampsia. *Hypertens Pregnancy* **22:** 143-148.

Walsh, C.P. and T.H. Bestor. 1999. Cytosine methylation and mammalian development. *Genes Dev* **13:** 26-34.

Watson, J.A., C.J. Watson, A.M. McCrohan, K. Woodfine, M. Tosetto, J. McDaid, E. Gallagher, D. Betts, J. Baugh, J. O'Sullivan, A. Murrell, R.W. Watson, and A. McCann. 2009. Generation of an epigenetic signature by chronic hypoxia in prostate cells. *Hum Mol Genet* **18:** 3594-3604.

Weaver, J.R., G. Sarkisian, C. Krapp, J. Mager, M.R. Mann, and M.S. Bartolomei. 2010. Domain-specific response of imprinted genes to reduced DNMT1. *Mol Cell Biol* **30:** 3916-3928.

Weber, M., J.J. Davies, D. Wittig, E.J. Oakeley, M. Haase, W.L. Lam, and D. Schubeler. 2005. Chromosome-wide and promoter-specific analyses identify sites of differential DNA methylation in normal and transformed human cells. *Nat Genet* **37:** 853-862.

Weber, M., I. Hellmann, M.B. Stadler, L. Ramos, S. Paabo, M. Rebhan, and D. Schubeler. 2007. Distribution, silencing potential and evolutionary impact of promoter DNA methylation in the human genome. *Nat Genet* **39:** 457-466.

Westerman, B.A., A. Poutsma, L.H. Looijenga, D. Wouters, I.J. van Wijk, and C.B. Oudejans. 2001. The Human Achaete Scute Homolog 2 gene contains two promotors, generating overlapping transcripts and encoding two proteins with different nuclear localization. *Placenta* **22:** 511-518.

Whitney, A.R., M. Diehn, S.J. Popper, A.A. Alizadeh, J.C. Boldrick, D.A. Relman, and P.O. Brown. 2003. Individuality and variation in gene expression patterns in human blood. *Proc Natl Acad Sci U S A* **100:** 1896-1901.

Wiles, N.J., T.J. Peters, D.A. Leon, and G. Lewis. 2005. Birth weight and psychological distress at age 45-51 years: results from the Aberdeen Children of the 1950s cohort study. *Br J Psychiatry* **187:** 21-28.

Winn, V.D., R. Haimov-Kochman, A.C. Paquet, Y.J. Yang, M.S. Madhusudhan, M. Gormley, K.T. Feng, D.A. Bernlohr, S. McDonagh, L. Pereira, A. Sali, and S.J. Fisher. 2007. Gene expression profiling of the human maternal-fetal interface reveals dramatic changes between midgestation and term. *Endocrinology* **148:** 1059-1079.

Wong, N.C., B. Novakovic, B. Weinrich, C. Dewi, R. Andronikos, M. Sibson, F. Macrae, R. Morley, M.D. Pertile, J.M. Craig, and R. Saffery. 2008. Methylation of the adenomatous

polyposis coli (APC) gene in human placenta and hypermethylation in choriocarcinoma cells. *Cancer Lett* **268:** 56-62.

Woodcock, D.M., P.J. Crowther, and W.P. Diver. 1987. The majority of methylated deoxycytidines in human DNA are not in the CpG dinucleotide. *Biochem Biophys Res Commun* **145:** 888-894.

Xu, Y., C.G. Goodyer, C. Deal, and C. Polychronakos. 1993. Functional polymorphism in the parental imprinting of the human IGF2R gene. *Biochem Biophys Res Commun* **197:** 747-754.

Xue, W.C., K.Y. Chan, H.C. Feng, P.M. Chiu, H.Y. Ngan, S.W. Tsao, and A.N. Cheung. 2004. Promoter hypermethylation of multiple genes in hydatidiform mole and choriocarcinoma. *J Mol Diagn* **6:** 326-334.

Yan, H., W. Yuan, V.E. Velculescu, B. Vogelstein, and K.W. Kinzler. 2002. Allelic variation in human gene expression. *Science* **297:** 1143.

Yan, H. and W. Zhou. 2004. Allelic variations in gene expression. *Curr Opin Oncol* **16:** 39-43.

Yoder, J.A. and T.H. Bestor. 1998. A candidate mammalian DNA methyltransferase related to pmt1p of fission yeast. *Hum Mol Genet* **7:** 279-284.

Yuen, R.K., L. Avila, M.S. Penaherrera, P. von Dadelszen, L. Lefebvre, M.S. Kobor, and W.P. Robinson. 2009. Human placental-specific epipolymorphism and its association with adverse pregnancy outcomes. *PLoS One* **4:** e7389.

Yuen, R.K., M.S. Penaherrera, P. von Dadelszen, D.E. McFadden, and W.P. Robinson. 2010. DNA methylation profiling of human placentas reveals promoter hypomethylation of multiple genes in early-onset preeclampsia. *Eur J Hum Genet* **18:** 1006-1012.

Yuen, R.K. and W.P. Robinson. 2011. Review: A high capacity of the human placenta for genetic and epigenetic variation: Implications for assessing pregnancy outcome. *Placenta*.

Zeng, S.M. and J. Yankowitz. 2003. X-inactivation patterns in human embryonic and extra-embryonic tissues. *Placenta* **24:** 270-275.

Zhang, A., D.A. Skaar, Y. Li, D. Huang, T.M. Price, S.K. Murphy, and R.L. Jirtle. 2011. Novel retrotransposed imprinted locus identified at human 6p25. *Nucleic Acids Res*.

Zhang, R., L. Zhou, Q. Li, J. Liu, W. Yao, and H. Wan. 2009. Up-regulation of two actin-associated proteins prompts pulmonary artery smooth muscle cell migration under hypoxia. *Am J Respir Cell Mol Biol* **41:** 467-475.

Zhao, X.D., X. Han, J.L. Chew, J. Liu, K.P. Chiu, A. Choo, Y.L. Orlov, W.K. Sung, A. Shahab, V.A. Kuznetsov, G. Bourque, S. Oh, Y. Ruan, H.H. Ng, and C.L. Wei. 2007. Whole-genome mapping of histone H3 Lys4 and 27 trimethylations reveals distinct genomic compartments in human embryonic stem cells. *Cell Stem Cell* **1:** 286-298.

Zou, Z., A. Anisowicz, M.J. Hendrix, A. Thor, M. Neveu, S. Sheng, K. Rafidi, E. Seftor, and R. Sager. 1994. Maspin, a serpin with tumor-suppressing activity in human mammary epithelial cells. *Science* **263:** 526-529.

Appendix 1: Supplementary tables and figures for Chapter 2

Supplementary Table 2.1. Summary of PCR Primers and conditions

Primers for bisulfite pyrosequencing

Gene	Primer	Sequence (5' to 3')	Annealing temperature (°C)	Product length (bp)
APC	Forward	TTTTTTGTTTGTTGGGGATTG	50	290
	Reverse	(5' biotinated)-AATCCRACAACACCTCCATTCTAT		
	Sequencing	TTTGTTGGGGATTGG		
DNAJC6	Forward	GTTGGTTTTTTATTTTGAGGGAAG	50	246
	Reverse	(5' biotinated)-ATTCTACAACCCTAACTTTTAATTTATCA		
	Sequencing	TTATTTTGAGGGAAGGA		
DNMT1	Forward	TGGAGGTTGGATTGGAATTGA	50	222
	Reverse	(5' biotinated)-ACCRACCATACCCAAAAAACAC		
	Sequencing	AATTGAGGATTTTATTTAAGG		
FAM50B	Forward	TTTTGTTTTTAYGTTGTGGGTAG	50	228
	Reverse	(5' biotinated)-ACAAACAATAATACRCAAATAATATTCAC		
	Sequencing	AGGGYGGGTTTTTAT		
	M-specific sequencing	GCGTGTTGAGTTTTTTC		
IGFBP1	Forward	AGAATTGGATTTTAATTGAGGGTTTGAA	50	189
	Reverse	(5' biotinated)-CCACTTACACCAAAAAATTAATAATTAACA		
	Sequencing	GAATTGGATTTTAATTGAGG		
LEP	Forward	(5' biotinated)-GGTTTYGYGAGGTGTATATTG	50	301
	Reverse	CATCCCTCCTAACTCAATTTCC		
	Sequencing	CCTACCAAAAAAAACCA		
MCCC1	Forward	GTGGAGAYGTTTTTATATTTTTGGAT	50	284
	Reverse	(5' biotinated)-CCTCTACCCACTAAACCATAACC		
	Sequencing	TTATATTTTTGGATTAGTTTAAAG		
RASGRF1	Forward	GGGGTTTYGTTGGTTTTTGAG	50	160
	Reverse	(5' biotinated)-CRCRAACCACTTAATTTACCATTT		
	Sequencing	GAGTATTATGTAGAAGGGGA		
RHOBTB3	Forward	GTATTTTYGGTTAAGGTTAAGAGGG	50	227
	Reverse	(5' biotinated)-AATTAATAAATACAACRCCCCAACC		
	Sequencing	AAGAGGGGGGGAAAT		
SORD	Forward	GTGTATTATTAGGGAAAGGTTGTTGG	50	163
	Reverse	(5' biotinated)-ACRCTTCTCCCAAACCCC		
	Sequencing	GTATTATTAGGGAAAGGTT		

Supplementary Table 2.1. Summary of PCR Primers and conditions

Primers for genotyping PCR

Gene	Primer	Sequence (5' to 3')	Annealing temperature (°C)	Product length (bp)
FAM50B	Forward	CGGGGCTCCTGTTTTCAC	57	149
	Reverse	(5' biotinated)-CCGTGTTGCAAGGCTCTCT		
	Sequencing	TGCTGAGCCTTCTCG		
MCCC1	Forward	TTCGTGGAGACGCCCTCA	57	102
	Reverse	(5' biotinated)-AACCCGTTCCTCCACTACGAAG		
	Sequencing	GGCTCCGACGGTGGC		
LEP	Forward	AGGCATGGAGCCCCGTAG	57	54
	Reverse	(5' biotinated)-CGGGGCCTTACCTTGCAAC		
	Sequencing	CCCGTAGGAATCGCA		

Primers for reverse transcription genotyping PCR

Gene	Primer	Sequence (5' to 3')	Annealing temperature (°C)	Product length (bp)
FAM50B	Forward	TTGGTTGTGCTATTGCTGATGT	60	70
	Reverse	(5' biotinated)-GGCAACACTAAAATACTCAGAAAAGACC		
	Sequencing	TGCTGATGTTATGCTTTG		
MCCC1	Forward	ATCAGCCCAAAGGTAGGCTCAG	60	271
	Reverse	(5' biotinated)-GTGGCTGTTGTGTACTTCATGG		
	Sequencing	AGGCTCAGGCTCCGAC		
LEP	Forward	GTAGGAATCGCAGCGCCA	60	66
	Reverse	(5' biotinated)-CACAAGAATCCGCACAGGG		
	Sequencing	GGAATCGCAGCGCCA		

Primers for bisulfite cloning PCR

Gene	Primer	Sequence (5' to 3')	Annealing temperature (°C)	Product length (bp)
FAM50B	Forward	TTTTGTTTTTAYGTTGTGGGTAG	52	228
	Reverse	ACAAACAATAATACRCAAATAATATTCAC		
MCCC1	Forward	GTGGAGAYGTTTTTATATTTTTGGAT	50	284
	Reverse	CCTCTACCCACTAAACCATAACC		

Supplementary Table 2.1. Summary of PCR Primers and conditions

Reaction condition and thermal profile for methylation and DNA genotyping

Reagents	Final conc.	Temperature		Cycle	
10X HotStarTaq Buffer	1X	Initial denaturation:	95°C	10 min	
$MgCl_2$	1.25mM	Denaturation:	95°C	40 sec	x 40 cycles
dNTP	0.2mM	Annealing:	50~60°C	40 sec	
Forward primer	200nM	Extension:	72°C	40 sec	
Reverse primer	200nM	Final extension:	72°C	7 min	
HotStarTaq	0.04U				
Total reaction volume	*25ul*				

Reaction condition and thermal profile for RNA genotyping

Reagents	Final conc.	Temperature		Cycle	
5X OneStep RT-PCR Buffer	1X	Reverse transcription:	50°C	30 min	
dNTP	0.4mM	Initial denaturation:	95°C	15 min	
Forward primer	200nM	Denaturation:	95°C	40 sec	x 40 cycles
Reverse primer	200nM	Annealing:	60°C	40 sec	
OneStep RT-PCR Enzyme Mix	-	Extension:	72°C	40 sec	
Total reaction volume	*25ul*	Final extension:	72°C	10 min	

Supplementary Table 2.2. PCR Primers for multiplex genotyping by Sequenom

SNP_ID	Forward primer	Reverse primer
rs4915691	TGGAATGGGAAGCAAGTCAG	GTCGGCAAAAGGATCCAGAG
rs2236600	GCTGTAGCTGGAGTCTGAAG	ATTAGGCAGACACTGGGTTC
rs2075667	ACCAGCAGCACAATTCTGTC	AGGAAGATCTCGTGATTGGG
rs2289292	GTGTATGGTAGAGGGAAGGG	CTACTCGGCTGCATTTCTGG
rs7908957	TGTGTGTGTACGTGCTTGTG	TCAATGTGCAGCTCTCCTTC
rs448475	TTCAGGAAGGAAGACTTCCC	TCCCTGCCTGTTAAGGAAAC
rs2070097	CTCCGGAAGTAGAGCTTCAG	ACCCACTGGTGGAGGGCTG
rs8444	AGCTGCCTCCCAGATTAATG	ACTCTCCTCTCACTTTCTCC
rs2269996	ATGTCATCCAGTACACCACC	GTGAAAGGCCTGGAACACTC
rs2230518	CAGTAACTTGATTGCTTCAG	CATTGTAGTTGTGGAGGCAG
rs867858	ACCGTGGGTTTTGCATTGTG	CAAACAGATGCCGTCATTCG
rs62076285	CCCTTCAGGTACAATTCCAC	CCTGGGAATTGCAGTCCTTG
rs937652	CAAACCCGTTCCTCCACTAC	ATCAGCCCAAAGGTAGGCTC
rs2167270	GTAGGAATCGCAGCGCCA	GCATTTTCCTTCCCAGGATG
rs1460924	AGAACACAGAAGGGTACCAG	CACACAATCCTGTCTGTTGG
rs2585	CCAAGCATGGGATTTTGCCG	ACACTGAATGTCACCTGTGC
rs34896	TCATCAAGGCTGTGGAGTTC	TATGTACCTCAGACAGAGGG
rs13077498	TGCCCCGGTAAATGCAAAAC	TTCAGGTGCCAAAATGGAGG
rs16999593	CCTGGCTAAAGTCAAATCCC	TTCCCGTTTTCTAGACGTCC
rs10230307	TCAGGTAATCACTGGAAAGC	CATAGAAAGTTGGGGATGTG
rs12259839	GCTACGCTCCAAGAATGATG	CCTGCATAATTCATTGGCCG
rs10502647	AGTAGGAGGAGAAGTGAATG	GACTCAAGATACACACAACTC
rs1050650	TGTTGCATGGGCTAATGAAG	ACACCATCATCATAGCAAGG
rs3813737	AAGGGACTCAGAGATGACAC	TAAGCGGTACGGCCTTTCAG
rs10057908	ACTGAATTTCAAGATGCTC	GACAGAGGACATTTAGATAC
rs2071203	GTGAAGGTGTAATTGGCTCC	GACGATGTCATCCAGTTTGC
rs4619	CATCTGGTTTCAGTTTTGTAC	TACCCTTGGAATGGGAAGAG
rs6597007	CATTGGTTGTGCTATTGCTG	GCAGAGCAATGCAGCAAATC
rs17029321	GACACATTCTCAATATTAGC	ATTTGCAAAGTGTTGTAGC
rs73261988	AACCGGAAGCAGTTGCTGAC	TCCTCCTGACCACTCCCCT
rs817343	CCGGGCACTGCTGCGGCT	ACCTGCTGCAGCACCTCCT
rs1065780	CACAGAAAAAAGCCCTAGAG	ATCTCGCCTTTCCTCACCTG
rs9617066	GCAATCACTTCCTGTCCAAC	AGGTACTGCAGCGATTATGG
rs34866491	TCCTCTTCCTGGCCTGTATC	ATGACGGAGACCAAGTGTGC
rs4762737	TATAAGACAACCGAGCTCAC	TTCTGCTCATTCCGGGTAAG
rs1057097	AGTACCACCACTCACAACAG	ATACTCGTCCCAATTGGCAG
rs3210458	TAAGACCCATCAGATCGAGG	GATGGTTTGGTTCAGGATGG
rs13396048	AGCTGGCAAATGACAACCAC	AGATGTTGTCCACCTGATGC
rs7873	GTGTTATATTCTGCCTCGCC	AGGATGGTTAGTGGCCCAG
rs203462	AGGAAGAGCTAGCTTGGAAG	ACGGTTGATCATACTGAGCC
rs7115806	AGCTGAGAAAATGGGAGCTG	TAATCCCTCCATTGGCTTCC

Supplementary Table 2.3. Gestational age and karyotype of triploidy cases

Sample name	Type	Gestational age	Karyotype
TP1	Digynic	<10 weeks	XXX
TP3	Digynic	<10 weeks	XXX
TP20	Digynic	<10 weeks	XXX
TP56	Digynic	8 weeks	XXY
TP58	Digynic	8 weeks	XXX
TP60	Digynic	9 weeks	XXY
TP61	Digynic	12 weeks	XXX
TP69	Digynic	9 weeks 6 days	XXX
TP84	Digynic	6-8 weeks	XXX
TP85	Digynic	7 weeks 3 days	XXX
TP6	Diandric	8 weeks	XXX
TP7	Diandric	<10 weeks	XXY
TP9	Diandric	13 weeks	XXX
TP24	Diandric	13 weeks	XXX
TP49	Diandric	9 weeks	XXY
TP54	Diandric	14 weeks 2 days	XXY
TP57	Diandric	8 weeks 3 days	XXX
TP74	Diandric	17 weeks	XXX
TP76	Diandric	15 weeks	XXX
TP86	Diandric	15 weeks	XXY

Supplementary Table 2.4. Summary of DNA methylation and copy number variation in identified imprinted DML

Gene	Known imprinted gene	M/P	TargetID	CNV	Average digynic	Std	Average diandric	Std	Difference	q value	Average CHM	Std	Average normal	Std
PLAGL1	Y	M	cg25350411		0.59	0.02	0.34	0.02	0.25	0	0.12	0.03	0.46	0.02
MCCC1	N	M	cg04991337		0.57	0.04	0.34	0.03	0.23	0	0.07	0.01	0.44	0.05
PEG10	Y	M	cg16492735	gain	0.54	0.02	0.31	0.02	0.22	0	0.08	0.03	0.42	0.02
DIRAS3	Y	M	cg22901840		0.66	0.03	0.45	0.04	0.21	0	0.18	0.04	0.55	0.02
PEG3	Y	M	cg18668753		0.54	0.03	0.33	0.02	0.21	0	0.17	0.03	0.42	0.02
L3MBTL	Y	M	cg23626798		0.68	0.02	0.47	0.02	0.21	0	0.09	0.02	0.57	0.02
ZIM2	Y	M	cg27519373		0.69	0.02	0.48	0.04	0.21	0	0.15	0.02	0.58	0.04
ZIM2	Y	M	cg02162069		0.74	0.02	0.53	0.02	0.21	0	0.10	0.04	0.64	0.02
ZIM2	Y	M	cg17663463		0.66	0.02	0.46	0.03	0.21	0	0.17	0.03	0.55	0.04
L3MBTL	Y	M	cg20091959		0.68	0.02	0.47	0.02	0.21	0	0.10	0.03	0.57	0.02
GRB10	Y	M	cg12903171		0.55	0.02	0.35	0.04	0.21	0	0.05	0.01	0.44	0.04
ZIM2	Y	M	cg22354595		0.69	0.02	0.48	0.03	0.21	0	0.08	0.02	0.58	0.04
SNURF	Y	M	cg18506672		0.65	0.03	0.45	0.03	0.20	0	0.24	0.05	0.53	0.04
DIRAS3	Y	M	cg16148270		0.72	0.02	0.52	0.04	0.20	0	0.22	0.07	0.61	0.03
PEG10	Y	M	cg08291000	gain	0.61	0.02	0.41	0.01	0.19	0	0.11	0.03	0.50	0.02
DIRAS3	Y	M	cg05392265		0.63	0.02	0.44	0.04	0.19	0	0.18	0.07	0.51	0.03
FAM50B	N	M	cg01570885		0.58	0.02	0.39	0.04	0.19	0	0.24	0.11	0.46	0.04
DIRAS3	Y	M	cg22500004		0.60	0.03	0.41	0.03	0.19	0	0.16	0.07	0.49	0.03
DIRAS3	Y	M	cg09118625		0.63	0.02	0.44	0.04	0.19	0	0.12	0.03	0.51	0.03
MEST	Y	M	cg18183281		0.71	0.02	0.52	0.03	0.19	0	0.14	0.05	0.63	0.03
PEG3	Y	M	cg19098268		0.77	0.02	0.59	0.02	0.18	0	0.11	0.05	0.68	0.03
GNAS	Y	M	cg07284407		0.68	0.03	0.50	0.03	0.18	0	0.21	0.13	0.61	0.04
PEG3	Y	M	cg19335327		0.56	0.01	0.38	0.02	0.18	0	0.09	0.02	0.45	0.03
PEG3	Y	M	cg14849423		0.66	0.02	0.49	0.02	0.17	0	0.09	0.04	0.56	0.03
SGCE	Y	M	cg18139769	gain	0.58	0.01	0.41	0.03	0.17	0	0.09	0.03	0.48	0.02
SGCE	Y	M	cg03682823	gain	0.49	0.02	0.32	0.02	0.17	0	0.05	0.02	0.40	0.02
DIRAS3	Y	M	cg13697378		0.60	0.01	0.45	0.03	0.15	0	0.13	0.04	0.51	0.01
PEG10	Y	M	cg06695761	gain	0.70	0.02	0.55	0.01	0.15	0	0.15	0.07	0.64	0.02
L3MBTL	Y	M	cg02611863		0.62	0.06	0.37	0.03	0.24	0.00001	0.15	0.04	0.57	0.09

Supplementary Table 2.4. Summary of DNA methylation and copy number variation in identified imprinted DML

Gene	Known imprinted gene	M/P	TargetID	CNV	Average digynic	Std	Average diandric	Std	Difference	q value	Average CHM	Std	Average normal	Std
SORD	N	M	cg26196700	gain/loss	0.54	0.05	0.32	0.05	0.23	0.00001	0.04	0.01	0.45	0.06
ZIM2	Y	M	cg02793099		0.60	0.02	0.38	0.07	0.22	0.00001	0.09	0.02	0.47	0.04
RHOBTB3	N	M	cg24274600		0.57	0.04	0.36	0.04	0.21	0.00001	0.03	0.00	0.52	0.04
GNAS	Y	M	cg21988465		0.77	0.03	0.56	0.05	0.21	0.00001	0.29	0.28	0.68	0.03
SORD	N	M	cg06424894	gain/loss	0.49	0.03	0.28	0.05	0.21	0.00001	0.10	0.01	0.38	0.03
PLAGL1	Y	M	cg17895149		0.69	0.02	0.48	0.06	0.21	0.00001	0.14	0.08	0.57	0.05
DIRAS3	Y	M	cg06191076		0.64	0.03	0.44	0.06	0.19	0.00001	0.18	0.08	0.48	0.03
C3orf62	N	M	cg20835282		0.44	0.05	0.26	0.04	0.19	0.00001	0.18	0.24	0.41	0.10
NAP1L5	Y	M	cg12759554		0.66	0.02	0.48	0.05	0.18	0.00001	0.27	0.14	0.58	0.05
ZIM2	Y	M	cg01656470		0.75	0.03	0.57	0.05	0.18	0.00001	0.15	0.09	0.66	0.04
SNURF	Y	M	cg02125271		0.64	0.04	0.46	0.05	0.18	0.00001	0.31	0.05	0.57	0.04
SLC46A2	N	M	cg07758904	gain/loss	0.55	0.04	0.38	0.05	0.17	0.00001	0.14	0.06	0.49	0.07
ARMC3	N	M	cg11673092		0.41	0.04	0.25	0.02	0.16	0.00001	0.06	0.02	0.33	0.03
PCK2	N	M	cg26402828		0.56	0.02	0.41	0.04	0.15	0.00001	0.06	0.01	0.47	0.14
PEG10	Y	M	cg19107595	gain	0.69	0.04	0.54	0.02	0.15	0.00001	0.16	0.04	0.65	0.03
DNMT1	N	M	cg15043801	loss	0.51	0.04	0.36	0.03	0.15	0.00001	0.06	0.02	0.46	0.04
CMTM3	N	M	cg23297477		0.56	0.05	0.35	0.06	0.21	0.00003	0.06	0.01	0.51	0.06
ZNF396	N	M	cg03776551		0.53	0.05	0.34	0.06	0.19	0.00003	0.05	0.01	0.45	0.03
GNAS	Y	M	cg14203179		0.55	0.05	0.36	0.06	0.20	0.00005	0.10	0.03	0.38	0.04
AIFM2	N	M	cg26699283	gain/loss	0.58	0.08	0.35	0.06	0.23	0.00006	0.07	0.01	0.48	0.05
CD83	N	M	cg01288598		0.61	0.04	0.46	0.05	0.15	0.00006	0.08	0.01	0.55	0.04
ZNF232	N	M	cg24680602	gain	0.48	0.03	0.33	0.05	0.15	0.00008	0.16	0.12	0.39	0.07
PCK2	N	M	cg15467148		0.65	0.03	0.50	0.06	0.15	0.00009	0.12	0.02	0.54	0.16
TMEM17	N	M	cg12385425		0.60	0.06	0.38	0.08	0.22	0.00010	0.10	0.01	0.56	0.03
NUDT12	Y	M	cg07655627		0.51	0.04	0.33	0.06	0.18	0.00010	0.12	0.03	0.39	0.10
FGF12	N	M	cg15543551		0.32	0.06	0.15	0.05	0.17	0.00010	0.07	0.01	0.22	0.04
IRF7	N	M	cg16541031	gain/loss	0.33	0.05	0.17	0.05	0.16	0.00010	0.06	0.01	0.25	0.07
KCNQ1	Y	M	cg27119222		0.70	0.03	0.51	0.08	0.18	0.00011	0.21	0.03	0.60	0.05
ST8SIA1	N	M	cg00769520	gain/loss	0.47	0.04	0.27	0.08	0.20	0.00012	0.05	0.02	0.40	0.04

Supplementary Table 2.4. Summary of DNA methylation and copy number variation in identified imprinted DML

Gene	Known imprinted gene	M/P	TargetID	CNV	Average digynic	Std	Average diandric	Std	Difference	q value	Average CHM	Std	Average normal	Std
ST8SIA1	N	M	cg24723331	gain/loss	0.48	0.05	0.30	0.06	0.18	0.00012	0.15	0.08	0.41	0.06
KCNQ1	Y	M	cg08007665		0.68	0.04	0.53	0.05	0.15	0.00012	0.32	0.08	0.57	0.07
DIRAS3	Y	M	cg19114595		0.58	0.05	0.43	0.05	0.15	0.00012	0.20	0.08	0.47	0.04
SNCB	N	M	cg05028467		0.47	0.08	0.25	0.06	0.21	0.00012	0.09	0.02	0.36	0.06
CYP2W1	N	M	cg15914863		0.60	0.04	0.44	0.06	0.16	0.00019	0.41	0.04	0.49	0.05
G0S2	N	M	cg17710021		0.57	0.03	0.41	0.07	0.15	0.00034	0.20	0.14	0.48	0.04
APC	N	M	cg16970232	loss	0.65	0.05	0.50	0.06	0.15	0.00037	0.23	0.09	0.65	0.08
RASGRF1	N	M	cg16154416	gain/loss	0.34	0.03	0.19	0.07	0.16	0.00039	0.06	0.02	0.26	0.06
L3MBTL	Y	M	cg01071811		0.68	0.05	0.50	0.09	0.19	0.00084	0.20	0.11	0.63	0.11
RASGRF1	Y	M	cg15156078	gain/loss	0.39	0.06	0.22	0.06	0.17	0.00085	0.09	0.02	0.29	0.07
GNAS	Y	P	cg20582984		0.54	0.02	0.75	0.02	-0.21	0	0.89	0.01	0.66	0.02
ZNF597	Y	P	cg14654875	gain	0.25	0.02	0.46	0.03	-0.21	0	0.62	0.08	0.33	0.05
GNAS	Y	P	cg01355739		0.56	0.02	0.76	0.02	-0.20	0	0.91	0.01	0.67	0.02
GNAS	Y	P	cg18619398		0.46	0.02	0.61	0.02	-0.15	0	0.85	0.04	0.52	0.02
DNAJC6	N	P	cg09082287		0.22	0.04	0.46	0.06	-0.24	0.00001	0.44	0.14	0.40	0.09
GNAS	Y	P	cg05558390		0.40	0.04	0.63	0.05	-0.23	0.00001	0.84	0.03	0.52	0.07
GNAS	Y	P	cg24975842		0.49	0.04	0.70	0.06	-0.21	0.00001	0.94	0.02	0.57	0.04
C10orf125	N	P	cg14607011	gain/loss	0.59	0.06	0.80	0.04	-0.21	0.00001	0.86	0.02	0.73	0.04
H19	Y	P	cg02657360	loss	0.29	0.04	0.49	0.06	-0.20	0.00001	0.84	0.04	0.40	0.03
H19	Y	P	cg21167159	loss	0.56	0.04	0.73	0.04	-0.16	0.00001	0.84	0.03	0.63	0.05
H19	Y	P	cg17769238	loss	0.40	0.04	0.58	0.05	-0.18	0.00002	0.79	0.05	0.49	0.08
SEMA3B	N	P	cg14911395	gain/loss	0.24	0.05	0.45	0.06	-0.20	0.00004	0.18	0.14	0.31	0.06
CMTM8	N	P	cg01617750		0.42	0.06	0.62	0.05	-0.20	0.00005	0.73	0.08	0.54	0.04
AKAP10	N	P	cg11630242		0.45	0.06	0.63	0.04	-0.18	0.00005	0.73	0.04	0.60	0.03
H19	Y	P	cg25852472	loss	0.44	0.05	0.60	0.04	-0.16	0.00005	0.78	0.03	0.50	0.04
ARHGAP4	N	P	cg06791102		0.49	0.04	0.65	0.05	-0.15	0.00005	0.72	0.08	0.62	0.10
MEG3	Y	P	cg05711886	gain	0.43	0.05	0.61	0.05	-0.17	0.00008	0.65	0.11	0.46	0.07
PARP12	N	P	cg07937272		0.47	0.05	0.63	0.05	-0.16	0.00008	0.78	0.05	0.50	0.03
SAMD10	N	P	cg03224418	gain/loss	0.42	0.05	0.60	0.06	-0.18	0.00008	0.60	0.11	0.53	0.07

Supplementary Table 2.4. Summary of DNA methylation and copy number variation in identified imprinted DML

Gene	Known imprinted gene	M/P	TargetID	CNV	Average digynic	Std	Average diandric	Std	Difference	q value	Average CHM	Std	Average normal	Std
MOV10L1	N	P	cg18638931	gain	0.28	0.04	0.44	0.05	-0.16	0.00008	0.52	0.14	0.30	0.05
H19	Y	P	cg15269875	loss	0.51	0.05	0.67	0.04	-0.16	0.00009	0.88	0.02	0.56	0.03
DNAJC6	N	P	cg26304237		0.12	0.02	0.29	0.07	-0.17	0.00010	0.28	0.12	0.21	0.06
SEMA3B	N	P	cg24816455	gain/loss	0.39	0.04	0.54	0.05	-0.15	0.00010	0.47	0.08	0.45	0.11
IGFBP1	N	P	cg05660795		0.23	0.04	0.38	0.05	-0.15	0.00010	0.42	0.13	0.25	0.03
GNAS	Y	P	cg14597908		0.46	0.06	0.64	0.06	-0.18	0.00012	0.86	0.03	0.48	0.06
CDKN1C	Y	P	cg05559445	gain/loss	0.40	0.04	0.56	0.06	-0.17	0.00012	0.65	0.02	0.44	0.05
ACPL2	N	P	cg00400028		0.39	0.04	0.54	0.05	-0.15	0.00012	0.63	0.08	0.49	0.04
CCR10	N	P	cg09509673		0.51	0.06	0.66	0.03	-0.15	0.00013	0.66	0.05	0.61	0.06
LEP	N	P	cg12782180	gain	0.54	0.08	0.74	0.05	-0.20	0.00015	0.86	0.06	0.73	0.08
REEP6	N	P	cg22759185	gain/loss	0.44	0.05	0.59	0.04	-0.15	0.00015	0.65	0.12	0.49	0.05
MEG3	Y	P	cg04291079	gain	0.37	0.05	0.60	0.09	-0.23	0.00019	0.66	0.16	0.40	0.08
LEP	N	P	cg19594666	gain	0.40	0.10	0.65	0.06	-0.25	0.00028	0.79	0.07	0.58	0.14
REEP6	N	P	cg02674804	gain/loss	0.53	0.07	0.72	0.05	-0.18	0.00028	0.78	0.08	0.58	0.08
FIGNL1	N	P	cg05072008		0.40	0.05	0.57	0.07	-0.17	0.00030	0.59	0.13	0.52	0.08
GATA4	N	P	cg13434842		0.31	0.05	0.48	0.06	-0.16	0.00040	0.45	0.10	0.36	0.08
FLJ37396	N	P	cg16075940		0.52	0.07	0.69	0.05	-0.17	0.00043	0.67	0.06	0.58	0.07
TBX6	N	P	cg14370448	gain/loss	0.60	0.06	0.76	0.06	-0.16	0.00048	0.76	0.07	0.73	0.08
PEX5	N	P	cg15754084		0.39	0.07	0.59	0.07	-0.20	0.00058	0.57	0.18	0.47	0.09
P2RY6	N	P	cg06637774		0.19	0.06	0.41	0.11	-0.23	0.00085	0.46	0.23	0.22	0.08
LASS2	N	P	cg18611122		0.52	0.07	0.71	0.07	-0.19	0.00085	0.72	0.10	0.68	0.07

Supplementary Table 2.6. Allele-specific methylation of *FAM50B* in blood and placenta

		Maternal blood		Preferential methylated		Fetal placenta		Preferential methylated
Sample	**Genotype**	**A**	**G**	**allele**	**Genotype**	**A**	**G**	**allele**
PM135	GA	2.2%	97.8%	G	AA	NI	NI	
PM143	GA	100.0%	0.0%	A	GA	66.9%	33.1%	A
PM144	GA	0.0%	100.0%	G	GG	NI	NI	
PM151	GG	NI	NI		GA	37.1%	62.9%[a]	G (maternal)
PM152	GG	NI	NI		GA	21.2%	78.8%[a]	G (maternal)
PM161	GA	100.0%	0.0%	A	GG	NI	NI	
PM165	GA	ND	ND		GA	56.6%	43.4%	A
PM171	GA	ND	ND		GA	88.1%	11.9%	A
PM172	GA	92.3%	7.7%	A	GG	NI	NI	
PM177	GA	ND	ND		GA	78.1%	21.9%	A
PM178	GA	0.0%	100.0%	G	GG	NI	NI	
PM180	GA	5.7%	94.3%	G	GA	0.0%	100.0%	G
PM181	GA	2.5%	97.5%	G	AA	NI	NI	
PM187	GA	ND	ND		GA	87.0%	13.0%	A
PM190	GA	4.0%	96.0%	G	GA	89.5%	10.5%	A
PM191	GA	ND	ND		GA	62.9%	37.1%	A
PM194	ND	ND	ND		GA	86.4%	13.6%	A
PM200	GA	100.0%	0.0%	A	GG	NI	NI	
PM201	GG	NI	NI		GA	0.0%	100%[a]	G (maternal)

[a]Cases with homozygous genotypes in maternal blood

NI: Not informative

ND: Not determined

Supplementary Table 2.6. Allelic expression of novel and known imprinted genes

DMR	Gene	SNP	Monoallelic cases	Percentage	Matched origin	Percentage
M	*FAM50B*	rs6597007	9/9	100%	5/5	100%
M	*DNMT1*	rs16999593	1/1	100%	1/1	100%
P	*MOV10L1*	rs9617066	8/9	89%	1/3	33%
M	*RHOBTB3*	rs34896	3/4	75%	2/2	100%
M	*SNCB*	rs2075667	3/4	75%	NI	NI
M	*ARMC3*	rs12259839	2/3	67%	2/2	100%
M	*ST8SIA1*	rs4762737	2/3	67%	0/1	0%
P	*ARHGAP4*	rs2070097	1/2	50%	NI	NI
M	*AIFM2*	rs7908957	2/8	25%	1/1	100%
M	*MCCC1*	rs937652	2/6	33%	NI	NI
P	*LEP*	rs2167270	1/15	7%	1/1	100%
P	*ACPL2*	rs3210458	0/3	0%	NI	NI
P	*AKAP10*	rs203462	0/11	0%	NI	NI
M	*APC*	rs448475	0/16	0%	NI	NI
M	*C3orf62*	rs13077498	0/4	0%	NI	NI
P	*DNAJC6*	rs4915691	0/8	0%	NI	NI
M	*FGF12*	rs1460924	0/4	0%	NI	NI
P	*GATA4*	rs867858	0/11	0%	NI	NI
P	*LASS2*	rs8444	0/13	0%	NI	NI
P	*P2RY6*	rs7115806	0/6	0%	NI	NI
P	*PARP12*	rs2269996	0/9	0%	NI	NI
P	*PEX5*	rs3813737	0/7	0%	NI	NI
M	*RASGRF1*	rs2230518	0/5	0%	NI	NI
P	*SAMD10*	rs817343	0/4	0%	NI	NI
P	*SEMA3B*	rs2071203	0/6	0%	NI	NI
M	*SLC46A2*	rs2236600	0/11	0%	NI	NI
P	*TBX6*	rs2289292	0/4	0%	NI	NI
M	*TMEM17*	rs13396048	0/1	0%	NI	NI
P	*C10orf125*	rs1057097	NI	NI	NI	NI
M	*CYP2W1*	rs73261988	NI	NI	NI	NI
M	*ZNF232*	rs62076285	NI	NI	NI	NI
M	*IGF2*	rs2585	8/8	100%	5/5	100%
M	*IGF2*	rs7873	3/3	100%	2/2	100%

NI: Not informative

Supplementary Table 2.7. Comparison of allelic expression measurement for *LEP* by pyrosequencing and Sequenom assays

	Pyrosequencing			Sequenom		
Sample	**G**	**A**	**Allelic ratio[a]**	**G**	**A**	**Allelic ratio[a]**
PM143	39.5%	60.5%	0.40	3.29	3.83	0.46
PM156	22.9%	77.1%	0.23	1.71	1.55	0.52
PM161	44.1%	55.9%	0.44	3.31	2.62	0.56
PM177	35.5%	64.5%	0.36	1.52	2.17	0.41
PM178	28.8%	71.2%	0.29	2.34	3.48	0.40
PM181	44.1%	55.9%	0.44	2.69	1.24	0.68
PM187	6.6%	93.4%	0.07	0.71	2.85	0.20
PM190	51.1%	48.9%	0.51	2.89	2.97	0.49
PM193	32.0%	68.0%	0.32	1.32	0.61	0.68
PM194	13.9%	86.1%	0.14	1.57	2.63	0.37
PM202	25.8%	74.2%	0.26	3.65	3.57	0.51
PM205	43.0%	57.0%	0.43	4.16	3.74	0.53

[a]Calculated by allele G/(allele G + allele A); correlation between pyrosequencing and Sequenom: $r=0.64$, $p<0.02$

Supplementary Table 2.8. DNA methylation of identified imprinted DMRs in different tissues

CHR	Gene	TargetID	q value	Average muscle	Std	Average brain	Std	Average kidney	Std	Average blood	Std	Average placenta	Std
12	*ST8SIA1*	cg00769520*	0	0.03	0.00	0.04	0.00	0.03	0.01	0.04	0.01	0.33	0.05
6	*CD83*	cg01288598*	0	0.05	0.01	0.07	0.02	0.05	0.01	0.07	0.01	0.49	0.05
3	*CMTM8*	cg01617750	0	0.48	0.03	0.47	0.04	0.30	0.08	0.43	0.06	0.60	0.04
20	*SAMD10*	cg03224418	0	0.73	0.02	0.66	0.02	0.64	0.07	0.42	0.04	0.55	0.05
18	*ZNF396*	cg03776551*	0	0.05	0.01	0.05	0.01	0.05	0.01	0.05	0.01	0.41	0.06
14	*MEG3*	cg04291079	0	0.57	0.05	0.58	0.04	0.58	0.04	0.92	0.03	0.52	0.10
3	*MCCC1*	cg04991337*	0	0.08	0.02	0.09	0.03	0.08	0.03	0.07	0.01	0.47	0.06
5	*SNCB*	cg05028467*	0	0.10	0.05	0.10	0.05	0.12	0.08	0.06	0.01	0.36	0.12
7	*FIGNL1*	cg05072008	0	0.38	0.05	0.57	0.05	0.50	0.06	0.35	0.09	0.58	0.06
11	*CDKN1C*	cg05559445	0	0.10	0.02	0.10	0.03	0.12	0.02	0.36	0.02	0.46	0.05
11	*P2RY6*	cg06637774	0	0.18	0.06	0.11	0.02	0.07	0.01	0.38	0.06	0.20	0.11
X	*ARHGAP4*	cg06791102*	0	0.25	0.15	0.25	0.14	0.24	0.18	0.46	0.07	0.61	0.10
5	*NUDT12*	cg07655627*	0	0.16	0.06	0.20	0.09	0.19	0.07	0.16	0.06	0.41	0.05
9	*SLC46A2*	cg07758904*	0	0.05	0.03	0.09	0.06	0.06	0.04	0.09	0.05	0.47	0.07
7	*PARP12*	cg07937272	0	0.43	0.06	0.23	0.06	0.50	0.03	0.53	0.04	0.42	0.06
11	*KCNQ1*	cg08007665	0	0.81	0.02	0.81	0.03	0.83	0.02	0.82	0.02	0.59	0.07
1	*DNAJC6*	cg09082287*	0	0.12	0.02	0.12	0.03	0.13	0.03	0.12	0.02	0.41	0.09
17	*CCR10*	cg09509673	0	0.47	0.05	0.23	0.07	0.48	0.08	0.86	0.03	0.68	0.08
17	*AKAP10*	cg11630242*	0	0.20	0.04	0.22	0.08	0.18	0.05	0.08	0.01	0.56	0.05
10	*ARMC3*	cg11673092*	0	0.11	0.02	0.07	0.01	0.09	0.01	0.06	0.02	0.32	0.04
2	*TMEM17*	cg12385425*	0	0.10	0.02	0.09	0.02	0.10	0.03	0.08	0.01	0.53	0.08
7	*LEP*	cg12782180*	0	0.13	0.05	0.13	0.03	0.13	0.03	0.45	0.04	0.73	0.07
8	*GATA4*	cg13434842*	0	0.06	0.01	0.07	0.00	0.07	0.01	0.17	0.03	0.40	0.07
16	*TBX6*	cg14370448*	0	0.32	0.05	0.28	0.07	0.15	0.02	0.05	0.01	0.67	0.04
10	*C10orf125*	cg14607011	0	0.67	0.04	0.57	0.10	0.75	0.04	0.87	0.02	0.75	0.04
3	*SEMA3B*	cg14911395	0	0.63	0.05	0.22	0.10	0.35	0.04	0.15	0.04	0.45	0.04
19	*DNMT1*	cg15043801*	0	0.06	0.02	0.06	0.02	0.06	0.02	0.07	0.01	0.44	0.08
11	*H19*	cg15269875	0	0.60	0.05	0.90	0.02	0.62	0.06	0.92	0.01	0.59	0.07

Supplementary Table 2.8. DNA methylation of identified imprinted DMRs in different tissues

CHR	Gene	TargetID	q value	Average muscle	Std	Average brain	Std	Average kidney	Std	Average blood	Std	Average placenta	Std
14	*PCK2*	cg15467148*	0	0.13	0.06	0.14	0.04	0.11	0.02	0.13	0.03	0.45	0.16
12	*PEX5*	cg15754084*	0	0.17	0.03	0.10	0.02	0.12	0.02	0.37	0.06	0.56	0.06
7	*CYP2W1*	cg15914863	0	0.31	0.06	0.49	0.08	0.30	0.03	0.89	0.02	0.48	0.06
15	*RASGRF1*	cg16154416*	0	0.04	0.01	0.04	0.01	0.03	0.00	0.13	0.02	0.31	0.12
5	*APC*	cg16970232*	0	0.08	0.04	0.09	0.04	0.09	0.05	0.06	0.01	0.66	0.08
1	*G0S2*	cg17710021*	0	0.05	0.00	0.06	0.01	0.05	0.01	0.06	0.01	0.45	0.10
1	*LASS2*	cg18611122*	0	0.22	0.05	0.11	0.03	0.24	0.05	0.15	0.02	0.73	0.05
7	*LEP*	cg19594666	0	0.14	0.07	0.13	0.03	0.11	0.05	0.43	0.06	0.47	0.11
3	*C3orf62*	cg20835282*	0	0.07	0.02	0.08	0.02	0.09	0.06	0.07	0.02	0.35	0.04
11	*H19*	cg21167159	0	0.65	0.05	0.87	0.01	0.68	0.04	0.88	0.01	0.63	0.09
16	*CMTM3*	cg23297477*	0	0.06	0.02	0.07	0.01	0.06	0.02	0.06	0.01	0.44	0.07
5	*RHOBTB3*	cg24274600*	0	0.03	0.00	0.03	0.01	0.03	0.00	0.03	0.00	0.47	0.04
17	*ZNF232*	cg24680602*	0	0.05	0.01	0.06	0.02	0.06	0.02	0.10	0.07	0.36	0.06
12	*ST8SIA1*	cg24723331*	0	0.07	0.03	0.07	0.02	0.08	0.03	0.10	0.03	0.34	0.06
3	*SEMA3B*	cg24816455	0	0.61	0.06	0.24	0.05	0.28	0.04	0.05	0.01	0.45	0.08
11	*H19*	cg25852472	0	0.47	0.05	0.72	0.05	0.53	0.04	0.81	0.02	0.50	0.06
15	*SORD*	cg26196700*	0	0.04	0.01	0.04	0.01	0.04	0.01	0.04	0.01	0.39	0.06
14	*PCK2*	cg26402828*	0	0.07	0.02	0.07	0.02	0.07	0.02	0.08	0.03	0.35	0.18
10	*AIFM2*	cg26699283*	0	0.06	0.01	0.06	0.01	0.06	0.02	0.08	0.02	0.45	0.07
6	*FLJ37396*	cg16075940	1.09E-05	0.60	0.05	0.38	0.07	0.56	0.06	0.63	0.08	0.65	0.08
7	*IGFBP1*	cg05660795	5.35E-05	0.10	0.03	0.07	0.02	0.07	0.02	0.16	0.03	0.27	0.05
15	*RASGRF1*	cg15156078*	9.25E-05	0.10	0.04	0.10	0.03	0.11	0.05	0.14	0.03	0.31	0.14
22	*MOV10L1*	cg18638931	9.25E-05	0.53	0.06	0.59	0.05	0.58	0.06	0.52	0.07	0.37	0.08
1	*DIRAS3*	cg19114595	0.000282	0.63	0.02	0.68	0.03	0.60	0.03	0.61	0.02	0.47	0.05
7	*PEG10*	cg19107595	0.000484	0.53	0.05	0.45	0.05	0.48	0.09	0.46	0.03	0.64	0.03

*Probes with predominant methylation in placenta (more than 15% on average higher than every tissue)

Supplementary Table 2.9. DNA methylation of identified imprinted DMRs in placenta with different gestational ages

CHR	Gene name	TargetID	q value	Average early	Std	Average mid	Std	Average term	Std
3	*SEMA3B*	cg14911395	0	0.31	0.06	0.45	0.04	0.32	0.06
12	*PEX5*	cg15754084	0	0.47	0.09	0.56	0.06	0.73	0.03
6	*FLJ37396*	cg16075940	0	0.58	0.07	0.65	0.08	0.78	0.04
1	*LASS2*	cg18611122	0	0.68	0.07	0.73	0.05	0.85	0.03
1	*DIRAS3*	cg19114595	0	0.47	0.04	0.47	0.05	0.31	0.06
1	*DNAJC6*	cg26304237	0	0.21	0.06	0.22	0.07	0.42	0.05
3	*CMTM8*	cg01617750	6.58E-05	0.54	0.04	0.60	0.04	0.66	0.05
1	*DNAJC6*	cg09082287	9.22E-05	0.40	0.09	0.41	0.09	0.58	0.05
19	*REEP6*	cg22759185	9.22E-05	0.49	0.05	0.57	0.05	0.67	0.09
20	*L3MBTL*	cg23626798	9.22E-05	0.57	0.02	0.56	0.03	0.50	0.04
3	*ACPL2*	cg00400028	0.00067	0.49	0.04	0.38	0.06	0.50	0.08
1	*DIRAS3*	cg09118625	0.000845	0.51	0.03	0.56	0.04	0.57	0.03

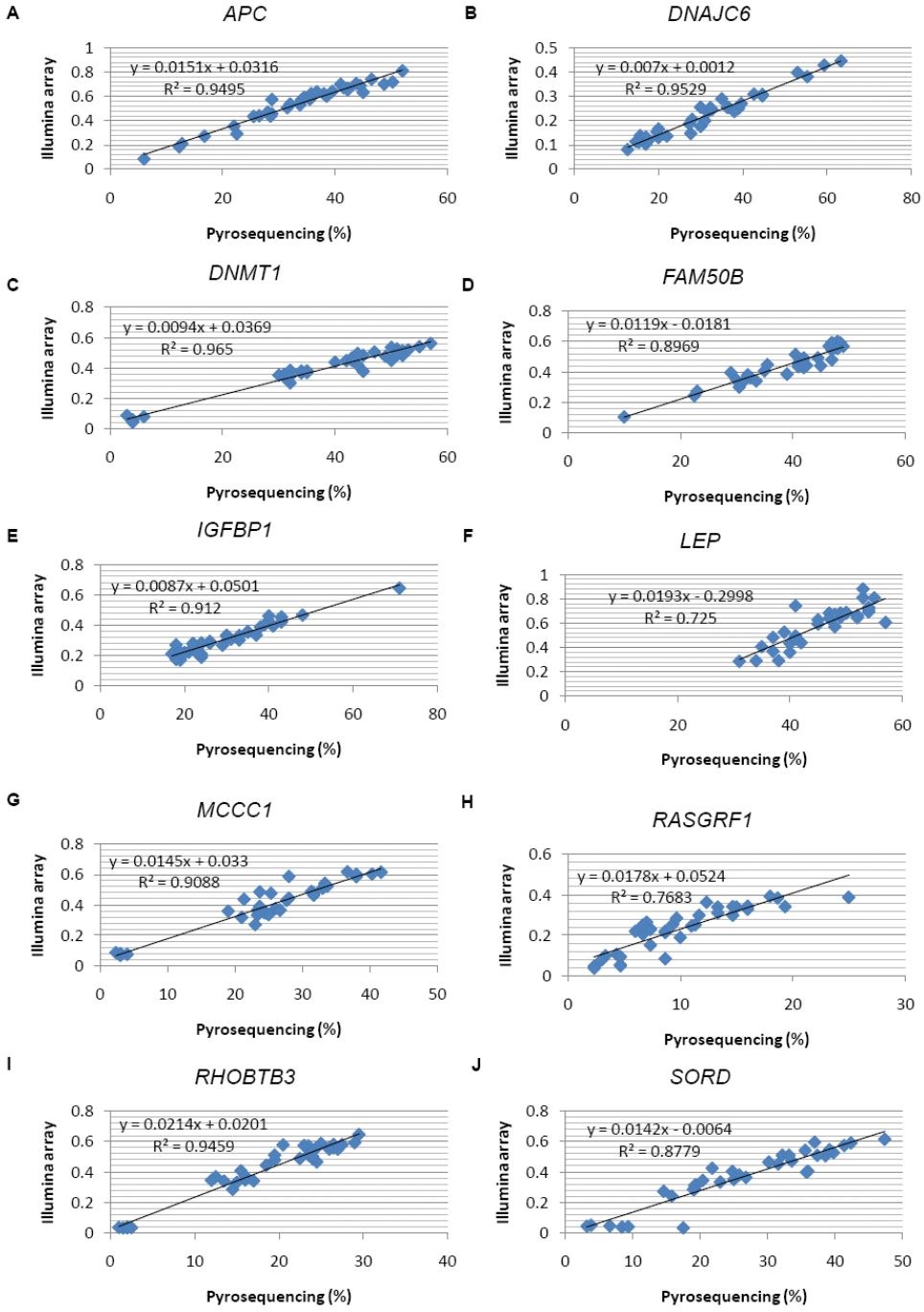

Supplementary Figure 2.1. Correlation of DNA methylation measurements between the Illumina array and pyrosequencing.

Methylation level measured by Illumina array (beta-value) for all the placental samples are compared against estimated percent methylation of the same CpG sites measured by pyrosequencing for (A) *APC*, (B) *DNAJC6*, (C) *DNMT1*, (D) *FAM50B*, (E) *IGFBP1*, (F) *LEP*, (G) *MCCC1*, (H) *RASGRF1*, (I) *RHOBTB3* and (J) *SORD*.

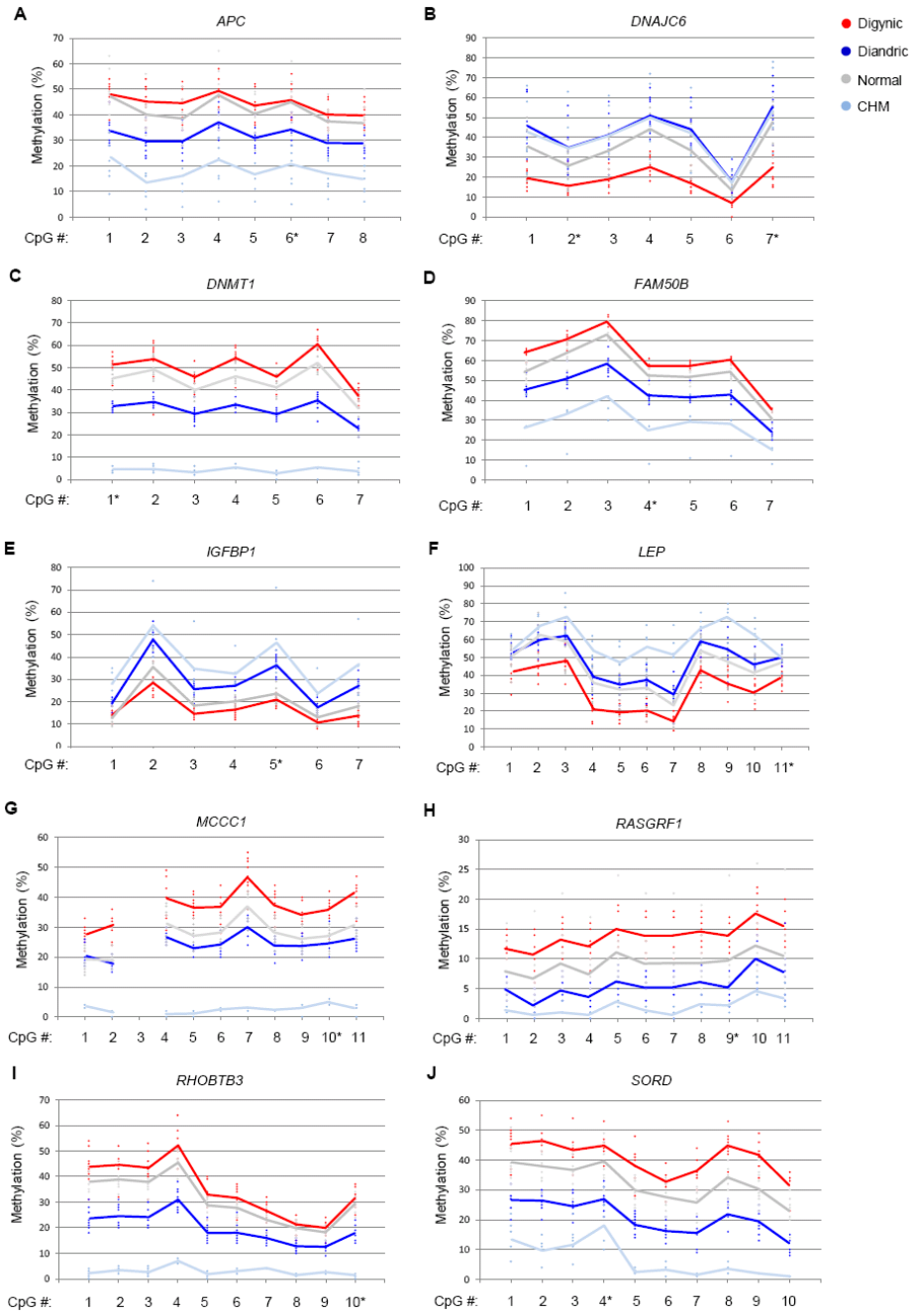

Supplementary Figure 2.2. DNA methylation patterns of all CpG sites measured within each individual pyrosequencing assay.

Methylation levels measured by pyrosequencing are shown for (A) *APC*, (B) *DNAJC6*, (C) *DNMT1*, (D) *FAM50B*, (E) *IGFBP1*, (F) *LEP*, (G) *MCCC1*, (H) *RASGRF1*, (I) *RHOBTB3* and (J) *SORD*. CpG numbers are assigned according to the ascending order of CpG sites covered by the pyrosequencing assay. CpG sites with an asterisk are the sites targeted by probes on the Illumina array. Values observed for each sample are indicated by coloured dots corresponding to the placental group, while lines connect the group averages at each site.

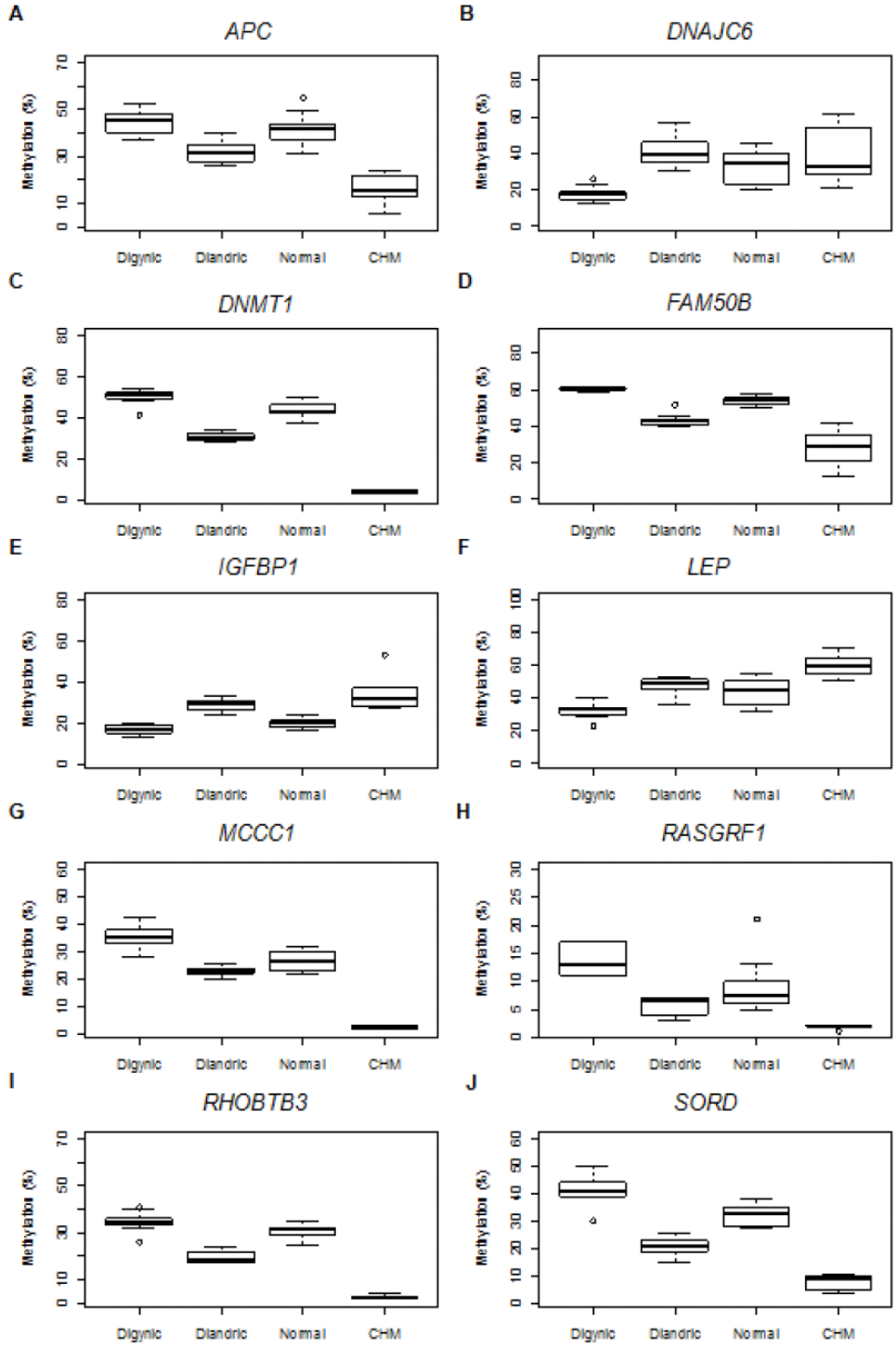

Supplementary Figure 2.3. Comparison of average DNA methylation level of identified imprinted DMRs between placental groups.

Boxplots of average methylation in each placental group are shown for (A) *APC*, (B) *DNAJC6*, (C) *DNMT1*, (D) *FAM50B*, (E) *IGFBP1*, (F) *LEP*, (G) *MCCC1*, (H) *RASGRF1*, (I) *RHOBTB3* and (J) *SORD*.

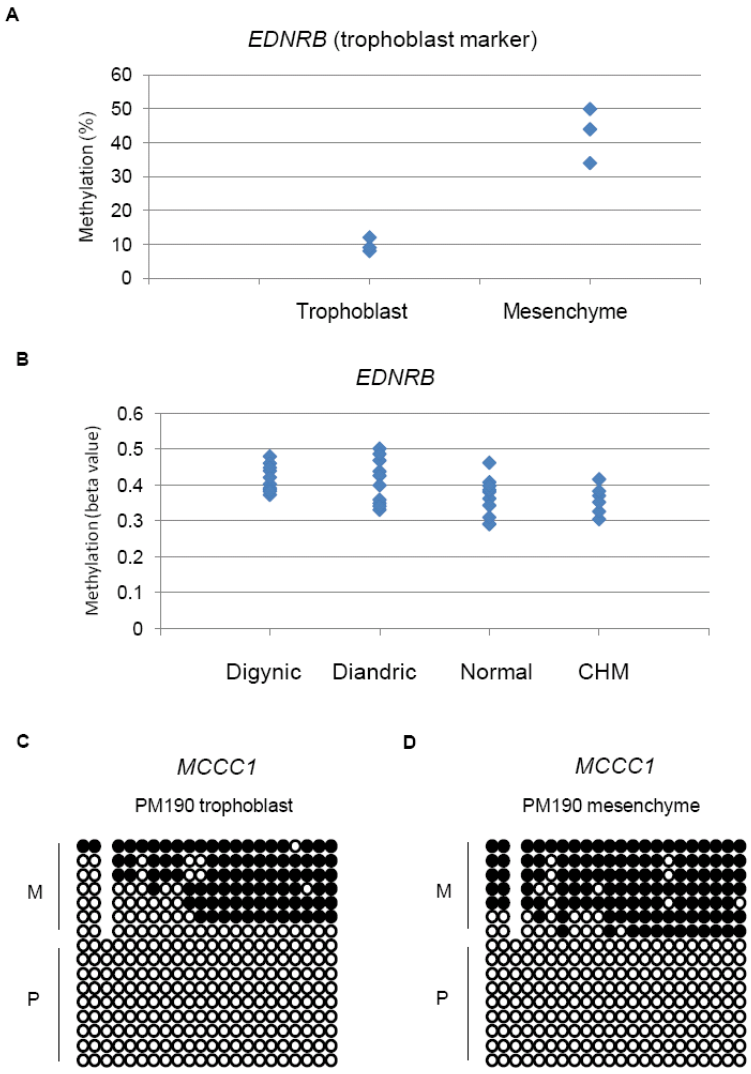

Supplementary Figure 2.4. Evaluation of cell composition as potential confounders to the imprinted DMR identification approach.

(A) Methylation level at the promoter region of *EDNRB* is used as a trophoblast marker as it has low methylation in trophoblast and is more highly methylated in mesenchymal cells. Ratio of trophoblasts to mesenchyme cells can be estimated by measuring the methylation level in the placenta. (B) *EDNRB* shows no differential methylation (i.e. no difference in trophoblasts to mesenchymal cell ratio) between digynic and diandric triploid placentas. (C, D) Parent-of-origin dependent allelic methylation of *MCCC1* can be found in both (C) trophoblasts and (D) mesenchymal cells.

Appendix 2: Supplementary tables and figures for Chapter 3

Supplementary Table 3.1. PCR primers and condition

Primers for bisulfite pyrosequencing

Gene	Primer	Sequence (5' to 3')	Product length (bp)
CDH17	Forward	TGATTGAAGTTGAAGGGAGAGGT	153
	Reverse	(5' biotinated)-CAACCCTTACCTTTCTATAAATCACAA	
	Sequencing	GGGAAGAGGGAGTGTT	
CRK	Forward	TATTYGTAGTGTAAGTGGAGTGTTAATAA	217
	Reverse	(5' biotinated)-CACCATATCRACCAAAATAATCTC	
	Sequencing	GGGAAGAGGGAGTGTT	
HOXA5	Forward	GGTTTTTTTTTTTTTYGAAGGTGATA	239
	Reverse	(5' biotinated)-CCTCRCAATTCCATTAAAATATACCA	
	Sequencing	TGATATTTGTATTTTTAAAATTTAG	
MEST	Forward	(5' biotinated)-GGGTTTTTTTTGGGAATAGGGTGAA	122
	Reverse	TTCCAAAATAAACTTAATCCATTCTCCRC	
	Sequencing	CCTTACCTACAAAACTCCAT	
MUSK	Forward	TGAATAGATTTAGATTTTTGGTTTGAGTT	129
	Reverse	(5' biotinated)-CAATAACAAAAAAACAATACCAAATACC	
	Sequencing	GATTTAGATTTTTGGTTTGAGT	

Reaction condition and thermal profile for all assays

Reagents	Final conc.	Temperature		Cycles
10X HotStarTaq Buffer	1X	Initial denaturation:	95°C	10 min
$MgCl_2$	1.25mM	Denaturation:	95°C	40 sec
NTP	200mM	Annealing:	50°C	40 sec x 40 cycles
Forward primer	200nM	Extension:	72°C	40 sec
Reverse primer	200nM	Final extension:	72°C	7 min
HotStarTaq	0.04U			
Total reaction volume	25ul			

Supplementary Table 3.2. Tissue-specific differentially methylated loci in normal fetuses

		Brain			Kidney			Lung			Skin			Muscle		
TargetID	**CpG island**	**Mean**	**Hyper**	**Hypo**	**Mean**	**Hyper**	**Hypo**	**Mean**	**Hyper**	**Hypo**	**Mean**	**Hyper**	**Hypo**	**Mean**	**Hyper**	**Hypo**
*CRK_P721_F	Y	0.9	Y	N	0.82	N	N	0.28	N	Y	0.66	N	N	0.79	N	N
*HOXA5_P479_F	Y	0.55	N	N	0.48	N	N	0.35	N	Y	0.95	Y	N	0.96	Y	N
*MEST_E150_F	Y	0.28	N	Y	0.75	N	N	0.58	N	N	0.74	N	N	0.92	Y	N
AATK_P519_R	Y	0.4	N	N	0.52	N	N	0.74	N	N	0.44	N	N	0.88	Y	N
AATK_P709_R	Y	0.35	N	N	0.38	N	N	0.61	N	N	0.25	N	Y	0.85	Y	N
APBA1_P644_F	Y	0.07	N	N	0.07	N	N	0.06	N	N	0.12	N	N	0.1	N	N
APC_P14_F	Y	0.12	N	N	0.11	N	N	0.33	N	N	0.14	N	N	0.13	N	N
AREG_P217_R	Y	0.49	N	N	0.31	N	N	0.3	N	N	0.21	N	N	0.26	N	N
BCR_P346_F	Y	0.82	N	N	0.39	N	Y	0.76	N	N	0.87	N	N	0.86	N	N
BCR_P422_F	Y	0.99	N	N	0.85	N	N	0.98	N	N	0.98	N	N	0.99	N	N
CREBBP_P712_R	Y	0.76	N	N	0.52	N	N	0.61	N	N	0.52	N	N	0.94	Y	N
CRIP1_P874_R	Y	0.17	N	N	0.01	N	Y	0.06	N	N	0.25	N	N	0.67	Y	N
DNMT2_P199_F	Y	0.45	N	Y	0.73	N	N	0.84	N	N	0.83	N	N	0.88	N	N
ERN1_P809_R	Y	0.93	Y	N	0.59	N	N	0.75	N	N	0.62	N	N	0.63	N	N
EYA4_P794_F	Y	0.09	N	N	0.01	N	Y	0.02	N	N	0.42	Y	N	0.56	Y	N
FGF6_P139_R	Y	0.99	N	N	0.89	N	N	0.99	N	N	0.99	N	N	0.99	N	N
GFI1_P208_R	Y	0.04	N	N	0.07	N	N	0.13	N	N	0.34	N	N	0.55	Y	N
GP1BB_E23_F	Y	0.46	N	N	0.19	N	Y	0.58	N	N	0.83	Y	N	0.61	N	N
HDAC1_P414_R	Y	0.95	N	N	0.8	N	N	0.93	N	N	0.91	N	N	0.97	N	N
HOXA11_E35_F	Y	0.02	N	N	0.04	N	N	0.03	N	N	0.07	N	N	0.2	N	N
HOXA11_P698_F	Y	0.13	N	Y	0.22	N	N	0.13	N	Y	0.87	Y	N	0.74	Y	N
HOXA5_E187_F	Y	0.08	N	Y	0.2	N	Y	0.19	N	Y	0.82	Y	N	0.89	Y	N
HOXA5_P1324_F	Y	0	N	N	0.02	N	N	0	N	N	0.19	N	N	0.27	N	N
HOXA9_P303_F	Y	0.21	N	N	0.01	N	N	0.12	N	N	0	N	N	0.01	N	N
HOXB2_P99_F	Y	0.25	N	Y	0.5	N	N	0.4	N	N	0.74	Y	N	0.49	N	N

Supplementary Table 3.2. Tissue-specific differentially methylated loci in normal fetuses

		Brain			Kidney			Lung			Skin			Muscle		
TargetID	**CpG island**	**Mean**	**Hyper**	**Hypo**	**Mean**	**Hyper**	**Hypo**	**Mean**	**Hyper**	**Hypo**	**Mean**	**Hyper**	**Hypo**	**Mean**	**Hyper**	**Hypo**
IFNGR2_P377_R	Y	0.93	Y	N	0.87	N	N	0.75	N	N	0.31	N	Y	0.7	N	N
IGFBP1_P12_R	Y	0.15	N	N	0.05	N	N	0.15	N	N	0.44	Y	N	0.17	N	N
MAD2L1_E93_F	Y	0.87	N	N	0.81	N	N	0.89	N	N	0.88	N	N	0.87	N	N
MAP2K6_P297_R	Y	0.46	N	N	0.16	N	N	0.2	N	N	0.3	N	N	0.24	N	N
MAP3K8_P1036_F	Y	0.96	N	N	0.9	N	N	0.9	N	N	0.72	N	N	0.97	N	N
MEST_P4_F	Y	0.13	N	Y	0.92	N	N	0.78	N	N	0.89	N	N	0.97	Y	N
MEST_P62_R	Y	0.26	N	Y	0.77	N	N	0.61	N	N	0.76	N	N	0.88	Y	N
MSH2_P1008_F	Y	0.98	N	N	0.47	N	Y	0.85	N	N	0.93	N	N	0.87	N	N
MST1R_E42_R	Y	0.83	N	N	0.94	N	N	0.81	N	N	0.77	N	N	0.78	N	N
MST1R_P392_F	Y	0.49	Y	N	0.09	N	N	0.23	N	N	0.15	N	N	0.45	N	N
MST1R_P87_R	Y	0.84	N	N	0.77	N	N	0.52	N	N	0.54	N	N	0.62	N	N
MT1A_P600_F	Y	0.14	N	N	0.14	N	N	0.18	N	N	0.48	Y	N	0.38	N	N
NFKB1_P496_F	Y	0.5	N	N	0.69	Y	N	0.45	N	N	0.25	N	Y	0.36	N	N
NNAT_P544_R	Y	0.87	N	N	0.94	N	N	0.9	N	N	0.97	N	N	0.87	N	N
PAX6_P1121_F	Y	0.06	N	N	0.05	N	N	0.07	N	N	0.26	N	N	0.12	N	N
PRKCDBP_E206_F	Y	0.08	N	N	0	N	N	0.01	N	N	0	N	N	0	N	N
PRKCDBP_P352_R	Y	0.62	Y	N	0.4	N	N	0.35	N	N	0.13	N	N	0.09	N	Y
PRSS8_E134_R	Y	0.68	N	N	0.42	N	Y	0.74	N	N	0.55	N	N	0.75	N	N
PTK6_E50_F	Y	0.99	N	N	0.99	N	N	0.99	N	N	0.9	N	N	0.99	N	N
RAB32_P493_R	Y	0.77	Y	N	0.48	N	N	0.27	N	N	0.31	N	N	0.46	N	N
RYK_P493_F	Y	0.5	N	N	0.58	Y	N	0.16	N	N	0.17	N	N	0.4	N	N
SEPT5_P441_F	Y	0.13	N	N	0.17	N	N	0.15	N	N	0.33	N	N	0.12	N	N
SEPT9_P374_F	Y	0.98	Y	N	0.94	Y	N	0.69	N	N	0.14	N	Y	0.7	N	N
SEPT9_P58_R	Y	0.97	N	N	0.96	N	N	0.88	N	N	0.43	N	Y	0.96	N	N
SLC22A3_P528_F	Y	0.27	N	N	0.46	N	N	0.28	N	N	0.44	N	N	0.76	Y	N
SLC5A5_E60_F	Y	0.6	N	N	0.4	N	N	0.4	N	N	0.35	N	N	0.39	N	N

Supplementary Table 3.2. Tissue-specific differentially methylated loci in normal fetuses

		Brain			Kidney			Lung			Skin			Muscle		
TargetID	**CpG island**	**Mean**	**Hyper**	**Hypo**	**Mean**	**Hyper**	**Hypo**	**Mean**	**Hyper**	**Hypo**	**Mean**	**Hyper**	**Hypo**	**Mean**	**Hyper**	**Hypo**
SMARCB1_P220_R	Y	0.28	N	N	0.42	N	N	0.24	N	N	0.15	N	N	0.11	N	N
SNCG_P98_R	Y	0.16	N	N	0.47	N	N	0.23	N	N	0.26	N	N	0.25	N	N
SOX2_P546_F	Y	0.06	N	N	0.07	N	N	0.06	N	N	0.07	N	N	0.58	Y	N
TBX1_P885_R	Y	0.04	N	Y	0.12	N	N	0.12	N	N	0.2	N	N	0.89	Y	N
TDGF1_E53_R	Y	0.4	N	Y	0.76	N	N	0.86	N	N	0.85	N	N	0.89	N	N
TGFB1_P833_R	Y	0.99	N	N	0.99	N	N	0.99	N	N	0.99	N	N	0.78	N	N
TNFRSF10D_P70_F	Y	0.21	N	N	0.14	N	N	0.12	N	N	0.11	N	N	0.42	Y	N
TNFSF8_P184_F	Y	0.86	N	N	0.83	N	N	0.81	N	N	0.95	N	N	0.81	N	N
TP73_P945_F	Y	0.05	N	N	0.07	N	N	0.09	N	N	0.09	N	N	0.26	N	N
VAV1_E9_F	Y	0.97	N	N	0.87	N	N	0.89	N	N	0.69	N	N	0.85	N	N
WRN_P969_F	Y	0.39	N	Y	0.76	N	N	0.92	N	N	0.97	N	N	0.92	N	N
ZNFN1A1_E102_F	Y	0.8	N	N	0.98	N	N	0.99	N	N	0.95	N	N	0.91	N	N
*CDH17_E31_F	N	0.97	N	N	0.52	N	Y	0.99	N	N	0.99	N	N	0.9	N	N
*MUSK_P308_F	N	0.98	N	N	0.99	N	N	0.98	N	N	0.98	N	N	0.85	N	N
ACTG2_P346_F	N	0.96	N	N	0.97	N	N	0.85	N	N	0.94	N	N	0.89	N	N
AGXT_P180_F	N	0.75	N	N	0.97	N	N	0.83	N	N	0.84	N	N	0.92	N	N
AOC3_P890_R	N	0.9	N	N	0.76	N	N	0.77	N	N	0.74	N	N	0.7	N	N
APOA1_P261_F	N	0.63	N	N	0.34	N	Y	0.79	N	N	0.96	Y	N	0.83	N	N
APOA1_P75_F	N	0.95	N	N	0.82	N	N	0.58	N	Y	0.96	N	N	0.94	N	N
ARHGDIB_P148_R	N	0.83	N	N	0.92	N	N	0.94	N	N	0.74	N	N	0.97	N	N
ASB4_E89_F	N	0.99	N	N	0.83	N	N	0.97	N	N	0.86	N	N	0.83	N	N
ASB4_P391_F	N	0.99	N	N	0.99	N	N	0.84	N	N	0.6	N	N	0.6	N	Y
ASB4_P52_R	N	0.99	Y	N	0.59	N	N	0.77	N	N	0.62	N	N	0.36	N	Y
B3GALT5_E246_R	N	0.97	N	N	0.99	N	N	0.95	N	N	0.96	N	N	0.76	N	N
BLK_P14_F	N	0.45	N	Y	0.98	N	N	0.98	N	N	0.98	N	N	0.94	N	N
CAPG_E228_F	N	0.98	N	N	0.86	N	N	0.85	N	N	0.84	N	N	0.72	N	N

Supplementary Table 3.2. Tissue-specific differentially methylated loci in normal fetuses

		Brain			Kidney			Lung			Skin			Muscle		
TargetID	**CpG island**	**Mean**	**Hyper**	**Hypo**	**Mean**	**Hyper**	**Hypo**	**Mean**	**Hyper**	**Hypo**	**Mean**	**Hyper**	**Hypo**	**Mean**	**Hyper**	**Hypo**
CARD15_P302_R	N	0.99	N	N	0.96	N	N	0.92	N	N	0.83	N	N	0.75	N	N
CASP10_E139_F	N	0.98	N	N	0.6	N	N	0.68	N	N	0.74	N	N	0.94	N	N
CASP10_P186_F	N	0.98	Y	N	0.57	N	N	0.49	N	N	0.37	N	Y	0.88	Y	N
CASP10_P334_F	N	0.97	Y	N	0.82	N	N	0.41	N	Y	0.65	N	N	0.86	N	N
CCKAR_E79_F	N	0.17	N	Y	0.1	N	Y	0.73	Y	N	0.35	N	N	0.66	Y	N
CCKAR_P270_F	N	0.4	N	Y	0.96	N	N	0.98	N	N	0.91	N	N	0.99	N	N
CCL3_P543_R	N	0.99	N	N	0.94	N	N	0.96	N	N	0.98	N	N	0.9	N	N
CD34_P780_R	N	0.98	N	N	0.97	N	N	0.91	N	N	0.89	N	N	0.94	N	N
CDH17_P376_F	N	0.99	N	N	0.98	N	N	0.93	N	N	0.99	N	N	0.99	N	N
CEACAM1_E57_R	N	0.92	Y	N	0.37	N	N	0.54	N	N	0.27	N	Y	0.69	N	N
CEACAM1_P44_R	N	0.99	N	N	0.99	N	N	0.98	N	N	0.92	N	N	0.98	N	N
CLDN4_P1120_R	N	0.88	N	N	0.74	N	N	0.65	N	N	0.76	N	N	0.9	N	N
CLK1_P538_F	N	0.48	Y	N	0.13	N	N	0.27	N	N	0.29	N	N	0.17	N	N
CPA4_E20_F	N	0.94	Y	N	0.94	Y	N	0.75	N	N	0.37	N	Y	0.69	N	N
CSF1R_P73_F	N	0.89	N	N	0.81	N	N	0.74	N	N	0.53	N	N	0.65	N	N
CSF2_P605_F	N	0.99	N	N	0.97	N	N	0.89	N	N	0.98	N	N	0.97	N	N
CSF3_P309_R	N	0.35	N	N	0.74	Y	N	0.59	N	N	0.57	N	N	0.32	N	N
CSF3R_P472_F	N	0.91	N	N	0.9	N	N	0.83	N	N	0.83	N	N	0.71	N	N
CSF3R_P8_F	N	0.69	Y	N	0.25	N	N	0.21	N	N	0.19	N	N	0.31	N	N
CTGF_P693_R	N	0.97	N	N	0.85	N	N	0.67	N	Y	0.97	N	N	0.99	N	N
DDR1_P332_R	N	0.01	N	N	0.12	N	N	0.38	Y	N	0.05	N	N	0.09	N	N
DDR2_E331_F	N	0.96	N	N	0.99	N	N	0.93	N	N	0.61	N	N	0.55	N	Y
DES_P1006_R	N	0.99	N	N	0.99	N	N	0.99	N	N	0.99	N	N	0.94	N	N
DLC1_E276_F	N	0.98	Y	N	0.88	N	N	0.43	N	Y	0.72	N	N	0.48	N	Y
DLC1_P695_F	N	0.99	N	N	0.99	N	N	0.89	N	N	0.78	N	N	0.97	N	N
DLC1_P88_R	N	0.97	Y	N	0.72	N	N	0.3	N	Y	0.67	N	N	0.29	N	Y

Supplementary Table 3.2. Tissue-specific differentially methylated loci in normal fetuses

		Brain			Kidney			Lung			Skin			Muscle		
TargetID	**CpG island**	**Mean**	**Hyper**	**Hypo**	**Mean**	**Hyper**	**Hypo**	**Mean**	**Hyper**	**Hypo**	**Mean**	**Hyper**	**Hypo**	**Mean**	**Hyper**	**Hypo**
EPHX1_E152_F	N	0.73	N	N	0.52	N	N	0.75	N	N	0.75	N	N	0.53	N	N
FAS_P322_R	N	0.38	Y	N	0.07	N	N	0.12	N	N	0.15	N	N	0.12	N	N
FER_P581_F	N	0.99	N	N	0.89	N	N	0.87	N	N	0.97	N	N	0.99	N	N
FGF1_E5_F	N	0.8	N	N	0.99	N	N	0.91	N	N	0.94	N	N	0.64	N	Y
FGF7_P44_F	N	0.42	N	Y	0.92	N	N	0.91	N	N	0.85	N	N	0.73	N	N
FRK_P36_F	N	0.99	Y	N	0.91	N	N	0.44	N	Y	0.52	N	Y	0.96	N	N
GFAP_P56_R	N	0.33	N	Y	0.96	N	N	0.93	N	N	0.92	N	N	0.7	N	N
GLI3_E148_R	N	0.85	N	N	0.95	N	N	0.88	N	N	0.77	N	N	0.95	N	N
GNG7_P903_F	N	0.98	N	N	0.99	N	N	0.97	N	N	0.88	N	N	0.95	N	N
HDAC7A_P344_F	N	0.81	N	N	0.99	N	N	0.99	N	N	0.99	N	N	0.97	N	N
HDAC9_E38_F	N	0.05	N	N	0.02	N	N	0.09	N	N	0.36	Y	N	0.02	N	N
HDAC9_P137_R	N	0.05	N	N	0.01	N	N	0.3	N	N	0.27	N	N	0.01	N	N
HLA-DPA1_P28_R	N	0.99	N	N	0.97	N	N	0.95	N	N	0.81	N	N	0.96	N	N
HLA-DPB1_E2_R	N	0.99	N	N	0.87	N	N	0.98	N	N	0.96	N	N	0.95	N	N
HOXB2_P488_R	N	0.13	N	Y	0.33	N	N	0.32	N	N	0.74	Y	N	0.65	Y	N
HPN_P374_R	N	0.1	N	N	0.11	N	N	0.19	N	N	0.15	N	N	0.56	Y	N
HPN_P823_F	N	0.19	N	N	0.17	N	N	0.4	N	N	0.17	N	N	0.63	Y	N
HTR2A_E10_R	N	0.59	N	Y	0.99	N	N	0.99	N	N	0.95	N	N	0.99	N	N
IGF1_E394_F	N	0.9	Y	N	0.89	Y	N	0.46	N	N	0.29	N	Y	0.23	N	Y
IGF1_P933_F	N	0.61	N	N	0.74	Y	N	0.33	N	N	0.42	N	N	0.11	N	Y
IL16_P93_R	N	0.61	N	N	0.89	N	N	0.72	N	N	0.62	N	N	0.86	N	N
IL1RN_E42_F	N	0.99	N	N	0.96	N	N	0.99	N	N	0.91	N	N	0.99	N	N
IL1RN_P93_R	N	0.66	N	N	0.99	Y	N	0.92	N	N	0.51	N	Y	0.86	N	N
IL6_E168_F	N	0.44	N	N	0.43	N	N	0.14	N	N	0.18	N	N	0.09	N	N
IL6_P213_R	N	0.81	Y	N	0.81	Y	N	0.08	N	Y	0.15	N	Y	0.24	N	N
IL8_E118_R	N	0.97	N	N	0.99	N	N	0.42	N	Y	0.93	N	N	0.95	N	N

Supplementary Table 3.2. Tissue-specific differentially methylated loci in normal fetuses

		Brain			Kidney			Lung			Skin			Muscle		
TargetID	**CpG island**	**Mean**	**Hyper**	**Hypo**	**Mean**	**Hyper**	**Hypo**	**Mean**	**Hyper**	**Hypo**	**Mean**	**Hyper**	**Hypo**	**Mean**	**Hyper**	**Hypo**
INS_P248_F	N	0.97	N	N	0.81	N	N	0.91	N	N	0.87	N	N	0.78	N	N
JAK3_P156_R	N	0.7	N	N	0.62	N	N	0.56	N	N	0.25	N	Y	0.53	N	N
KLK11_P103_R	N	0.98	N	N	0.97	N	N	0.98	N	N	0.96	N	N	0.82	N	N
KRT5_P308_F	N	0.87	N	N	0.91	N	N	0.87	N	N	0.87	N	N	0.78	N	N
LEFTY2_P719_F	N	0.98	N	N	0.99	N	N	0.97	N	N	0.88	N	N	0.68	N	Y
LMO2_P794_R	N	0.99	N	N	0.85	N	N	0.99	N	N	0.99	N	N	0.98	N	N
LRRK1_P834_F	N	0.87	N	N	0.86	N	N	0.62	N	N	0.77	N	N	0.75	N	N
MAPK10_E26_F	N	0.97	N	N	0.74	N	N	0.9	N	N	0.99	N	N	0.94	N	N
MAPK4_E273_R	N	0.99	N	N	0.65	N	N	0.91	N	N	0.98	N	N	0.7	N	N
MAS1_P469_R	N	0.99	N	N	0.99	N	N	0.97	N	N	0.92	N	N	0.96	N	N
MMP10_E136_R	N	0.44	N	Y	0.72	N	N	0.71	N	N	0.77	N	N	0.71	N	N
MMP19_P306_F	N	0.98	N	N	0.99	N	N	0.99	N	N	0.9	N	N	0.97	N	N
MPL_P62_F	N	0.96	N	N	0.96	N	N	0.97	N	N	0.88	N	N	0.81	N	N
MPL_P657_F	N	0.2	N	Y	0.44	N	N	0.76	Y	N	0.6	N	N	0.49	N	N
MPO_P883_R	N	0.85	Y	N	0.78	N	N	0.58	N	N	0.49	N	N	0.3	N	Y
NAT2_P11_F	N	0.96	N	N	0.67	N	N	0.81	N	N	0.77	N	N	0.63	N	N
NOTCH4_E4_F	N	0.88	Y	N	0.69	N	N	0.22	N	Y	0.38	N	N	0.39	N	N
NQO1_P345_R	N	0.11	N	N	0.14	N	N	0.23	N	N	0.2	N	N	0.07	N	N
P2RX7_P597_F	N	0.98	N	N	0.91	N	N	0.96	N	N	0.99	N	N	0.97	N	N
PDGFB_P719_F	N	0.6	N	N	0.84	N	N	0.79	N	N	0.62	N	N	0.91	N	N
PDGFRA_E125_F	N	0.48	N	N	0.41	N	N	0.45	N	N	0.41	N	N	0.69	Y	N
PGR_P790_F	N	0.95	N	N	0.94	N	N	0.94	N	N	0.92	N	N	0.86	N	N
PIK3R1_P307_F	N	0.73	N	Y	0.99	N	N	0.99	N	N	0.99	N	N	0.98	N	N
PLA2G2A_E268_F	N	0.98	N	N	0.97	N	N	0.94	N	N	0.97	N	N	0.91	N	N
PLG_E406_F	N	0.5	N	Y	0.99	N	N	0.99	N	N	1	N	N	0.97	N	N
PTHLH_E251_F	N	0.55	N	N	0.4	N	Y	0.72	N	N	0.86	N	N	0.82	N	N

Supplementary Table 3.2. Tissue-specific differentially methylated loci in normal fetuses

		Brain			Kidney			Lung			Skin			Muscle		
TargetID	**CpG island**	**Mean**	**Hyper**	**Hypo**	**Mean**	**Hyper**	**Hypo**	**Mean**	**Hyper**	**Hypo**	**Mean**	**Hyper**	**Hypo**	**Mean**	**Hyper**	**Hypo**
PTHLH_P15_R	N	0.92	N	N	0.82	N	N	0.94	N	N	0.98	N	N	0.98	N	N
PTHR1_P258_F	N	0.65	N	N	0.9	N	N	0.93	N	N	0.86	N	N	0.81	N	N
PYCARD_P393_F	N	0.77	Y	N	0.73	N	N	0.58	N	N	0.36	N	N	0.27	N	Y
RARA_P1076_R	N	0.98	Y	N	0.7	N	N	0.18	N	Y	0.19	N	Y	0.75	N	N
S100A2_E36_R	N	0.98	N	N	0.56	N	Y	0.89	N	N	0.83	N	N	0.76	N	N
S100A2_P1186_F	N	0.99	N	N	0.99	N	N	0.98	N	N	0.98	N	N	0.83	N	N
S100A4_E315_F	N	0.93	Y	N	0.68	N	N	0.72	N	N	0.25	N	Y	0.39	N	Y
S100A4_P194_R	N	0.99	N	N	0.99	N	N	0.99	N	N	0.83	N	N	0.98	N	N
S100A4_P887_R	N	0.97	N	N	0.99	N	N	0.97	N	N	0.84	N	N	0.95	N	N
SERPINA5_E69_F	N	0.98	N	N	0.94	N	N	0.98	N	N	0.73	N	N	0.81	N	N
SERPINA5_P156_F	N	0.61	Y	N	0.16	N	N	0.34	N	N	0.41	N	N	0.11	N	Y
SFTPB_P689_R	N	0.94	N	N	0.96	N	N	0.86	N	N	0.74	N	N	0.9	N	N
SLC14A1_P369_R	N	0.99	N	N	0.99	N	N	0.99	N	N	0.81	N	N	0.85	N	N
SPDEF_P6_R	N	0.88	N	N	0.64	N	N	0.66	N	N	0.7	N	N	0.59	N	N
SPP1_E140_R	N	0.19	N	N	0.23	N	N	0.47	Y	N	0.27	N	N	0.17	N	N
SPP1_P647_F	N	0.91	N	N	0.8	N	N	0.93	N	N	0.93	N	N	0.88	N	N
SRC_E100_R	N	0.99	N	N	0.91	N	N	0.91	N	N	0.99	N	N	0.98	N	N
SRC_P164_F	N	0.96	N	N	0.91	N	N	0.91	N	N	0.93	N	N	0.94	N	N
STAT5A_E42_F	N	0.95	N	N	0.93	N	N	0.82	N	N	0.85	N	N	0.36	N	Y
STAT5A_P704_R	N	0.93	N	N	0.94	N	N	0.92	N	N	0.8	N	N	0.7	N	N
TDGF1_P428_R	N	0.17	N	Y	0.37	N	N	0.38	N	N	0.35	N	N	0.59	Y	N
TEK_E75_F	N	0.8	N	N	0.85	N	N	0.58	N	N	0.6	N	N	0.94	N	N
TEK_P526_F	N	0.86	N	N	0.85	N	N	0.84	N	N	0.76	N	N	0.48	N	Y
TFF1_P180_R	N	0.99	N	N	0.98	N	N	0.93	N	N	0.97	N	N	0.91	N	N
TFF2_P178_F	N	0.98	N	N	0.58	N	Y	0.93	N	N	0.91	N	N	0.9	N	N
TGFB3_E58_R	N	0.88	Y	N	0.64	N	N	0.46	N	N	0.57	N	N	0.42	N	N

Supplementary Table 3.2. Tissue-specific differentially methylated loci in normal fetuses

		Brain			Kidney			Lung			Skin			Muscle		
TargetID	**CpG island**	**Mean**	**Hyper**	**Hypo**	**Mean**	**Hyper**	**Hypo**	**Mean**	**Hyper**	**Hypo**	**Mean**	**Hyper**	**Hypo**	**Mean**	**Hyper**	**Hypo**
THBS2_P605_R	N	0.97	Y	N	0.55	N	N	0.47	N	Y	0.6	N	N	0.94	Y	N
TMPRSS4_E83_F	N	0.99	N	N	0.94	N	N	0.94	N	N	0.97	N	N	0.99	N	N
TNFSF10_E53_F	N	0.31	N	N	0.21	N	Y	0.59	N	N	0.63	N	N	0.48	N	N
TRIM29_P135_F	N	0.98	N	N	0.8	N	N	0.99	N	N	0.95	N	N	0.99	N	N
TRIM29_P261_F	N	0.98	N	N	0.56	N	Y	0.98	N	N	0.87	N	N	0.98	N	N
TSC2_E140_F	N	0.91	Y	N	0.6	N	N	0.44	N	Y	0.61	N	N	0.79	N	N
UGT1A1_P315_R	N	0.65	N	Y	0.99	N	N	0.97	N	N	0.98	N	N	0.97	N	N
UGT1A1_P564_R	N	0.86	N	N	0.94	N	N	0.94	N	N	0.97	N	N	0.92	N	N
VAMP8_E7_F	N	0.89	Y	N	0.34	N	Y	0.61	N	N	0.68	N	N	0.79	N	N
VAMP8_P114_F	N	0.79	N	N	0.51	N	N	0.74	N	N	0.68	N	N	0.77	N	N
VAMP8_P241_F	N	0.97	N	N	0.79	N	N	0.93	N	N	0.95	N	N	0.98	N	N
WEE1_P924_R	N	0.98	N	N	0.85	N	N	0.97	N	N	0.85	N	N	0.79	N	N
WNT8B_P216_R	N	0.77	N	N	0.99	N	N	0.99	N	N	0.99	N	N	0.99	N	N
ZAP70_P220_R	N	0.94	N	N	0.72	N	N	0.94	N	N	0.75	N	N	0.88	N	N

*Loci confirmed with pyrosequencing

Supplementary Table 3.3. Tissue-specific differentially methylated loci in normal fetal and adult tissues

			Brain		Kidney		Lung		ANOVA
Stage	**Feature ID**	**CGI**	**Mean**	**SD**	**Mean**	**SD**	**Mean**	**SD**	***p* value**
Fetal	MEST_P4_F	Y	0.13	0.05	0.92	0.03	0.78	0.04	8.20717E-15
	*S100A2_E36_R	N	0.98	0.01	0.56	0.05	0.89	0.02	4.64039E-13
	TFF2_P178_F	N	0.98	0.01	0.58	0.05	0.93	0.01	1.09584E-12
	*RARA_P1076_R	N	0.98	0.02	0.70	0.10	0.18	0.06	8.10347E-12
	TRIM29_P135_F	N	0.98	0.02	0.80	0.03	0.99	0.00	3.86138E-11
	*IL6_P213_R	N	0.81	0.05	0.81	0.08	0.08	0.09	3.89587E-11
	*SEPT9_P374_F	Y	0.98	0.02	0.94	0.04	0.69	0.03	1.18536E-10
	*CSF3R_P8_F	N	0.69	0.05	0.25	0.07	0.21	0.04	1.35425E-10
	CRK_P721_F	Y	0.90	0.05	0.82	0.06	0.28	0.10	2.0841E-10
	*CASP10_P334_F	N	0.97	0.02	0.82	0.06	0.41	0.08	2.18999E-10
	CDH17_E31_F	N	0.97	0.07	0.52	0.07	0.99	0.00	3.94217E-10
	TRIM29_P261_F	N	0.98	0.01	0.56	0.10	0.98	0.01	7.7881E-10
	*CEACAM1_E57_R	N	0.92	0.07	0.37	0.06	0.54	0.06	9.60336E-10
	GFAP_P56_R	N	0.33	0.14	0.96	0.01	0.93	0.02	1.53407E-09
	DLC1_E276_F	N	0.98	0.02	0.88	0.05	0.43	0.12	3.19134E-09
	IGF1_E394_F	N	0.90	0.08	0.89	0.03	0.46	0.07	3.33161E-09
	DNMT2_P199_F	Y	0.45	0.06	0.73	0.06	0.84	0.02	3.78665E-09
	MSH2_P1008_F	Y	0.98	0.02	0.47	0.09	0.85	0.07	4.0123E-09
	FAS_P322_R	N	0.38	0.04	0.07	0.05	0.12	0.03	4.2182E-09
	ASB4_P391_F	N	0.99	0.00	0.99	0.00	0.84	0.04	6.33634E-09
	*VAMP8_E7_F	N	0.89	0.05	0.34	0.06	0.61	0.10	7.23868E-09
	APOA1_P261_F	N	0.63	0.06	0.34	0.09	0.79	0.06	2.2338E-08
	CLK1_P538_F	N	0.48	0.06	0.13	0.04	0.27	0.06	2.37276E-08
	ERN1_P809_R	Y	0.93	0.03	0.59	0.07	0.75	0.05	3.25586E-08
	VAMP8_P241_F	N	0.97	0.01	0.79	0.03	0.93	0.04	4.11725E-08
	MAPK10_E26_F	N	0.97	0.03	0.74	0.05	0.90	0.02	4.38852E-08
	TDGF1_E53_R	Y	0.40	0.11	0.76	0.05	0.86	0.03	6.01413E-08
	NAT2_P11_F	N	0.96	0.06	0.67	0.05	0.81	0.03	6.18362E-08
	WEE1_P924_R	N	0.98	0.01	0.85	0.04	0.97	0.01	7.34002E-08
	LMO2_P794_R	N	0.99	0.00	0.85	0.05	0.99	0.00	7.51879E-08
	SNCG_P98_R	Y	0.16	0.04	0.47	0.07	0.23	0.05	1.03409E-07
	*PTHR1_P258_F	N	0.65	0.07	0.90	0.04	0.93	0.02	1.54614E-07
	*VAMP8_P114_F	N	0.79	0.03	0.51	0.07	0.74	0.03	1.54859E-07
	MAPK4_E273_R	N	0.99	0.00	0.65	0.10	0.91	0.04	1.60541E-07
	PLG_E406_F	N	0.50	0.17	0.99	0.01	0.99	0.00	1.61043E-07
	MAP2K6_P297_R	Y	0.46	0.05	0.16	0.03	0.20	0.07	1.73846E-07
	*NOTCH4_E4_F	N	0.88	0.07	0.69	0.11	0.22	0.16	2.02324E-07

Supplementary Table 3.3. Tissue-specific differentially methylated loci in normal fetal and adult tissues

			Brain		Kidney		Lung		ANOVA
Stage	**Feature ID**	**CGI**	**Mean**	**SD**	**Mean**	**SD**	**Mean**	**SD**	***p* value**
	*CCKAR_E79_F	N	0.17	0.14	0.10	0.05	0.73	0.14	2.06322E-07
	ZAP70_P220_R	N	0.94	0.02	0.72	0.07	0.94	0.03	3.11561E-07
	BLK_P14_F	N	0.45	0.19	0.98	0.01	0.98	0.01	3.3188E-07
	HDAC9_P137_R	N	0.05	0.04	0.01	0.02	0.30	0.09	3.7434E-07
	MEST_E150_F	Y	0.28	0.12	0.75	0.06	0.58	0.07	4.01871E-07
	*PYCARD_P393_F	N	0.77	0.04	0.73	0.02	0.58	0.04	5.77277E-07
	RAB32_P493_R	Y	0.77	0.14	0.48	0.05	0.27	0.08	9.53574E-07
	MEST_P62_R	Y	0.26	0.06	0.77	0.14	0.61	0.09	1.11125E-06
	*THBS2_P605_R	N	0.97	0.02	0.55	0.08	0.47	0.16	1.28163E-06
	DLC1_P695_F	N	0.99	0.01	0.99	0.00	0.89	0.04	1.35378E-06
	MST1R_P87_R	Y	0.84	0.05	0.77	0.04	0.52	0.10	1.40084E-06
	*WRN_P969_F	Y	0.39	0.18	0.76	0.04	0.92	0.03	1.41694E-06
	CPA4_E20_F	N	0.94	0.03	0.94	0.02	0.75	0.07	1.44316E-06
	*PRKCDBP_E206_F	Y	0.08	0.03	0.00	0.00	0.01	0.02	2.11803E-06
	CSF3_P309_R	N	0.35	0.12	0.74	0.06	0.59	0.04	2.56769E-06
	FRK_P36_F	N	0.99	0.00	0.91	0.07	0.44	0.20	2.69633E-06
	*SPDEF_P6_R	N	0.88	0.05	0.64	0.06	0.66	0.06	2.9193E-06
	*IL8_E118_R	N	0.97	0.02	0.99	0.00	0.42	0.24	3.09912E-06
	ACTG2_P346_F	N	0.96	0.03	0.97	0.01	0.85	0.04	3.18262E-06
	CSF2_P605_F	N	0.99	0.01	0.97	0.02	0.89	0.03	3.80231E-06
	DLC1_P88_R	N	0.97	0.02	0.72	0.12	0.30	0.23	3.95807E-06
	*MPO_P883_R	N	0.85	0.05	0.78	0.04	0.58	0.08	4.02927E-06
	MAD2L1_E93_F	Y	0.87	0.02	0.81	0.03	0.89	0.01	4.06192E-06
	HDAC1_P414_R	Y	0.95	0.02	0.80	0.05	0.93	0.03	4.44984E-06
	SPP1_P647_F	N	0.91	0.04	0.80	0.03	0.93	0.03	4.48799E-06
	BCR_P346_F	Y	0.82	0.11	0.39	0.08	0.76	0.11	4.65558E-06
	SRC_E100_R	N	0.99	0.01	0.91	0.02	0.91	0.02	4.74637E-06
	*CASP10_E139_F	N	0.98	0.02	0.60	0.05	0.68	0.14	4.98921E-06
	TGFB3_E58_R	N	0.88	0.08	0.64	0.09	0.46	0.11	5.95661E-06
	*HTR2A_E10_R	N	0.59	0.18	0.99	0.00	0.99	0.00	6.09759E-06
	TNFSF10_E53_F	N	0.31	0.09	0.21	0.07	0.59	0.10	6.41022E-06
	GP1BB_E23_F	Y	0.46	0.11	0.19	0.07	0.58	0.09	7.5239E-06
	IGF1_P933_F	N	0.61	0.15	0.74	0.04	0.33	0.07	1.07709E-05
	SRC_P164_F	N	0.96	0.01	0.91	0.02	0.91	0.02	1.37586E-05
	UGT1A1_P315_R	N	0.65	0.16	0.99	0.00	0.97	0.02	1.65744E-05
	FGF6_P139_R	Y	0.99	0.00	0.89	0.05	0.99	0.00	1.67632E-05
	MMP10_E136_R	N	0.44	0.11	0.72	0.04	0.71	0.07	1.77554E-05

Supplementary Table 3.3. Tissue-specific differentially methylated loci in normal fetal and adult tissues

			Brain		Kidney		Lung		ANOVA
Stage	**Feature ID**	**CGI**	**Mean**	**SD**	**Mean**	**SD**	**Mean**	**SD**	***p* value**
	MPL_P657_F	N	0.20	0.18	0.44	0.13	0.76	0.10	1.78135E-05
	*HDAC7A_P344_F	N	0.81	0.09	0.99	0.00	0.99	0.00	1.89964E-05
	CTGF_P693_R	N	0.97	0.05	0.85	0.05	0.67	0.11	1.9297E-05
	ASB4_P52_R	N	0.99	0.00	0.59	0.16	0.77	0.06	1.95083E-05
	CCKAR_P270_F	N	0.40	0.28	0.96	0.04	0.98	0.01	2.02498E-05
	ZNFN1A1_E102_F	Y	0.80	0.10	0.98	0.01	0.99	0.01	2.5732E-05
	LRRK1_P834_F	N	0.87	0.06	0.86	0.03	0.62	0.11	2.75636E-05
	AREG_P217_R	Y	0.49	0.06	0.31	0.05	0.30	0.06	2.83482E-05
	SFTPB_P689_R	N	0.94	0.02	0.96	0.02	0.86	0.04	3.28488E-05
	FGF7_P44_F	N	0.42	0.26	0.92	0.01	0.91	0.04	3.36433E-05
	*DDR1_P332_R	N	0.01	0.01	0.12	0.10	0.38	0.15	3.82735E-05
	SERPINA5_P156_F	N	0.61	0.08	0.16	0.13	0.34	0.15	4.03793E-05
	ASB4_E89_F	N	0.99	0.00	0.83	0.08	0.97	0.01	4.09699E-05
	KRT1_P798_R	N	0.97	0.01	0.97	0.01	0.90	0.03	4.1004E-05
	INS_P248_F	N	0.97	0.03	0.81	0.06	0.91	0.04	4.1506E-05
	*NNAT_P544_R	Y	0.87	0.02	0.94	0.02	0.90	0.02	4.17063E-05
	*PIK3R1_P307_F	N	0.73	0.14	0.99	0.00	0.99	0.00	4.74398E-05
	KLK10_P268_R	N	0.58	0.07	0.75	0.05	0.53	0.07	5.14423E-05
	PDGFA_P78_F	Y	0.24	0.05	0.47	0.08	0.36	0.04	5.29117E-05
Adult	TNFRSF10D_P70_F	Y	0.74	0.09	0.03	0.01	0.05	0.03	3.36348E-13
	MST1R_P392_F	Y	0.82	0.08	0.10	0.10	0.08	0.03	1.80431E-11
	*CEACAM1_E57_R	N	0.74	0.09	0.10	0.05	0.09	0.06	2.34435E-11
	MST1R_E42_R	Y	0.89	0.04	0.86	0.02	0.49	0.06	3.98474E-11
	*CASP10_E139_F	N	0.59	0.10	0.03	0.02	0.07	0.04	7.72887E-11
	*RARA_P1076_R	N	0.82	0.07	0.53	0.07	0.17	0.09	1.46269E-09
	EYA4_P794_F	Y	0.70	0.08	0.17	0.07	0.14	0.07	1.59655E-09
	*CASP10_P334_F	N	0.75	0.09	0.16	0.12	0.12	0.07	4.39413E-09
	BMP4_P123_R	Y	0.52	0.09	0.14	0.05	0.13	0.02	1.65006E-08
	CSF1_P339_F	Y	0.30	0.08	0.00	0.00	0.01	0.01	1.68014E-08
	HLA-DPB1_E2_R	N	0.88	0.05	0.36	0.16	0.20	0.08	2.37459E-08
	*SPDEF_P6_R	N	0.83	0.05	0.66	0.04	0.46	0.07	2.45852E-08
	SHB_P691_R	Y	0.42	0.09	0.03	0.02	0.11	0.06	3.06817E-08
	FGF1_P357_R	N	0.42	0.11	0.86	0.04	0.85	0.06	4.347E-08
	*CSF3R_P8_F	N	0.86	0.10	0.56	0.06	0.29	0.09	4.38761E-08
	TNFRSF10A_P171_F	Y	0.34	0.08	0.03	0.06	0.02	0.02	4.89965E-08
	HLA-DPA1_P205_R	N	0.77	0.05	0.68	0.08	0.31	0.09	5.4486E-08
	CDK2_P330_R	N	0.33	0.10	0.01	0.02	0.00	0.00	8.47771E-08

Supplementary Table 3.3. Tissue-specific differentially methylated loci in normal fetal and adult tissues

			Brain		Kidney		Lung		ANOVA
Stage	**Feature ID**	**CGI**	**Mean**	**SD**	**Mean**	**SD**	**Mean**	**SD**	***p* value**
	S100A4_E315_F	N	0.94	0.02	0.76	0.07	0.36	0.15	1.10322E-07
	CASP10_P186_F	N	0.72	0.18	0.07	0.08	0.09	0.07	1.17657E-07
	MKRN3_P108_F	N	0.84	0.05	0.99	0.00	0.98	0.01	1.22699E-07
	RAD50_P191_F	Y	0.23	0.09	0.57	0.12	0.78	0.06	1.26016E-07
	RIPK3_P124_F	N	0.92	0.01	0.79	0.08	0.39	0.14	1.54734E-07
	TNFRSF10A_P91_F	Y	0.31	0.08	0.02	0.05	0.02	0.03	3.53011E-07
	*IL6_P213_R	N	0.50	0.12	0.08	0.07	0.09	0.03	4.05076E-07
	DNAJC15_P65_F	Y	0.47	0.10	0.84	0.11	0.95	0.04	4.11151E-07
	FGFR2_P460_R	Y	0.53	0.07	0.14	0.12	0.17	0.03	5.38071E-07
	CARD15_P302_R	N	0.80	0.08	0.46	0.14	0.23	0.09	6.04426E-07
	*DDR1_P332_R	N	0.42	0.07	0.49	0.14	0.89	0.04	6.98272E-07
	SOD3_P460_R	N	0.69	0.03	0.94	0.02	0.86	0.08	9.91889E-07
	TMPRSS4_P552_F	N	0.98	0.01	0.96	0.02	0.89	0.02	1.29709E-06
	*WRN_P969_F	Y	0.48	0.18	0.93	0.03	0.96	0.03	1.30247E-06
	*THBS2_P605_R	N	0.82	0.04	0.47	0.13	0.31	0.12	1.48527E-06
	TNFRSF10D_E27_F	Y	0.35	0.13	0.01	0.00	0.01	0.01	1.95251E-06
	HOXA5_P1324_F	Y	0.02	0.02	0.26	0.05	0.16	0.06	2.08844E-06
	HLA-DPA1_P28_R	N	0.80	0.09	0.42	0.20	0.16	0.06	2.11977E-06
	*PYCARD_P393_F	N	0.40	0.05	0.35	0.08	0.12	0.04	2.27864E-06
	HOXA11_P698_F	Y	0.18	0.11	0.49	0.09	0.08	0.06	3.054E-06
	*HDAC7A_P344_F	N	0.63	0.14	0.96	0.01	0.96	0.03	3.14158E-06
	UGT1A1_P564_R	N	0.86	0.05	0.97	0.01	0.98	0.01	4.0071E-06
	PTHLH_P15_R	N	0.95	0.02	0.87	0.06	0.63	0.11	4.33638E-06
	*VAMP8_E7_F	N	0.83	0.05	0.53	0.17	0.34	0.07	4.69861E-06
	EPHA5_P66_F	Y	0.12	0.07	0.51	0.15	0.50	0.02	4.83834E-06
	STAT5A_E42_F	N	0.60	0.09	0.38	0.08	0.21	0.09	5.15623E-06
	*PRKCDBP_E206_F	Y	0.36	0.13	0.05	0.05	0.01	0.02	5.56334E-06
	*PTHR1_P258_F	N	0.87	0.07	0.45	0.14	0.72	0.06	6.22111E-06
	*SEPT9_P374_F	Y	0.75	0.04	0.56	0.20	0.18	0.09	6.47591E-06
	ICAM1_P386_R	Y	0.43	0.12	0.16	0.10	0.03	0.05	7.18535E-06
	PTCH2_E173_F	Y	0.10	0.04	0.23	0.08	0.39	0.08	8.15143E-06
	*IL8_E118_R	N	0.69	0.12	0.47	0.21	0.05	0.09	8.6181E-06
	*MPO_P883_R	N	0.67	0.07	0.36	0.21	0.10	0.07	9.71424E-06
	*CCKAR_E79_F	N	0.65	0.15	0.25	0.22	0.91	0.05	9.96775E-06
	IL1RN_E42_F	N	0.99	0.00	0.89	0.03	0.95	0.02	1.07368E-05
	SHB_P473_R	Y	0.08	0.04	0.00	0.00	0.00	0.01	1.24075E-05
	SLC22A18_P216_R	N	0.88	0.06	0.79	0.06	0.47	0.16	1.29257E-05

Supplementary Table 3.3. Tissue-specific differentially methylated loci in normal fetal and adult tissues

			Brain		Kidney		Lung		ANOVA
Stage	**Feature ID**	**CGI**	**Mean**	**SD**	**Mean**	**SD**	**Mean**	**SD**	***p* value**
	POMC_P400_R	Y	0.73	0.13	0.46	0.16	0.19	0.09	1.38997E-05
	CTSD_P726_F	Y	0.29	0.12	0.66	0.08	0.56	0.06	1.42284E-05
	MMP2_P303_R	Y	0.45	0.17	0.17	0.06	0.03	0.02	1.47758E-05
	IRF7_E236_R	Y	0.32	0.08	0.08	0.06	0.11	0.04	1.47863E-05
	CEACAM1_P44_R	N	0.93	0.03	0.65	0.12	0.47	0.15	1.53488E-05
	*S100A2_E36_R	N	0.91	0.04	0.60	0.18	0.44	0.07	1.5406E-05
	KRT13_P676_F	N	0.95	0.03	0.91	0.04	0.83	0.01	1.57811E-05
	ZP3_P220_F	N	0.75	0.05	0.88	0.02	0.87	0.02	1.58545E-05
	*NNAT_P544_R	Y	0.84	0.01	0.94	0.04	0.95	0.03	1.58939E-05
	PECAM1_E32_R	Y	0.91	0.04	0.87	0.06	0.51	0.17	1.73817E-05
	PTHLH_E251_F	N	0.71	0.07	0.45	0.10	0.41	0.07	1.97686E-05
	IL18BP_P51_R	N	0.79	0.09	0.70	0.24	0.20	0.11	2.27466E-05
	*VAMP8_P114_F	N	0.81	0.04	0.45	0.12	0.41	0.14	2.28115E-05
	SH3BP2_P771_R	Y	0.12	0.11	0.43	0.10	0.11	0.06	2.33836E-05
	*PIK3R1_P307_F	N	0.68	0.12	0.96	0.02	0.92	0.04	2.49519E-05
	TIE1_E66_R	N	0.93	0.03	0.85	0.06	0.54	0.17	2.8007E-05
	*HTR2A_E10_R	N	0.65	0.13	0.92	0.06	0.95	0.02	2.80838E-05
	*NOTCH4_E4_F	N	0.76	0.12	0.52	0.18	0.17	0.16	2.96012E-05
	ALOX12_E85_R	Y	0.33	0.10	0.57	0.15	0.78	0.04	3.01041E-05
	PECAM1_P135_F	Y	0.91	0.05	0.80	0.05	0.51	0.17	3.11722E-05
	CCL3_P543_R	N	0.99	0.01	0.92	0.03	0.98	0.01	3.34116E-05
	MKRN3_E144_F	Y	0.86	0.06	0.99	0.00	0.98	0.02	3.85033E-05
	GLI2_P295_F	Y	0.97	0.02	0.85	0.05	0.94	0.02	4.04581E-05
	HOXB2_P488_R	N	0.45	0.09	0.70	0.07	0.73	0.08	4.10335E-05
	APBA2_P305_R	N	0.99	0.00	0.92	0.03	0.97	0.01	4.46724E-05
	PTPN6_E171_R	Y	0.56	0.10	0.10	0.07	0.56	0.21	4.51675E-05
	PRKCDBP_P352_R	Y	0.70	0.08	0.38	0.26	0.10	0.04	4.66356E-05

*Loci common in fetal and adult stage

Supplementary Table 3.4. Loci demonstrating age-dependent differential methylation between normal fetal and adult tissues

		Fetal		Adult		
Tissue	**Feature ID**	**Mean**	**SD**	**Mean**	**SD**	**Difference**
Brain	ACVR1_P983_F	0.27	0.12	0.82	0.09	0.56
	ALOX12_P223_R	0.11	0.05	0.56	0.24	0.45
	BMP4_P123_R	0.06	0.06	0.52	0.09	0.46
	BMP4_P199_R	0.14	0.11	0.75	0.07	0.61
	CCKAR_E79_F	0.17	0.14	0.65	0.15	0.48
	CCKAR_P270_F	0.40	0.28	0.85	0.08	0.45
	DDR1_P332_R	0.01	0.01	0.42	0.07	0.41
	EYA4_P794_F	0.09	0.15	0.70	0.08	0.61
	FGF7_P44_F	0.42	0.26	0.91	0.04	0.49
	GFI1_P208_R	0.04	0.04	0.91	0.05	0.86
	MMP14_P13_F	0.21	0.09	0.67	0.08	0.46
	MT1A_P600_F	0.14	0.17	0.73	0.03	0.59
	POMC_P400_R	0.04	0.04	0.73	0.13	0.68
	PTPN6_E171_R	0.06	0.06	0.56	0.10	0.51
	RIPK3_P124_F	0.45	0.12	0.92	0.01	0.47
	TDGF1_E53_R	0.40	0.11	0.84	0.05	0.44
	TNFRSF10D_P70_F	0.21	0.14	0.74	0.09	0.53
	APC_E117_R	0.66	0.08	0.13	0.04	-0.53
	BCR_P346_F	0.82	0.11	0.23	0.13	-0.59
	CPA4_E20_F	0.94	0.03	0.53	0.18	-0.41
	CSF1R_P73_F	0.89	0.02	0.46	0.17	-0.43
	CTSD_P726_F	0.92	0.08	0.29	0.12	-0.63
	DDB2_P613_R	0.62	0.10	0.12	0.10	-0.50
	DNAJC15_P65_F	0.89	0.08	0.47	0.10	-0.42
	E2F5_P516_R	0.60	0.15	0.19	0.07	-0.41
	ELL_P693_F	0.79	0.11	0.05	0.05	-0.74
	GABRB3_P92_F	0.57	0.07	0.07	0.01	-0.49
	GADD45A_P737_R	0.45	0.13	0.04	0.02	-0.41
	IGF1_E394_F	0.90	0.08	0.32	0.10	-0.58
	IGF1_P933_F	0.61	0.15	0.15	0.05	-0.46
	MAPK10_E26_F	0.97	0.03	0.57	0.12	-0.40
	NFKB1_P496_F	0.50	0.03	0.04	0.03	-0.46
	PEG3_E496_F	0.95	0.03	0.49	0.16	-0.47
	RAB32_P493_R	0.77	0.14	0.33	0.17	-0.44
	RYK_P493_F	0.50	0.16	0.00	0.01	-0.49
	SPI1_E205_F	0.90	0.04	0.45	0.14	-0.44
	TSC2_E140_F	0.91	0.07	0.34	0.14	-0.57
	ZNF264_P397_F	0.65	0.34	0.15	0.11	-0.50
Kidney	ALOX12_E85_R	0.00	0.00	0.57	0.15	0.57

Supplementary Table 3.4. Loci demonstrating age-dependent differential methylation between normal fetal and adult tissues

		Fetal		Adult		
Tissue	**Feature ID**	**Mean**	**SD**	**Mean**	**SD**	**Difference**
	ALOX12_P223_R	0.12	0.04	0.59	0.14	0.47
	APOA1_P261_F	0.34	0.09	0.77	0.13	0.43
	CREBBP_P712_R	0.52	0.13	0.92	0.04	0.40
	GFI1_P208_R	0.07	0.06	0.67	0.08	0.60
	HPN_P374_R	0.11	0.08	0.66	0.14	0.55
	HPN_P823_F	0.17	0.10	0.90	0.02	0.73
	KCNK4_P171_R	0.16	0.13	0.58	0.07	0.42
	LY6G6E_P45_R	0.21	0.09	0.66	0.15	0.45
	NPY_P295_F	0.04	0.04	0.50	0.24	0.46
	APC_E117_R	0.63	0.04	0.13	0.04	-0.50
	ARHGDIB_P148_R	0.92	0.05	0.47	0.26	-0.44
	CARD15_P302_R	0.96	0.04	0.46	0.14	-0.50
	CASP10_E139_F	0.60	0.05	0.03	0.02	-0.58
	CASP10_P186_F	0.57	0.13	0.07	0.08	-0.50
	CASP10_P334_F	0.82	0.06	0.16	0.12	-0.66
	CPA4_E20_F	0.94	0.02	0.50	0.16	-0.44
	CRK_P721_F	0.82	0.06	0.42	0.14	-0.41
	DDB2_P613_R	0.69	0.07	0.23	0.24	-0.46
	EFNB3_E17_R	0.74	0.05	0.33	0.05	-0.41
	ELL_P693_F	0.73	0.12	0.32	0.15	-0.42
	GABRB3_P92_F	0.55	0.04	0.09	0.03	-0.46
	HDAC1_P414_R	0.80	0.05	0.28	0.15	-0.52
	HLA-DPA1_P28_R	0.97	0.01	0.42	0.20	-0.55
	HLA-DPB1_E2_R	0.87	0.07	0.36	0.16	-0.50
	HLA-DRA_P77_R	0.89	0.04	0.36	0.18	-0.52
	IGF1_E394_F	0.89	0.03	0.43	0.25	-0.46
	IL6_P213_R	0.81	0.08	0.08	0.07	-0.73
	IL8_E118_R	0.99	0.00	0.47	0.21	-0.52
	MPO_P883_R	0.78	0.04	0.36	0.21	-0.42
	NFKB1_P496_F	0.69	0.10	0.11	0.15	-0.58
	PEG3_E496_F	0.92	0.04	0.50	0.13	-0.41
	PTHR1_P258_F	0.90	0.04	0.45	0.14	-0.45
	PYCARD_P150_F	0.91	0.03	0.41	0.13	-0.51
	RYK_P493_F	0.58	0.10	0.14	0.20	-0.43
	STAT5A_E42_F	0.93	0.04	0.38	0.08	-0.55
	TNFSF10_P2_R	0.95	0.04	0.28	0.22	-0.67
Lung	ALOX12_E85_R	0.01	0.02	0.78	0.04	0.77
	ALOX12_P223_R	0.08	0.01	0.69	0.07	0.61
	DDR1_P332_R	0.38	0.15	0.89	0.04	0.51
	HOXA5_E187_F	0.19	0.12	0.75	0.12	0.56

Supplementary Table 3.4. Loci demonstrating age-dependent differential methylation between normal fetal and adult tissues

		Fetal		Adult		
Tissue	**Feature ID**	**Mean**	**SD**	**Mean**	**SD**	**Difference**
	HOXB2_P488_R	0.32	0.06	0.73	0.08	0.40
	HPN_P823_F	0.40	0.13	0.82	0.09	0.42
	PTPN6_E171_R	0.08	0.09	0.56	0.21	0.48
	RAD50_P191_F	0.33	0.04	0.78	0.06	0.46
	TGFB3_E58_R	0.46	0.11	0.87	0.05	0.41
	APC_E117_R	0.68	0.04	0.12	0.04	-0.56
	ARHGDIB_P148_R	0.94	0.03	0.40	0.10	-0.54
	CAPG_E228_F	0.85	0.11	0.35	0.18	-0.50
	CARD15_P302_R	0.92	0.05	0.23	0.09	-0.69
	CASP10_E139_F	0.68	0.14	0.07	0.04	-0.61
	CASP10_P186_F	0.49	0.22	0.09	0.07	-0.40
	CASP8_E474_F	0.88	0.03	0.37	0.15	-0.51
	CD34_P780_R	0.91	0.03	0.42	0.14	-0.49
	CEACAM1_E57_R	0.54	0.06	0.09	0.06	-0.45
	CEACAM1_P44_R	0.98	0.01	0.47	0.15	-0.51
	EFNB3_E17_R	0.76	0.05	0.34	0.04	-0.42
	ERN1_P809_R	0.75	0.05	0.25	0.07	-0.50
	GABRB3_P92_F	0.61	0.04	0.09	0.02	-0.53
	HDAC1_P414_R	0.93	0.03	0.40	0.06	-0.53
	HLA-DPA1_P205_R	0.83	0.03	0.31	0.09	-0.52
	HLA-DPA1_P28_R	0.95	0.03	0.16	0.06	-0.79
	HLA-DPB1_E2_R	0.98	0.01	0.20	0.08	-0.78
	HLA-DRA_P77_R	0.71	0.06	0.14	0.07	-0.57
	IL18BP_P51_R	0.88	0.02	0.20	0.11	-0.68
	IL8_P83_F	0.99	0.00	0.49	0.25	-0.50
	KLK10_P268_R	0.53	0.07	0.10	0.02	-0.43
	LTB4R_E64_R	0.98	0.01	0.52	0.14	-0.46
	MPO_P883_R	0.58	0.08	0.10	0.07	-0.48
	PECAM1_E32_R	0.98	0.02	0.51	0.17	-0.47
	PECAM1_P135_F	0.98	0.01	0.51	0.17	-0.47
	PEG3_E496_F	0.95	0.03	0.53	0.06	-0.42
	PYCARD_P150_F	0.92	0.03	0.41	0.17	-0.51
	PYCARD_P393_F	0.58	0.04	0.12	0.04	-0.46
	S100A2_E36_R	0.89	0.02	0.44	0.07	-0.45
	SEPT9_P374_F	0.69	0.03	0.18	0.09	-0.51
	SLC22A18_P216_R	0.97	0.02	0.47	0.16	-0.50
	SPI1_E205_F	0.89	0.05	0.45	0.21	-0.45
	STAT5A_E42_F	0.82	0.05	0.21	0.09	-0.61
	TNFSF10_E53_F	0.59	0.10	0.12	0.10	-0.47
	TNFSF10_P2_R	0.99	0.00	0.39	0.21	-0.60

Supplementary Table 3.4. Loci demonstrating age-dependent differential methylation between normal fetal and adult tissues

		Fetal		Adult		
Tissue	**Feature ID**	**Mean**	**SD**	**Mean**	**SD**	**Difference**
	TRIP6_P1090_F	0.99	0.00	0.53	0.21	-0.46
	TRIP6_P1274_R	0.99	0.01	0.47	0.20	-0.51
	VAV1_E9_F	0.89	0.02	0.47	0.23	-0.42

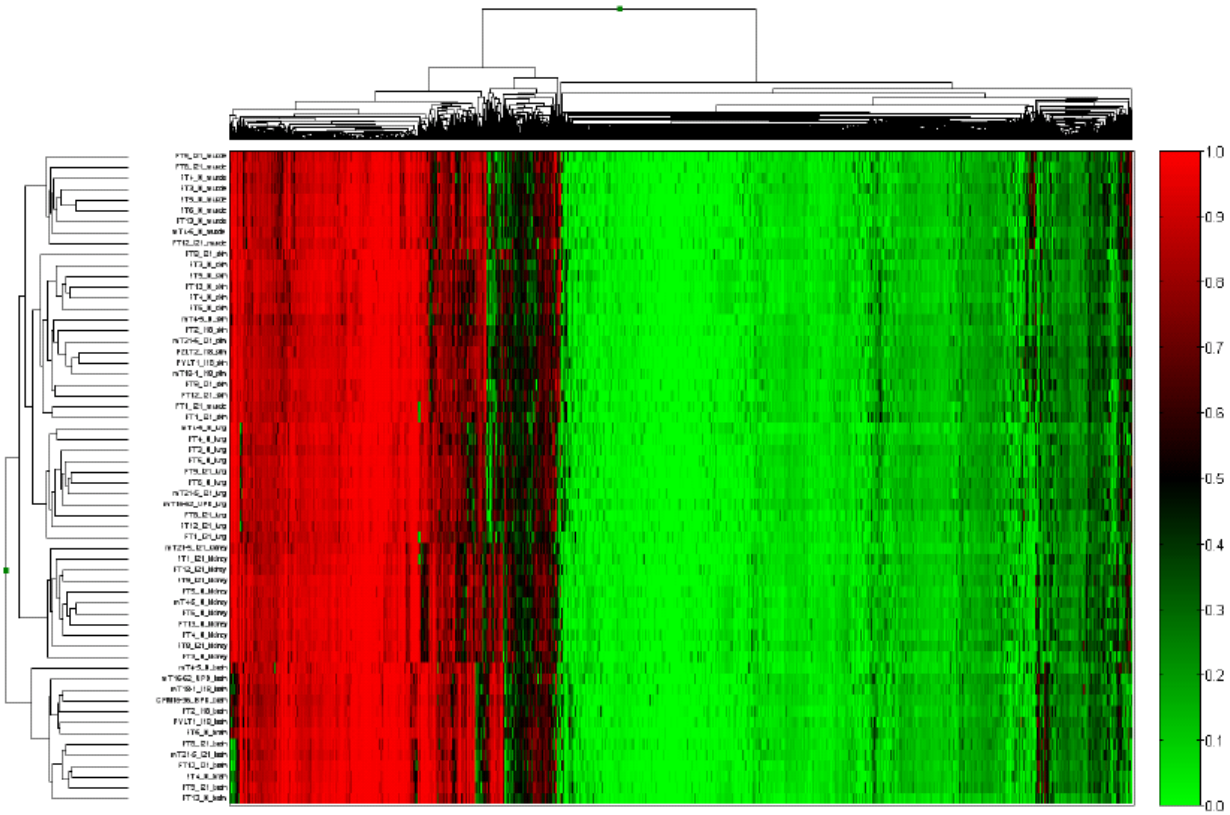

Supplementary Figure 3.1. Heat-map of the methylation array data.

Hierarchical clustering of CpGs (columns) and samples (rows) is based on 1-r of the β values (Illumina Beadstudio software). A beta value of zero (indicated in bright green) represents an unmethylated locus and one (indicated in bright red) represents a methylated locus.

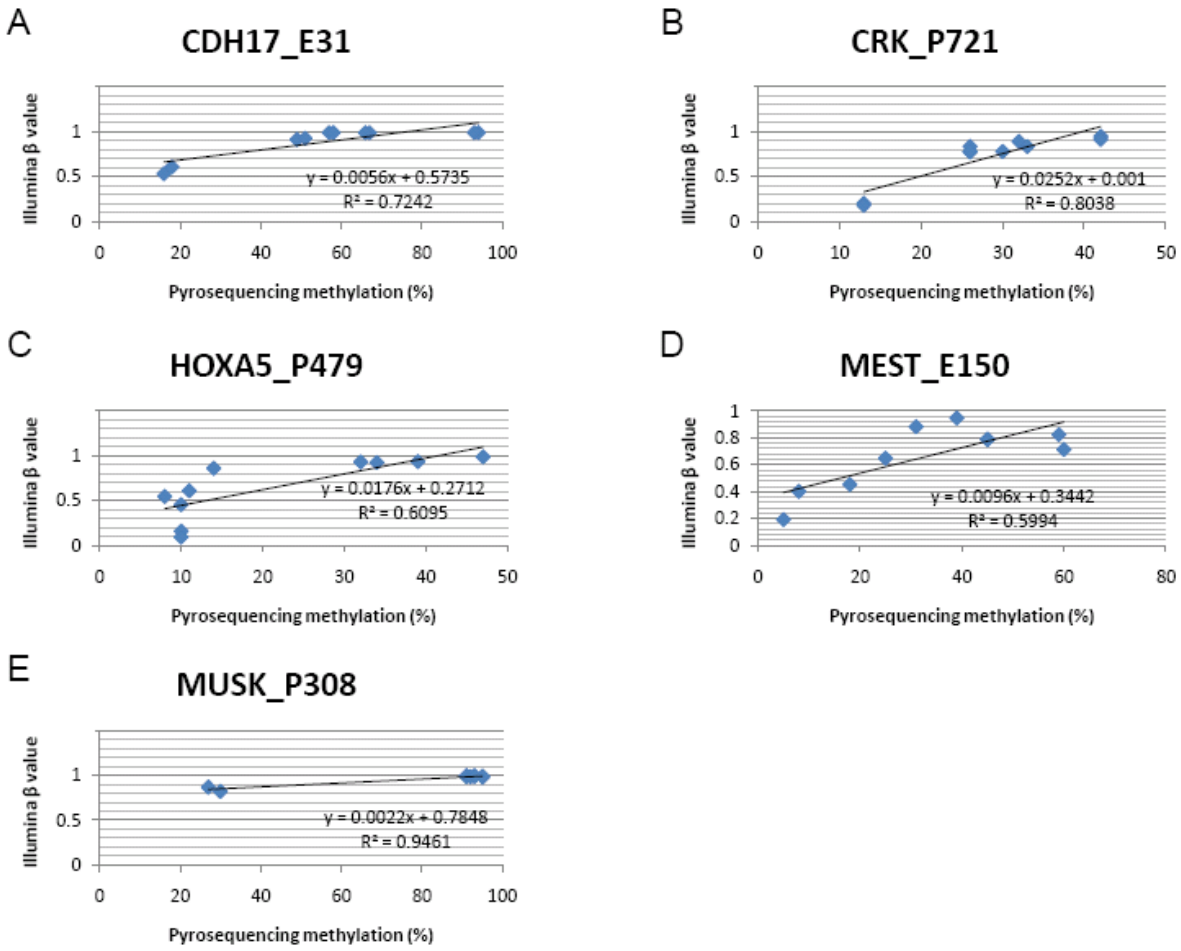

Supplementary Figure 3.2. Correlations of DNA methylation measurements between Illumina methylation array and bisulfite pyrosequencing.

Methylation level (β value) measured by Illumina methylation array is plotted against methylation level measured by bisulfite pyrosequencing for (A) CDH17_E31, (B) CRK_P721, (C) HOXA5_P479, (D) MEST_P150 and (E) MUSK_P308. Linear trendline and R^2 are shown for each comparison. Values for all 5 loci are significantly correlated (p<0.005).

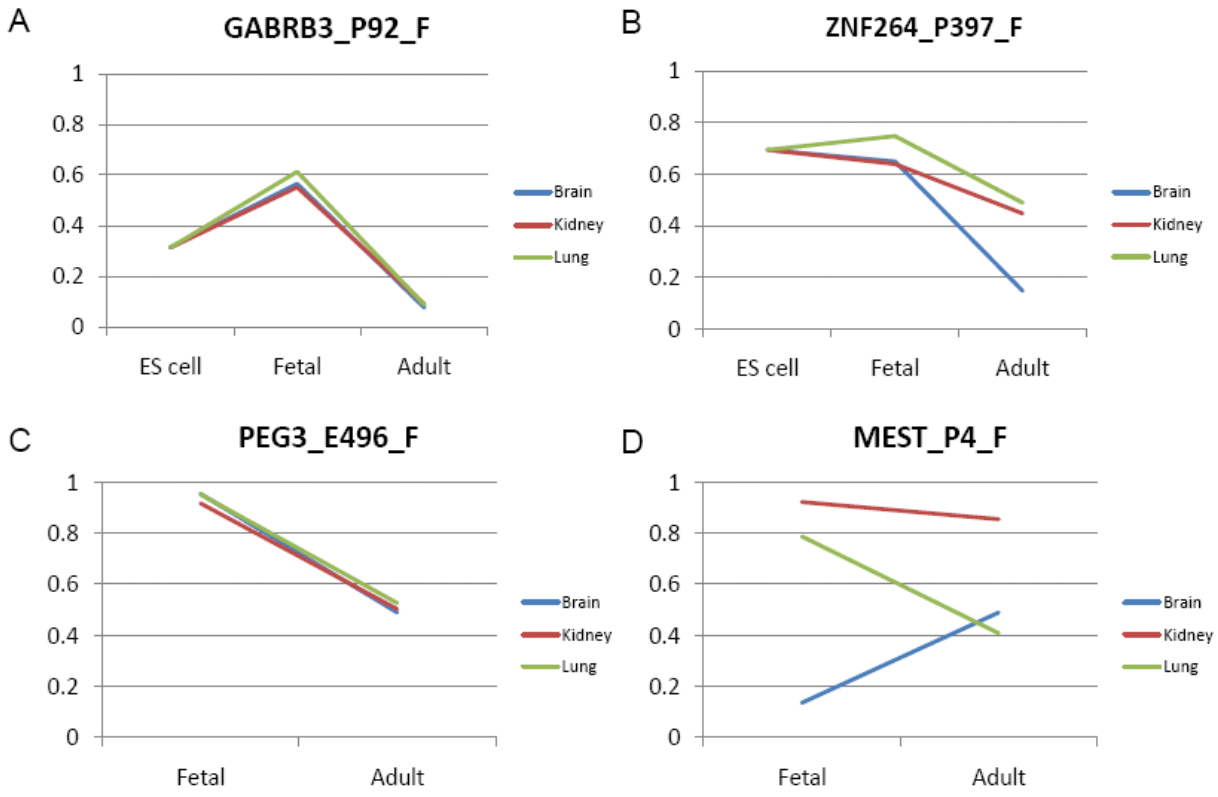

Supplementary Figure 3.3. Graphs representing different patterns of age-dependent differentially methylation at sites associated with imprinted genes.

Average methylation level (β value) is given for (A) GABRB3_P92, (B) ZNF264_P397 in ES cell, fetal and adult tissues, (C) PEG3_E496 and (D) MEST_P4 in fetal and adult tissues. In some cases changes occur in different tissues concordantly over time (e.g. GABRB3_P92_F and PEG_E496_F) while for others the changes are tissue specific (e.g. MEST_P4_F).

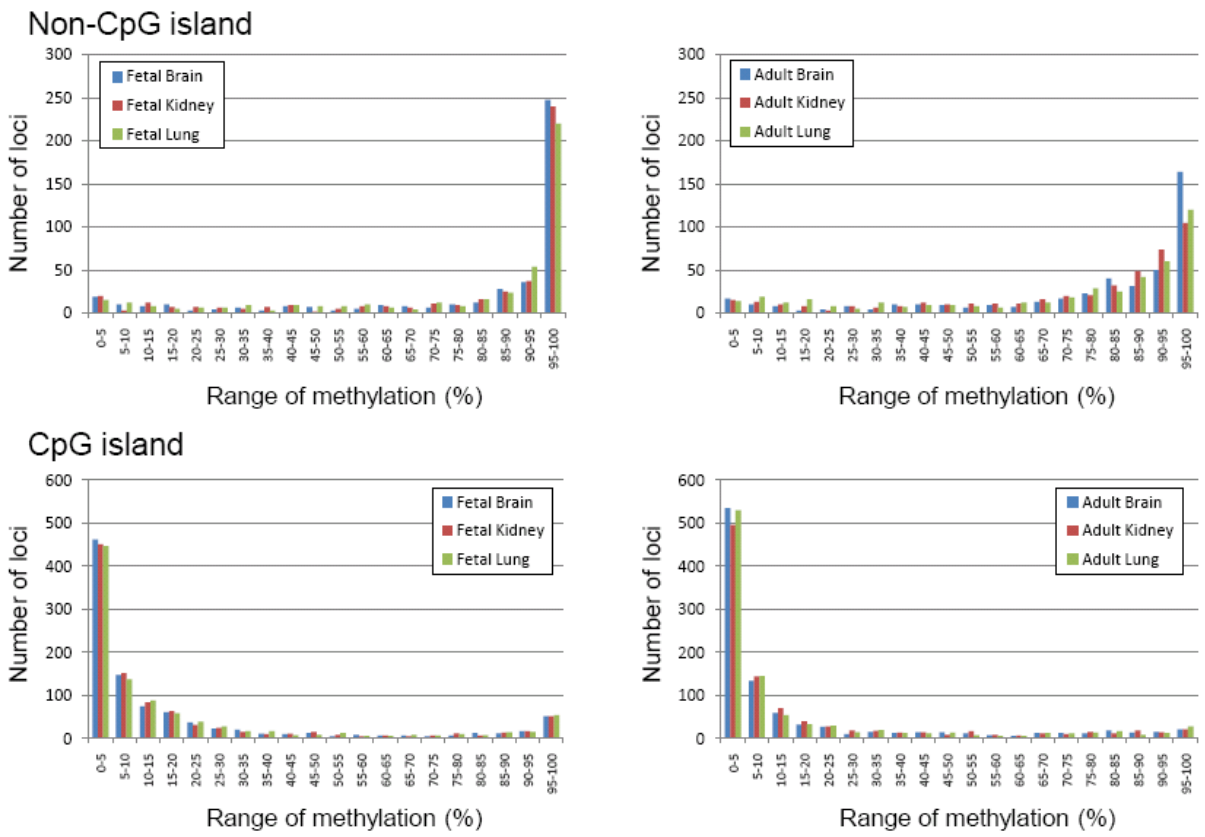

Supplementary Figure 3.4. DNA methylation distribution of all CpG loci in fetal and adult tissues.

The number of CpG sites (y-axis) for a given methylation range (X-axis) is given for brain, kidney and lung considering (A) non-CpG island in fetus, (B) non-CpG island in adult, (C) CpG island in fetus and (D) CpG island in adult.

Appendix 3: Supplementary tables and figures for Chapter 4

Supplementary Table 4.1. PCR Primers and conditions

Primers for bisulfite pyrosequencing

Gene	Primer	Sequence (5' to 3')	Annealing temperature (°C)	Product length (bp)
EPHB4	Forward	GGYGAGGGTTTTTTAAATTTAGT	50	113
	Reverse	(5' biotinated)-AAAAACTCACCTTCCAAAACTAC		
	Sequencing	GGYGAGGGTTTTTTAAAT		
TUSC3	Forward	TAATTGGGTTTAGTAGTAGGATGGTT	50	218
	Reverse	(5' biotinated)-CAAAAAAAAAAACTAACAAAACATCC		
	Sequencing	TTTAGGGTTAAAGGATTAT		
WNT2	Forward	AAGTAATGAGTTGAGAATTATTTTTGGATT	50	195
	Reverse	(5' biotinated)-AAAACCTTTAAAAAAACTCCAAACC		
	Sequencing	TTAGGGATTTGTTTGTTAG		
MKRN3	Forward	TTTTTTGTTAATGTTTTGTTGGTGA	50	179
	Reverse	(5' biotinated)-CTTTTTTTATTCACTCCATCTTATATCTA		
	Sequencing	TTTAGAAATTTTAGAAAATA		
NOD2	Forward	TGATGTAGTTGTTGGGAGGATAGA	50	144
	Reverse	(5' biotinated)-TTACACACCAAACCTAAAACAACC		
	Sequencing	TTGTTGGGAGGATAGAG		
ID2	Forward	ATTTATTGTATTGTATTTTATTTATTATTTTAGTTGGGT	57	178
	Reverse	(5' biotinated)-ACTTCCCTTCRTCCCCATTAA		
	Sequencing	ATTTATTATTTTAGTTGGGT		
Ephb4	Forward	TAGATTTGGGGGGGTTAGGGTTT	50	135
	Reverse	(5' biotinated)-AACACCCCAAAAAAACTCACCTTCT		
	Sequencing	GGGTTAGGGTTTTTTAAAT		
Tusc3	Forward	GTTAGAGGTGAAAGTAAGGGGTTATTT	50	251
	Reverse	(5' biotinated)-AACAACCTCTCCTAACCAAAACCT		
	Sequencing	GGTTATTTTTTGATGTTTG		
Wnt2	Forward	TGTGTATTATTGGTTAGGAATTTTTTAAA	50	280
	Reverse	(5' biotinated)-AACCAATTCCCCAAACACTA		
	Sequencing	TTTTTTTTATTTTTTAATAAAATT		

Supplementary Table 4.1. PCR Primers and conditions

Primers for *Bst*UI pre-digestion PCR

Gene	Primer	Sequence (5' to 3')	Annealing temperature (°C)	Product length (bp)
ID2	Forward	CCAGCCCCGCACTTACTGT	56	226
	Reverse	GCGGCTTTTATCCGCACTC		
TUSC3	Forward	GGTGAACCGGATGCTCTGTC	56	186
	Reverse	(5' biotinated)-CGGCAGGGCAGTGTCTCC		
	Sequencing	GGGTCCCTCGCAAAG		

Primers for Reverse Transcription PCR

Gene	Primer	Sequence (5' to 3')	Annealing temperature (°C)	Product length (bp)
TUSC3	Forward	AGTCTCCTCCTCTGCGTCCT	60	337
	Reverse	(5' biotinated)-TCAGCTGCTCTACTTTTTCAGC		
	Sequencing	GGGTCCCTCGCAAAG		
EPHB4	Forward	AGGAACATCACAGCCAGACC	60	303
	Reverse	CTGCACCAATCACCTCTTCA		
WNT2	Forward	CTGTATCAGGGACCGAGAGG	60	475
	Reverse	TGACTGCAGAACACCAGGAG		

Primers for bisulfite cloning PCR

Gene	Primer	Sequence (5' to 3')	Annealing temperature (°C)	Product length (bp)
TUSC3	Forward	TAATTGGGTTTAGTAGTAGGATGGTT	50	218
	Reverse	CAAAAAAAAAAACTAACAAAACATCC		
EPHB4	Forward	GGYGAGGGTTTTTTAAATTTAGT	50	234
	Reverse	ATCCRAAATATTTAAAACTACAATA		
WNT2	Forward	AAGTAATGAGTTGAGAATTATTTTTGGATT	50	195
	Reverse	AAAACCTTTAAAAAAACTCCAAACC		

Supplementary Table 4.1. PCR Primers and conditions

Reaction condition and thermal profile for all PCR

	Final conc.			
10X HotStarTaq Buffer	1X	Initial denaturation:	95°C	10 min
$MgCl_2$	1.25mM	Denaturation:	95°C	40 sec
dNTP	200uM	Annealing:	50~60°C	40 sec } x 40 cycles
Forward primer	200nM	Extension:	72°C	40 sec
Reverse primer	200nM	Final extension:	72°C	7 min
HotStarTaq	0.04U			
Total reaction volume	*25ul*			

Supplementary Table 4.2. Sequence independence of MAP

EPHB4	Sample Name	rs2571607 (promoter)	rs314315 (promoter)	rs2247445 (promoter)	rs2289058 (exon 6)	rs144173 (exon 7)	rs314359* (exon 9)	rs2230585 (exon 12)	rs34918225 (exon 15)
Methylated	**PM20**	GG	AA	GG	CC	CT	CT	CT	CC
	#PM74	AG	AA	AG	CC	CT	CT	CT	CC
	PM85	AG	AA	AG	CC	CC	CC	CC	CC
	PM96	AA	AA	AA	CC	CC	CC	CC	CC
	PM97	AG	AA	AG	CC	CT	CT	CT	CC
	#PM151	-	AA	GG	CC	CT	CT	CT	CC
	PM182	AG	AA	AG	CC	CC	CC	CC	CC
Unmethylated	**PM10**	AA	AA	AA	CC	CC	CC	CC	CC
	PM17	AA	AA	AA	CC	CC	CC	CC	CC
	PM34	GG	AA	GG	CC	CT	CT	CT	CC
	PM41	AG	AA	AG	CC	CT	CT	CT	CC
	PM47	AA	AA	AA	-	CC	CC	CC	CC
	PM50	GG	AA	GG	CC	CC	CC	CC	CC
	PM53	AA	-	AA	CC	CC	CC	CC	CC
	PM55	AG	AA	AG	CC	CC	CC	CC	CC
	PM58	AA	AA	AA	CC	CC	CC	CC	CC
	PM64	GG	AA	GG	CC	CT	CT	CT	CC
	PM82	AG	AA	AG	CC	CC	CC	CC	CC
	PM84	AG	AA	AG	CC	CC	CC	CC	CC
	PM90	AG	AA	AG	CC	CC	CC	CC	CC
	PM98	AG	AA	AG	CC	CT	CT	CT	CC
	PM104	GG	AA	GG	CC	TT	TT	TT	CC
	PM118	GG	AA	GG	CC	TT	TT	TT	CC
	PM122	AG	AA	AG	CC	CT	CT	CT	CC
	PM123	AG	AA	AG	CC	CT	CT	CT	CC
	PM131	GG	AA	GG	CC	CT	CT	CT	CC
	#PM133	GG	AA	GG	CC	CT	CT	CT	CC
	PM150	GG	AA	GG	CC	CT	TT	CT	CC
	PM158	AG	AA	AG	CC	CC	CC	CC	CC
	#PM181	AG	AA	AG	CC	CT	CT	CT	CC

Supplementary Table 4.2. Sequence independence of MAP

TUSC3	Sample Name	rs9325758 (promoter)	rs6993637 (promoter)	rs11545035 (exon 2)	rs17121892 (exon 8)
Methylated	**PM10**	TT	AA	TT	CC
	PM34	TT	AA	TT	CC
	PM47	TT	AA	TT	CC
	PM53	TT	AA	TT	CC
	PM55	TT	AA	TT	CC
	PM58	TT	AA	TT	CC
	PM82	TT	AA	TT	CC
	PM84	TT	AA	TT	CC
	PM90	CT	AA	TT	CC
	PM97	TT	AA	TT	CC
	PM98	TT	AA	TT	CC
	PM104	TT	AA	TT	CC
	PM118	TT	AA	TT	CC
	PM133	TT	AA	CT	CC
	PM150	CT	AA	TT	CC
	PM181	TT	AA	TT	CC
Unmethylated	**PM17**	CT	AA	TT	CC
	PM20	TT	AA	TT	CC
	PM41	TT	AA	TT	CC
	PM50	TT	AA	TT	CC
	PM64	TT	AA	TT	CC
	PM74	TT	AA	TT	CC
	PM85	TT	AA	TT	CC
	PM96	TT	AA	TT	CC
	PM122	TT	AA	TT	CC
	PM123	TT	AA	TT	CC
	PM131	TT	AA	TT	CC
	PM151	TT	AA	TT	CC
	PM158	CT	AA	TT	CC
	PM182	TT	AA	TT	CC

Supplementary Table 4.2. Sequence independence of MAP

WNT2	Sample Name	rs39317 (promoter)	rs2051714 (promoter)	rs39316 (promoter)	rs39315 (promoter)	rs1051751 (exon 5)	rs2228946* (exon 5)	rs6972479 (exon 5)	rs2024233 (exon 5)
Methylated	**PM10**	AA	TT	GG	CC	GG	GG	GG	AG
	PM17	AA	CT	CG	CC	GG	AG	AG	AG
	PM20	AG	CC	GG	CT	GG	GG	GG	GG
	PM21	AG	CT	GG	CT	GG	GG	GG	AA
	PM50	GG	CC	GG	TT	GG	AG	AG	AG
	PM84	AG	CC	GG	CT	GG	AG	AG	AA
	#PM94	AG	CT	GG	CT	GG	AG	AG	AG
	PM130	AG	CT	GG	CT	GG	GG	GG	AA
	PM152	AG	CT	GG	CT	GG	GG	GG	AG
	PM154	GG	CC	GG	TT	GG	AG	AA	GG
	PM157	GG	CC	GG	TT	GG	GG	GG	AG
	#PM165	GG	CC	GG	TT	GG	AG	AG	AG
	PM172	AG	CT	GG	CT	GG	GG	GG	AA
Unmethylated	**PM5**	GG	CC	GG	TT	GG	GG	GG	AG
	PM6	AG	CT	GG	CT	GG	GG	GG	GG
	PM60	AG	CT	GG	CT	GG	GG	GG	AG
	PM62	AG	CT	GG	CT	GG	GG	GG	AA
	#PM64	AG	CC	CG	CT	GG	AG	AG	AG
	PM80	AG	CC	CG	CT	GG	AG	AG	GG
	PM89	AG	CC	CG	CT	GG	AG	AG	AG
	#PM100	AG	CC	CG	CT	GG	AG	AG	AG
	PM104	GG	CC	GG	TT	GG	GG	GG	AG
	PM122	AG	CT	GG	CT	GG	GG	GG	AG
	PM139	GG	CC	GG	TT	GG	GG	GG	AG
	PM150	GG	CC	GG	TT	GG	GG	GG	AA
	PM181	GG	CC	GG	TT	GG	GG	GG	AA

Sample used for allele-specific methylation and gene expression studies

* SNP used for cDNA genotyping

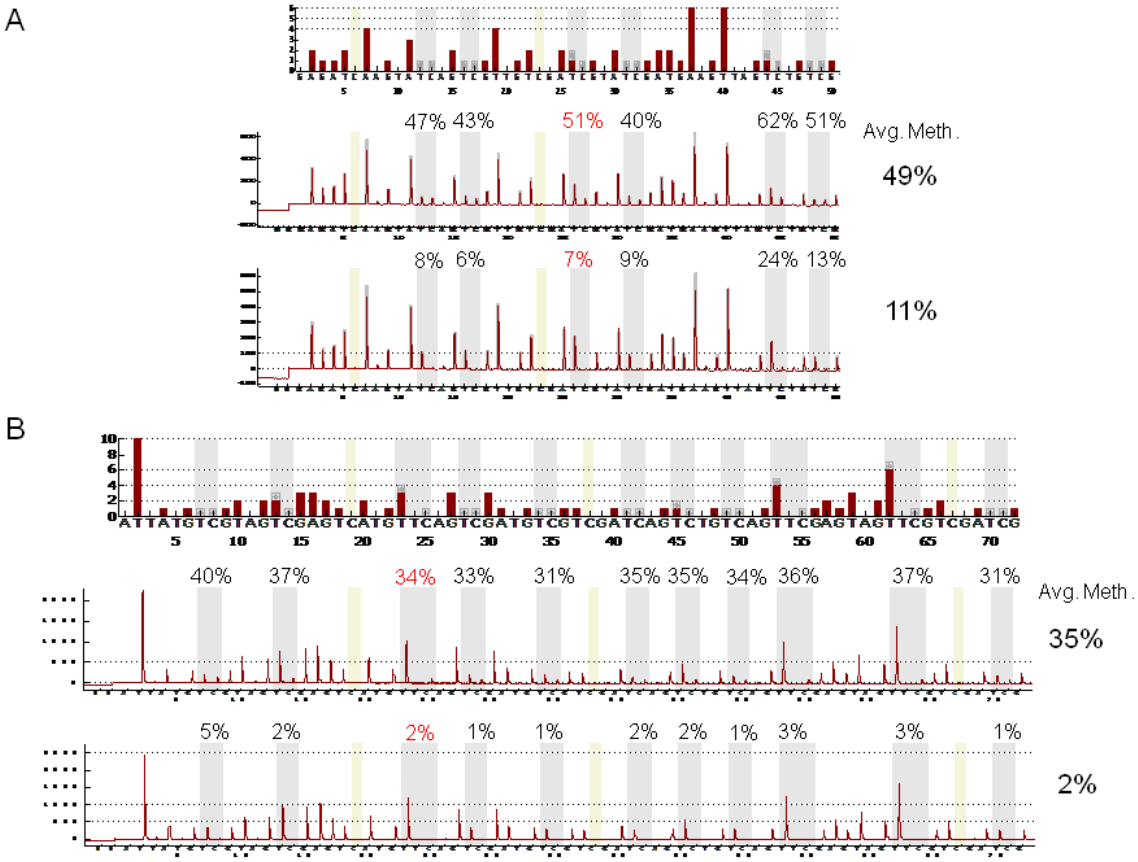

Supplementary Figure 4.1. Validation of variable methylation at (A) *MKRN3* and (B) *TUSC3* by pyrosequencing.

Pyrograms from one methylated sample and one unmethylated sample are shown. Reference pyrograms are shown on top. Methylation level of CpG sites that are targeted by the Illumina probes are highlighted in red.

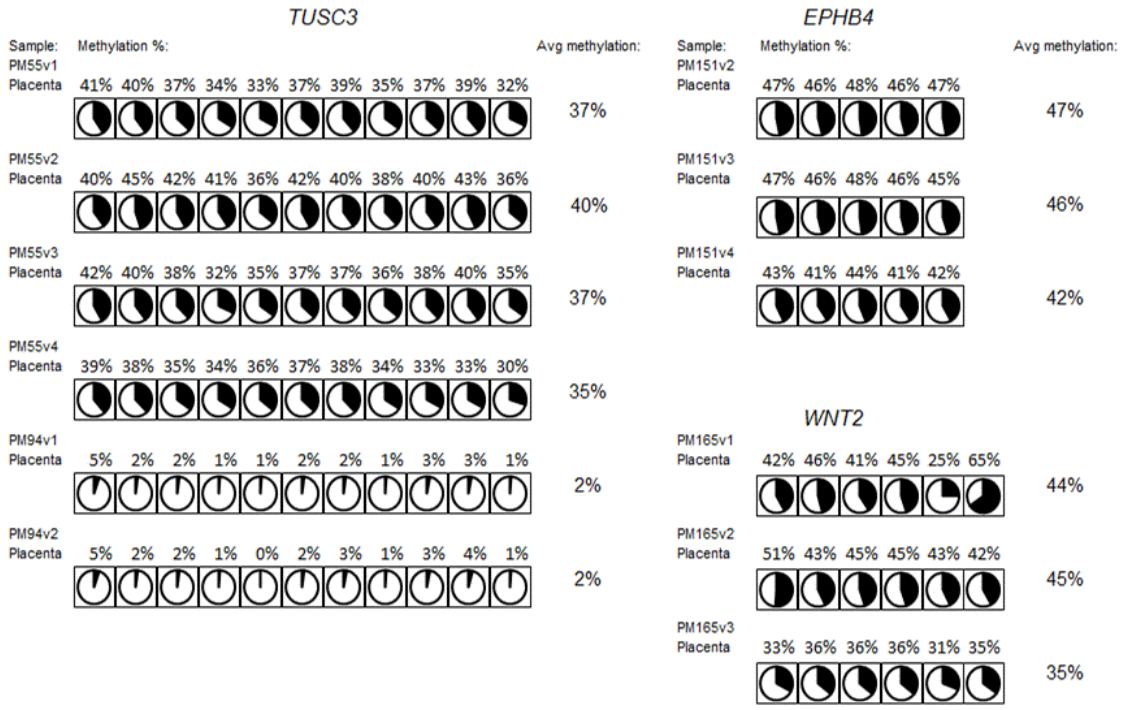

Supplementary Figure 4.2. Intra-individual variability of DNA methylation on MAP.

DNA methylation level of (A) *TUSC3*, (B) *EPHB4* and (C) *WNT2* is given for multiple whole villous samples taken from the same placenta (four sites for PM55, two sites for PM94). On-or-off DNA methylation pattern was consistent from different samples within the same placenta. Each circle represents a CpG site within a sample. The area shaded in black is proportional to the methylation level of the CpG site indicated by pyrosequencing.

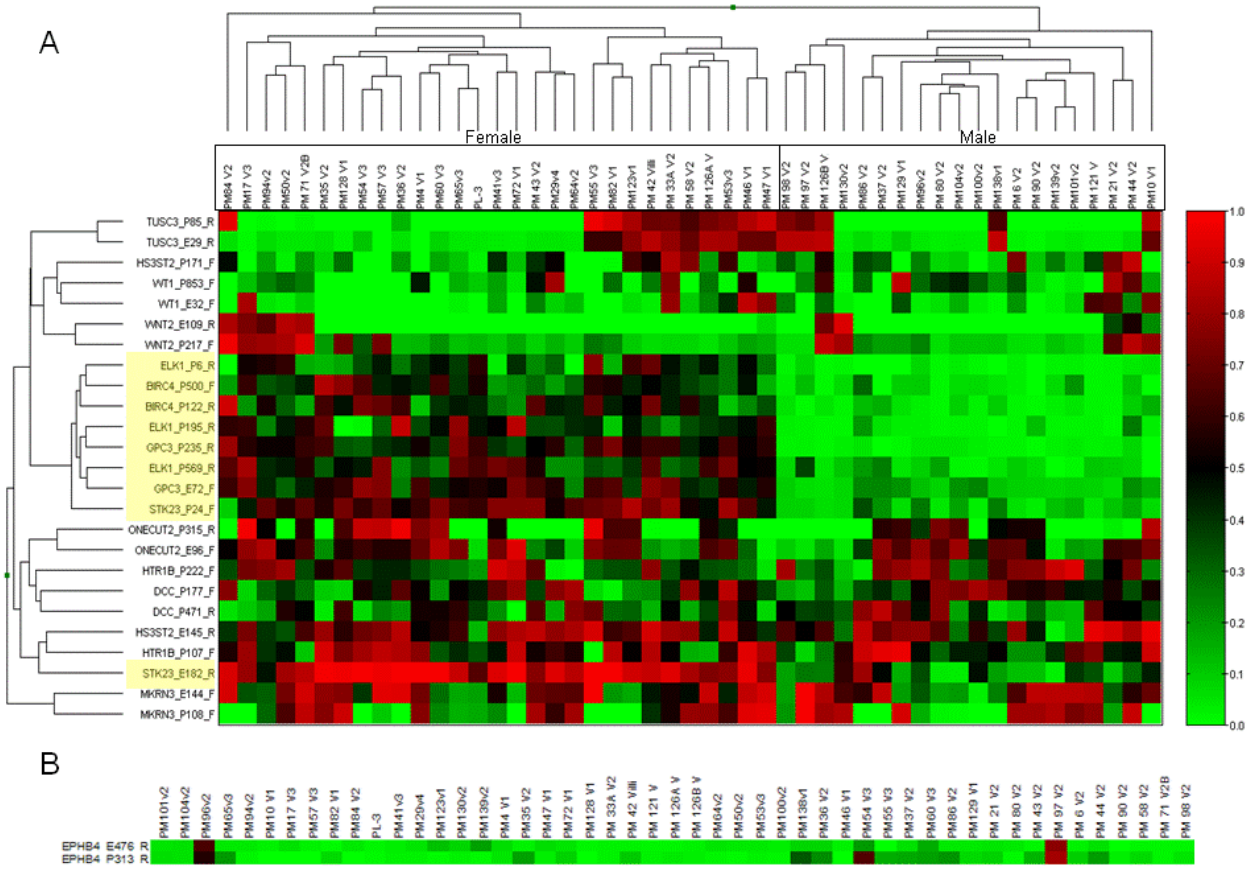

Supplementary Figure 4.3. Genes exhibiting high inter-individual variance in methylation values in a large population of human placentas.

(A) Heat-map of 12 genes with at least 2 probes having methylation variance greater than 1.5 SD from the mean. Probes and sample names are shown and with hierarchical clustering of beta values based on 1-r (Illumina Beadarray software). A beta value of zero (indicated in bright green) represents an unmethylated locus and one (indicated in bright red) represents a methylated locus. Probes for genes on the X chromosome are highlighted by a yellow box. (B) Heat-map of *EPHB4* in 49 human placentas.

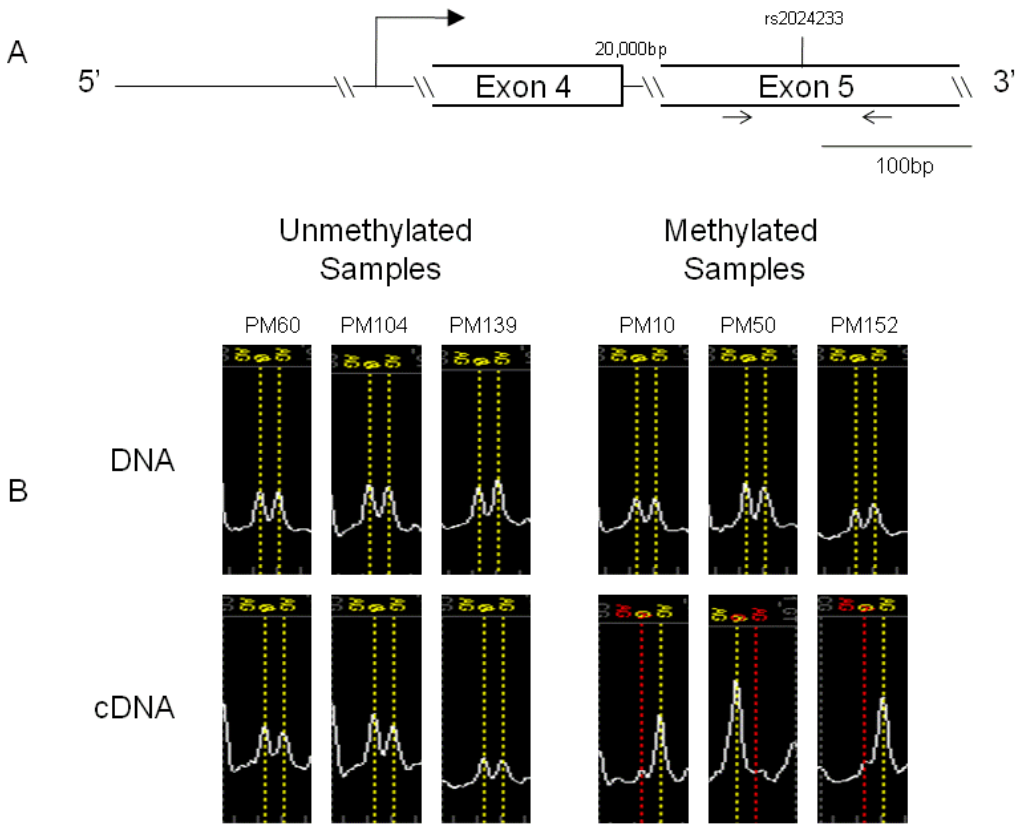

Supplementary Figure 4.4. Allele-specific mRNA expression in *WNT2*.

(A) Schematic of *WNT2* locus showing the regions investigated by genotyping assays within exon 5 of 3 methylated samples and 3 unmethylated samples. PCR primers for DNA and cDNA genotyping by Sequenom are indicated by black arrows. (B) Allele-specific expression of *WNT2* is observed based on the A/G allele of rs2228946 in DNA and cDNA by iPlex. Peak height of the alleles corresponds to the relative amount of alleles present in the sample.

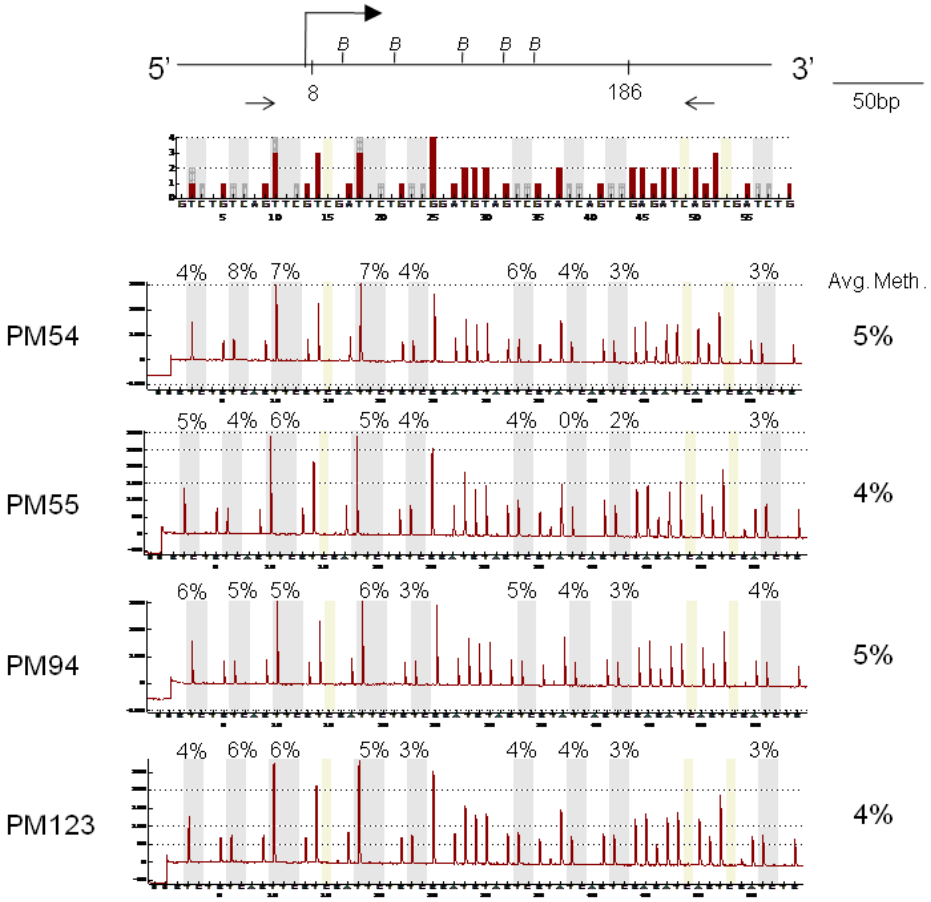

Supplementary Figure 4.5. CpG methylation status of *ID2* on *Bst*UI digestion sites.

Schematic of *ID2* locus showing the regions investigated by bisulfite pyrosequencing is shown on top (8 to 186 relative to the transcriptional start site according to NM_002166). PCR primers for bisulfite pyrosequencing are indicated by black arrows. Enzyme digestion sites of *Bst*UI are indicated by "B". Reference pyrogram is provided. CpG sites were unmethylated for this region of *ID2* in the 4 samples investigated.

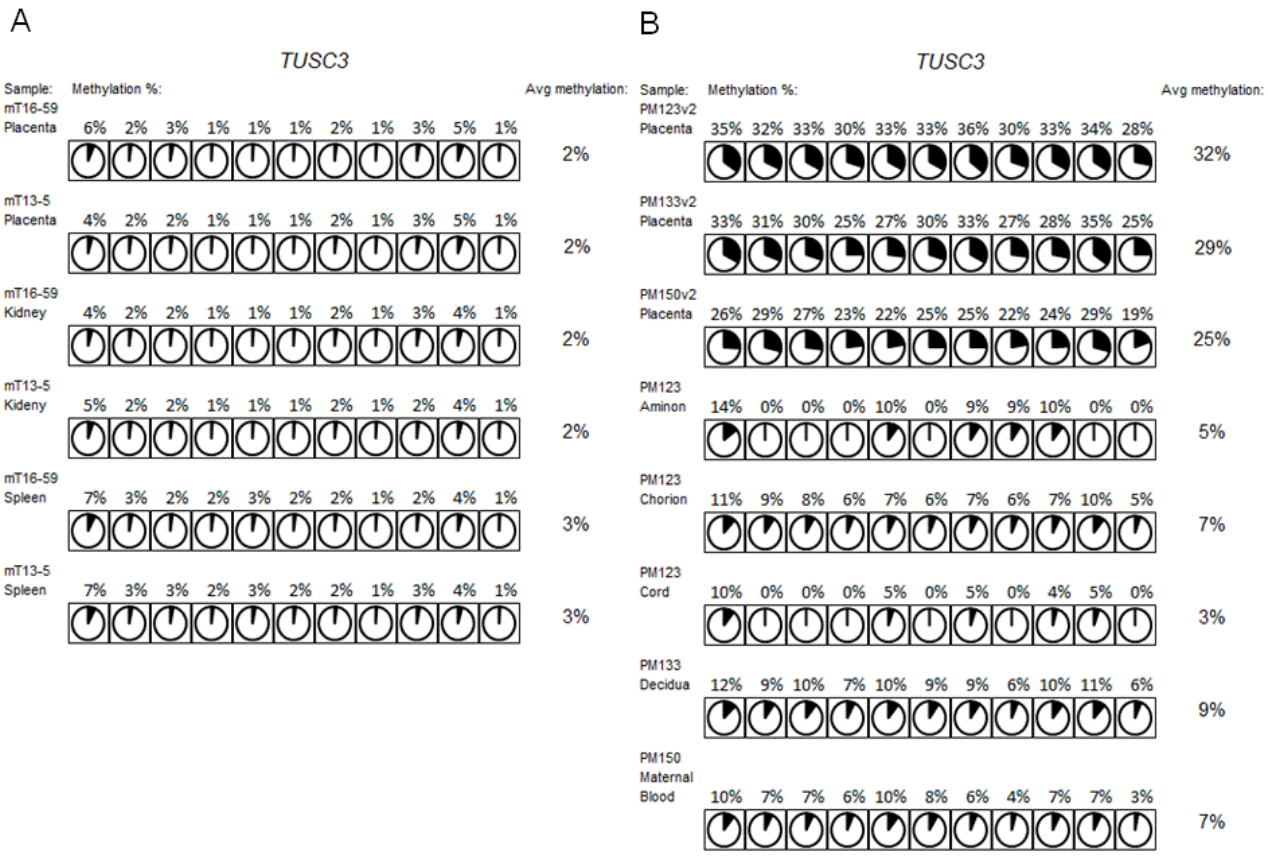

Supplementary Figure 4.6. Tissue-specific DNA methylation of *TUSC3*.

(A) DNA samples from two independent fetuses with placentas unmethylated in *TUSC3* promoter were investigated by bisulfite pyrosequencing. None of the cases were methylated in other tissues. (B) DNA samples from 3 independent placentas with trophoblastic villi methylated in *TUSC3* promoter were investigated by bisulfite pyrosequencing. None of the tissues (Aminon, chorion, cord, decidua and maternal blood) other than whole villi was highly methylated. Each circle represents a CpG site in a sample. Area shaded in black is proportional to the methylation level of the CpG site indicated by pyrosequencing.

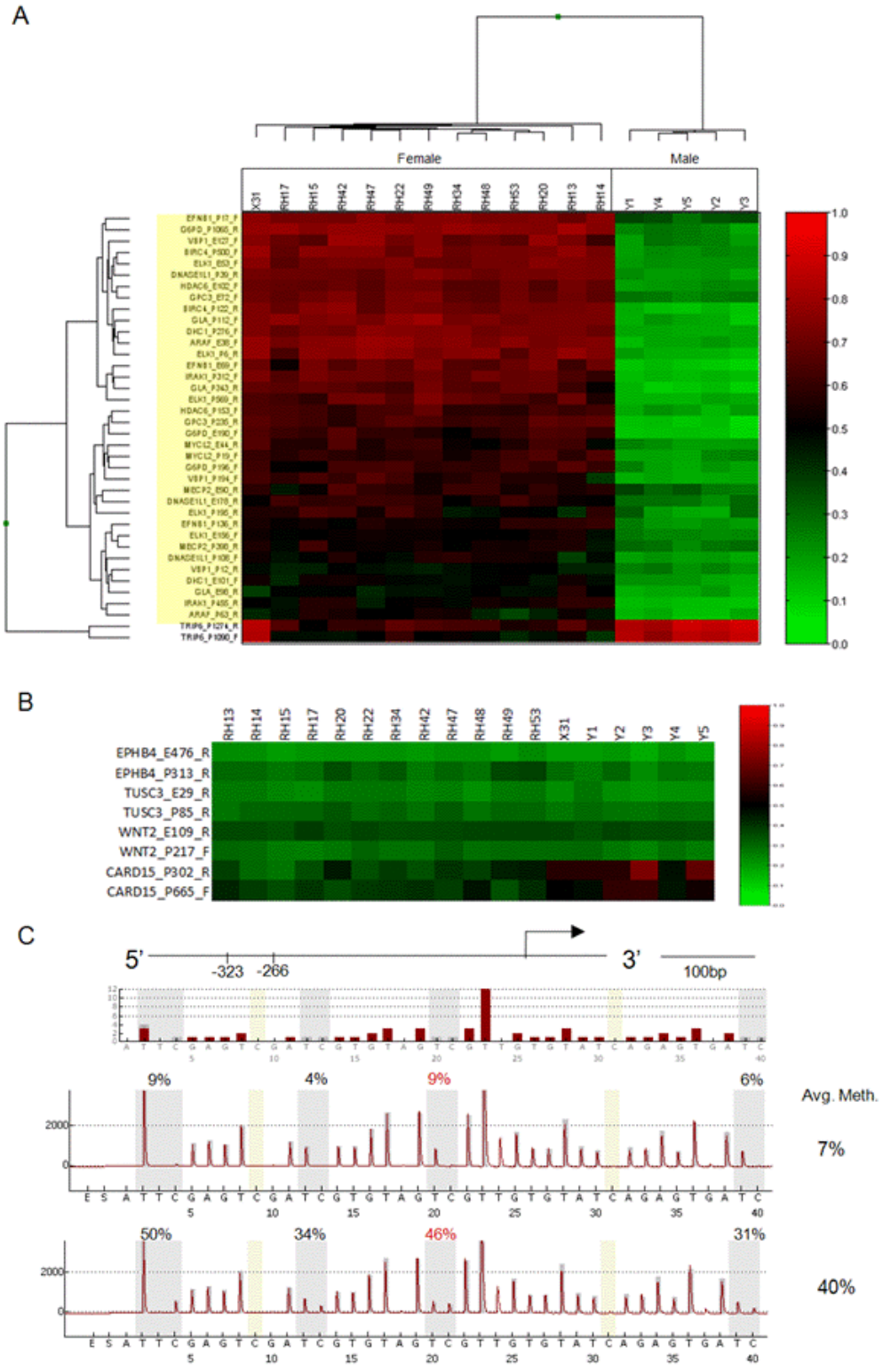
A
Female
Male
X31
RH17
RH15
RH42
RH47
RH22
RH49
RH34
RH48
RH53
RH20
RH13
RH14
Y1
Y4
Y5
Y2
Y3
1.0
0.9
0.8
0.7
0.6
0.5
0.4
0.3
0.2
0.1
0.0
B
RH13
RH14
RH15
RH17
RH20
RH22
RH34
RH42
RH47
RH48
RH49
RH53
X31
Y1
Y2
Y3
Y4
Y5
EPHB4_E476_R
EPHB4_P313_R
TUSC3_E29_R
TUSC3_P85_R
WNT2_E109_R
WNT2_P217_F
CARD15_P302_R
CARD15_P665_F
C
5'
3'
-323
-266
100bp
9%
4%
9%
6%
Avg. Meth.
7%
50%
34%
46%
31%
40%

Supplementary Figure 4.7. Inter-individual variance of methylation values in the human blood cells.

(A) Heat-map of 14 genes with at least 2 probes having methylation variance greater than 1.5 SD from the mean. Probes and sample names are shown and with hierarchical clustering of beta values based on 1-r (Illumina Beadarray software). A beta value of zero (indicated in bright green) represents an unmethylated locus and one (indicated in bright red) represents a methylated locus. Probes for genes on the X chromosome are highlighted by a yellow box. (B) Heat-map of *EPHB4*, *TUSC3*, *WNT2* and *NOD2* (CARD15) in human blood generated by Illumina GoldenGate Methylation Array. (C) Validation of variable methylation of *NOD2* by bisulfite pyrosequencing. Schematic of NOD2 locus showing the regions investigated by bisulfite pyrosequencing (−323 to −266 relative to the transcriptional start site according to NM_022162). One methylated sample and one unmethylated sample are shown. Reference pyrograms are shown on top. Methylation level on CpG sites that targeted by the Illumina probe is highlighted in red.

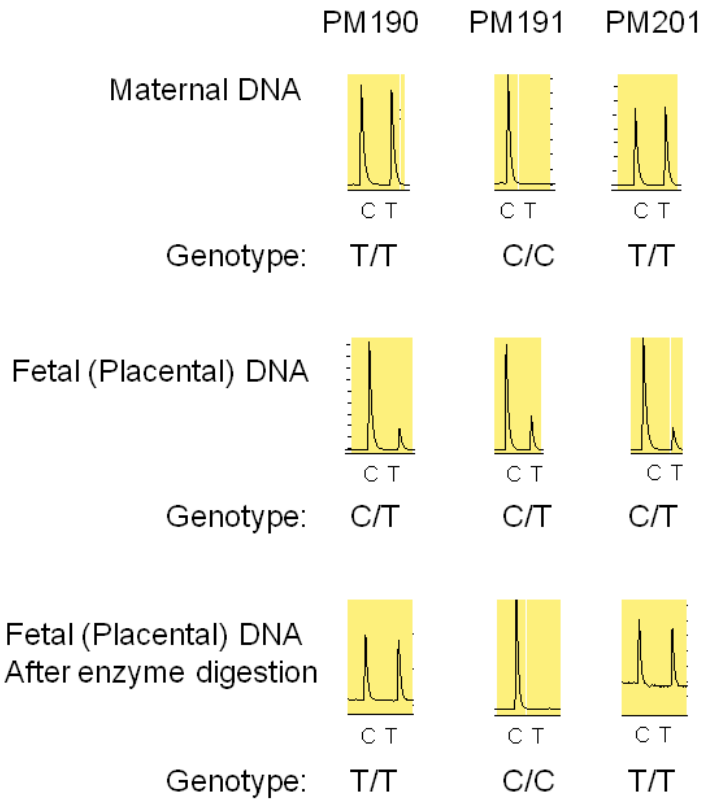

Supplementary Figure 4.8. Parental-origin of DNA methylation in *TUSC3* promoter.

Three informative cases (homozygous in mother and heterozygous in fetus) which have DNA methylation in the placenta showed that the methylated alleles were originated from the mother using methylation-sensitive restriction enzyme treatment followed by genotyping.

Appendix 4: Supplementary tables and figures for Chapter 5

Supplementary Table 5.1. Clinical information of the placental samples

Case	Group	Gestational age (wks)	Maternal age (yrs)	Birth weight (g)	SD	Gender	Condition	Mode of delivery/ Other complication	Average systolic BP (mmHg)	Average diastolic BP (mmHg)	*Proteinuria (g/L)	*Protein Excretion (g/d)	Placenta Weight (g)	Ethnicity
PL-1	Early control	29.29	36.7	N/A	N/A	male	normal	Abruption	N/A	N/A	N/A	N/A	N/A	N/A
PL-2	Early control	27.43	N/A	913.0	1.34	female	normal	C/s	N/A	N/A	N/A	N/A	N/A	N/A
PM174	Early control	33.86	34.6	1940	-0.65	male	normal	Abruption	N/A	N/A	N/A	N/A	N/A	N/A
PM175	Early control	28.00	36.8	1290	1.16	female	normal	Abruption	N/A	N/A	N/A	N/A	N/A	N/A
PM21	EOPET	33.71	34.8	1650	-1.87	male	IUGR & EoPET	C/s	N/A	N/A	0.50	0.63	N/A	N/A
PM43	EOPET	31.71	32.3	1440	-0.88	female	EoPET	VD	148	84	7.95	11.03	300	N/A
PM97	EOPET	26.00	23.8	440	-2.20	male	IUGR & EoPET	VD	150	105	1.00	N/A	90	Egyptian
PM6	EOPET	32.71	42.3	1160	-3.45	male	IUGR & EoPET	C/s	136	93	0.09	0.17	195	N/A
PM74	Late control	37.86	36.0	3460	0.59	male	normal	SVD	N/A	N/A	N/A	N/A	405	N/A
PM85	Late control	38.00	35.9	2750	-1.23	female	normal	SVD	N/A	N/A	N/A	N/A	440	Asian
PM118	Late control	39.14	37.9	3835	1.22	male	normal	SVD	N/A	N/A	N/A	N/A	N/A	Chinese
PM122	Late control	37.00	35.8	2730	-0.45	male	normal	SVD	N/A	N/A	0.15	N/A	N/A	Caucasian
PM136	Late control	38.00	40.2	3145	-0.22	female	normal	C/s	N/A	N/A	N/A	N/A	N/A	Caucasian
PM53	LOPET	38.57	35.0	4400	2.52	female	LoPET	C/s	146	93	0.70	N/A	740	N/A
PM58	LOPET	37.00	37.2	3010	0.09	female	LoPET	C/s	124	84	1.83	N/A	500	N/A
PM71	LOPET	38.86	38.9	2675	-1.47	female	LoPET	VD	N/A	N/A	0.89	0.81	290	Caucasian
PM98	LOPET	37.43	34.7	3310	0.68	male	LoPET	SVD	N/A	N/A	0.17	0.36	N/A	Indonesian
PM33B	Control	32.00	42.0	2015	1.76	male	normal	C/s	105	65	N/A	N/A	210	Caucasian
PM90	Control	38.29	36.7	3505	0.70	male	normal	SVD	N/A	N/A	N/A	N/A	N/A	Caucasian
PM117	Control	39.86	36.5	3665	0.41	male	normal	VD	N/A	N/A	N/A	N/A	N/A	Caucasian
PM112	Control	38.71	30.2	3495	0.43	female	normal	SVD	N/A	N/A	N/A	N/A	N/A	N/A
PM113	Control	40.14	34.3	3885	0.89	male	normal	C/s	N/A	N/A	N/A	N/A	N/A	Caucasian

Supplementary Table 5.1. Clinical information of the placental samples

Case	Group	Gestational age (wks)	Maternal age (yrs)	Birth weight (g)	SD	Gender	Condition	Mode of delivery/ Other complication	Average systolic BP (mmHg)	Average diastolic BP (mmHg)	*Proteinuria (g/L)	*Protein Excretion (g/d)	Placenta Weight (g)	Ethnicity
PM33A	IUGR	32.00	42.0	1440.0	-0.88	female	IUGR	C/s	105	65	N/A	N/A	410	Caucasian
PM42	IUGR	26.00	33.7	450	-2.14	female	IUGR	SVD	120	70	N/A	N/A	N/A	N/A
PM126A	IUGR	36.57	36.7	2080	-0.81	female	IUGR	C/s	100	60	N/A	N/A	640	Caucasian
PM126B	IUGR	36.57	36.7	1895	-1.33	male	IUGR	C/s	100	60	N/A	N/A	640	Caucasian
PM12	EOPET	31.71	39.3	1305	-1.50	male	IUGR & EoPET	C/s	150	97	N/A	N/A	N/A	N/A
PM15	EOPET	32.86	36.1	1480	-2.03	female	IUGR & HELLP	C/s	146	94	0.19	0.36	N/A	N/A
PM26	EOPET	31.71	36.2	940	-3.17	female	IUGR & EoPET	C/s	160	100	17.89	N/A	540	N/A
PM39	EOPET	32.00	19.7	1700	0.31	male	IUGR & EoPET	VD	151	101	3.02	8.92	295	N/A
PM48A	EOPET	31.00	40.2	395	-5.67	female	IUGR & EoPET	SVD	N/A	N/A	1.57	5.52	N/A	Iranian
PM51	EOPET	34.00	42.9	1400	-2.92	female	IUGR & EoPET	C/s	126	77	0.29	0.81	260	Chinese
PM60	EOPET	33.29	39.8	1465	-2.65	female	IUGR & EoPET	C/s	173	105	0.14	0.19	320	Filipino
PM62	EOPET	27.14	41.0	480	-4.21	male	IUGR & EoPET	C/s	N/A	N/A	0.40	0.98	80	N/A
PM64	EOPET	33.29	27.7	1728	-0.94	female	HELLP	VD	155	109	1.53	2.88	315	Caucasian
PM80	EOPET	28.57	35.8	1095	-1.47	male	EoPET	C/s	140	87	0.30	N/A	230	N/A
PM86	EOPET	24.86	34.9	545	-1.64	male	IUGR & EoPET	C/s	N/A	N/A	N/A	N/A	N/A	N/A
PM116	EOPET	32.43	26.0	1480	-0.70	male	IUGR & EoPET	C/s	140	80-114	1.01 (AVG)	1.13	N/A	Caucasian
PM138	EOPET	34.00	38.3	3685	6.68	male	EoPET	C/s	N/A	N/A	1.32	2.95	N/A	Caucasian
PL-4	Early control	30.43	36.0	1535	2.42	male	normal	C/s	N/A	N/A	N/A	N/A	180	N/A
PL-5	Early control	26.43	35.6	850	-0.02	female	normal	SVD	N/A	N/A	N/A	N/A	175	N/A
PL-7	Early control	30.14	22.2	1615	3.13	male	normal	N/A	N/A	N/A	N/A	N/A	320	Mexican

Supplementary Table 5.1. Clinical information of the placental samples

Case	Group	Gestational age (wks)	Maternal age (yrs)	Birth weight (g)	SD	Gender	Condition	Mode of delivery/ Other complication	Average systolic BP (mmHg)	Average diastolic BP (mmHg)	*Proteinuria (g/L)	*Protein Excretion (g/d)	Placenta Weight (g)	Ethnicity
PL-8	Early control	26.57	40.7	875	1.59	female	normal	N/A	N/A	N/A	N/A	N/A	185	N/A
PL-9	Early control	27.43	23.2	995	-0.79	male	normal	C/s	N/A	N/A	NEGATIVE	N/A	255	N/A
PL-11	Early control	33.71	35.0	2495	1.68	male	normal	C/s	N/A	N/A	NEGATIVE	N/A	N/A	N/A
PL-12	Early control	25.86	29.6	915	0.33	male	control	C/s	N/A	N/A	N/A	N/A	210	N/A
PL-14	Early control	33.14	31.3	2375	1.90	male	normal	Abruption	N/A	N/A	NEGATIVE	N/A	420	Hungarian
PL-15	Early control	28.57	30.8	N/A	N/A	male	normal	N/A	N/A	N/A	N/A	N/A	210	N/A
PL-17	Early control	33.29	27.2	2025	0.36	male	normal	N/A	N/A	N/A	NEGATIVE	N/A	335	N/A
PL-18	Early control	29.00	36.9	1135	-1.12	female	normal	C/s	N/A	N/A	NEGATIVE	N/A	355	N/A
PL-20	Early control	28.71	28.8	1276	0.13	male	normal	Abruption	N/A	N/A	0.25	N/A	315	N/A
PL-21	Early control	28.57	34.7	1455	1.72	male	normal	Abruption	N/A	N/A	NEGATIVE	N/A	245	Indian
PM65	Control	41.43	30.9	3250	-0.58	female	normal	N/A	N/A	N/A	N/A	N/A	N/A	Caucasian
PM94	Control	40.29	36.1	3580	0.22	female	normal	N/A	N/A	N/A	N/A	N/A	N/A	Caucasian
PM96	Control	40.00	33.9	3900	0.92	male	normal	N/A	N/A	N/A	N/A	N/A	N/A	Polish
PM101	Control	38.00	34.3	2885	-0.88	male	normal	C/s	N/A	N/A	N/A	N/A	N/A	N/A
PM104	Control	40.71	30.3	3360	-0.37	male	normal	VD	N/A	N/A	N/A	N/A	N/A	Caucasian

*NOTE: measured many times, recorded values closest to delivery

N/A: Not available

VD: Vaginal delivery

C/s: Caesar Section

Supplementary Table 5.2. PCR primers and condition

Primers for bisulfite pyrosequencing

Gene	Primer	Sequence (5' to 3')	Product length (bp)	Number of CpGs
CAPG	Forward	GTGGTTGGGGTAGTTAGAGAAGTAA	176	2
	Reverse	(5' biotinated)-CTACCCACCCAAAAAAATACCAA		
	Sequencing	GTGGGGTAGGTTGGAA		
GLI2	Forward	TGGGTTTTTTGGTAAGTAAGTGAAGTT	223	3
	Reverse	(5' biotinated)-CRTAATATCCCACTTATACTAACCATTCAT		
	Sequencing	AAAAGATATAGGATTGTGAAA		
KRT13	Forward	TGAAGGTTAAATGAGATGATGAGTGTA	141	2
	Reverse	(5' biotinated)-CCATCAAACACAACTATAAAAACTCA		
	Sequencing	GTGTAAAGTAATTTTATTTAGT		
TIMP3	Forward	GTTAAAGTGTTTAAAGGGGAAAAAGGA	199	2
	Reverse	(5' biotinated)-CCRCTTCATCCTATTAAAAATACCACA		
	Sequencing	AAAATGTTTTTGGAAATATTA		
MEST	Forward	(5' biotinated)-GGGTTTTTTTTGGGAATAGGGTGAA	122	4
	Reverse	TTCCAAAATAAACTTAATCCATTCTCCRC		
	Sequencing	CCTTACCTACAAAACTCCAT		

Reaction condition and thermal profile for all assays

Reagents	Final conc.	Temperature		Cycles
10X HotStarTaq Buffer	1X	Initial denaturation:	95°C	10mins
$MgCl_2$	1.25mM	Denaturation:	95°C	40 sec
dNTP	200mM	Annealing:	50°C	40 sec } x 40 cycles
Forward primer	200nM	Extension:	72°C	40 sec
Reverse primer	200nM	Final extension:	72°C	7 min
HotStarTaq	0.04U			
Total reaction volume	25ul			

Supplementary Table 5.3. Correlation between Illumina array and bisulfite pyrosequencing assay measurements

	Illumina array	Bisulfite pyrosequencing assay	Correlation of the same CpG site between assays		Correlation of overall CpG sites between assays	
	difference (%)	difference (%)	coefficient	*p* value	coefficient	*p* value
CAPG	10.58	8.50	0.73	<0.05	0.72	<0.05
GLI2	21.97	4.25	0.93	<0.005	0.82	<0.05
KRT13	18.03	7.75	0.77	<0.05	0.76	<0.05
TIMP3	19.23	18.25	0.94	<0.001	0.95	<0.001
MEST	15.50	10.50	0.94	<0.001	0.95	<0.001

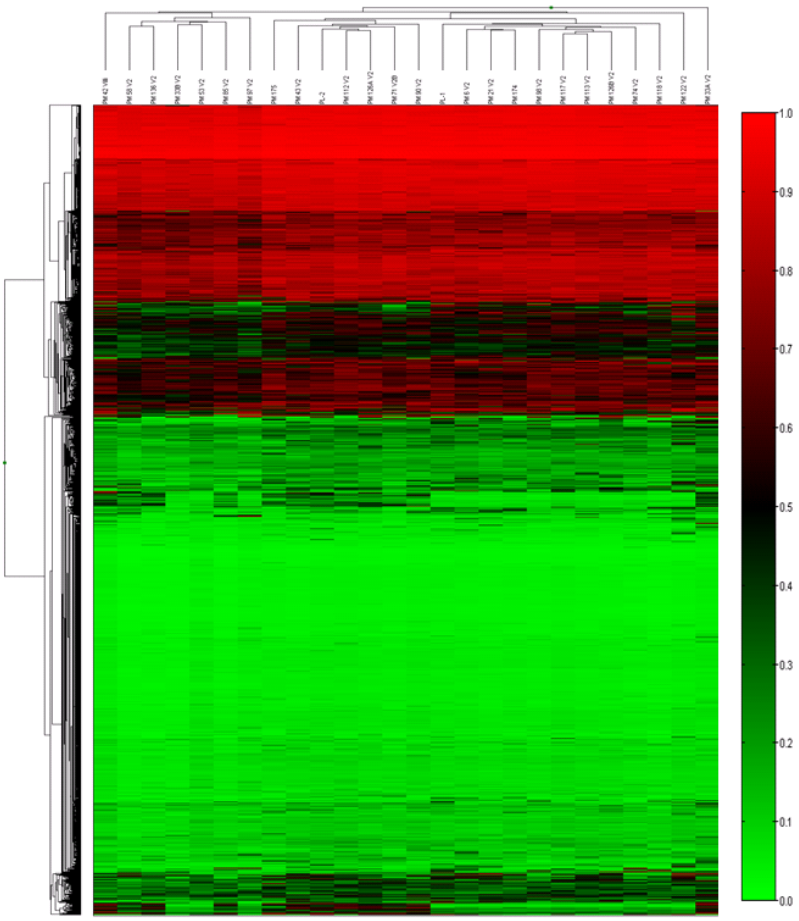

Supplementary Figure 5.1. Heat-map of the methylation array data.

Probes and sample names are shown and with hierarchical clustering of beta values based on 1-r (Illumina Beadarray software). A beta value of zero (indicated in bright green) represents an unmethylated locus and one (indicated in bright red) represents a methylated locus.

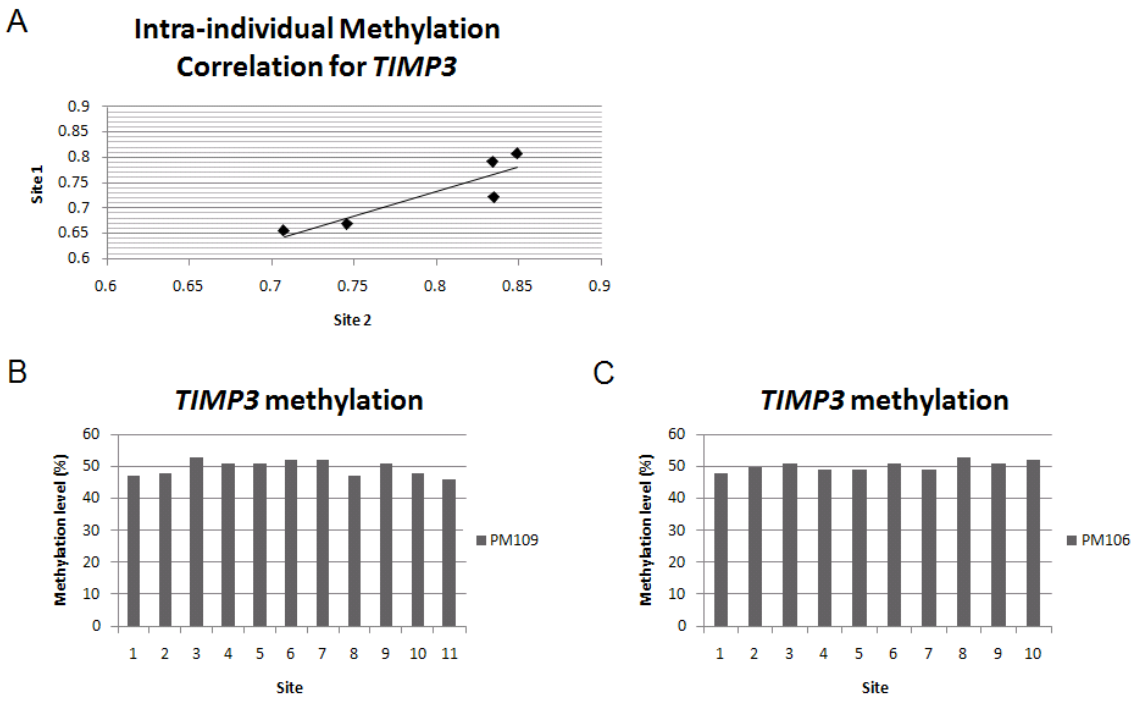

Supplementary Figure 5.2. Intra-individual methylation analysis of *TIMP3* methylation in placenta.

(A) Correlation of *TIMP3* methylation between two independent sites from 5 control placentas. *TIMP3* methylation analysis in (A) 11 sampling sites from case PM109 and (B) 10 sampling sites from case PM106.

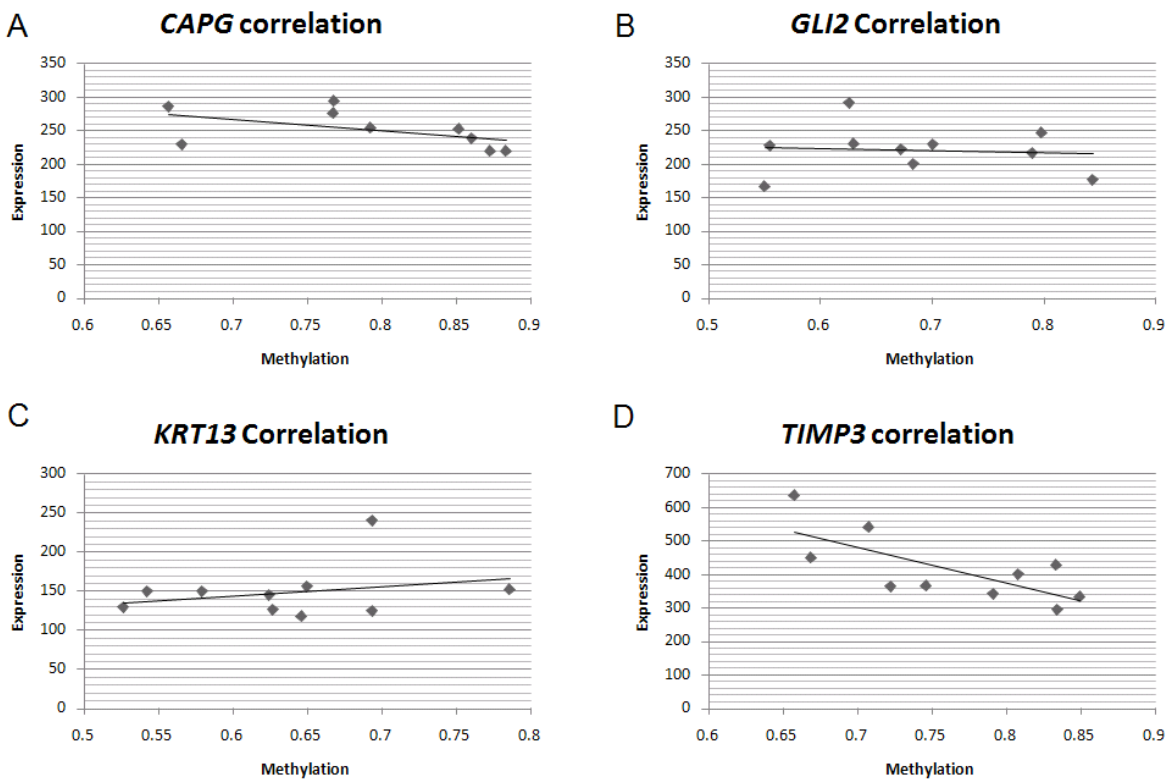

Supplementary Figure 5.3. Correlation of DNA methylation with gene expression from array data.

Correlation of (A) *CAPG* (R=-0.29; *p*=0.4), (B) *GLI2* (R=-0.08; *p*=0.82), (C) *KRT13* (R=0.27; *p*=0.44) and (D) *TIMP3* (R=-0.72; *p*=0.02) based on 5 placentas with 2 sampling sites each.